

https://dspace.org/

Pillared clays as "green chemstry" catalysts for wastewater treatment

Baloyi, Siwela Jeffrey

2019

https://hdl.handle.net/10539/28045

Baloyi, Siwela Jeffrey. (2019). Pillared clays as "green chemistry" catalysts for wastewater treatment. University of the Witwatersrand, https://hdl.handle.net/10539/28045

Downloaded from a DSpace repository. https://dspace.org/

Pillared clays as “green chemistry” catalysts for wastewater treatment



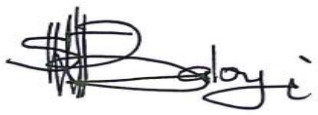
Siwela Jeffrey Baloyi

January 2019

A thesis submitted to the Faculty of Science, University of the Witwatersrand, Johannesburg, in fulfilment of the requirements for the degree of Doctor of Philosophy.

Declaration

I **Siwela Jeffrey Baloyi,** hereby declare that the work reported on this thesis is my own unaided work under the supervision of Dr Moma and Dr Thabang Ntho. This work has not been submitted in substance for any other degree or award at this or any other university or i learning, nor is being submitted concurrently in candidature for any degree or other award.



08 /01 /2019

Candidate

Siwela Jeffrey Baloyi

Date

Abstract

In this study, the CWAO (catalytic wet air oxidation) of phenol was studied in a batch and plug-flow reactors operated in continuous mode, using a highly active and stable heterogeneous catalysts. Three pillared clay-based heterogeneous catalysts, Al/Zr-PILCs (aluminium/zirconia pillared interlayered clays), Al/Fe-PILCs (aluminium/iron pillared interlayered clays) and Al/Cr-PILCs (aluminium/chromium zirconia pillared interlayered clays) were synthesized using ultrasonic treatment method and screened for their efficiency in removing phenol in aqueous medium in a batch autoclave reactor. The method of hydrolysis and ion exchange were successfully achieved by direct addition of the clay into the pillaring solution using ultrasonic treatment both during the formation of the pillaring solution and in the intercalation process, respectively. The preparation method used in this study significantly reduced the synthesis time and the water consumption required compared to conventional method discussed in the literature, indicating advantages of potential scale-up of the pillared clay preparation. Calcination of the synthesized pillared clay catalysts at 500 °C for 120 minutes yielded optimum physical properties with BET (Brunauer–Emmett–Teller) surface area of 180 - 230 m^2/g and basal spacing of 1.50 - 1.92 nm and with good thermal stability. All catalysts achieved a complete removal of phenol and above 80% TOC conversion after 120 min in aqueous solution under mild reaction conditions of 100 °C and 10 bar. Of the catalysts, screened Al/Zr-PILCs catalyst, especially with Al/Zr ratio of 3:1 was the most active catalyst in terms of phenol removal, TOC conversion and stability. For practical purposes, Al/Zr-PILCs as the best selected PILCs (pillared interlayered clays) catalytic powder was fixed on a monolithic substrate. Since the use of monolithic catalysts to the oxidation of phenol in wastewaters can minimize the pressure drop in the flow reactor.

The cordierite monoliths coated with Al/Zr pillared bentonite clay powder were synthesized, characterized and tested in phenol oxidation. The BET specific surface area and mean pore size of the monolithic catalysts obtained by N_2 adsorption–desorption isotherm studies shows that the catalyst are mesoporous by showing type IV adsorption isotherms. The HRSEM (high resolution scanning electron microscopy) characterization results confirmed the active

components were well deposited on the channel walls and the washcoat is observed in all the corners of the washcoated monolith cross section, while the EDX (energy dispersive X-ray spectrometer) revealed the presence of the Zr and Fe elements in the cordierite monolithic catalyst walls. Ultrasound experiments used to estimate the coating adherence show that the washcoated Al/Zr pillared bentonite powder is well anchored on the cordierite. Kinetics of CWAO of phenol was studied over powder Al/Zr-PILCs and monolithic catalyst using a batch autoclave reactor and flow reactor, respectively. During the CWAO of phenol reaction, aromatic ring intermediates (*p*-benzoquinone, catechol acid and hydroquinone) and short chain carboxylic acids (oxalic acid, maleic acid, formic acid, acetic acid and malonic acid) were identified. Kinetic parameters of the model that describes the formation and oxidation of intermediate aromatic compounds and short chain carboxylic acids were determined. The proposed CWAO of phenol kinetic model account for internal and external diffusion limitations, assuming the pseudo-first order reaction. Therefore, the proposed approach can be used for scaling-up the CWAO of phenol in plug flow reactor. The reaction pathway for the CWAO of phenol was proposed.

These findings show that the novel Al/Zr-PILCs monolithic catalyst have a great potential for application in CWAO of phenol, since the materials used in the process are inexpensive, abundant and require minimal modifications. To best of our knowledge, the application of Al/Zr-PILCs/cordierite monolith catalyst for this reaction has not been previously reported.

Keywords: Bentonite clay, Al/Zr-pillared clay, Al/Fe-pillared clay, Al/Cr-pillared clay, ultrasonic treatment, cordierite honeycomb monolith, washcoating, wastewater treatment, flow reactor, reaction pathway and kinetics, phenol, catalytic wet air oxidation (CWAO).

Dedication

To My Late Mother
Mphephu Baloyi
1948 - 2002

I dedicate this thesis to Almighty God of Mount Zion my creator, my strong pillar, my source of inspiration, wisdom, knowledge and understanding. He has been the source of my strength throughout this PhD program and on His wings only have I soared. He always stood with me and strengthened me. I also dedicate this work to my family for creating a conducive environment for me to complete my studies in record time without any pressure. Indeed I gave it all it takes to finish that which I started within three years.

Acknowledgement

I would like to begin by thanking a number of people for their help and support throughout my PhD studies.

I cannot thank my supervisor, **Dr John Moma**, enough for giving me a great opportunity to study at the University of the Witwatersrand. He was very supportive in guiding me through my research and was always there, with his open door policy, if I needed his advice. He was like a brother I never had, he would sacrificed his family time and making long calls after office hours about my work progress.

I would also like to extend my thanks to my industrial supervisor, **Dr Thabang Ntho**, from Mintek for financial support and technical guidance. I have learned lots of things from his way of thinking and his research methodology style. I can honestly say that this PhD thesis could not have gone ahead without his outstanding input, supervision, scientific knowledge and experience in catalysis.

I am also grateful of the time my former supervisors, **Professor Kalala Jalama** and **Professor Esther Akinlabi**, spent supporting me during my initial stages of this PhD study at the University of Johannesburg.

Special thanks to **Mr Kabelo Ledwaba,** for letting me use their BET surface area analysis and FTIR; **Ms Pumeza Gqogqa** for her assistance with HPLC training and to Mr **Mbavhalelo Maumela** for his assistance with HRSEM analysis.

To all the members of **CATMAT group (Wits University) and Catalysis group (Mintek),** for all the great scientific discussions and constructive criticism during seminars and practice talks. It was a great experience being with all of you.

I thank **Mr Tladi Makatsa** and **Mr Sibusiso Mavuso** for their technical help in designing and commissioning plug flow monolith reactor.

Mr Petrus Mafulako and **Ms Pumeza Gqogqa,** for encouraging me during toughest times.

Financial support by the **Department of Science and Technology (DST)** and **National Research Foundation (NRF)** of South Africa, **University of Witwatersrand, University of Johannesburg and Mintek** is acknowledged.

My deepest gratitude goes to my Family for their moral and spiritual support in all that I do, *Xikwembu xi mikatekisa.*

And last but not least, special thanks to my supportive girlfriend, for her patience, understanding and encouragement. We started dating before I started my PhD studies so she had to put up with the stress all the way through. Thank you very much.

Publications, Presentations and Awards

Publications

1. **J. Baloyi**, T. Ntho, J. Moma, Synthesis and application of pillared clay heterogeneous catalysts for wastewater treatment: a review, RSC Adv. 8 (2018) 5197–5211. doi:10.1039/C7RA12924F.

2. **J. Baloyi**, T. Ntho, J. Moma, Synthesis of highly active and stable Al/Zr pillared clay as catalyst for catalytic wet oxidation of phenol, J. Porous Mater. (2018). doi:10.1007/s10934-018-0667-3.

3. J. Moma, **J. Baloyi**, T. Ntho, Synthesis and characterization of an efficient and stable Al/Fe pillared clay catalyst for the catalytic wet air oxidation of phenol, RSC Adv. 8 (2018) 30115–30124. doi:10.1039/C8RA05825C.

4. **Baloyi, J.**, Ntho, T., & Moma, J. (2018). A Novel Synthesis Method of Al/Cr Pillared Clay and its Application in the Catalytic Wet Air Oxidation of Phenol. Catalysis Letters, 148(12), 3655-3668.

5. **J. Baloyi**, T. Ntho, J. Moma. Influence of operational parameters and kinetic modelling of catalytic wet air oxidation of phenol by Al/Zr pillared clay catalyst. **Accepted for publication in Iranian Journal of Chemistry and Chemical Engineering (IJCCE).**

6. **J. Baloyi**, T. Ntho, J. Moma. Catalytic wet air oxidation of phenol by cordierite honeycomb washcoated with Al/Zr pillared bentonite. **Submitted for publications in Applied Catalysis B: Environmental.**

7. **J. Baloyi**, T.A Ntho and J. Moma. An Effective Pillared South African Bentonite Clay: Synthesis and Application as Green Chemistry Catalyst for Wastewater Treatment. Int'l Conference Proceeding: 9th International Conference on Advances in Science, Engineering, Technology and Waste Management (ASETWM17) November 27-28, 2017 Parys (South Africa) ***(First Prize)*.** Conference paper, ISBN: 978-81-934174-6-1.

Presentations

1. Title: An Effective Pillared South African Bentonite Clay: Synthesis and Application as Green Chemistry Catalyst for Wastewater Treatment. **Oral presentation**. Authors: Jeffrey Baloyi, T.A Ntho and J Moma. Conference: 9th International Conference on Advances in Science, Engineering, Technology and Waste Management (ASETWM17) November 27-28, 2017 Parys (South Africa) ***(First Prize)***. ISBN: 978-81-934174-6-1

2. Title: Pillared Bentonite Clay Washcoating into Cordierite Honeycomb Monolith Reactors for Application in Wastewater Treatment: Effect of Powder Characteristics. **Oral presentation**. Authors: **Jeffrey Baloyi**, T.A Ntho and J Moma. Conference: 9th International Conference on Research in Chemical, Agricultural, Biological and Environmental Sciences (RCABES-2017) November 27-28, 2017 Parys (South Africa). ISBN: 978-81-934174-6-1

3. Synthesis of low-cost Al/Zr pillared from South African natural clay: Application for catalytic wet air oxidation of phenol. **Oral presentation.** Authors: **Jeffrey Baloyi**, T.A Ntho and J Moma. Conference: Catalysis South Africa (CATSA17) November 19-23, 2017 Sun City (South Africa).

4. Title: Preparation of novel Al/Cr pillared clays catalyst for catalytic wet oxidation of phenol: effect of ultrasonic time. **Oral presentation.** Authors: **Jeffrey Baloyi**, T.A Ntho and J Moma. Conference: 8th World Congress on Oxidation Catalysis (WCOC17) September 3-8, 2017 Krakow (Poland). ISBN: 978-83-60514-27-6.

5. Title: Highly active and stable Al/Fe pillared South African bentonite clay: Synthesis, characterization and application for CWAO of phenol under mild conditions. **Poster presentation**. Authors: **Jeffrey Baloyi**, T.A Ntho and J Moma. Conference: 8th World Congress on Oxidation Catalysis (WCOC17) September 3-8, 2017 Krakow (Poland). ISBN: 978-83-60514-27-6.

6. Title: Effect of ultrasonic treatment time on the preparation of novel Al/Zr pillared clays as catalyst for catalytic wet oxidation of phenol. **Poster presentation**. Authors: **Jeffrey Baloyi**, T.A Ntho, J.A Moma, J. Kalala and E.T. Akinlabi. Conference: International Conference on Environment, Materials and Green Technology, Nov. 24-25, 2016 Sebokeng (South Africa). ISBN: 978-1-77012-141-6.

7. Title: High catalytic activity at low temperature in oxidation of phenol with South African pillared bentonite clay. **Poster presentation.** Authors: **Jeffrey Baloyi**, T.A Ntho and J Moma. Conference: 8th Wits Cross-Faculty Graduate Symposium, University of the Witwatersrand, Oct. 25-26, 2017 Johannesburg (South Africa).

Awards

1. **Session Best Paper and Best Oral presentation:** International Conference of Eminent Association of Pioneers (EAP), November 2017, Parys, South Africa.
2. **DST/NRF Professional Graduate Programme PhD Scholarship:** 2015-2018, Mintek.
3. **Postgraduate PhD Merit award:** 2016-2017, University of the Johannesburg.
4. **Postgraduate PhD Merit award:** 2017-2018, University of the Witwatersrand.
5. **PhD Researcher Travel Grant:** 8th World Congress on Oxidation Catalysis and XII European Workshop Meeting in Innovation in Selective Oxidation Catalysis 2017, Krakow, Poland.

Contents

Declaration i

Abstract ii

Dedication iv

Acknowledgement v

Publications, Presentations and Awards vii

Chapter 1 1

Introduction to pillared clays as catalysts for wastewater treatment 1

1. Background 2

1.1. Problem statement 5

1.2. Justification 7

1.3. Aim and objectives of the present work 7

1.4. Scope and structure of this thesis 8

Reference 10

Chapter 2 15

Literature review 15

Chapter 3 30

Synthesis and characterization of Al/Zr pillared clay catalyst 30

Chapter 4 46

Synthesis and characterization of an efficient and stable Al/Fe pillared clay catalyst 46

Chapter 5 57

A novel synthesis method of Al/Cr pillared clay catalysts 57

Chapter 6 72

Influence of operational parameters and kinetic modelling in a batch reactor 72

Chapter 7 98

Cordierite honeycomb washcoated with Al/Zr pillared bentonite catalyst: mechanistic studies, reaction pathway and kinetic modelling 98

Chapter 8 137

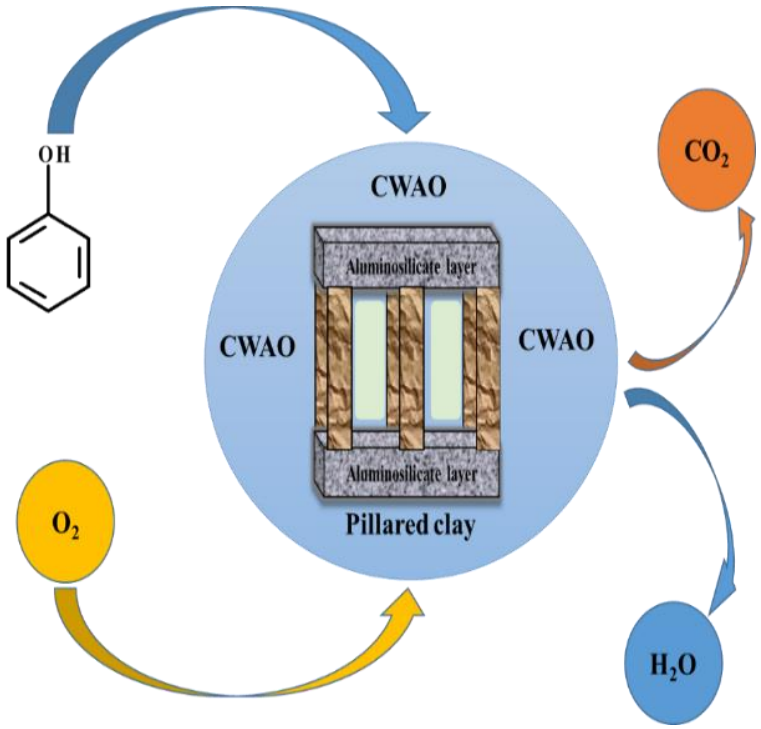
General conclusions and recommendations 137

APPENDICES 141

Supplementary materials 142

Chapter 1

Introduction to pillared clays as catalysts for wastewater treatment



1. Background

The basic human right of access to clean and safe water has been compromised by the rising global population, urbanization, and climate change as well as domestic, agricultural and environmental changes. Around the world, 780 million people do not have access to safe and clean drinking water for consumption [1]. It has been estimated that by 2025; about 3 billion people will be forced to survive under water scarcity as estimated by World Water Council [2]. Almost 1.1 billion people don't have facility to improve drinking water bodies throughout the world, and 2.6 billion are under sanitation [3]. Water scarcity can affect economic growth and human health, since this jeopardizes the industrial production and shrinks the availability of hygienic foods, and drinks [4]. Water scarcity is among the main problems to be faced by many societies and the World in the 21st century. Water scarcity is both a natural and a human made phenomenon. Therefore, continuous release of wastewater into the environment without treatment is causing growing concern to the whole world and is environmentally unacceptable.

Amongst the many organic contaminants that can be present in wastewaters, phenol is proved important because of the global demand for the industrial phenol market that has been increasing steadily over the last few years mainly because of the demand for its derivatives from the end-use segment. Phenol and phenolic substances are widely used in many industries and discharged in the wastewater from various industries, such as phenolic resin and pharmaceutical, oil refineries, petrochemical plants, ceramic plants, steel plants, coal conversion processes and pesticides manufacturing [5]. Moreover phenol is considered to be an intermediate product in the oxidation pathway of higher-molecular-weight aromatic hydrocarbons [6]. Many of the materials produced by the phenol industry are toxic and cannot be discharged without treatment. Typical concentrations of phenolic compounds in these industrial wastewaters are in the range of 200 to 1500 mg/L whilst the Environmental Protection Authority's limit for wastewater discharge are 0.5 mg/L for surface water and 1 mg/L for sewerage water [7]. In the past years, wastewater-containing phenol has received increased attention because of its extreme toxicity to the aquatic life and poor biodegradability [8-13]. Therefore, it is very important to eliminate these contaminants to environmentally harmless species before their discharge into water bodies.

The conventional processes for removal of phenols from industrial wastewaters include extraction, adsorption (e.g. using activated carbon), biological, chemical oxidation,

electrochemical techniques and irradiation etc. All of these methods suffer from serious shortcomings such as high costs, incompleteness of purification, formation of hazardous by-products, long time of the treatment, the large area of land, easily influenced by seasons, low efficiency and applicability to a limited concentration range [14, 15]. Therefore, there is urgent need to develop a safe and effective phenol wastewater treatment technique.

As a result, many studies over the past decade have focused on alternative treatment methods, which are direct and effective, for removal of phenols from wastewater. Advanced oxidation processes (AOPs) can be a useful option. Advanced oxidation processes include wet air oxidation (WAO), catalytic wet air oxidation (CWAO), H_2O_2-promoted catalytic wet air oxidation (H_2O_2-CWAO) and Fenton process [16]. The efficiency of AOPs results from the fact that the in-situ generated hydroxyl radicals ($^{\bullet}OH$) are highly reactive species (E^0 = +2.8V), which attack the majority of organic molecules causing their oxidation to other products and ultimately to CO_2 and H_2O [17, 18]. They are also characterized by low selectivity of attack, which is a useful attribute for an oxidant used in wastewater treatment and for solving pollution problems [19]. Contaminants are mainly oxidized through the use of four different reagents: ozone, hydrogen peroxide, oxygen, and air or their combination. To choose the most appropriate technology, some aspects such as the concentration and nature of the pollutants and the volume of wastewater must be considered.

In AOPs, CWAO is one of the promising methods for the oxidation of refractory compounds such as phenol using oxygen or air to CO_2 and H_2O, without emissions of toxic gases such as NOx, SO_2, HCl, dioxins, furans, fly ash, etc. [20]. The advantages of CWAO includes simultaneous treatment of total organic carbon (TOC), sulfur compounds and refractory organic compounds in one stage, low running costs (using robust catalysts), a compact plant design for low space requirements, stably continuous and automatic operation, the process is extremely clean since it does not involve the use of any harmful chemical reagents and no secondary contaminants formed [21, 22]. Moreover, the wastewater after CWAO treatment may be reused and steam from the oxidation reaction of the wastewater may be recycled into energy. The main drawbacks are high capital investment and high operating costs due to severe reaction conditions and the lack of stable and active catalysts, which prevent industrial commercialization. Therefore, various research efforts have been committed to reduce the harshness of the operating conditions through the development of robust solid catalysts [13, 23]. Guo et al. [23] reported that if stable solid catalysts can be developed that work

efficiently below 125 °C and 25 bar, CWAO would be a potential technology for the treatment of organic compounds in wastewater streams. The use of a novel class of heterogeneous pillared interlayered clays (PILCs) catalysts in CWAO has been proposed as a way to efficiently reduce the harshness of the reaction conditions, reduce reaction time and improve the oxidation rate of refractory organic contaminants [24]. Since clay minerals are natural, abundant, environmentally friendly and low cost these characteristics make pillared clays more suitable catalysts compared to other expensive noble metal based catalysts.

The present work focuses on the use of South African natural bentonite clay to obtain heterogeneous pillared clays catalysts for wastewater treatment. Natural clays have been widely used as ion exchangers, catalysts and adsorbents due to their local and abundant availability and the capability to undergo modification to enhance the surface area, adsorption capacity and range of application [25]. However, their lack of permanent high porosity limits their further application in industry. To solve this problem, bulky inorganic polycations obtained from polymerization of multivalent inorganic cations (e.g. Al^{3+}, Zr^{4+}, Cr^{3+}, Ti^{4+} and Fe^{3+}) are intercalated into the interlayer region of the clays by cation exchange. This is done because when the clays are dispersed in water, they swell significantly owing to the hydration of the interlamellar cations that act as counterions to balance the negative charges of the clay layers. Therefore, polycations in aqueous solutions can be intercalated into the interlayer gallery by cation exchange. The intercalated polycations increase the basal spacing of the clays, and upon heating in the calcination stage at a high temperature, the intercalated species undergo dehydration and dehydroxylation and hence are converted to temperature-stable oxide pillars, propping the clay layers apart and preventing its collapse. The final pillared clays present a two-dimensional porous network, showing a dramatic improvement in catalytic and adsorption applications [26, 27]. The final properties of pillared clays can be modulated by carefully choosing the different parameters, such as nature of the pillaring agent, type of clay and particle size, pillaring procedure and the thermal treatment, thus offering a very powerful flexible way to design tailored catalysts. Solids with very high surface areas, a broad spectrum of properties (structural, chemical and catalytic, etc), and controlled internal structures can be obtained by controlling the pillaring process.

However, conventional method involves prolonged periods of synthesis, high volumes of water and high energy costs. These conditions present major drawbacks in the scale up of the synthesis of pillared clays [28-31]. Therefore, the synthesis method has gained considerable

attention with many studies aimed at reducing synthesis time and energy costs by finding novel ways to economize the method for commercial feasibility. In an attempt to overcome these synthesis drawbacks, novel simplified synthesis methods for PILCs catalysts with single and mixed pillaring metals have been developed by the use of ultrasound [29, 32, 33], microwave [29, 33, 34] and one-step high-temperature high-pressure synthesis [28] during aging of the pillaring solution and interaction with the powdered raw natural clay. In addition, the use of the raw natural clay without further purification has been reported to reduce synthesis time [32] and the addition of a second pillaring metal such as Cr, Zr, Fe and Ti to the Al pillaring solution is also recommended, in order to improve the porosity, pore volume, specific surface area, thermal stability and acidity of mononuclear inorganic PILCs catalysts [35-41]. Moreover, the commercialization of PILCs catalysts is not only influenced by the optimization of preparation parameters but also by the ability to shape the powder material into conformed products such as monoliths or washcoating into monolith which aid in a separation of used catalysts from treated water. This study is focused on the design of novel pillared bentonite clay catalysts for phenol wastewater treatment by CWAO under mild reactions conditions.

1.1. Problem statement

The biggest challenges for the next generation are adequate supplies of fresh water and climate change. It has been reported by WHO, that more than 80 countries including South Africa accounting for 40% of the world's population are facing major water crises and about 1.2 billion people are already estimated to be drinking unclean water [42]. Moreover, more than 10 million people die annually due to various diseases caused by the consumption of polluted water. Therefore, treatment of wastewater for reuse to overcome scarcity of water has been a global challenge for many countries like South Africa as water scarce country. The rapid increase in the demand of clean water has attracted much of the attention of government organisations and water industries to develop robust, environmental friendly and cost effective technologies for wastewater treatment.

Currently, the various treatment methods that have been actively investigated to remove organic pollutants from wastewater are chemical, physical (adsorption, reserve osmosis, etc.), adsorption, biological, incineration, AOPs, etc. The selection of wastewater treatment process among these methods is very critical and has to be made considering the contaminants present

in wastewater in terms of toxicities and concentration of the pollutants in the wastewater stream. Chemical and petroleum industries generate a wide variety of highly toxic organic wastes. Among organic pollutants, phenol and phenol derivates, used as raw materials in petrochemical, chemical and pharmaceutical industries, have received increased attention in the last years due to their toxicity. This situation is mainly due to phenol's high solubility in water. These phenols when discharged into the environment end up in surface waters like lakes and rivers, as well as underground water and as a result contaminate them. Due to high toxicity of phenol, it is important to treat wastewater containing phenols to bring their concentrations to levels prescribed by law before they are discharged into the water bodies.

Of the above listed methods, the most favoured treatment method for phenol removal is the AOPs such as CWAO. However, this method has not seen wide scale industrial application due largely to the high cost of operation involved emanating from severity of the reaction conditions [18]. Although the use of biological treatment is generally cheaper than all the methods known, it fails when the phenol concentration in the wastewater is higher than 200 mg/L [43]. Pauli and Franke, [44] and Katzer et al. [45] reported this limit at 50 and 70 mg/L, respectively. In many cases all the above limits are exceeded in most of the actual wastewater streams. Moreover, biodegradation processes are inherently slow and do not allow for high degrees of removal and sludge is still major factors of environmental pollution [46]. The CWAO is very attractive for treating wastewaters that are too toxic for biological technology to be treated and too dilute for incineration to be eliminated. The heterogeneous CWAO has gained some attention as the addition of catalysts decreases the severe operating conditions, enhances the reaction rate, and shortens the reaction time and remarkable economy-scale advantages [22, 23, 46, 47]. Therefore, further research on the discovery of solids heterogeneous catalysts that are robust, cheap, and efficient solid catalysts, ensuring the total oxidation of refractory organic compounds to water, carbon dioxide and less toxic biogradable compounds, at mild reaction conditions is a big scientific and technological concern worldwide. Gitari et al. [48] reported that South Africa has large deposits of bentonite clay that is likely to be extracted in the next 60 years, if the demand does not increase.

This research study is aimed at the design of pillared bentonite clay as "green chemistry" catalysts using South African bentonite clay and suitability of pillared clays for the treatment of refractory organic wastewater containing phenol by using CWAO process. In this study the severity of oxidation conditions can be reduced by the use of a suitable (cheap, stable,

environmental friendly and resistant to poisoning) solids catalyst. Not only can the treatment use milder conditions (temperature and pressure), but, in principle, the designed catalyst can also be easily recovered, regenerated, and reused without significant catalyst leaching and deactivation.

1.2. Justification

The incapability of conventional methods to effectively remove refractory organic wastewater such as phenol has made it evident that new, compact and more efficient systems are needed. The AOPs such as CWAO seems to be better economically and technologically feasible for treating the highly toxic organic wastewater [46, 49-51]. Using CWAO, the reaction is operated at mild conditions, the reaction time is shortened, and much higher oxidation rate is achieved. In this respect, the presence of environmental catalyst in CWAO performs an essential role in minimizing the release of toxic compounds and the development of energy saving, residue-free processes. The design of new effective suitable and inexpensive catalytic materials is one of the main challenges to achieve this goal [52].

Therefore, the application of pillared bentonite clay as heterogeneous catalysts offers a variety of potential advantages in CWAO wastewater treatment technology, from both the sustainable green chemistry and engineering point of view. The preparation of PILCs as novel heterogeneous catalysts and its application in CWAO is still in its developmental stage, efficient evaluation of this novel technology requires deep understanding of PILCs catalyst design. Several research studies have been reported on the preparation and characterization of PILCs and CWAO removal of refractory organic wastewater using PILCs. None has been recorded on the CWAO removal of refractory organic wastewater using South African bentonite clay minerals in the preparation of PILCs. Moreover, no commercialised preparation process has been reported in the literature. To the best of our knowledge, this is the first study that investigates the CWAO of phenol by PILCs using South African natural bentonite clay as starting material. Hence, it was decided to embark on this study.

1.3. Aim and objectives of the present work

The **main objective** of this research is to apply pillared clay catalysts prepared from natural bentonite clay for treatment of phenol in aqueous solution by CWAO.

In order to achieve the research objective, the **specific objectives** of this study are:-

a. To prepare and characterize heterogeneous pillared clay catalysts from naturally occurring South African bentonite clay mineral.
b. To evaluate the activity, stability and regeneration of pillared clay catalysts for use in catalytic wet oxidation of phenol wastewater.
c. To investigate the effect of operational parameters such as reaction temperature, initial pH, initial phenol concentration, catalyst dosage and oxygen partial pressure.
d. To washcoat cordierite honeycomb monolith with pillared clay powder catalyst.
e. To study the mechanistic studies as well as kinetic modelling.
f. To design and construct a monolith reactor and process instrumentation diagrams for the reactions.

1.4. Scope and structure of this thesis

The current study is primarily focused on the development of a pillared clay catalysts for CWAO of phenol in aqueous solution, which will include a cordierite monolithic support structure carrying a catalyst. This development will consist of the aim and specific objectives listed above, and will be limited to the catalytic materials developments and catalytic activity testing in both batch and trickle bed monolithic reactors, putting aside the comprehensive engineering reactor simulations.

The thesis contents are structured as outlined below.

In **Chapter 1,** a detailed background, problem statement, justification for the study, main and specific objectives of the research are covered.

In **Chapter 2**, detailed literature review about preparation of pillared clays, water pollution by refractory organic compounds and advanced oxidation processes based on the previous and recent work relating to this study is explained. This chapter has been published as; **J. Baloyi**, T. Ntho, J. Moma, Synthesis and application of pillared clay heterogeneous catalysts for wastewater treatment: a review, RSC Adv. 8 (2018) 5197–5211. doi:10.1039/C7RA12924F.

In **Chapter 3,** synthesis, characterization and CWAO application of Al/Zr pillared clay catalyst is presented. This chapter has been published as; **J. Baloyi**, T. Ntho, J. Moma, Synthesis of highly active and stable Al/Zr pillared clay as catalyst for catalytic wet oxidation of phenol, J. Porous Mater. (2018). doi:10.1007/s10934-018-0667-3. The published paper fully fulfilled the specific objectives a and b.

In **Chapter 4,** synthesis, characterization and CWAO application of Al/Fe pillared clay catalyst is presented. This chapter has been published as; J. Moma, **J. Baloyi**, T. Ntho, Synthesis and characterization of an efficient and stable Al/Fe pillared clay catalyst for the catalytic wet air oxidation of phenol, RSC Adv. 8 (2018) 30115–30124. doi:10.1039/C8RA05825C. The published paper fully fulfilled the specific objectives a and b.

In **Chapter 5,** synthesis, characterization and CWAO application of Al/Cr pillared clay catalyst is presented. This chapter has been published as; **Baloyi, J**., Ntho, T., & Moma, J. (2018). A Novel Synthesis Method of Al/Cr Pillared Clay and its Application in the Catalytic Wet Air Oxidation of Phenol. *Catalysis Letters*, *148*(12), 3655-3668. The published paper fully fulfilled the specific objectives a and b.

In **Chapter 6,** influence of operational parameters and kinetic modelling of catalytic wet air oxidation of phenol is presented. This chapter has been accepted for publication in Iranian Journal of Chemistry and Chemical Engineering (IJCCE) as; **J. Baloyi**, T. Ntho, J. Moma. Influence of operational parameters and kinetic modelling of catalytic wet air oxidation of phenol by Al/Zr pillared clay catalyst. This paper addresses objectives c and e.

Chapter 7 presents wash coating of cordierite honeycomb with Al/Zr pillared bentonite for CWAO of phenol with the design of monolithic plug flow reactor. This chapter is submitted for publication in Applied Catalysis B: Environmental as; **J. Baloyi**, T. Ntho, J. Moma. Catalytic wet air oxidation of phenol by cordierite honeycomb washcoated with Al/Zr pillared bentonite. This paper addresses objectives d, e and f.

Finally in **Chapter 8** general conclusions are summarized and recommendations for future studies are presented.

Reference

[1] C. Sealy, Cleaning up water on the nanoscale, Nano Today, 8 (2013) 337-338.

[2] U. Urgency, Water Caucus Summary, World Water Council (WWC), Marseille, France, (2007).

[3] O. World Health, Persistent organic pollutants: impact on child health, (2010).

[4] M. Kaufmann, K. Melia-Teevan, Turning the Tides of Crisis, 2009 (access date 02/03/2018).

[5] Z. Liu, H. Meng, H. Zhang, J. Cao, K. Zhou, J. Lian, Highly efficient degradation of phenol wastewater by microwave induced H2O2-CuOx/GAC catalytic oxidation process, Separation and Purification Technology, 193 (2018) 49-57.

[6] H. Ejhed, J. Fång, K. Hansen, L. Graae, M. Rahmberg, J. Magnér, E. Dorgeloh, G. Plaza, The effect of hydraulic retention time in onsite wastewater treatment and removal of pharmaceuticals, hormones and phenolic utility substances, Science of The Total Environment, 618 (2018) 250-261.

[7] E.S.Z. El-Ashtoukhy, Y.A. El-Taweel, O. Abdelwahab, E.M. Nassef, Treatment of petrochemical wastewater containing phenolic compounds by electrocoagulation using a fixed bed electrochemical reactor, Int. J. Electrochem. Sci, 8 (2013) 1534-1550.

[8] E. Guélou, J. Barrault, J. Fournier, J.-M. Tatibouët, Active iron species in the catalytic wet peroxide oxidation of phenol over pillared clays containing iron, Applied Catalysis B: Environmental, 44 (2003) 1-8.

[9] A. Eftaxias, J. Font, A. Fortuny, A. Fabregat, F. Stüber, Catalytic wet air oxidation of phenol over active carbon catalyst: global kinetic modelling using simulated annealing, Applied Catalysis B: Environmental, 67 (2006) 12-23.

[10] M. Ahmaruzzaman, D.K. Sharma, Adsorption of phenols from wastewater, Journal of colloid and interface science, 287 (2005) 14-24.

[11] D. Fu, F. Zhang, L. Wang, F. Yang, X. Liang, Simultaneous removal of nitrobenzene and phenol by homogenous catalytic wet air oxidation, Chinese Journal of Catalysis, 36 (2015) 952-956.

[12] A.M. Khaksar, S. Nazif, A. Taebi, E. Shahghasemi, Treatment of phenol in petrochemical wastewater considering turbidity factor by backlight cascade photocatalytic reactor, Journal of Photochemistry and Photobiology A: Chemistry, 348 (2017) 161-167.

[13] H. Sassi, G. Lafaye, H.B. Amor, A. Gannouni, M.R. Jeday, J. Barbier, Wastewater treatment by catalytic wet air oxidation process over Al-Fe pillared clays synthesized using microwave irradiation, Frontiers of Environmental Science & Engineering, 12 (2018) 2.
[14] A. Babuponnusami, K. Muthukumar, A review on Fenton and improvements to the Fenton process for wastewater treatment, Journal of Environmental Chemical Engineering, 2 (2014) 557-572.
[15] H. Wei, X. Yan, S. He, C. Sun, Catalytic wet air oxidation of pentachlorophenol over Ru/ZrO_2 and $Ru/ZrSiO_2$ catalysts, Catalysis Today, 201 (2013) 49-56.
[16] A. Rubalcaba, M.E. Suárez-Ojeda, F. Stüber, A. Fortuny, C. Bengoa, I. Metcalfe, J. Font, J. Carrera, A. Fabregat, Phenol wastewater remediation: advanced oxidation processes coupled to a biological treatment, Water science and technology, 55 (2007) 221-227.
[17] J. Carriazo, E. Guelou, J. Barrault, J.M. Tatibouët, R. Molina, S. Moreno, Synthesis of pillared clays containing Al, Al–Fe or Al–Ce–Fe from a bentonite: characterization and catalytic activity., Catal. Today, 107-108 (2005) 126-132.
[18] J. Baloyi, T. Ntho, J. Moma, Synthesis and application of pillared clay heterogeneous catalysts for wastewater treatment: a review, RSC Advances, 8 (2018) 5197-5211.
[19] S. Malato, J. Blanco, A. Vidal, C. Richter, Photocatalysis with solar energy at a pilot-plant scale: an overview, Applied Catalysis B: Environmental, 37 (2002) 1-15.
[20] G. Yang, H. Chen, H. Qin, X. Zhang, Y. Feng, Effect of nitrogen doping on the catalytic activity of activated carbon and distribution of oxidation products in catalytic wet oxidation of phenol, The Canadian Journal of Chemical Engineering, (2017) n/a-n/a.
[21] F. Arena, R. Di Chio, C. Espro, A. Palella, L. Spadaro, Catalytic Wet Air Oxidation (CWAO) of Industrial Wastewaters: Mechanistic Evidences, Catalyst Development and Kinetic Modeling, in, Springer, pp. 349-353.
[22] K.-H. Kim, S.-K. Ihm, Heterogeneous catalytic wet air oxidation of refractory organic pollutants in industrial wastewaters: a review, Journal of hazardous materials, 186 (2011) 16-34.
[23] J. Guo, M. Al-Dahhan, Activity and stability of iron-containing pillared clay catalysts for wet air oxidation of phenol, Applied Catalysis A: General, 299 (2006) 175-184.
[24] J. Guo, M. Al-Dahhan, Catalytic Wet Oxidation of Phenol by Hydrogen Peroxide over Pillared Clay Catalyst, Industrial & Engineering Chemistry Research, 42 (2003) 2450-2460.
[25] C.B. Molina, J.A. Casas, A.H. Pizarro, J.J. Rodriguez, Pillared clays as green chemistry catalysts: application to wastewater treatment, Clay: Types, Properties and Uses, (2011) 435-474.

[26] L.A. Galeano, H.J. Muñoz, A.M. García, A. Gil, M.Á. Vicente, Development of Mn or Fe sulfides in the interlayer space of raw and Al-pillared bentonite, Applied clay science, 157 (2018) 31-40.
[27] T.J. Pinnavaia, M.S. Tzou, S.D. Landau, New chromia pillared clay catalysts, Journal of the American Chemical Society, 107 (1985) 4783-4785.
[28] M. Ding, S. Zuo, C. Qi, Preparation and characterization of novel composite AlCr-pillared clays and preliminary investigation for benzene adsorption, Applied Clay Science, 115 (2015) 9-16.
[29] A. Olaya, S. Moreno, R. Molina, Synthesis of pillared clays with Al 13-Fe and Al 13-Fe-Ce polymers in solid state assisted by microwave and ultrasound: Characterization and catalytic activity, Applied Catalysis A: General, 370 (2009) 7-15.
[30] J.T. Kloprogge, L.V. Duong, R.L. Frost, A review of the synthesis and characterisation of pillared clays and related porous materials for cracking of vegetable oils to produce biofuels, Environmental Geology, 47 (2005) 967-981.
[31] M.A. Vicente, A. Gil, F. Bergaya, Pillared clays and clay minerals, Handbook of Clay Science, 5 (2013) 524.
[32] F. Tomul, The effect of ultrasonic treatment on iron–chromium pillared bentonite synthesis and catalytic wet peroxide oxidation of phenol, Applied Clay Science, 120 (2016) 121-134.
[33] V. Singh, V. Sapehiyia, G.L. Kad, Ultrasound and microwave activated preparation of ZrO 2-pillared clay composite: catalytic activity for selective, solventless acylation of 1, n-diols, Journal of Molecular Catalysis A: Chemical, 210 (2004) 119-124.
[34] G. Fetter, P. Bosch, Microwave effect on clay pillaring, in: Pillared Clays and Related Catalysts, Springer, 2010, pp. 1-21.
[35] Z.U.O. Shufeng, Z. Renxian, Q.I. Chenze, Synthesis and characterization of aluminum and Al/REE pillared clays and supported palladium catalysts for benzene oxidation, Journal of Rare Earths, 29 (2011) 52-57.
[36] C.B. Molina, J.A. Casas, J.A. Zazo, J.J. Rodríguez, A comparison of Al-Fe and Zr-Fe pillared clays for catalytic wet peroxide oxidation, Chemical Engineering Journal, 118 (2006) 29-35.
[37] J.G. Carriazo, E. Guelou, J. Barrault, J.M. Tatibouët, S. Moreno, Catalytic wet peroxide oxidation of phenol over Al–Cu or Al–Fe modified clays, Applied Clay Science, 22 (2003) 303-308.

[38] J.M. Oades, Interactions of polycations of aluminum and iron with clays, Clays Clay Miner, 32 (1984) 49-57.
[39] M.L. Occelli, New routes to the preparation of pillared montmorillonite catalysts, Journal of Molecular Catalysis, 35 (1986) 377-389.
[40] J.G. Carriazo, M.A. Centeno, J.A. Odriozola, S. Moreno, R. Molina, Effect of Fe and Ce on Al-pillared bentonite and their performance in catalytic oxidation reactions, Applied Catalysis A: General, 317 (2007) 120-128.
[41] W.Y. Lee, R.H. Raythatha, B.J. Tatarchuk, Pillared-clay catalysts containing mixed-metal complexes: I. Preparation and characterization, Journal of Catalysis, 115 (1989) 159-179.
[42] F.R. Rijsberman, Water scarcity: fact or fiction?, Agricultural water management, 80 (2006) 5-22.
[43] B.B. Pruden, H. Le, Wet air oxidation of soluble components in waste water, The Canadian Journal of Chemical Engineering, 54 (1976) 319-325.
[44] O. Pauli, G. Franke, Behaviour and degradation of technical preservatives in the biological purification of sewage, Biodeterioration of Materials, 2 (1972) 52.
[45] J.R. Katzer, H.H. Ficke, A. Sadana, An evaluation of aqueous phase catalytic oxidation, Journal (Water Pollution Control Federation), (1976) 920-933.
[46] F. Arena, R. Di Chio, B. Gumina, L. Spadaro, G. Trunfio, Recent advances on wet air oxidation catalysts for treatment of industrial wastewaters, Inorganica Chimica Acta, 431 (2015) 101-109.
[47] A. Cybulski, Catalytic wet air oxidation: are monolithic catalysts and reactors feasible?, Industrial & Engineering Chemistry Research, 46 (2007) 4007-4033.
[48] W.M. Gitari, Attenuation of metal species in acidic solutions using bentonite clay: implications for acid mine drainage remediation, Toxicological & Environmental Chemistry, 96 (2014) 201-217.
[49] A. Quintanilla, J.A. Casas, A.F. Mohedano, J.J. Rodríguez, Reaction pathway of the catalytic wet air oxidation of phenol with a Fe/activated carbon catalyst, Applied Catalysis B: Environmental, 67 (2006) 206-216.
[50] J. Levec, A. Pintar, Catalytic wet-air oxidation processes: a review, Catalysis Today, 124 (2007) 172-184.
[51] J. Fu, G.Z. Kyzas, Wet air oxidation for the decolorization of dye wastewater: An overview of the last two decades, Chinese Journal of Catalysis, 35 (2014) 1-7.

[52] F. Arena, C. Italiano, L. Spadaro, Efficiency and reactivity pattern of ceria-based noble metal and transition metal-oxide catalysts in the wet air oxidation of phenol, Applied Catalysis B: Environmental, 115 (2012) 336-345.

Chapter 2

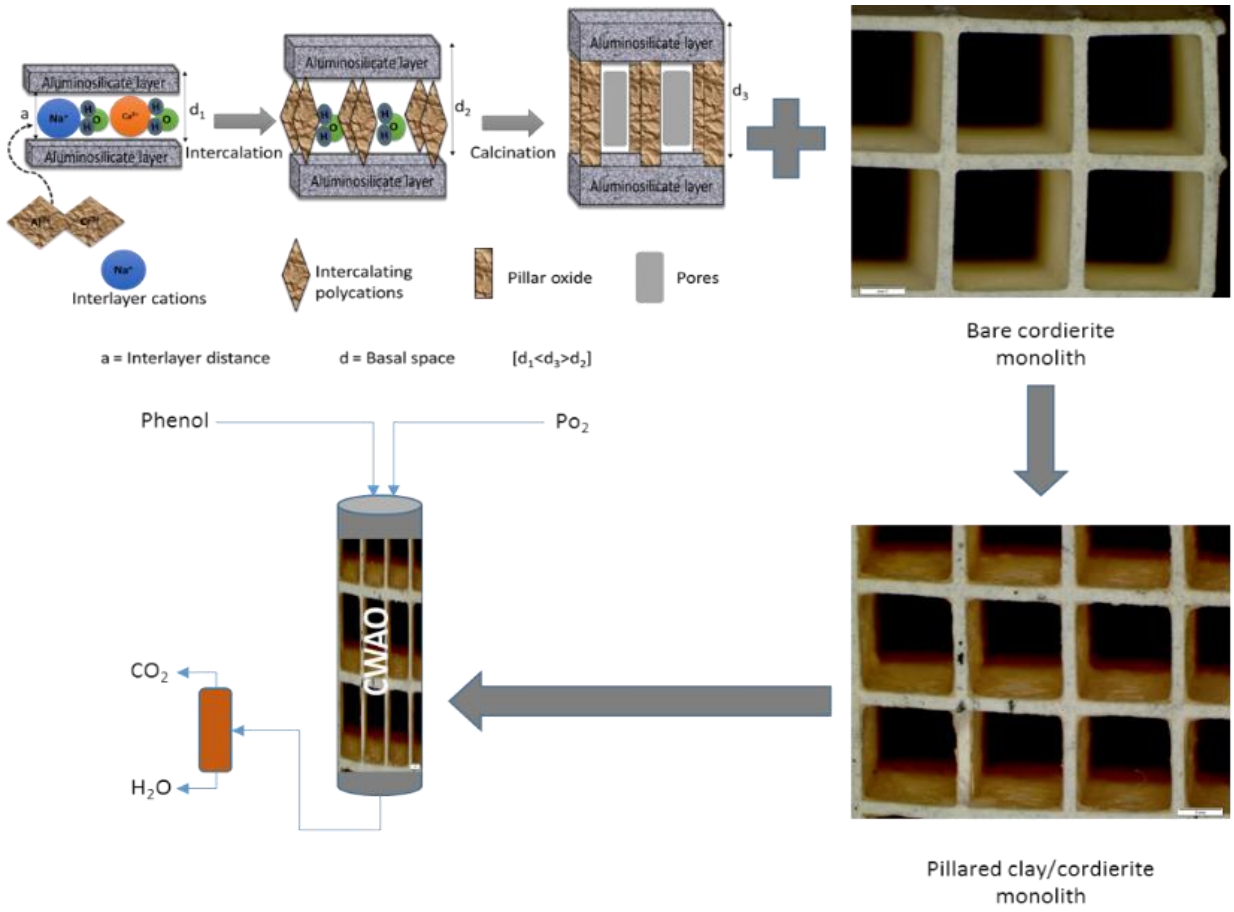
Literature review

This chapter has been published as **J. Baloyi,** T. Ntho, J. Moma, Synthesis and application of pillared clay heterogeneous catalysts for wastewater treatment: a review, RSC Adv. 8 (2018) 5197–5211. doi:10.1039/C7RA12924F.

J. Baloyi – 70% (conducted the research, wrote the first draft and addressed the reviewers comments);

T. Ntho – 15% (industrial (Mintek) supervisor, oversees the handling of experiments and obtained results);

J. Moma – 15% (academic (Wits) supervisor, reviewed the manuscript and approved the revised manuscript).



RSC Advances

REVIEW



Cite this: *RSC Adv.*, 2018, **8**, 5197

Synthesis and application of pillared clay heterogeneous catalysts for wastewater treatment: a review

Jeffrey Baloyi,[ab] Thabang Ntho[b] and John Moma[*a]

Received 30th November 2017
Accepted 23rd January 2018

DOI: 10.1039/c7ra12924f

rsc.li/rsc-advances

The use of pillared interlayered clays (PILCs) as heterogenous catalysts in wastewater treatment technologies, particularly advanced oxidation processes (AOPs), is gaining popularity for the treatment of refractory wastewater effluents. The recent literature involving these solid materials is reviewed, with more focus on studies that aim at reducing the synthesis costs and escalating the synthesis process to industrial scale. Their role as active solid materials in the AOPs such as photocatalysis, catalytic wet peroxide oxidation (CWPO), the Fenton process and catalytic wet air oxidation (CWAO) of refractory organic compounds in polluted aqueous streams is also reviewed. These processes are evaluated to evidence their main direction for future research, particularly with reference to possible industrial use of these technologies to treat refractory organic wastewater using pillared clay-based catalysts. The pillared clay catalysts demonstrate good application prospects for the removal of refractory wastewater effluents using AOP technology. The reviewed studies suggest that the photocatalytic process is useful in low concentrations of these compounds, while CWPO, the Fenton process and CWAO are recommended for higher concentrations. However, catalyst development to reduce the severity of oxidation reaction conditions, with focus on the low cost, catalyst stability, reusability and environmental friendliness are the key aspects to be addressed by future research work.

1. Introduction

The use of green chemistry and green engineering intimates the design of chemical products, processes that reduce or eliminate the use or generation of hazardous substances from all sources and overall cost minimization.[1] Moreover, the minimization of toxicity and hazards as well as the maximization of safety practices are important considerations. When these terms are applied to the performances of individual chemical reactions, chemical processes, and chemical synthesis plants, they deal with the same issues. Advances in both green chemistry and green engineering address the presence of toxic substances in the environment, hazards associated with global issues such as climate change, energy demands, global warming, availability of a safe and adequate water supply and interest in sustainability. These concepts have then become very popular. In recent years there has been an increasing interest in the use of pillared clays minerals, also called pillared interlayered clays (PILCs), as green heterogeneous catalysts in the wastewater treatment.[2–4]

Applications of clay minerals have attracted a lot of interest due to their potential use in heterogeneous catalysis.[5,6] However, clay minerals inherently have the shortcoming of poor access to their active sites which decreases their performance for catalytic reactions. Nevertheless, modification of natural clay minerals by pillaring using suitable pillaring agents has emerged as a promising technique because it allows for opening of the clay layers, producing high resistance and thermal stability, increased porosity, surface area and basal spacing as well as other physicochemical characteristics.[7,8] The pillaring method is based on a mechanism of cationic exchange in which robust inorganic molecules are introduced in the interlayer space of the clay minerals forming oxides strongly bound to layers of the minerals.[9] The hydroxyl polycations of polynuclear metals, such as Al, Fe, Zr, Cr and Ti, are types of inorganic pillaring agents that have been widely studied. Numerous studies have discussed these solid materials in details and are cited in the literature.[10,11] Incorporation of a second pillaring agent (*e.g.*, M = Zr, Fe, Cr and Ti) in the Al inorganic agents to create mixed oxide PILCs have emerged.[11,12] The general preparation process of mixed oxides pillaring agents (*e.g.* Al/M) is similar to the preparation of a single metal oxide agent, except that the base solution (*e.g.* NaOH or Na_2CO_3) is titrated into the $Al(NO_3)_3$ and M pillaring agent solutions with different Al/M molar ratios. Incorporation of a second metal oxide is reported to further improve the structure by increasing the pore volume and specific surface area (200–300 $m^2\ g^{-1}$), thermal stability and acidity of the catalyst compared to single metal oxide PILCs.

The conventional preparation of PILCs consists of two important stages: the preparation of the metal oxide pillaring

[a]*Molecular Science Institute, School of Chemistry, University of the Witwatersrand, P/Bag 3, WITS 2050, Johannesburg, South Africa. E-mail: john.moma@wits.ac.za*
[b]*Advanced Materials Division, Mintek, Private Bag X3015, Randburg 2125, South Africa*

This journal is © The Royal Society of Chemistry 2018

agent in solution and the mixing of pillaring agent with a suspension (typical 2% in weight) of clay in water.[13] This method involves long periods of time and large amount of water, and such requirements represent a considerable shortcoming when trying to scale-up the pillaring method to industrial scale.[14] Therefore, the use of PILCs as heterogeneous solids catalysts has not been escalated to commercial levels, due to the fact that it has been challenging to perform the conventional laboratory synthesis method at industrial scale.[15] In order to reduce the large volume of water required, currently the pillaring method is focused on application of concentrated clay suspension, dry clay and concentrated pillaring agent solution.[4] Similarly, direct addition of clay to pillaring solutions decreases the time required for the preparation process and methods such as ultrasound,[4] microwave[16] and one-step high-temperature synthesis[10] have recently emerged as a powerful and green approaches for synthesis of PILCs. All these methods, obtain solid materials with comparable characteristics to those of the solid materials synthesized by means of the conventional method, however, within shorter time for the process. Moreover, several studies reported that when using the conventional method, the aging time may vary by hours or days (1–5 days) depending on the pillars.[17–19] With ultrasound, microwave and one-step high-temperature synthesis methods, the aging and ion exchange process occur in minutes (5–30 minutes), therefore facilitating its extension to an industrial scale. However, commercialization of PILCs catalysts is not only influenced by the optimization of preparation parameters but also by the ability to shape the powder material into conformed products such as pellets, monoliths and agglomerates, *etc.* The prepared catalytic solids materials are expected to keep their chemical properties and catalytic activity as well as maintain their stability during the reaction process. Mohino *et al.*[20] and Sanabria *et al.*[21] used the extrusion method to manufacture raschig rings, pellets and monoliths that involve pillared bentonite clay minerals. Numerous studies available in literature on the manufacture of extrudates are related to ceramic monoliths such as sepiolite, cordierite, mullite, zirconia, titania, α- and γ-alumina and mixture of these materials.[22,23] However, few studies have been reported relating to fabrication of extrudates based on pillared clay catalysts, which remains an important aspect for PILCs to be used at an industrial scale level.[21] Therefore, there is a great need for creative strategies which should enable PILCs to be engineered to "designer catalysts" for applications in green, eco-friendly and sustainable wastewater treatment processes. Wastewater contaminated by phenol and its derivatives is one of the most common and essential representatives of refractory organic wastewater produced by industrial methods such as petrochemical, paper, paint, fabric and chemical industries, because of its high toxicity even at low concentrations. Phenol is listed as a primary pollutant by WHO (World Health Organisation). It is considered toxic at concentration above 2 mg L^{-1}, and when it is present in natural water streams it can lead to the formation of harmful chlorine solutions during disinfection by chlorination.[24] Typical concentrations of phenolic compounds in these industrial wastewaters are in the range of 200–1500 mg L^{-1} whilst the Environmental Protection Authority's limit for wastewater disposal discharge is 0.5 mg L^{-1} for surface water and 1 mg L^{-1} for sewerage water.[25] In the past years, wastewater containing phenol has received increased attention because of its extreme toxicity to aquatic life and resistance to biodegradation.[24,26] Consequently, with regards to human health and the environment, it is crucial to purify water contaminated with phenol and its derivatives, which can be present in almost all industrial wastewater streams.

Conventional processes for removal of phenol from industrial wastewaters include biological, adsorption, extraction, chemical oxidation, electrochemical methods and irradiation *etc.* The above mentioned methods suffer from serious shortcomings such as high costs, incompleteness of purification, formation of hazardous by-products, low efficiency and applicability to a limited concentration range (these methods are not suitable for treating moderate to high concentration organic pollutants such as phenol).[27,28] Therefore, it is of great importance to find innovative and simple methods and approaches to tackle environmental problems associated with wastewater contaminated by phenol. The use of advanced oxidation processes (AOPs) in the presence of PILCs to treat environmental contamination by refractory organic wastewater containing phenol is one of the most promising methods that have received increased attention in recent years.[4,21,29] AOPs, especially using PILCs catalysts as cheap natural materials are able to remove organic contaminants from aqueous effluents without high costs and complex technical requirements. Catalytic wet air oxidation (CWAO), catalytic wet peroxide oxidation (CWPO), Fenton-like process and photocatalytic treatment of wastewater are some of the successful AOPs processes, utilising catalysis for the removal of pollutants in industrial wastewater in the presence of an active catalyst.[30] AOPs are all based on the high reactivity together with low selectivity of attack displayed by hydroxyl radicals ($HO^{\bullet}$). AOPs may achieve full mineralization of most of the refractory organic contaminants to CO_2 and H_2O, or at least partial degradation of the substrates releasing less harmful by-products.[28] Therefore, these processes play crucial roles as green engineering processes in the wastewater treatment of moderate to high concentration of organic contaminants such as refractory organic pollutants.

In this context, this article aims at undertaking a systematic review of heterogeneous pillared clay catalysts syntheses processes based on recent and previous studies. The green route syntheses, modification and applications of the pillared clays catalysts in AOPs have been discussed in detail. The synthesis and application of pillared clay catalysts for refractory organic wastewater treatment will be reviewed with focus on aspects that have not yet been comprehensively reviewed such as a new insight into understanding the role of new robust sustainable green synthesis methods and their eco-friendly approach towards commercialization.

2. Synthesis of pillared interlayered clays (PILCs)

Pillared inter-layered clays (PILCs) are an imperative group of microporous inorganic solids with great catalytic potential for

This journal is © The Royal Society of Chemistry 2018

applications in catalytic processes.[31] PILCs have attracted increasing attention, particularly from industry, due to their microporous nature and wide range of applications such as catalytic oxidation, hydrogenation, dehydrogenation, hydroxylation, esterification, catalytic cracking, and others.[13] All of the above-mentioned reactions are potentially interesting in general green engineering industrial methods and green chemistry techniques.

The phenomenon used in the synthesis of pillared clays is the ion exchange of interlamellar cations by bulky cationic species that act as supports to keep the structure open. It is well known that only swelling clay minerals that are capable of cation exchange such as smectite group (bentonite) can be pillared. The first step in the pillaring of PILCs involves the synthesis of the pillaring agent. In this step the pillaring solution undergoes hydrolysis, polymerization and complexation with the anion in the solution.[32] The hydrolysis conditions such as temperature, pH and aging time, play an important role in the formation of PILCs. In the case of Al^{3+} polyoxocation, a base (NaOH or Na_2CO_3) is added to $AlCl_3$ or $Al(NO_3)_3$ solutions with OH/Al^{3+} ratios up to 2.5. Kloprogge[17] analyzed the polyoxocation complex produced during the process and is thought to be the Keggin ion $[AlO_4Al_{12}(OH)_{24}(H_2O)_{12}]^{7+}$. The conventional process involves prolonged times and this makes the pillaring process not applicable in an industrial scale. This stage of the synthesis process has gained considerable attention with many studies aimed to reduce time and energy costs by finding ways to economize the process for commercial feasibility. Martinez-Ortiz *et al.*,[33] Olaya *et al.*[12] and Sivaiah *et al.*[34] used microwave radiation during the synthesis of pillaring solution with a reduction in the synthesis time needed from several hours to less than 30 minutes. Tomul[4] recently investigated the use of ultrasound treatment during the preparation of iron–chromium pillaring solution. The Fe/Cr pillaring solutions was aged for less than 20 minutes compared to hours or days required when conventional method is used. The characteristics and catalytic behavior of the resulting pillared solids confirmed the beneficial effect of using ultra sound treatment.

The synthesis of the pillaring agent is followed by slow addition of the polyoxocation pillaring solution to the clay suspension. This allows the interlayer inorganic cations in the clay to exchange with the polyoxocation in solution through intercalation.[6] This results in up to five times increase in basal spacing (d_{001}) of the clay mineral, which is generally determined by XRD. When the conventional method is used, this process can take up to hours or days to complete depending on the pillars, as the pillaring solution is added drop-wise and the mixture is stirred for at least hours with heat supplied.[10,15,35–37] Although this method has been successful in laboratory synthesis of pillared clays, it is not an ideal method for industrial scale production because of the large amounts of water and heat required. However, using an ultrasound or a microwave treatment method, the ion exchange occurs in minutes. Duong *et al.*[38] studied the intercalation of montmorillonite and found ultrasonic treatment to reduce the intercalation time from several hours with the conventional method to less than 20 minutes. They however found prolonged ultrasonic treatment to result in partial destruction of the pillared structure. The obtained solids were comparable in physical and catalytic properties to that from the conventional method. Most importantly, no heat was needed in the pillaring process, with the added advantages of cost saving and minimal safety risks. Lastly, the amount of water used and space were minimized by use of a more concentrated clay suspension compared to conventional method. Therefore, the synthesis of PILCs on a commercial scale can be attained since the intercalation of the pillaring complexes can be achieved within a short period of time without losing catalytic activity. Numerous studies also concluded that ultrasound treatment method can enhance and promote dispersion of the active metal on the carrier, therefore, improving the catalytic performance of the pillared clay catalysts.[12,19,39,40]

The application of microwave radiation has also been reported to reduce the time of the synthesis during intercalation stage. Olaya *et al.*[12] reported the synthesis of Al pillared clay catalyst using a concentrated suspension of the pillaring solution and the clay with microwave radiation. It was found that the solids synthesized using microwave irradiation exhibited better characteristics than those of solids synthesized by the conventional method. They concluded that the synthesis of Al pillared clays using concentrated suspensions of clay and microwave provided advantages at the industrial level compared with the conventional method. This can be attributed to the fact that it decreases the time and volume of water required in the process, and also generates solids with high catalytic activity. A number of studies also reported PILCs materials synthesized using microwave irradiation with characteristics that can be matched with those of PILCs materials synthesized by means of the conventional methods.[15,36,41,42]

Another problem which hinders the commercialization of PILCs at industrial scale is that the clay dispersion is diluted by the use of high volumes of water during the synthesis process, and addition of pillaring solutions to the clay suspension takes a long time. As reported by numerous studies water consumption can be significantly reduced by using concentrated clay suspensions and dry clay.[14,37,43] It has been reported that starting with dry clay generated the highest degree of modification. This could be attributed to strong interaction of vibrating molecules due to microwave radiation and generation of higher resistance in the medium, which also results in higher dielectric heating than in a diluted system.

The final step is the washing and then calcination of the dried obtained solids. This step results in the dehydration and dihydroxylation of the polyoxocation where it changes to stable oxide clusters. This step is also referred to as thermal activation. Thermally stable porous solids are obtained after calcination. During calcination the bond between the interlayer species and clay layers is thought to shift from ionic to near covalent which results in the stabilisation of the porous network, by converting hydroxide pillars to stable oxides.[6] The basal spacing may decrease, but should not collapse due to calcination at high temperatures. It is also suggested that the intercalation species must not fill the entire interlayer clay space in order to have accessible porosity with high specific surface areas.[44] Excess

ions such as chlorides or nitrates that can still be found in the solid materials prior to calcination can also be removed in this step. Due to the re-suspension of the separated clay minerals in high purity water, the washing step is also considered as more time consuming step. The washing step is repeated several times until the chlorides or nitrates ions are completely removed from solid clay materials. The high volume of water required during the washing step hinders the industrial scale-up of the solid clay materials. The effect of washing step on Al-PILCs was investigated by Thomas and Occelli.[45] The samples which were repeatedly washed up to 4 times with 400 cm^3 of high purity water and the samples with no washing were compared. The XRD results revealed a broad weak peak for the unwashed sample, which then shifted to 18.9 Å with the first washing, and then became sharper with consecutive washing. Their study concluded that the initial cations present in the interlayer space were formed "*in situ*" by base hydrolysis of the different oligomers present instead of Keggin. Therefore, the washing step is found to be necessary to form stable Al-PILCs as their stability is linked to the creation of Keggin ions. Molina[46] was the first to publish a method in which concentrated (40% w/w) clay slurries, contained in dialysis bags, were equilibrated in an Al-pillaring solution. Subsequently, del Riego *et al.*[47] used the same method to pillar concentrated (10% w/w) raw and purified bentonite clay and found that the use of dialysis membranes aided the recovery of the concentrated suspensions of pillared clay materials and the number of washing cycles was decreased. However, the procedure was time-consuming and high volumes of solutions were required since the pillaring solution remained dilute. The use of dialysis compared to conventional washing methods was examined by Aceman *et al.*[48] who found that at first Al was adsorbed into the interlayer space either in a monomeric state or as small oligomers. The hydrolytic oligomerization to form Keggin ions with these species were achieved after a number of days, given that the excess ions such as Al, Cl and Na were removed through washing or dialysis. Intercalated clay sample inside the Visking dialysis bag was put in double distilled water for 7 days at room temperature in the dialysis experiments. The thermal stability of dialyzed intercalated montmorillonite clay samples was similar to non-dialysed samples, while intercalated laponite and hectorite clay samples resulted in poor thermal stability for both dialyzed samples and the washed samples. Both dialyzed intercalated beidellite and saponite clay samples demonstrated high thermal stability as revealed by more intense sharper XRD peaks compared to those washed 4 times. Sampieri *et al.*[49] investigated the effect of washing. For solids samples washed with a large volume of water (2 L g^{-1} of montmorillonite clay), the larger silica species were expelled irrespective of the synthesis method used in the study. The study concluded that the washing step is critical in synthesis methods, as it determines the interlayer space, thermal stability and the porosity of the pillared montmorillonite. However, the pillared structures were stable up to 600 °C, but collapsed at 700 °C. Fig. 1 displays schematically the pillaring process.

In general the current problems associated with the above preparation procedure are long synthesis periods and high energy costs, high volumes of water usage and mixing of clay solutions.

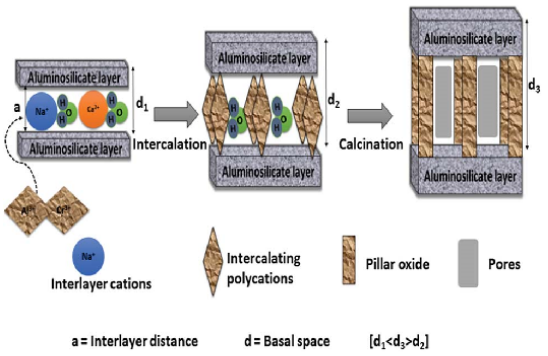


Fig. 1 Schematic representation of clay pillaring process (basal spacing; $d_1 < d_3 > d_2$).

Therefore, due to the above-mentioned problems PILCs have not been applied as commercial catalysts. This is because of the difficulties in escalating the laboratory scale developed pillaring process to an industrial scale. In order to produce PILCs at an industrial scale, the above mentioned procedure must be simplified.

3. Recent advances in the synthesis of PILCs

Commercially, when huge amounts of PILCs are required to be synthesized, conventional methods become uneconomical, since enormous equipment as well as the use of large volumes of water are required in the process.[37] The synthesis of pillared clays requires several optimizations to enable them to be applied at industrial scale. These include the use of raw natural clays without further purification[4,12,13] and the use of advanced green chemistry synthesis methods such as ultrasound, microwave radiation and one-step high-temperature high-pressure syntheses.[10,14,15,50] In addition, in order to improve the structure and acidity of mononuclear inorganic PILCs, the addition of a second pillaring agent such as Cr, Zr, Fe and Ti to the Al pillaring agent solution is also recommended.

The effect of addition of second metal oxides (*e.g.* M = Fe, Zr, Cr and Ti, *etc.*) to the Al inorganic pillaring solution has been extensively investigated. Carriazo *et al.*,[44] Molina *et al.*[51] and Zuo *et al.*[52] obtained solids with higher surface areas (increase from 200 to 300 m^2 g^{-1}) and pore volumes than single metal oxide (Al-PILCs). However, the drawbacks of the synthesis methods of the pillaring agent solutions are not considerably improved.

The removal of traces of organic matter, iron oxides and soluble salts from the natural clay before pillaring has also been investigated. Prior to pillaring process high content of iron oxides in the surface are generally removed from raw natural clay due to reports that they affect the synthesis process, textural properties and catalytic activity of PILCs as a result of the fact that excessive iron oxides content may change the colloidal and

This journal is © The Royal Society of Chemistry 2018

rheological behavior of both the suspended natural clay and the cation exchange capacity of the mineral clay present.[53] For more cutting-edge green chemistry processes some excellent properties of shaped PILCs such as extruded solids, pellets, agglomerates and monolith macro-structures are preferred. However, excessive iron oxides content may reduce both the thermal and mechanical stability of the solid materials. The PILCs catalysts' acidic and redox properties could be modified due to the excessive iron oxides content present in the raw natural clay. However, the use of purified clays is not preferred for the industrial scale process due to the fact that this cation exchange involves the use of high volumes of water and sodium salts. Therefore, the use of raw natural smectite clays with high swellability such as sodium bentonite is preferred, as it makes it easier to incorporate large metal polyoxo complexes.

The methodology for the synthesis of PILCs with single and mixed metal oxides that was developed by the use of ultrasound, microwave and one-step high-temperature high-pressure method during aging of the pillaring solution and interaction with the powdered raw natural clay has been reported to decrease the synthesis time as well as the volume of water used in the pillaring process by approximately by 90 and 95%, respectively. At an industrial scale, this leads to a significant reduction in the cost of the synthesis processes.[10,12,13,15]

Several studies[4,13,15,35,40,54,55] found the use of ultrasonic treatment to reduce the synthesis time of PILCs to less than 20 minutes. The obtained PILCs had a basal spacing ranging from 18 to 20.6 Å and a BET surface area in the range of 134 to 362 $m^2\ g^{-1}$. In order to test their thermal and hydrothermal stabilities, the PILCs were heated at temperatures ranging between 400 to 900 °C in a muffle furnace for 2 to 8 hours. The PILCs intercalated by the conventional method were exposed to comparable conditions. The results showed that the structure of PILCs prepared by conventional method collapsed at around 600 to 700 °C while the PILCs prepared by ultrasonic treatment partially maintained their structure at 900 °C. This stability was attributed to the uniform pillaring obtained by the use of ultrasonic treatment. Ultrasonic treatment did not change properties such as acidity and catalytic activity of the PILCs but was found to improve the incorporation of pillars of larger size and higher homogeneity into the clay, compared to the conventional synthesis. The ultrasonic treatment method offers several advantages to the scale up of these PILCs. Firstly, it reduces the time required from several hours or days to less than 20 minutes. It also requires no heat for the process, thereby offering a considerable saving in energy costs. In conclusion, the dry raw natural clay can be directly added to the pillaring solution and the resulting clay suspension can be highly concentrated compared to conventional methods, therefore using less water, shorter period and volumes.

The use of microwave irradiation has been reported by various authors to also speed up the PILCs synthesis process[12,16,18,33,56,57] requiring less than 15 minutes for the intercalation. Fetter *et al.*[56] investigated ways to accelerate the intercalation step during the synthesis of PILCs by using microwave irradiation. In their study 10 wt% clay suspension was slowly added to Al chlorohydrate to give an Al/clay ratio of 5 mmol g^{-1}. The solid sample was sealed and exposed to microwave irradiation for different time periods and then pillared by the conventional method. It was found that the specific surface areas of the solids prepared using microwave irradiation increased by 20–30% compared to samples synthesized by the conventional method. The microwave irradiation time was found to have little effect on the specific surface area, attaining 340 $m^2\ g^{-1}$ in 5 minutes of irradiation compared to 18 hours using the conventional method. Similarly, Fetter *et al.*[57] synthesized PILCs solids materials *via* microwave irradiation for 7 minutes using highly concentrated starting clay slurry of 50 wt% and obtained a specific surface area of 331 $m^2\ g^{-1}$, which was 27% higher compared to solids samples synthesized by the conventional method. Olaya *et al.*[12] developed a novel methodology for the synthesis of composite Al/Fe and Al/Fe/Ce pillared clays. The starting raw clay was added directly to pillaring solution and microwave radiation was applied during both the synthesis of the pillaring solution and in the intercalation process. The amount of water used and the processing time were reduced by 90–95%, offering new routes for the industrial scale up of the synthesis of the PILCs. The most promising materials prepared by the methodology proposed in their study, were synthesized using between 50 and 90% less Fe and Ce than the PILCs synthesized by the conventional method. The XRD patterns showed more intense and homogeneous (001) diffraction lines with a high content of both Al and Ce while BET results showed higher specific surface areas compared to PILCs prepared *via* conventional methods. Their activities and selectivities in the oxidation of phenol in wastewater were found to be superior compared to PILCs from conventional preparation method with higher Fe content. A lower Ce was found to have a positive effect on the incorporation of Al, the homogeneity of the (001) diffraction lines, the high specific surface area and high catalytic activity, demonstrating that the catalytic activity of the solid materials depends on the success of the pillaring process. The study by Sanabria *et al.*[16] also found that the synthesis of PILCs composites Al/Fe and Al/Ce/Fe by microwave radiation in a concentrated medium resulted in a 90–95% reduction in amount of water used as well as the intercalation time by 70–93%. The PILCs synthesized by this method were comparable in their catalytic activity and selectivity to those from the conventional synthesis procedure in a dilute medium. The active phase was reported to be more stable during the reaction and the leaching of Fe was less than 0.18 mg L^{-1}.

Recently, Ding *et al.*[10] proposed a method for the synthesis of AlCr pillaring agents *via* one-step high-temperature high-pressure hydrothermal procedure, and the composite of Al/Cr-PILCs were synthesised using ion exchange. Variations in synthesis parameters such as reaction temperature, Al/Cr molar ratio and reaction time were found to affect the structure and textural properties of Al/Cr-PILCs. The specific surface area, pore volume, and maximum basal spacing of Al/Cr-PILCs reached 266 to 362 $m^2\ g^{-1}$, 0.16–0.22 $cm^3\ g^{-1}$, and 2.06 nm, respectively, after 4 hours of calcination at 550 °C. The as-synthesized composite Al/Cr-PILCs were porous materials with outstanding structures and performance compared to

mononuclear Al-PILCs and Cr-PILCs. The synthesis procedure significantly reduced the number of steps as well as the amount of materials used compared to conventional methods. Therefore, this new proposed one-step method can be extensively applied to the synthesis of PILCs.

4. Synthesis of PILCs extrudates and monoliths

The scale up of catalysts based on PILCs to a commercial level for industrial applications also depends on the ability to match the synthesized powder pillared clay materials from laboratory scale to commercial shapes such as pellets, Raschig rings, monoliths *etc.* These materials after formation should keep their chemical properties, catalytic activity and stability during the reaction similar to the powder pillared clay materials. The synthesis of pillared bentonite clay materials with different shapes such as pellets, Raschig rings and monoliths has been achieved *via* extrusion techniques.[20,21,58] There are four steps that are involved in the extrusion process; the mixing and kneading of powder components in dry state is considered as the first step. In this step powder materials are selected based on the final solid material's chemical composition. In order to impart plasticity and lubrication to the solid mixture throughout extrusion, liquids such as water and plasticizers are added in the second step. In the third step, high-shear mixing, extrusion and thermal processing are applied to fix the solid structures and impart to the green body mechanical strength. The synthesis schematic representation of the extrusion process is shown in Fig. 2.

To date, most of the studies on the manufacture of monoliths, investigated the catalysts materials based on conventional supports such as alumina,[59] cordierite,[60] activated carbon,[61] zeolite,[62] titania[63] and mixtures of these materials.[23] On the other hand, in developing new catalyst systems, it would be appropriate to explore the opportunity of synthesizing monoliths materials with stable, less expensive and high surface area materials. Generally, monolithic catalyst structures have several advantages over conventional solid particle catalysts. These include low pressure drop, high mass transfer, short internal diffusion distance, very low bed flooding, high liquid velocity, good thermal and mechanical properties, simplicity in scale up, *etc.*[23]

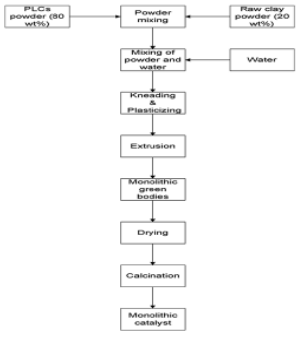


Fig. 2 Schematic representation of extrusion process.

Sanabria *et al.*[21] developed extrudates on Al/Fe and Al/Ce/Fe pillared bentonite composites which were shaped as pellets, Raschig rings and monoliths and the precursor materials were Na- or Ca-bentonite clay as binder. The catalytic activities of these composite materials were investigated for the oxidation of phenol in wastewater. The mechanical resistance of the extrudate materials depended on the calcination temperature and at 500 °C, good mechanical strength and sufficient stability to immersion in water were achieved. The as-synthesized extrudate materials retained the structural and textural properties of the powder materials. However, there was a decrease in specific surface area and pore volumes, which was reported to be due to the added bentonite as binder. The formed extrude materials preserved the catalytic properties of powder form. However, longer reaction times were required to accomplish a comparable phenol oxidation activity as well as TOC reduction, likely due to the diffusional limitations inherently present in the extrudates.

Mohino *et al.*[20] investigated features linked to the composition of the paste in the synthesis of monoliths of Al-PILCs as well as the effect of parameters such as temperature and pH on the physicochemical properties of the synthesized monoliths. In their study PILCs were introduced as starting material to prepare monoliths, and described the manufacturing conditions under which the resulting extruded materials offer the suitable combination of both physicochemical and mechanical properties as to be used as catalyst materials or catalytic supports. This study showed that extruded monolithic honeycombs with high surface area can be easily synthesized using Al-PILCs as starting raw material. The original properties of the PILCs were improved by the obtained monolith catalysts. These improved properties such as high surface area, acidity and reactivity, a good mechanical strength and resistance to pH and temperature makes the PILCs to be able to be applied as green catalyst in catalytic processes. It was therefore concluded that the Al-PILCs can be regarded as a competitive material for any other high specific surface area materials for instance zeolites, to conform monoliths either as catalysts or as active phase carriers in a number of catalytic processes. Generally, in the manufacturing process, the composition of the mixture to be extruded is of capital significance and in order to get the desired physicochemical properties of the product. In that sense, they concluded that the addition of the natural parent clay as a binder in a ratio 80/20 and of water in a solid/liquid ratio of 0.53 seems profitable.

Dominguez *et al.*[64] performed the deposition of Al–Fe pillared bentonite and gold supported Al/Fe pillared bentonite on metallic monoliths. The synthesized catalysts were characterized and their efficiency was investigated in the gaseous oxidation of CO as well as the oxidation of phenol in aqueous medium. They found that the deposition of pillared bentonite clay (with and without gold) was successful without changing the structural characteristics of the catalysts. The use of monoliths was found to enhance the catalytic activity in both

This journal is © The Royal Society of Chemistry 2018

oxidation reactions; however, more improvement was evident in the oxidation of phenol. The monolith assisted with the separation of the catalyst from the reaction medium in the liquid phase.

Han *et al.*[65] synthesised a series of acidic montmorillonite/cordierite monolithic catalysts by a coating method using silica sol as the binder. The catalysts performances were investigated in the conversion of cumene hydroperoxide (CHP). They reported that acidic montmorillonite was homogeneously distributed on the surface of cordierite honeycomb monolith. The specific surface area of the cordierite honeycomb monolith considerably increased with an increase in the acidic montmorillonite. The catalysts were found to have a higher catalytic activity and selectivity towards conversion of CHP. It was also reported that this novel catalyst can be reused for several times without significant decrease in the activity.

Recently, Gatica *et al.*[66] studied the use of pillared clays in the synthesis of washcoated clay honeycomb monoliths as support for manganese catalysts for the total oxidation of VOCs. Based on the physicochemical properties of the catalyst it was shown that the pillared clay played a positive role in optimizing the active phase deposited onto the surface of the honeycomb monolith surface by increasing its amount while keeping a relatively dispersed firmly bound active phase on the surface of the honeycomb monolith. The synthesized catalyst showed high efficiency and stability towards removal of the two model VOCs (acetone and propane) investigated. It was concluded that the data collected in their studies together with the intrinsic advantages of the honeycomb monolithic design, demonstrate the potential of the synthesised catalyst as a competitive material in the field of VOCs removal.

5. Catalytic application of PILCs catalysts in wastewater treatment

5.1 Overview

In the last decade of the 21st century wastewater and water industries have come up with innovative trends focused on green and sustainable development.[67] In general, sustainable technologies strengthen diverse products and services that deliver performance at lower costs, greatly reduce or remove environmental impact without forming secondary pollution and thereby improving the quality of life. Adsorbents and catalysts are significant for sustainable development in the green engineering wastewater industry. They aid in the treatment of wastewater contaminated by harmful substances in a resource protective way, with less energy usage and, in some cases, without any formation of harmful by-products and wastes. The catalysts, specifically if applied in a structured way, play a significant role in the so-called combined or integrated approach to environmental protection, such as integration of various wastewater treatment processes. These processes include separation, chemical reaction, momentum transfer and heat exchange. The result of such process integration is the decrease of investment costs, which is often combined with major energy recovery and space saving.

Recently, PILCs have been defined as porous materials of the 21st century and have attracted much attention from both academic and industrial research point of view.[68–71] Their high specific surface area, large micropore volume, upper acid site concentration, increased hydrophobicity and the increase in the density of sorption sites make them an excellent adsorbent and catalyst for removal of pollutants in wastewater.[4,71] The removal of contaminants present in wastewater streams generated by various industrial processes has emerged as a significant concern during past decade.[72,73] This is because of the decline in the amount and quality of available fresh water in the world due to the increase in water demands and long periods of drought. Many extremely toxic and hazardous compounds such as phenol and its derivatives are considered as persistent organic contaminants that occupy a prominent position on the WHO contaminants list owing to their high toxicity for microorganisms, high chemical oxygen demand and low biodegradability.[74] Typical concentrations of phenol in industrial wastewaters are in the range of 200–1500 mg L^{-1} whilst the Environmental Protection Authority's limit for wastewater discharge are 0.5 mg L^{-1} for surface water and 1 mg L^{-1} for sewerage water.[74,75] Therefore, effective removal of pollutants such as phenol in wastewater turns out to be a challenging task since environmental laws and regulations are becoming more stringent with time. Wastewater discharges such as phenols that are too dilute to incinerate and yet too toxic to be treated by biological process can suitably be dealt with by AOPs. AOPs have been defined as aqueous phase oxidation processes mainly based on the generation of highly active and non-selective hydroxyl radicals (HO$^{\bullet}$) in its mechanism, that contribute to the breakdown of the organic pollutants in wastewater.[76] The first step in the removal of organic contaminants by AOPs is adsorption, due to the fact that their mode of action occurs on the surface of the catalyst and both adsorption and AOPs processes would take place concurrently and the final removal would be due to the result of both removal by adsorption and AOPs. Low adsorption of these organic contaminants onto the surface of the PILCs, results in significantly low AOPs reaction rates. Consequently, increasing the adsorption capacity of organic contaminants onto PILCs may significantly increase the removal rate of organic contaminants.

In recent years, the modification of clay mineral to increase its adsorption capacity for the removal of contaminants from wastewater has been studied.[37,77,78] Several research groups have focused on the improvement of the structural and textural properties of bentonite clays and their applications in wastewater treatment.[4,79,80] Ding *et al.*[10] prepared a novel Al/Cr-pillared montmorillonite clays materials and tested them for adsorption of benzene. The benzene adsorption capacity of the prepared Al/Cr-PILCs was found to be higher compared to the starting raw clay minerals. Furthermore, the results indicated that the material had excellent benzene adsorption performance, and complete desorption could be achieved at a temperature far below its calcination temperature, indicating that the material can be reused. Therefore, the prepared Al/Cr-PILCs were found to be good materials for adsorption. El Miz *et al.*[81] synthesized Al-PILCs using Al_{13} [OH/Al = 2.4] from

Moroccan clay and studied its aqueous thymol adsorption capacities using a batch equilibrium technique. The prepared materials were found to possess excellent adsorption capacity for aqueous thymol removal. The intraparticle diffusion plot in the study confirmed that the sorption process was controlled by particle diffusion. The amount of thymol released (desorbed) from the Al-PILCs was negligible in water. Mechanisms involved in the adsorption that describe the high thymol adsorption capacity and irreversibility, were the molecule fixed by the adsorbed clay on polar groups (Al–OH and Si–OH) (remaining) sites onto the basal plane and on the layer silicate edges. Owing to these properties, the Al-PILCs showed a high potential for use as an adsorbent for thymol in wastewater. Although adsorption seems to be an effective and simple method, the regeneration of the adsorbent increases the operational cost.[37,78–80] In contrast, quite reasonable results are obtained in the removal of organic contaminants by AOPs as compared to adsorption due to the fact that hydroxyl radicals are not selective and have high oxidation capacity.[76]

Recently, Tomul *et al.*[37] synthesized Ti-pillared bentonite, Cu, Ag and Fe modified Ti-pillared bentonite and Cu/Ti- and Fe/Ti pillared bentonite composites using different Ti sources *via* direct synthesis or by modification after synthesis. The synthesized materials were investigated for both adsorption and oxidation of aqueous bisphenol A. The bisphenol A adsorption capacity of the Fe/PTi-PILCs sample was observed to be higher compared to other samples. The adsorption of bisphenol A by the pillared bentonite tested was found to fit the Langmuir isotherm. On the other hand the PTi-PILCs, Cu/PTi-PILCs and Fe/PTi-PILCs, values close to complete bisphenol A conversion were obtained within 30 minutes of reaction time while the conversion rate was only 85% in the Ag/PTi-PILCs sample for the same reaction time. It was concluded that the synthesized pillared bentonite materials were effective for both adsorption and oxidation of bisphenol A from aqueous solution. Tomul[4] synthesized the Fe/Cr-mixed bentonite pillared clay and investigated its activity for the oxidation of phenol. It was found that the temperature have major effect, compared to other studied parameters, increasing both the phenol oxidation and TOC removal while also retarding iron and chromium leaching from Fe/Cr-pillared bentonite catalyst. The iron and chromium leaching was not significant as were reported to be less than 0.71 and 1.13 mg L^{-1}, respectively. These values were found to be less than the maximum allowed by the legislation for these metals.[74] Moreover, during the oxidation of phenol, aromatic intermediates such as catechol, hydroquinone and benzoquinones were obtained and then it was observed that these intermediates are oxidized to organic acids such as oxalic acid, formic acid, maleic acid and fumaric acid.

Guo and Al-Dahhan[29] evaluated extrudates of Al/Fe-PILCs in the packed-bed operations for wastewater treatment by a wet oxidation process. The oxidation of phenol in aqueous solution was investigated using a semi-batch reactor under mild conditions. The Al/Fe-PILCs attained complete oxidation of phenol and high removal of TOC. Intermediate products such as catechol, benzoquinone, hydroquinone, oxalic acid and acetic acid were identified. The catalyst was found to be reusable for several reaction cycles without any significant change in its catalytic activity with low amount of Fe leached from the catalyst into solution. The as-synthesized Al/Fe-PILCs was thus found to be a promising catalyst for industrial wastewater treatment. Nikolopoulos *et al.*[82] investigated the removal of phenol using extrudates prepared with pillared bentonite clay at room temperature and atmospheric pressure. Extrudates with B-Al/Fe and B-Al/Ce/Fe were reported to attain total removal of phenol and TOC between 30 and 62%, in 9 hours reaction time. Thereafter, the catalyst was removed from the solution and the leachate was recovered and analysed, indicating Fe values in the range of 0.11–0.14 mg L^{-1}. The differences in phenol and TOC removal time for the extruded materials compared to the powdered materials were attributed to a consequence of the agglomeration process and the inherent diffusional limitations. The extruded catalyst retained its catalytic activity during at least 10 consecutive tests (80 hours).

Sanabria *et al.*[21] synthesized extrudates developed from Al/Fe and Al/Ce/Fe pillared bentonite shaped as pellets, Raschig rings and monoliths with Na- or Ca-bentonite as binder. The Al/Fe and Al/Ce/Fe-PILCs were investigated as catalyst in the removal of phenol. The synthesized extrudate materials were reported to maintain their chemical and catalytic properties of the synthesized materials in a powder form. The observed differences in the reaction time required to achieve similar phenol and TOC removal, were attributed to diffusional limitations inherently present in the extrudate materials.

5.2 Advanced oxidation processes

AOPs have gained recognition as alternative wastewater treatment processes against conventional methods, targeting the removal of non-biodegradable and toxic organic compounds.[83,84] In general, the main objective of any AOPs design is to produce and use hydroxyl free radicals as strong oxidants to destroy chemical compounds which cannot be removed by conventional oxidants. AOPs technology has gained popularity as an imperative technology for oxidation and mineralization of refractory compounds in wastewater.[67] Oxidizing power is one of the most important factors to be considered when selecting an oxidant for oxidation processes.[84] Table 1 shows the relative oxidation potentials of several chemical oxidizers. The $HO^{\bullet}$ is the second strongest oxidant (second highest powerful oxidant after the fluorine) with a relative to oxidation power of 2.86 eV. These radicals are produced by means of oxidizing agent such as H_2O_2 and O_3,

Table 1 Oxidation potentials of some commonly oxidants

Substance	Potential (eV)
Fluorine (F_2)	3.06
Hydroxyl radical ($HO^{\bullet}$)	2.86
Oxygen (O)	2.42
Ozone molecule (O_3)	2.07
Hydrogen peroxide (H_2O_2)	1.78
Oxygen molecule (O_2)	1.23

This journal is © The Royal Society of Chemistry 2018

ultrasound, ultraviolet irradiation, and homogeneous or heterogeneous catalysts. The HO˙ radicals are non-selective in nature and they can react without any other additives with a wide range of contaminants and attack organic compounds by either abstracting a hydrogen atom or adding hydrogen atom to the double bonds.[85,86] The HO˙ radicals oxidize organic compounds to lower molecular weight intermediates or carbon dioxide and water in case of complete mineralization.[86]

AOPs include wet air oxidation (WAO), photocatalysis, catalytic wet peroxide oxidation (CWPO), catalytic wet air oxidation (CWAO) and Fenton processes.[30] In recent decades, these methods have been applied successfully for the removal of recalcitrant pollutants based on the high oxidative power of the HO˙ radical.[4,86,87] These methods are promising in converting toxic and biologically resistant compounds into less harmful intermediates compounds or carbon dioxide and water. However, most noticeable drawback of AOPs is their operating cost compared to other conventional physicochemical or biological treatments. This is due to the use of catalysts that are sensitive to poisoning and expensive. Therefore, AOPs cannot be easily implemented to industrial scale to achieve complete mineralization of non-biodegradable compounds due to this limitation. One of the most reasonable solutions to this problem is the use of abundant, inexpensive and environment friendly catalyst such as PILCs or coupling AOPs with less expensive conventional treatment methods. This process is justified commercially in the industrial application if the used catalyst can be less expensive, non-poisonous, reduce the severity of the operating conditions and completely mineralize the organic compounds. PILCs have been applied in AOPs as a catalyst or catalyst support due to their stability, structure, abundant availability, and cost-effectiveness. The use of PILCs in AOPs as a catalyst that helps in the removal of high toxic organic compounds has been frequently reported in the literature with promising selectivities suitable for various organic contaminants.[51,88–91]

5.2.1 Photocatalysis. Heterogeneous photocatalysis is one of the AOPs technologies which is expected to develop to industrial scale in the near future. This is due to the fact that it does not need any chemicals addition, it is suitable for treating wastewater with low concentrations of organic pollutants, it is non-specific, and it can lead to the total mineralization of organic compounds.[92] This technology can use solar energy, which can be of particular interest for countries with prolonged periods of sunlight.[93] Heterogeneous photocatalytic process is one of the most important AOPs and it is based on the oxidation of organic compounds present in wastewater by means of a photochemical reaction occurring on a semiconductor catalytic solid surface activated by light with a specific wavelength. The use Ti-PILCs has attracted increasing interest because of their low toxicity, such kind of materials are being used as photocatalysts for efficient treatment of wastewaters containing toxic organic compounds.[92] The photocatalytic oxidation of different organic compounds such as phenol, 4-chlorophenol, dimethyl phthalate ester and dyes using Ti-PILCs catalysts has been reported.[94–99]

However, most of the above mentioned studies reported photocatalytic activities of Ti-PILCs to be low compared to commercial available P25 TiO_2. The possible reasons are related to lower amount of TiO_2 in Ti-PILCs compared to pure TiO_2, the difficulty in obtaining well crystallized nanocrystals, and the quantum-size effect, due to small TiO_2 nanocrystals present (a blue shift in the absorption edge). Moreover, it appears that doping of the Ti-PILCs with silver decreases the catalytic activity in agreement with its lower adsorption capacity. Another most common problem associated with the photocatalysis process is the reduced efficiency of Ti-PILCs photocatalyst with continuous operation possibly due to the adsorption of contaminants at the solid surface and blocking of the UV activated sites, which makes them unavailable for the destruction of targeted organic compounds and the need to treat highly diluted wastewater. Therefore, the practical applicability of photocatalysis using Ti-PILCs in industrial scale is not eco-friendly. However, many researches at laboratory scale to date are investigating ways which are aimed at improving the process to escalate it to industrial scale. The use of natural sunlight is significant compared to the use of artificial UV lamps which are reported not feasible in the photocatalytic process. Therefore, the current need is to study how to use the PILCs catalysts structure to promote catalytic activity under sunlight and also to apply the hydrophobic micro environment of PILCs to absorb the non-polar pollutants.

So far, only few studies have reported the use of PILCs catalyst structure as heterogeneous catalyst to promote sunlight activity. Yang *et al.*[100] and Zhang *et al.*[101] prepared a composite TiO_2-PILCs photocatalyst for the removal fuchsine and 4BS dye under sunlight. The photocatalytic activities in both studies were found to be comparable to that of commercial Degussa P25 TiO_2 using sunlight irradiation. However, it was reported that the use of dyes adsorbing in the visible region is not appropriate valuation to study the photocatalytic properties of PILCs materials in the visible region, due to the dye self-sensitizer effect in the visible region.

5.2.2 Photo-Fenton. Fenton peroxidation process has a long-established reliability to generate the powerful oxidant, hydroxyl radicals (HO˙) and is judged to be effective in the elimination of organic compounds in wastewater.[102] In addition, it is relatively environmentally friendly due to the fact that it does not involve the use of harmful chemical reagents such as Fe^{2+} ions and hydrogen peroxide (H_2O_2) and the generated hydroxyl radicals (HO˙) are nontoxic.[103,104] However, the conventional homogeneous Fenton processes require the removal of the ferric hydroxide sludge after wastewater treatment and it requires acidic conditions, typically below pH 3.0. Additionally, separation and reuse of these homogeneous catalysts are rather difficult at the end of the Fenton oxidation treatment process. These drawbacks limit the application of this process in the industrial scale, due to the high costs involved in terms of labour, reagents, acidification during processing and neutralization after treatment and time.[89] To overcome these drawbacks, much attention has been paid to the development of immobilized Fenton catalysts, such as heterogeneous Fenton-like catalysts, which can promote a heterogeneous Fenton process.

Since the beginning of the 21st century, efforts have been made to improve heterogeneous processes such as iron supported on materials like clays.[88,105–109] PILCs have been

commonly used in heterogeneous photo-Fenton applications.[110] This is due to the low cost and abundance of clay minerals, together with the ease of the pillaring process, resulting in the successful immobilization of iron ions on the surface of a material with relatively larger specific surface area. Therefore, pillared clay catalysts have been employed in the photo-Fenton removal of organic contaminants such phenol and its derivatives,[107,108] organic dyes,[105] toluene,[111] tyrosol[112] and other persistent compounds.[113,114] The catalyst physiochemical characteristics, as well as the operational parameters used in a specific reaction are reported to have a strong influence on the removal efficiency of organic contaminants in wastewater. As a result, it is essential to assess the effect of these factors on the effectiveness of the PILCs catalysts for removal of organic pollutants using heterogeneous Fenton process.

The first study which investigated the performance of pillared laponite clay-based Fe nanocomposites in the photo-Fenton (H_2O_2 + UV radiation) mineralization of azo-dye Acid Black was reported by Sum *et al.*[115] They achieved a 100% mineralization of azo-dye Acid Black, whereas only trace amounts of leached Fe ions were detected. The study by Li *et al.*[89] investigated the photo-Fenton removal of an organic azo-dye (Orange II) using Fe-pillared bentonite. They compared the reaction rates of the heterogeneous photo-Fenton process and homogeneous photo-Fenton process, in which it was found that the heterogeneous photo-Fenton process was much faster. It was further shown that the synthesized catalyst materials can also be easily recovered, regenerated, and re-used in the process. The photo-Fenton oxidation of Methylene Blue using Fe-PILCs catalysts with two different sized particle fractions (<250 μm and within the range of 250–450 μm, respectively) was studied by De León *et al.*[106] Both PILCs catalysts performed very well for the removal of the dye from aqueous solution, but the differences in catalyst performance were linked to textural properties. Recently, Bel Hadjltaief *et al.*[109] synthesized an iron-pillared Tunisian clay (Fe-PILCs) and used as the catalyst in the heterogeneous photo-Fenton oxidation of Red Congo and Malachite Green in aqueous solution. They found that both dyes were successfully removed from the aqueous solutions using a heterogeneous photo-Fenton process in the presence of Fe-PILCs as the catalyst. Furthermore, stability and leaching tests showed that the catalyst was stable over the evaluated reaction time and cycles.

Heterogeneous Fenton oxidation using PILCs has been demonstrated in full laboratory scale applications as a feasible technology for the treatment of a wide diversity of organic pollutants in aqueous solutions. However, many studies were carried out using H_2O_2 and UV light, which is not economically feasible at a commercial scale. Therefore the possibility of using sunlight is necessary for commercial scalability. The economy of this technology is very dependent on the H_2O_2 consumption; and therefore safe handling of H_2O_2 and minimal usage of H_2O_2 when dealing with high organic loads are important considerations.

5.2.3 Catalytic wet peroxide oxidation (CWPO). CWPO processes using H_2O_2 (hydrogen peroxide) as the oxidant instead of oxygen have emerged as a feasible alternative for the wastewater treatments of medium-high refractory pollutants and TOC concentrations.[116] This process operates at milder reaction conditions (temperature lower than 100 °C and atmospheric pressure) and does not need expensive reactors, offering significantly lower operative and fixed capital costs. The absence of a gas/liquid boundary in the CWPO process removes mass-transfer limitations and the H_2O_2 acts as a free-radical initiator, providing radicals ($HO^{\bullet}$) that promote the removal of organics pollutants in wastewater. This results in reduction of reaction times and allows conversion under milder reaction conditions. However, it should be noted that H_2O_2 is a more expensive reactant compared to oxygen (air). One of the major drawbacks of this process is the instability of the solid catalyst due to the chemical leaching of active metal such as Fe and Cu into the liquid phase of reaction. In order to increase the breakdown of H_2O_2 to hydroxyl radicals the use of an inexpensive, stable, ecofriendly and superior activity catalysts is highly desirable.

Among different solid catalytic materials that have been used in CWPO process, PILCs are receiving increasing attention.[8,117] Therefore, these materials can be used as a new class of micro- and mesoporous materials for catalytic applications in both acid–base and oxidative reactions.[8,118,119] PILCs with mixed oxides of aluminium/iron or aluminium/copper have been seen as a feasible option for the removal of organic pollutants such as dyes and phenolic compounds from wastewaters.[8,119] PILCs catalysts have been reported by Galeano *et al.*[3] to achieve high rates of pollutants removal with a very high stability and a minimal leaching of the interlayered metal species.[7,118,120] Garrido-Ramírez *et al.*[120] and Zhou *et al.*[7] reported that PILCs can also perform over a wide range of pH and temperature and can be readily separated from the aqueous solution and retain their catalytic activity in repeated cycles. They reported relatively short operation times owing to the high catalytic activity of the PILCs.

Barrault *et al.*[121] were amongst the first to study the removal of phenol in wastewater under mild reaction conditions (70 °C and atmospheric pressure) using mixed Al/Fe-PILCs in CWPO. Their study showed that approximately 80% of the phenol present was converted into CO_2 and H_2O within 2 hours reaction time. The stability of Al/Fe-PILCs catalyst was reported to be superior, even after three cycles of the reaction and only less than 1 mg L^{-1} of iron leached to the solution. Barrault *et al.*[121,122] were also amongst the first researchers to report the good performances of mixed Al/Cu-PILCs synthesized from a crude bentonite clay mineral in phenol oxidation with H_2O_2. They reported that the introduction of copper in pillaring position resulted in more effective catalysts, although the amount of copper which can be introduced was limited to less than 0.5 wt%. This catalytic material was reported to be stable against leaching and the catalyst was reusable in consecutive batch reactor tests. Caudo *et al.*[123] compared Cu-PILCs and Fe-PILCs in the CWPO of both model phenolic compounds (*p*-coumaric and *p*-hydroxybenzoic acids) and real olive oil milling wastewater. The synthesized solid materials exhibited similar performances in all these reactions, although Cu-PILCs showed a lower formation of oxalic acid (main reaction

This journal is © The Royal Society of Chemistry 2018

intermediate) compared to Fe-PILCs. Both catalysts showed a high resistance to leaching of active metal and a good catalytic performance.

The first study to investigate the removal of the refractory contaminants in the coffee wet processing wastewater (CWPW) produced in Colombia using CWPO was reported by Peralta *et al.*[124] In their study the oxidation of the phenolic compounds in CWPW was examined using Al/Fe-PILCs extrudates which were shaped into Raschig rings. The investigation was conducted at mild operating conditions (temperature of 25 °C and atmospheric pressure), the Al/Fe-PILCs extrudates were found to be effective catalysts for the removal of phenolic compounds and TOC reduction in CWPW. The catalyst extrudates were reported to have achieved a 62.4 and 67.5% phenol removal and selectivity toward CO_2 after 96 hours of the reaction time. Moreover, the Al/Fe-PILCs extrudates showed superior catalytic activity during eight successive oxidation experiments without significant Fe leaching. Therefore, the use of Al/Fe-PILCs extrudates in the removal of phenolic compounds demonstrated the potential for treatment of real wastewaters contaminated by phenolic compounds. This study showed a positive contribution to the eco-friendly and sustainable development in the use of CWPO for real wastewater treatment. This is mainly due to the fact that the Al/Fe extrudates materials can keep the properties of the pillared clay (high specific surface area and reactivity), show good mechanical stability and do not disintegrate upon contact with real wastewater. In addition, the expensive separation step (filtration or centrifugation) is not compulsory as the extrudates can be easily separated from wastewater after reaction, unlike powder solids catalysts materials. Therefore, these features make PILCs catalyst extrudates an attractive alternative for treating wastewater using CWPO.

In summary, several studies showed interesting and stable performances of PILCs-based catalysts for CWPO process. They can be used for practical applications, although studies on their practical industrial application in CWPO are limited, as most of the studies in the literature only focus on the use of model compounds. However, up to date there are few commercial CWPO processes using solid catalysts materials. These include the OXY-PURE of Delta Umwelttechnik which is developed to remove cyanide, phenols and other organic species from heavily organic loaded and turbid wastewaters and the USP Technologies (formerly known as US Peroxide processes) for treatment of municipal wastewater, drinking water treatment and industrial wastewater.[124]

5.2.4 Catalytic wet air oxidation (CWAO). Among the methods employed to oxidize recalcitrant organic contaminants, the CWAO is of significant interest due to its high oxidizing ability and complete mineralization.[125] The CWAO is a liquid-phase oxidation process using a solid catalyst in which organic and inorganic compounds, present in the solution, is oxidized by oxygen or air basically to CO_2 and H_2O, without any toxic gaseous emissions such as NOx, SO_2, HCI, dioxins, furans, fly ash, *etc.* CWAO is considered an attractive and useful method for treatment of organic contaminants effluents with concentrations which are too low for incineration and too high for biological treatment, *e.g.* in the case of harmful organic effluent such as phenol.[71] The incineration process is reported to be uneconomically feasible due to additional fuel cost or when heat recovery would result in only marginal saving.[126] The reaction is typically carried out at elevated temperatures (200–325 °C) and pressures (5–20 MPa) in order to optimize the oxygen concentration in the dissolved phase and consequently improve the CWAO process efficiency.[126] Although, CWAO has shown excellent potential to treat industrial wastewater, its application is limited due to the high capital investment and the high operating costs involved.[127] This is due to the severity of operating conditions and the lack of stable and active catalysts, which prevent a wider industrial commercialization. Therefore, many research efforts have been devoted to decrease the severity of the operating conditions through the development of appropriate solid catalysts.[127–129] If a stable solid catalysts can be developed that works effectively below 125 °C and 2.5 MPa, CWAO would be a potential wastewater treatment process for more general water treatment.[130] The use of PILCs catalysts in the CWAO has been proposed as this can effectively decrease the severity of the operating conditions, shorten reaction time and enhance the oxidation efficiency of organic compounds.[29]

Guo and Al-Dahhan *et al.*[29] studied the use of PILCs catalyst in the CWAO of aqueous phenol solution. The CWAO kinetics of an aqueous solution of phenol was investigated using Al/Fe-PILCs extrudates (cylindrical, approximately 2 × 8 mm) in the temperature range of 90–150 °C and air pressure range of 0.8–2.5 MPa. The reaction temperature, air pressure, initial solution pH, initial phenol concentration, and catalyst loading were the operating parameters studied. The employed conditions in their studies were much milder compared to typical industrial operating conditions. The comparison between results obtained without hydrogen peroxide and using hydrogen peroxide oxidation were done in this study. This is one of the few studies in open literature wherein a good comparison between the performances in catalytic oxidation with wet air and H_2O_2 (CWAO and CWPO, respectively) of the same catalyst was investigated. In the presence of H_2O_2 the Al/Fe-PILCs was reported to have attained a total removal of phenol and significant mineralization (80–100%) of TOC conversion without significant Fe leaching and catalyst deactivation. However, the cost and noticeable corrosion issues associated with H_2O_2 restricted their efforts on H_2O_2 oxidation and focused on the oxidation by air only. The total removal of phenol by CWAO was achieved at optimum pH of 4 and low pressure of 1.5 MPa. The optimum temperature was found to be between 130 and 150 °C, above which the operating pressure was reported to exceed the vapour pressure of the liquid phase which was uneconomical. The deactivation of the Al/Fe-PILCs extrudates catalyst due to fouling and Fe leaching was reported to be insignificant, although the solution was acidic and at high temperature. Therefore, the PILCs catalyst was found to be stable and maintained its activity for long-term experimental reaction.

The development of commercial CWAO processes based on homogenous catalysts (*e.g.*, Ciba-Geigy, LOPROX, WPO, ORCAN and ATHOS processes) started as early as the mid-fifties in the United States.[131,132] Homogeneous transition metal catalysts

Table 2 Commercial CWAO processes for the treatment of industrial wastewater[131–133]

Process	Catalyst/oxidant	Temperature, °C	Pressure, MPa	Application
LoProxBaye	Fe^{2+}-acid/O_2	<300	0.5–2	Chemical/pharmaceutical waste
Ciba-Geigy	Cu^{2+}/air	~300	~15	Chemical/pharmaceutical waste
Athos	Cu^{2+}/O_2	235–250	4.4–5.5	Residual sludge
WPO	Fe–Cu–Mn/H_2O_2	90–130	0.1–0.5	Aquifer decontamination
Orcan	Fe^{2+}/air + H_2O_2	120	0.3	Refractory waste pre-treatment
The Nippon Shkubai (NS-LC)	TiO_2 supported multi-metal catalysts (oxides of lanthanide series and transition metals)	160–270	0.9–8	Can treat acetic acid, phenol, formaldehyde and ammonia
Osaka gas	ZrO_2 or TiO_2 with noble or base metals (Fe–Co–Ni–Ru–Pd–Pt–Cu–Au–W)	250	6	High COD and ammonia containing wastewaters
Kurita	Supported Pt	170	—	Ammonia
CALIPHOX	CuO–ZnO–Al_2O_3	180	4	Industrial wastewaters

based on Cu^{2+} or Fe^{2+} ions are currently used in numerous commercial CWAO plants, which are operating successfully to treat different industrial discharges and residual sludge. Table 2 summarises some commercial CWAO processes. Ciba-Geigy was the first to commercialize CWAO process that applies a copper salt as a catalyst. Currently, there are three plants operating in Germany and Switzerland, these plants are dedicated to the treatment of chemical and pharmaceutical wastes. These plants operate at 300 °C and pressure above 15 MPa and have accomplished high oxidation efficiencies (95–99%) of chemical and pharmaceutical wastewaters. However, there is a need to remove the homogeneous transition metal catalysts from wastewater stream after treatment in a subsequent step and recycle to the reactor inlet or discard it. On the other hand the heterogeneous catalysts can be separated from treated wastewater easily and reused, while maintaining their catalytic activity for sufficiently long periods.

Therefore, three commercial heterogeneous CWAO processes (*e.g.* NS-LC, Osaka Gas and Kurita) have been developed in Japan since mid-eighties.[133] These heterogeneous CWAO processes are based on heterogeneous catalysts containing precious metals deposited on titania or titania–zirconia supports and are able to oxidize different refractory compounds, therefore, allowing the treated wastewater to be discharged directly to water bodies or reused as process water. The NS-LC process uses a vertical monolith reactor with a Pt/Pd/TiO_2–ZrO_2 honeycomb heterogeneous catalyst. The operating conditions are in the range of 160–270 °C and 0.9–8 MPa with space velocity of 2 L h^{-1} and can treat different organic effluents such as acetic acid, phenol, formaldehyde and ammonia, up to more than 99% conversion. The Osaka gas process applies a combination of precious and base metals on titania or zirconia–titania supports (Fe–Co–Ni–Ru–Pd–Pt–Cu–Au–W) in a form of honeycomb or sphere as heterogeneous catalyst. Typical operating conditions are 250 °C and 6 MPa, with 200 L h^{-1} feed of wastewater and this process targets wastewater effluent containing high COD and ammonia. The Kurita process uses nitrite as oxidant instead of oxygen in the presence of a supported Pt catalyst. This process is more effective at lower temperatures, around 170 °C and is used to treat wastewater effluent containing ammonia. The CALIPHOX process is the most recently developed process to treat industrial wastewaters using metal oxide catalyst extrudates in a trickle-bed reactor. This process was developed by the National Institute of Chemistry of Slovenia and an engineering firm and operates at relatively mild conditions (180 °C and 4 MPa).

In conclusion, as it can be observed from Table 2, there have been more CWAO commercialised processes based on homogenous catalysis than heterogeneous catalysis. Moreover, the industrial applications of CWAO operate at temperatures and pressures that are not considerably low compared to those used in non-catalytic wet oxidation. This observation indicates the urgent need for the development of more active, eco-friendly, cheap and stable heterogeneous catalysts, which can reduce the severity of the reaction conditions. However, it is also interesting to note that majority of these heterogeneous processes have used transition metal catalysts either as sole active component or in combination with other active components instead of expensive noble metals.

6. Conclusions and future prospects

The application of pillared clays as heterogeneous catalysts offers a variety of potential benefits in AOPs wastewater treatment technologies, from both the sustainable green chemistry and engineering perspective. However, it is essential to further advance background knowledge to completely understand limitations and advantages towards commercialization. The current reviewed results are promising to fill some specific gaps, which prevent the process to be escalated to industrial scale. Up to date however, no industrial examples of the use of pillared clays as catalysts in AOPs exist. The next step involves a more rational design and engineering of catalysts materials and reactors. Along this review, important aspects of AOPs technologies have been reviewed and studies on treatment of wastewaters on the industrial scale/commercialized processes demonstrate the potential of these technologies. The possible benefits such as mineralization of highly toxic refractory compounds, mild reaction conditions and shorter residence times and the formation of harmless products, from AOPs specifically CWAO process, will be a key driver for more research studies in the field. The main current problem in the

This journal is © The Royal Society of Chemistry 2018

development of successful industrial-scale heterogeneous CWAO process for the treatment of industrial wastewater seems to be the design of appropriate catalyst that is highly active, stable, economical, easy to recover, reusable and environmentally friendly. Improvements to overcome high operational costs of CWAO process offer attractive alternatives, such as PILCs materials as inexpensive robust catalysts for CWAO of refractory organic contaminants. Therefore, further research in the area of catalyst development, with the focus on the low cost, catalyst stability, reusability and environmental friendliness such as PILCs, will lead to the discovery of solids heterogeneous catalysts that are effective for many industrial-scale CWAO processes. The use of novel green synthesis methods such as microwave radiation and ultrasonic treatment has proven to be effective methods with more improved physicochemical properties and high catalytic activity of PILCs compared to conventional methods. The new developments in the synthesis of PILCs substantially mitigate deactivation of catalysts due to leaching, long period of synthesis and high water consumption, which are the most important drawback in industrial scale application of wastewater treatment.

Conflicts of interest

On behalf of all authors, there are no conflicts to declare.

Acknowledgements

This research was financially supported by the National Research Foundation (NRF)/Department of Science and Technology (DST) of South Africa under Professional Development Programme (PDP) Project No. 96719 and Mineral Science Council of South Africa (Mintek) under CWO of Wastewater Project No. ADE 164.

References

1 R. L. Lankey and P. T. Anastas, *Ind. Eng. Chem. Res.*, 2002, **41**, 4498–4502.
2 C. Molina, J. Casas, A. Pizarro and J. Rodriguez, *Clay: Types, Properties and Uses*, 2011, pp. 435–474.
3 L. A. Galeano, A. Gil and M. A. Vicente, *Appl. Catal., B*, 2010, **100**, 271–281.
4 F. Tomul, *Appl. Clay Sci.*, 2016, **120**, 121–134.
5 J. G. Carriazo, M. A. Centeno, J. A. Odriozola, S. Moreno and R. Molina, *Appl. Catal., A*, 2007, **317**, 120–128.
6 A. Gil, L. M. GandÍA and M. A. Vicente, *Catal. Rev.*, 2000, **42**, 145–212.
7 S. Zhou, C. Zhang, X. Hu, Y. Wang, R. Xu, C. Xia, H. Zhang and Z. Song, *Appl. Clay Sci.*, 2014, **95**, 275–283.
8 W. Ye, B. Zhao, H. Gao, J. Huang and X. Zhang, *J. Porous Mater.*, 2016, **23**, 301–310.
9 M. F. Brigatti, E. Galan and B. K. G. Theng, in *Developments in Clay Science*, ed. B. K. G. T. Faïza Bergaya and L. Gerhard, Elsevier, 2006, vol. 1, pp. 19–86.
10 M. Ding, S. Zuo and C. Qi, *Appl. Clay Sci.*, 2015, **115**, 9–16.
11 M. Kurian and R. Babu, *J. Environ. Chem. Eng.*, 2013, **1**, 86–91.
12 A. Olaya, S. Moreno and R. Molina, *Appl. Catal., A*, 2009, **370**, 7–15.
13 J. T. Kloprogge, L. V. Duong and R. L. Frost, *Environ. Geol.*, 2005, **47**, 967–981.
14 G. Fetter and P. Bosch, in *Pillared Clays and Related Catalysts*, Springer, 2010, pp. 1–21.
15 M. Vicente, A. Gil and F. Bergaya, *Handbook of Clay Science*, 2013, 5, p. 524.
16 N. R. Sanabria, M. A. Centeno, R. Molina and S. Moreno, *Appl. Catal., A*, 2009, **356**, 243–249.
17 J. Kloprogge, *J. Porous Mater.*, 1998, **5**, 5–41.
18 V. Singh, V. Sapehiyia and G. L. Kad, *J. Mol. Catal. A: Chem.*, 2004, **210**, 119–124.
19 M. R. Pérez, I. Pavlovic, C. Barriga, J. Cornejo, M. C. Hermosín and M. A. Ulibarri, *Appl. Clay Sci.*, 2006, **32**, 245–251.
20 F. Mohino, A. B. Martin, P. Salerno, A. Bahamonde and S. Mendioroz, *Appl. Clay Sci.*, 2005, **29**, 125–136.
21 N. R. Sanabria, P. Ávila, M. Yates, S. B. Rasmussen, R. Molina and S. Moreno, *Appl. Clay Sci.*, 2010, **47**, 283–289.
22 P. Forzatti, D. Ballardini and L. Sighicelli, *Catal. Today*, 1998, **41**, 87–94.
23 P. Avila, M. Montes and E. E. Miró, *Chem. Eng. J.*, 2005, **109**, 11–36.
24 D. Fu, F. Zhang, L. Wang, F. Yang and X. Liang, *Chin. J. Catal.*, 2015, **36**, 952–956.
25 E. El-Ashtoukhy, Y. El-Taweel, O. Abdelwahab and E. Nassef, *Int. J. Electrochem. Sci.*, 2013, **8**, 1534–1550.
26 E. Guélou, J. Barrault, J. Fournier and J.-M. Tatibouët, *Appl. Catal., B*, 2003, **44**, 1–8.
27 A. O. Ibhadon and P. Fitzpatrick, *Catalysts*, 2013, **3**, 189–218.
28 J.-M. Herrmann, *Catal. Today*, 1999, **53**, 115–129.
29 J. Guo and M. Al-Dahhan, *Ind. Eng. Chem. Res.*, 2003, **42**, 2450–2460.
30 A. Rubalcaba, M. Suárez-Ojeda, F. Stüber, A. Fortuny, C. Bengoa, I. Metcalfe, J. Font, J. Carrera and A. Fabregat, *Water Sci. Technol.*, 2007, **55**, 221–227.
31 N. Sanabria, A. Álvarez, R. Molina and S. Moreno, *Catal. Today*, 2008, **133–135**, 530–533.
32 L. C. A. Oliveira, R. M. Lago, J. D. Fabris and K. Sapag, *Appl. Clay Sci.*, 2008, **39**, 218–222.
33 M. J. Martinez-Ortiz, G. Fetter, J. M. Domınguez, J. A. Melo-Banda and R. Ramos-Gómez, *Microporous Mesoporous Mater.*, 2003, **58**, 73–80.
34 M. V. Sivaiah, S. Petit, J. Brendlé and P. Patrier, *Appl. Clay Sci.*, 2010, **48**, 138–145.
35 A. Gil, S. A. Korili, R. Trujillano and M. A. Vicente, *Pillared clays and related catalysts*, Springer, 2010.
36 S. T. Khankhasaeva, D. V. Dambueva, E. T. Dashinamzhilova, A. Gil, M. A. Vicente and M. N. Timofeeva, *J. Hazard. Mater.*, 2015, **293**, 21–29.
37 F. Tomul, F. Turgut Basoglu and H. Canbay, *Appl. Surf. Sci.*, 2016, **360**, 579–593.
38 L. V. Duong, J. T. Kloprogge, R. L. Frost and J. Van Veen, *J. Porous Mater.*, 2007, **14**, 71–79.
39 M. J. Pérez-Zurita, G. J. Pérez-Quintana, H. Alfonso, J. A. Maldonado, C. U. De Navarro, A. De Abrisqueta and C. E. Scott, *Clays Clay Miner.*, 2005, **53**, 528–535.

40 F. Rahmani, M. Haghighi and P. Estifaee, *Microporous Mesoporous Mater.*, 2014, **185**, 213–223.
41 G. Fetter, V. Hernández, V. Rodríguez, M. A. Valenzuela, V. H. Lara and P. Bosch, *Mater. Lett.*, 2003, **57**, 1220–1223.
42 M. E. Gyftopoulou, M. Millan, A. V. Bridgwater, D. Dugwell, R. Kandiyoti and J. A. Hriljac, *Appl. Catal., A*, 2005, **282**, 205–214.
43 A. Aouad, T. Mandalia and F. Bergaya, *Appl. Clay Sci.*, 2005, **28**, 175–182.
44 J. G. Carriazo, E. Guelou, J. Barrault, J. M. Tatibouët and S. Moreno, *Appl. Clay Sci.*, 2003, **22**, 303–308.
45 S. Thomas and M. Occelli, *Clays Clay Miner.*, 2000, **48**, 304–308.
46 R. Molina, *Clays Clay Miner.*, 1992, **40**, 480–482.
47 A. del Riego, I. Herrero, C. Pesquera, C. Blanco, I. Benito and F. González, *Appl. Clay Sci.*, 1994, **9**, 189–197.
48 S. Aceman, N. Lahav and S. Yariv, *Appl. Clay Sci.*, 2000, **17**, 99–126.
49 A. Sampieri, G. Fetter, P. Bosch and S. Bulbulian, *J. Porous Mater.*, 2004, **11**, 157–162.
50 B. González-Rodríguez, R. Trujillano, V. Rives, M. A. Vicente, A. Gil and S. A. Korili, *Appl. Clay Sci.*, 2015, **118**, 124–130.
51 C. B. Molina, J. A. Casas, J. A. Zazo and J. J. Rodríguez, *Chem. Eng. J.*, 2006, **118**, 29–35.
52 S. Zuo, R. Zhou and C. Qi, *J. Rare Earths*, 2011, **29**, 52–57.
53 L. Storaro, M. Lenarda, R. Gazerla and A. Rinaldi, *Microporous Mater.*, 1996, **6**, 55–63.
54 S. P. Katdare, V. Ramaswamy and A. V. Ramaswamy, *Microporous Mesoporous Mater.*, 2000, **37**, 329–336.
55 A. Pérez, M. A. Centeno, J. A. Odriozola, R. Molina and S. Moreno, *Catal. Today*, 2008, **133–135**, 526–529.
56 G. Fetter, G. Heredia, A. M. Maubert and P. Bosch, *J. Mater. Chem.*, 1996, **6**, 1857–1858.
57 G. Fetter, G. Heredia, L. A. Velázquez, A. M. Maubert and P. Bosch, *Appl. Catal., A*, 1997, **162**, 41–45.
58 A. Louloudi and N. Papayannakos, *Appl. Clay Sci.*, 2016, **123**, 47–55.
59 J. Benbow and J. Bridgewater, *Paste flow and extrusion*, Oxford University Press, UK, 1993, p. 153.
60 I. M. Lachman, R. D. Bagley and R. M. Lewis, *Am. Ceram. Soc. Bull.*, 1981, **60**, 202.
61 M. Yates, J. Blanco, P. Avila and M. P. Martin, *Microporous Mesoporous Mater.*, 2000, **37**, 201–208.
62 C. D. Madhusoodana, R. N. Das, Y. Kameshima, A. Yasumori and K. Okada, *Microporous Mesoporous Mater.*, 2001, **46**, 249–255.
63 R. M. Heck, S. Gulati and R. J. Farrauto, *Chem. Eng. J.*, 2001, **82**, 149–156.
64 M. I. Dominguez, N. Sanabria, W. Y. Hernandez, S. Moreno, R. Molina, J. A. Odriozola and M. A. Centeno, *Appl. Catal., A*, 2009, **364**, 166–173.
65 L. Han, Y. Wang, J. Zhang, Z. Lei, C. Huang and B. Chen, *Chin. J. Chem. Eng.*, 2014, **22**, 854–860.
66 J. M. Gatica, J. Castiglioni, C. de los Santos, M. P. Yeste, G. Cifredo, M. Torres and H. Vidal, *Catal. Today*, 2017, **296**, 84–94.
67 A. Buthiyappan, R. Abdul Aziz Abdul and A. Wan Daud Wan Mohd, in *Reviews in Chemical Engineering*, 2016, vol. 32, p. 1.
68 T. Nakato, J. Kawamata and S. Takagi, in *Inorganic Nanosheets and Nanosheet-Based Materials: Fundamentals and Applications of Two-Dimensional Systems*, ed. T. Nakato, J. Kawamata and S. Takagi, Springer Japan, Tokyo, 2017, pp. 3–31.
69 B. Sun, F.-A. Khan, G. Süss-Fink and B. Therrien, in *Encapsulated Catalysts*, Academic Press, 2017, pp. 387–441.
70 G. Potsi, A. K. Ladavos, D. Petrakis, A. P. Douvalis, Y. Sanakis, M. S. Katsiotis, G. Papavassiliou, S. Alhassan, D. Gournis and P. Rudolf, *J. Colloid Interface Sci.*, 2018, **510**, 395–406.
71 H. Sassi, G. Lafaye, H. B. Amor, A. Gannouni, M. R. Jeday and J. Barbier, *Front. Environ. Sci. Eng.*, 2018, **12**, 2.
72 A. M. Khaksar, S. Nazif, A. Taebi and E. Shahghasemi, *J. Photochem. Photobiol., A*, 2017, **348**, 161–167.
73 Z. Wang, M. Xu, F. Wang, X. Liang, Y. Wei, Y. Hu, C. G. Zhu and W. Fang, *Electrochim. Acta*, 2017, **247**, 535–547.
74 D. Pittet, B. Allegranzi and J. Boyce, *Infection Control & Hospital Epidemiology*, 2009, **30**, 611–622.
75 M. Ahmaruzzaman, *Adv. Colloid Interface Sci.*, 2008, **143**, 48–67.
76 V. Cleveland, J.-P. Bingham and E. Kan, *Separation and Purification Technology*, 2014, **133**, 388–395.
77 M. El Miz, S. Salhi, I. Chraibi, A. El Bachiri, M. Fauconnier and A. Tahani, *Open J. Phys. Chem.*, 2014, **4**, 98–116.
78 J. R. Kim, S. G. Huling and E. Kan, *Chem. Eng. J.*, 2015, **262**, 1260–1267.
79 G. Xiao, L. Fu and A. Li, *Chem. Eng. J.*, 2012, **191**, 171–176.
80 M. Umar, F. Roddick, L. Fan and H. A. Aziz, *Chemosphere*, 2013, **90**, 2197–2207.
81 M. El Miz, S. Salhi, I. Chraibi, A. El Bachiri, M.-L. Fauconnier and A. Tahani, *Open J. Phys. Chem.*, 2014, **4**, 98–116.
82 A. N. Nikolopoulos, O. Igglessi-Markopoulou and N. Papayannakos, *Ultrason. Sonochem.*, 2006, **13**, 92–97.
83 S. Chen, Y. Wu, G. Li, J. Wu, G. Meng, X. Guo and Z. Liu, *Appl. Clay Sci.*, 2017, **136**, 103–111.
84 K.-Y. A. Lin and Z.-Y. Zhang, *Chem. Eng. J.*, 2017, **313**, 1320–1327.
85 A. Buthiyappan, A. A. Abdul Raman and W. M. A. W. Daud, *RSC Adv.*, 2016, **6**, 25222–25241.
86 L. Ma, H. He, R. Zhu, J. Zhu, I. D. R. Mackinnon and Y. Xi, *Catal. Sci. Technol.*, 2016, **6**, 6066–6075.
87 M. F. Abid, G. M. Alwan and L. A. Abdul-Ridha, *Arabian J. Sci. Eng.*, 2016, **41**, 2659–2670.
88 O. Sze Nga Sum, J. Feng, X. Hu and P. Lock Yue, *Chem. Eng. Sci.*, 2004, **59**, 5269–5275.
89 Y. Li, Y. Lu and X. Zhu, *J. Hazard. Mater.*, 2006, **132**, 196–201.
90 O. Ayodele, H. Auta and N. M. Nor, *Ind. Eng. Chem. Res.*, 2012, **51**, 16311–16319.
91 L.-A. Galeano, M. Á. Vicente and A. Gil, *Catal. Rev.*, 2014, **56**, 239–287.
92 G. Jing, Z. Sun, P. Ye, S. Wei and Y. Liang, *Water Practice and Technology*, 2017, **12**, 432–443.

This journal is © The Royal Society of Chemistry 2018

Chapter 3

Synthesis and characterization of Al/Zr pillared clay catalyst

This chapter has been published as: **J. Baloyi**, T. Ntho, J. Moma, Synthesis of highly active and stable Al/Zr pillared clay as catalyst for catalytic wet oxidation of phenol, J. Porous Mater. (2018). doi:10.1007/s10934-018-0667-3.

J. Baloyi – 70% (conducted the research, wrote the first draft and addressed the reviewers comments);

T. Ntho – 15% (industrial (Mintek) supervisor, oversees the handling of experiments and obtained results);

J. Moma – 15% (academic (Wits) supervisor, reviewed the manuscript and approved the revised manuscript).

Journal of Porous Materials
https://doi.org/10.1007/s10934-018-0667-3

Synthesis of highly active and stable Al/Zr pillared clay as catalyst for catalytic wet oxidation of phenol

Jeffrey Baloyi[1,2] · **Thabang Ntho**[2] · **John Moma**[1]

© Springer Science+Business Media, LLC, part of Springer Nature 2018

Abstract
Natural bentonite clay was used in the synthesis of single and mixed oxide Al/Zr pillared clay catalysts by means of ultrasonic treatment during the aging and intercalation steps. The raw bentonite and pillared clay catalysts were characterized using high resolution scanning electron microscopy with energy dispersive system (HRSEM-EDS), powder X-ray diffraction (PXRD), N_2 adsorption/desorption, Fourier transform infrared spectroscopy, thermogravimetric analysis, cation exchange capacity, zeta potential and all the catalysts evaluated in the catalytic wet air oxidation (CWAO) of phenol. Calcination of the synthesized Al/Zr-PILCs at 500 °C for 120 min yielded optimum physical properties with BET surface area of 230 m^2/g, pore volume of 0.115 cm^3/g and basal spacing of 1.92 nm and with good thermal stability. Complete removal of phenol was obtained after 120 min and 88% TOC was removed after 180 min in aqueous solution under mild reaction conditions of 100 °C and 10 bar after. Catalyst reusability studies showed that the Al/Zr-PILCs catalyst demonstrated excellent chemical and structural stability with insignificant leaching of Zr^{4+} after six consecutive catalytic runs. The Al/Zr-PILCs catalyst therefore demonstrated excellent catalytic properties in the CWAO of phenol in aqueous solution.

Keywords Al/Zr pillared clay · Ultrasonic treatment · Phenol · Catalytic wet air oxidation

1 Introduction

The steady growth in global population and industrialization presents challenges in the treatment of wastewaters that usually contain an extensive diversity of persistent, toxic and poorly biodegradable organic pollutants. Phenol and its compounds are usually detected in various wastewaters streams due to their wide usage in numerous industries such as refineries, paint, coking operations, petrochemicals, pulp, paper, pharmaceuticals, wood products, resin manufacturing and plastics [1–4]. Phenol is characterized by low solubility, a poor ionization capacity and a very low vaporization pressure. Moreover, phenolic compounds are complex, toxic to living organisms and poisonous to soil microbes [5]. Phenolic compounds have been listed as priority water pollutants by the World Health Organisation (WHO) and the department of water and sanitation of South Africa in its reviewed national water resource strategy (NWRS) published in June 2013 [6–8]. Phenolic compounds in various industrial wastewater streams are usually present in the concentration range of 200–1500 mg/L whilst the Environmental Protection Authority (EPA) has set limit for water purity standard of less than 1 µg/L for phenol in surface water [9]. The toxicity levels typical range between 10 and 24 mg/L for human beings and 9–25 mg/L for fish and aquatic ecosystem [3].

Several physical and chemical wastewater treatment techniques have been used to mitigate the aquatic pollution impact of phenol. These include biological, adsorption, extraction, chemical oxidation, electrochemical and irradiation methods. The above mentioned conventional treatment techniques suffer from limitations such as incomplete removal of the organic compounds, high costs, low efficiency, generation of hazardous by-products and applicability to a limited concentration range [10]. As a result, it

Electronic supplementary material The online version of this article (https://doi.org/10.1007/s10934-018-0667-3) contains supplementary material, which is available to authorized users.

✉ John Moma
john.moma@wits.ac.za

[1] Molecular Science Institute, School of Chemistry, University of the Witwatersrand, P/Bag 3, Johannesburg WITS 2050, South Africa

[2] Advanced Materials Division, MINTEK, Private Bag X3015, Randburg 2125, South Africa

Published online: 10 August 2018

is important to develop and implement innovative technologies for treatment of wastewater pollutants such as phenol at high efficiencies, low cost and low energy consumption. Advanced oxidation processes (AOPs) such as catalytic wet air oxidation (CWAO) have been well-defined as promising alternatives to oxidize refractory compounds such as phenol using oxygen or air to CO_2 and H_2O, without emissions of toxic gases such as NOx, SO_2, HCI, dioxins, furans, fly ash, etc. [10]. The main drawbacks are high capital investment and high operating costs due to severe reaction conditions and the lack of stable and active catalysts, which prevent industrial commercialization. Consequently, numerous research efforts have been committed to decrease the severity of the operating conditions through the development of robust solid catalysts [11]. If a stable solid catalyst can be developed that works efficiently below 125 °C and 25 bar, CWAO would be a potential technology for the treatment of organic compounds in wastewater streams. The use of a novel class of heterogeneous pillared interlayered clays (PILCs) catalysts in CWAO has been proposed as a way to efficiently reduce the severity of the reaction conditions, reduce reaction time and improve the oxidation rate of organic compounds [12]. Since clay minerals are natural, abundant, environmentally friendly and low cost these characteristics make pillared clays more suitable catalysts compared to other expensive noble metal based catalysts.

However, the conventional method for the synthesis of PILCs involves long synthesis times, high water volumes and high energy costs. These conditions present major setbacks in the scale up of the synthesis of pillared clays [13–17]. Consequently, the synthesis process has gained considerable attention with many studies aimed at reducing time and energy costs by finding new ways to economize the process for commercial feasibility. In an attempt to overcome these synthesis drawbacks, new simplified synthesis methods for PILCs catalysts with single and mixed pillaring metals have been developed by the use of ultrasound [14, 18, 19], microwave [14, 19, 20] and one-step high-temperature high-pressure synthesis [13] during aging of the pillaring solution and interaction with the powdered raw natural clay. In addition, the use of the raw natural clay without further purification has been reported to reduce synthesis time [18] and the addition of a second pillaring metal such as Cr, Zr, Fe and Ti to the Al pillaring solution is also recommended, in order to improve the porosity, pore volume, specific surface area, thermal stability and acidity of mononuclear inorganic PILCs catalysts [21, 22]. In spite of PILCs being robust heterogeneous microporous catalyst materials derived from natural sources and having very fascinating properties, there is very little information reported in the literature aimed at improving the synthesis method of PILCs by addition of the raw clay directly to pillaring solutions and using ultrasonic treatment method during the intercalation stage as well as the application of mixed transition metal oxides PILCs as catalysts for the CWAO of phenol. Although there are some research articles available in the literature investigating the use of ultrasonic method for syntheses of PILCs catalysts with different single metal oxides as well as their application in wastewater treatment, to the best of our knowledge there is no report on the combination of Al/Zr metal oxides in PILCs synthesis by direct addition of the natural clay to the pillaring solution without purification for applications in CWAO of phenol in wastewater treatment. One interesting aspect on using Al/Zr-PILCs is based on the fact that both Al and Zr are well-known highly active single transition metal oxides applied to oxidize many organic wastewater reactions by different researches [23–28].

The present study aims to synthesize and catalytically apply composite Al/Zr-PILCs catalysts with different Al/Zr molar ratios for CWAO of phenol in the liquid phase under mild reactions conditions. Our objectives are to (i) synthesize and characterize Al/Zr-PILCs prepared from natural bentonite clay, (ii) investigate the potential of Al/Zr-PILCs for the CWAO of phenol in aqueous solution, and (iii) study the catalyst stability and its regeneration.

2 Materials and methods

2.1 Chemicals

Bentonite clay mined by ECCA Holdings (Pty) Ltd., from Cape Town, South Africa was used as starting material for the preparation of Al/Zr pillared clay and used without any further purification. Analytical grade $Al(NO_3)_3{\cdot}9H_2O$, $Zr(NO_3)_4{\cdot}5H_2O$, HCl and NaOH used for preparation of pillaring agents and pillared bentonite were purchased from Merck Chemicals (Pty) Ltd. The phenol used for catalytic experiments was supplied by Sigma-Aldrich Chemical Co. Analytical-grade hydroquinone, benzoquinone, catechol, oxalic acid, acetic acid, maleic acid, malonic acid and formic acid used to identify the reaction intermediates were also purchased from Sigma-Aldrich Chemical Co. Acetic acid and methanol of chromatographic grade were obtained from Merck.

2.2 Preparation of pillaring solutions

NaOH solution (0.4 M, 500 mL) was added dropwise at a rate of 5 mL/min into either $Al(NO_3)_3{\cdot}9H_2O$ (0.4 M, 250 mL) or $Zr(NO_3)_4{\cdot}5H_2O$ (0.4 M, 250 mL) solution at 25 °C under vigorous stirring. After complete addition, the mixture was stirred for 2 h and ultrasonicated for 10 min at room temperature. Our preliminary investigation found 10 min to be the optimum ultrasonic treatment time. The mixed Al/Zr pillaring solutions (Al/Zr molar ratios of 1:3, 1:1, 3:1 and

6:1) were prepared by dropwise addition of 0.4 M NaOH solution into a mixture of 0.4 M $Al(NO_3)_3{\cdot}9H_2O$ and 0.4 M $Zr(NO_3)_4{\cdot}5H_2O$ solutions with the desired Al/Zr ratio under vigorous stirring until an $[OH^-]/[Al^{3+}+Zr^{4+}]$ molar ratio of 2:1 was reached. The resulting mixture was subjected to ultrasonic treatment at 25 °C for 10 min.

2.3 Pillaring of the bentonite clay

The pillared clay catalysts were synthesized using a modified method described by Tomul [18]. Ultrasonic treatment starting with dry clay material was used to prepare the pillared bentonite clay, in order to decrease material consumption and reaction time compared to conventional pillared clays synthesis method. In a typical preparation procedure for obtaining Al/Zr-pillared bentonite clay, the dry clay was added directly to the pillaring solutions to yield a 10 mmol ratio of (Al + Zr)/g sodium bentonite (25 mL pillaring solution/1 g) and stirred at room temperature for 30 min. The resulting suspensions were ultrasonicated for 10 min at 25 °C for the ion exchange to occur, followed by 8 min of centrifugation. The resultant solid was washed with high purity water (5 times each with 200 mL portions) to remove any nitrates and chlorides (negative to $AgNO_3$ test), oven-dried at 120 °C for 16 h followed by calcination in air at 500 °C for 2 h. After cooling, the solid catalyst was grounded and sieved to a particle size range of less than 150 µm.

2.4 Materials characterization

High resolution scanning electron microscopy (HRSEM) was carried out using FEI Nova NanoSem equipped with an energy dispersive X-ray spectroscope (EDS). The samples were sputtered with a thin layer of gold or carbon to avoid static electricity effect and enhance image quality. X-ray diffraction (XRD) was performed using a high resolution Bruker AXS D8 X-ray advanced powder diffractometer with CoKα-radiation (40 kV, 40 mA, 1.78897 Å) using a LinxEye detector recorded over 5°–80° of 2θ range at scanning speed of 0.02°/s. The basal spacing (d_{001}) values were also determined from XRD patterns. The BET surface areas, average pore diameters and pore volumes were determined by N_2 adsorption/desorption at 77 K, using a Micromeritics ASAP TrisStar 3000 unit. Fourier transform infra-red (FTIR) spectra were measured using a Varian 640-IR FTIR spectrometer with a Miracle single bounce diamond attenuated total reflectance (ATR) cell from PIKE Technologies. The FTIR was operated at a resolution of 4 cm^{-1} in the wavelength range of 400–4000 cm^{-1} over 200 scans. The surface acidity properties were evaluated by adsorption of pyridine as probe molecule and the nature of the acid sites characterized on the basis of the FTIR spectral data of the pyridine pre-adsorbed samples measured using a Varian 640-IR FTIR spectrometer in the spectral wavelength range of 1650 and 1350 cm^{-1} with 200 scans and at a resolution of 4 cm^{-1}. The pyridine adsorption and FTIR spectral measurements were carried out in-situ in the spectrometer. Thermogravimetric analysis (TGA) curves were obtained using a simultaneous thermal analyser (STA) (Perkin-Elmer model 6000). The point of zero charge (PZC) pH were determined by a Zetasizer Nano ZS (Malvern Instruments, UK). The cation exchange capacity (CEC) was obtained by the Kjeldahl technique using ammonium acetate to exchange the ions of the sample with the ammonium ion and the amount of ammonium ion retained determined using a Kjeldahl unit.

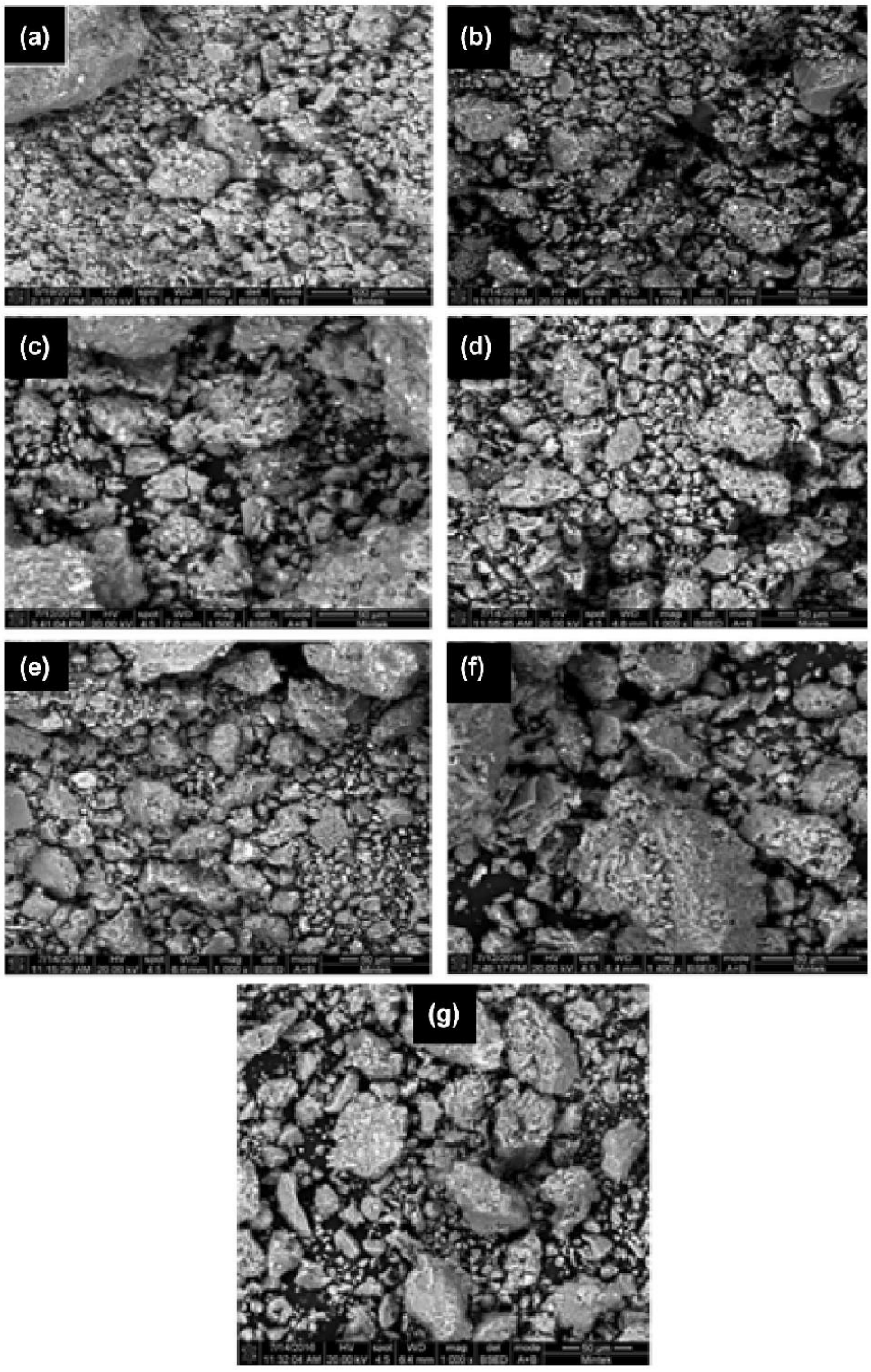
2.5 Catalytic wet air oxidation (CWAO) of phenol

The experiments in the CWAO of phenol were carried out in a high pressure semi-batch type autoclave reactor (Parr Instruments Co., model 4531M) equipped with a magnetically driven stirrer and fittings to enable gas addition to the reactor and for liquid sampling. The temperature of the reactor was measured by a thermocouple and controlled by a PID regulator. All experiments were carried out under optimized reaction conditions determined in our preliminary investigations for CWAO process with Al/Zr pillared clay catalyst (Figs. S2–S7 in Supplementary Materials). The 350 mL glass liner vessel of the reactor was charged with 200 mL of phenol solution (initial concentrations of 1000 mg/L) and the 2 g/L of catalyst. The reactor mixture was purged with pure nitrogen (at 5 bars) for 5 min and the nitrogen evacuated. The reactor was then heated to the desired temperature (100 °C), with the stirrer set at 800 rpm. Once the desired temperature was attained, the mixture was stirred for 60 min and the reaction initiated by supplying pure oxygen (10 bars) to the reactor. Prior to initiating the reaction, a sample from the reactor was analysed to determine the amount of phenol adsorbed by the catalyst. The extent of the reaction was the determined by withdrawing samples from the reactor at regular time intervals and determining their phenol concentration. The extent of the reaction was calculated by using the following equation.

$$A(\%) = \frac{(C_0 - C_t)}{C_0} \times 100 \quad (1)$$

where C_0 is the initial phenol concentration, C_t is the phenol concentration at time t and A is the percentage phenol conversion.

It was found that the amount of phenol adsorbed by the catalyst was not significant. Throughout the CWAO


(a)
(b)
(c)
(d)
(e)
(f)
(g)

◂**Fig. 1** HRSEM images of the different clay samples: **a** natural bentonite clay, **b** Al-PILCs, **c** Zr-PILCs, **d** Al/Zr-PILCs (1:3), **e** Al/Zr-PILCs (1:1), **f** Al/Zr-PILCs (3:1) and **g** Al/Zr-PILCs (6:1)

experiments, 5 mL samples were withdrawn from the reaction suspension and immediately filtered by nylon micro filter of 0.45 µm pore size prior to analysis. All catalytic experiments were carried out in triplicate and the average values reported.

The phenol concentration was determined by high performance liquid chromatography (HPLC) (Shimadzu LC-10AD) using an ODS-3 column and a UV detector. A mixture of 60/40 V/V of methanol and water was used as mobile phase at a flow rate of 1 mL/min. The column was operated at a constant temperature of 30 °C. The evolution of phenol intermediates during the reaction were analysed by HPLC following the method described by Ma et al. [29]. Total organic carbon (TOC) was measured to evaluate the mineralization degree of short-chain organic compounds acids by a Shimadzu TOC analyzer. A Mettler-Toledo FE 20 pH meter was used to determine the pH of solutions. The total Zr^{4+} leached from the solid catalysts during CWAO of phenol reactions were evaluated by inductively coupled plasma-atomic emission spectroscopy (ICP-AES).

2.6 Catalyst stability and regeneration

The spent catalyst was recovered by separating the solid catalyst from the liquid reaction medium at the end of each run, added to 100 mL $CaCl_2$ solution (4%) and stirred for 120 min at room temperature to remove all adsorbed organics. It was then rinsed with high purity water and oven-dried at 120 °C for 5 h and reused for the next catalytic reaction under the same conditions. The leached Zr^{4+} from the catalyst at the end of each catalytic reaction was quantified using ICP-AES. XRD and BET surface area analyses were also used to study the catalyst after successive catalytic runs.

3 Results and discussion

3.1 Characterization of Al/Zr pillared bentonite clay

The morphologies of the natural bentonite and pillared bentonite clays are shown in Fig. 1. A tightly packed pattern with highly porous and rough surface was observed in the structure of both natural bentonite and pillared bentonite clays. The morphology of the pillared bentonite samples is similar to the morphology of the natural bentonite; no clusters of ZrO_2 were identified. Therefore, zirconium nanoparticles seem to be homogenously dispersed in the pillared bentonite clay samples and no differences between the natural bentonite and pillared bentonite clay was visualized. The natural bentonite clay structure remained intact after pillaring process, thus, indicating that the mechanical structure of natural bentonite clay was not affected by the pillaring process. Similar results were reported by Nissam et al. [30]. The EDS analyses confirmed the presence of Zr in the bentonite clay lattice after pillaring process. The elemental analysis of natural and pillared bentonite clays, as obtained from EDS analysis, are shown in Table 1. The chemical composition of natural bentonite clay confirms the presence of oxides of Si and Al together with other mineral impurities such as Fe, Na, Mg, Ca, K and Fe. The high content of Si and Al oxides revealed the presence of quartz and muscovite [31, 32]. This result was also confirmed by XRD analysis. As shown in Table 1, significant amounts of Al or Zr were incorporated during the pillaring process. Pillaring resulted in a decrease in the amount of exchangeable K, Na and Ca cations which confirms the insertion of Al, Zr or Al/Zr pillars into the interlamellar spacing of the natural bentonite clay through ion exchange. The EDS analysis also confirmed the increase and presence of aluminium and zirconium in the pillared bentonite clay which correspond to the decrease in the amount of exchangeable cations, further confirming the successful ion exchange between the interlayer cations and Al, Zr and/ or Al/Zr species.

CEC is defined as the total capacity of a material to bind exchangeable cations. These cations such as Ca^{2+}, Mg^{2+}, Na^{+} and K^{+} as determined by EDS analysis are held by the negatively charged clay sheets through electrostatic forces. The obtained results of CEC of natural and pillared bentonite clay are presented in Table 1. In order to evaluate the influence of the pillaring process, the CEC of the natural as well as the pillared bentonite clays were measured using ammonium acetate exchange method [23, 33]. As shown in Table 1, the CEC of natural bentonite clay is higher than the CEC of all pillared bentonite samples, suggesting that the intercalated polycations are hardly exchanged. Moreover, this might be attributed to the heterostructure formation mechanism of the bentonite clay which is not an exchange type but a template assisted self-assembling mechanism [34]. This decrease of CEC bentonite clay after pillaring might be an indication that the ion exchange process took place. The results support the fact that the high CEC enables the bentonite clay to eliminate low-density chemical species such as Ca^{2+}, Mg^{2+}, Na^{+} and K^{+} from the bentonite clay matrices over isomorphous substitution by high density poly-cationic species. The CEC residual value of Zr-PILCs is found to be low compared to that of Al-PILCs which confirms that zirconium polyhydroxycations are more effective in blocking negative charge than Al-PILCs. Similar trends were reported by Mnasri-Ghnimi et al. [23].

The plot of the zeta potentials of the natural and pillared clays at different pH values are shown in Fig. 2. The point of zero charge for the different samples are derived from

Table 1 Physicochemical characteristics of natural and pillared bentonite clay samples by EDS, CEC and XRD

Sample	Al/Zr ratio	Na (%)	Mg (%)	Al (%)	Si (%)	K (%)	Ca (%)	Fe (%)	Zr (%)	CEC (meq/100 g)	d_{001} (nm)
Bentonite	–	3.73	3.29	15.31	65.09	2.39	1.09	9.10	0.00	78.6	1.56
Al-PILCs	–	0.96	1.24	31.98	59.14	1.82	0.27	4.55	0.00	40	1.72
Zr-PILCs	–	0.88	1.33	11.74	41.83	1.57	0.11	4.35	38.19	21	1.79
Al/Zr-PILCs	1:3	0.19	1.88	18.06	54.98	1.31	0.09	1.51	21.98	28	1.81
Al/Zr-PILCs	1:1	0.98	1.25	20.27	56.38	1.45	0.76	1.31	17.60	27	1.88
Al/Zr-PILCs	3:1	0.26	1.29	23.65	54.47	1.41	0.04	1.61	17.31	26	1.92
Al/Zr-PILCs	6:1	0.58	1.59	25.89	52.64	1.36	0.57	0.99	16.38	30	1.78

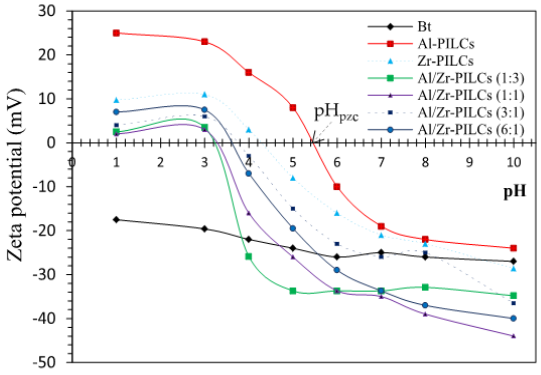
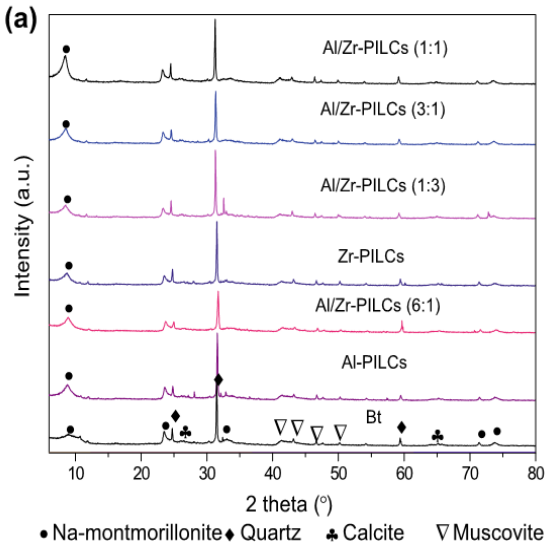


Fig. 2 Zeta potential (mV) values as a function of pH for natural and pillared bentonite clays

the plot [35]. It is seen that the natural bentonite clay (Bt) has negative zeta potential values in the pH range of 1–10. A similar observation was reported by various researchers [36–38]. The high content of permanent negative charge on the basal surface of Bt clay particles can be attributed to arise from the high degree of isomorphous substitution of structural Si^{4+} in the tetrahedral layer by Fe^{3+} or Al^{3+} while Al^{3+} in the octahedral layer is substituted by Fe^{2+} or Mg^{2+} [39] as well as the pH independent charge arising from the hydroxyl groups at the edges of the Bt clay particles. The decrease in negative zeta potential from 27 to 17.5 mV with increasing pH values (H^+ ions) in the solution can be attributed to this pH independent charge. In contrast, the pillared clays have higher zeta potentials than the natural clay, which reflect that positive charges have been introduced into Bt resulting in a less negatively charged Bt after intercalation. This can be related to the oxide pillars formed between Bt layers due to the hydration of zirconium or aluminium polycations intercalated into the intermellar space, upon calcination. In addition, it was observed that the increase of OH^- ions reduces the positive charge of pillared Bt resulting in negative zeta potential values at basic pH values and the PZC values of mixed metal oxides pillared clay were lower compared to the single metal oxides. This is due to the combination of more hydroxyl groups (–OH) by mixed Al/Zr polyoxycations, which is likely to be present as $\{[Al_xZr_y(OH)_z(H_2O)_n]^{(3x+4y-z)+}\}$, on the mixed Al/Zr-PILCs surfaces [38]. In the case of single Al or Zr polyoxycations, the well-known Keggin Al_{13} cations is presumably present as $\{[Al_{13}O_4(OH)_{24}(H_2O)_{12}]^{7+}\}$ while the tetrametric $\{[Zr(OH)_2{\cdot}4H_2O_4]^{8+}\}$ cations present in the phase of Zr. This results in a lower positive charge and PZC values of the mixed metal oxides pillared clay compared to single oxides. When the solid phase Al or Zr dissolves in water they produce deprotonated species with reduced charge [40]. Due to its positive charge, pillared bentonite clay can be expected to decrease the repulsion between its particles and negatively charged substances at acidic pH values, thereby increasing the adsorption of phenol on its surface, which consequently increase the catalytic oxidation of phenol.

XRD analysis confirms the success of pillaring process by indication of an increase in basal spacing (d_{001}) which results from the intercalation of Al, Zr or Al/Zr metal oxides clusters between the bentonite clay sheets. Figure 3 shows the XRD patterns of raw bentonite and the pillared clays. The basal spacing (d_{001}) values for materials are listed in Table 1. XRD analysis results as shown in Table 1 confirm the increase in the d_{001} values of the bentonite after pillaring with Al, Zr or Al/Zr metal oxide clusters into the bentonite clay silicate layers. The XRD patterns of natural bentonite and pillared clays exhibit a shift of the signal related to (001) smectite (for sodium bentonite) planes at $2\theta = 8.8°$ to $2\theta = 7.3°$–$6.88°$. This corresponds to the increase in the d_{001} values of the raw bentonite from 1.56 nm to 1.72–1.92 nm for the pillared clays because of the pillaring process [13, 41]. This finding indicates a successful intercalation of active metal oxide clusters (Al, Zr or Al/Zr) into Keggin structure by cation exchange process, since a shift of the signal corresponding to sodium bentonite to lesser 2 theta degrees values is observed with evident increase in its d_{001} values [23, 24]. XRD data indicate that the raw bentonite mineral clay matrices contain mineral phases such as montmorillonite which is dominant and other impurities such as



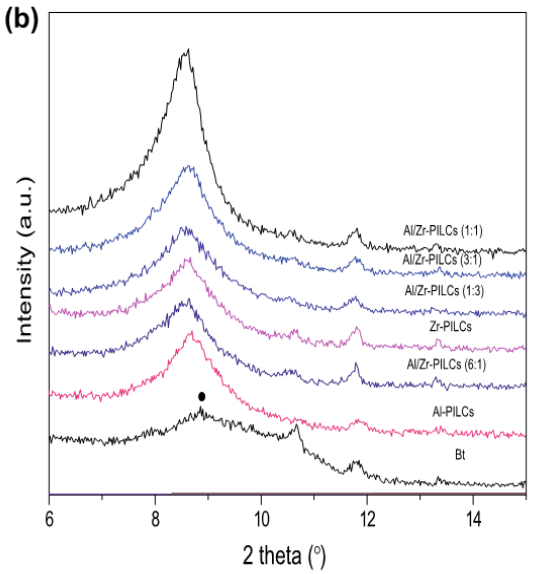


Fig. 3 XRD patterns of the natural and pillared bentonite clay; **a** wide angle p-XRD and **b** low angle p-XRD patterns

quartz, muscovite and calcite [42, 43]. After modification by pillaring the mineral phases present in the natural clay are inherited by the pillared clay materials. Therefore, the main characteristic diffraction reflection corresponding to natural clay observed in all pillared materials shows that the crystalline structure of pillared materials inherited from the raw bentonite clay was not strongly affected by the pillaring process. Similar observations for pillared clay have been reported by different research groups [24, 44, 45]. In addition, the zirconium oxide (ZrO_2 particles) and mixed-Al_2O_3/ZrO_2 oxide phases peaks were not detected in the XRD analysis, which indicate that these active metals were either very well distributed over the catalyst surface or resulted in amorphous phases [30, 46].

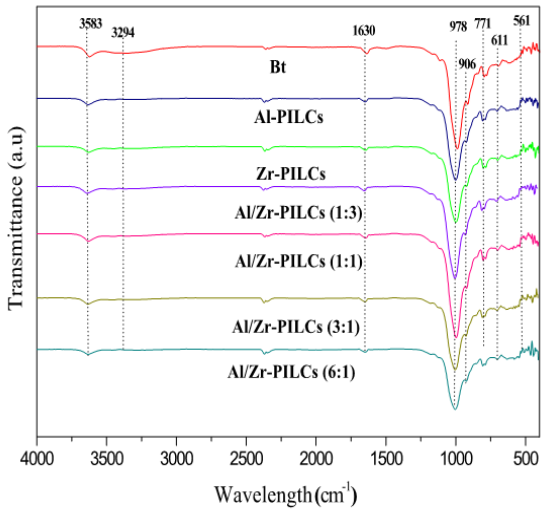


Fig. 4 FTIR spectra for natural and pillared bentonite clay samples

The FTIR spectra (400–4000 cm^{-1}) of the natural and pillared bentonite clay materials are shown in Fig. 4. The shapes of the spectra of the natural as well as the pillared clay materials are similar, demonstrating that the peaks which correspond to natural bentonite clay structure were retained after the pillaring process. This therefore suggests that the layered crystal structure of natural bentonite clay was not affected by the pillaring process for both the single and mixed metal oxides, in agreement with the XRD and SEM analyses results. For the natural bentonite clay, the peaks corresponding to –OH stretching vibrations of structural hydroxyls groups in the bentonite clay and the water molecules (H-bonded water) in the interlayer are observed at approximately 3583 and 3294 cm^{-1}, respectively [41, 42]. The peak near 1630 cm^{-1} corresponds to H–O–H bending vibration of water, while the peak at approximately 978 cm^{-1} corresponds to the siloxane (Si–O–Si) group stretching vibration in the tetrahedral structure of the bentonite clay [25, 41], but the peak shifted to higher wavelength (978–1088 cm^{-1}) due to pillaring in all pillared materials. Similar observations have been reported by different researchers [24, 47, 48]. The peaks at 906 and 771 cm^{-1} were attributed to the Al-OH and MgO-H stretching vibrations, respectively [41]. The peaks resulting from Si-O bending and Al-O stretching vibration are observed at approximately 561–611 cm^{-1} [47]. Although the spectra of both raw and pillared bentonite are similar, minor differences

regarding the decrease in the peaks intensity of all pillared materials at high wavelength (3583–3294 cm^{-1}) and low wavelength of 978–400 cm^{-1} range were observed. The observed decrease in the intensity of H-bonded-OH stretching near 3583 and 3294 cm^{-1} was due to the hydration of the interlayer water molecules after intercalation. Moreover, broadening of the peak at 3294 cm^{-1} could be attributed to the existence of Keggin-OH and Keggin-H_2O stretches, indicating the presence of Keggin ions in the Al, Zr or mixed Al/Zr pillared bentonite [49, 50]. The decrease in the siloxane (Si–O–Si) group peak intensity at approximately 978 cm^{-1} can be attributed to the formation of protonic sites (Si–O–Si, Si–O–Al or Si–O–metal peaks) during calcination of the intercalated cation [51, 52]. The slight changes in the peak intensity at 561–611 cm^{-1} might also be attributed to the formation of Si–O–metal (Al, Zr) pillars after the intercalation of metal ions into natural bentonite layer structure [25, 53, 54].

The textural properties of the natural and pillared bentonite clays are presented in Table 2. Pillaring of natural clay leads to a significant increase in the specific surface area and micropore volume. The results confirm the successful intercalation of Al, Zr or Al/Zr polyoxycations into the bentonite clay layers. It is seen this increase is lower for the single metal oxide (Al or Zr) pillared clays compared with those for the mixed metal oxides (Al/Zr) for all the Al/Zr ratios. The specific surface area and the micropore volume of the natural bentonite clay increased from 61 to 230 m^2/g and 0.089 to 0.115 cm^3/g, respectively and as the mixed metal oxides (Al/Zr) molar ratio differs, the specific surface area and micropore volumes vary with Al/Zr-PILCs (3:1) having the highest specific surface area as well as micropore volume. The higher specific surface area shows that the pillared bentonite clay samples have a microporous structure. These results are in a good agreement with the results from XRD which confirmed successful pillaring of the raw bentonite clay. Similar results in the case of Al, Zr or Al/Zr pillared clays were observed by different researchers [23, 55–59].

The nitrogen adsorption–desorption isotherms of the raw and pillared bentonite samples are shown in Fig. 5. The isotherms of the raw and pillared bentonite samples are combinations of type II and type IV isotherms with well-defined hysteresis loops corresponding to type H4 [60]. At lower equilibrium pressures $P/P_0 \leq 0.4$, the adsorption–desorption isotherms have the shape of type II suggesting microporous structure according to Brunauer, Deming, Deming and Teller (BDDT) classification [61]. At higher equilibrium pressures, the adsorption–desorption isotherms exhibit a well-defined type H4 hysteresis loop indicating slit-shaped pores between plate-like particles according to the IUPAC classification. Accordingly, type IV isotherms indicate mesoporous materials while H4 hysteresis loops are generally characteristic of materials containing both micropores and mesopores structure [60].

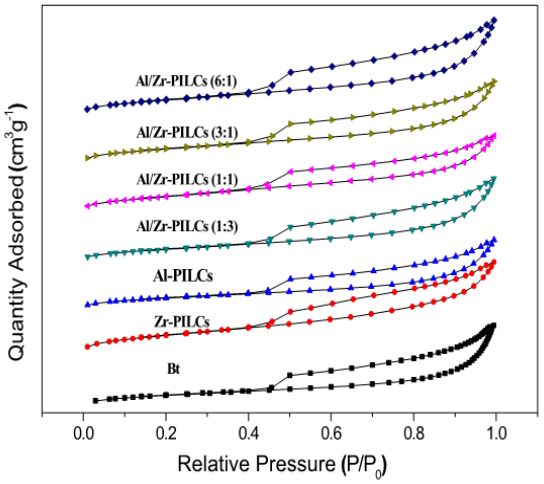


Fig. 5 Nitrogen adsorption–desorption isotherms for natural and pillared bentonite clay samples with single and mixed oxide pillars

Table 2 Surface properties of prepared catalysts and raw bentonite clay

Sample	S_{BET} [a] (m^2/g)	V_{pore} [b] (cm^3/g)	V_{mic} [c] (cm^3/g)	d_{pore} [d] (nm)
Bentonite	61	0.11	0.089	10.1
Zr-PILCs	150	0.33	0.106	8.5
Al-PILCs	147	0.32	0.099	8.2
Al/Zr-PILCs (1:3)	206	0.35	0.110	7.2
Al/Zr-PILCs (1:1)	210	0.36	0.113	7.6
Al/Zr-PILCs (3:1)	230	0.38	0.115	7.1
Al/Zr-PILCs (6:1)	182	0.34	0.108	7.8

[a]Specific surface area (SBET)

[b]Total pore volume at $p/p_0 \sim 0, 99$

[c]Micropore volume

[d]Pore diameter

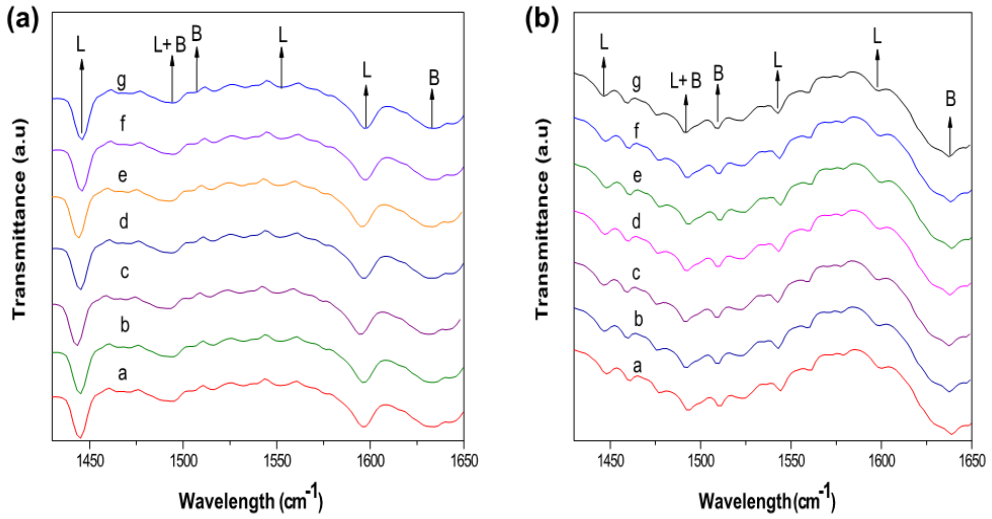


Fig. 6 FTIR spectra of pyridine adsorption on Na-bentonite and pillared natural bentonite samples at 25 °C (**a**) and after calcination at 400 °C (**b**). [(*a*) Bt, (*b*) Al-PILCs, (*c*) Zr-PILCs, (*d*) Al/Zr-PILCs (1:3), (*e*) Al/Zr-PILCs (1:1), (*f*) Al/Zr-PILCs (3:1) and (*g*) Al/Zr-PILCs (6:1)]

The nature of the acidity of the samples determined by pyridine adsorption and FTIR spectroscopy are shown in Fig. 6. The FT-IR spectra of adsorbed pyridine base molecule were used to discriminate the Lewis and Brönsted acid sites on the samples. The FT-IR spectra of all of samples after pyridine adsorption exhibit IR bands at 1443, 1491, 1522, 1541, 1558 and 1635 cm^{-1}. The IR bands at 1443 and 1541 cm^{-1} are associated with Brönsted acid site (B) [23, 57]. The IR band at 1558 cm^{-1} corresponds to pyridine adsorbed to both Lewis and Brönsted acid (L + B) sites of the samples [23, 57, 62–64] while the IR bands at 1491, 1522 and 1635 cm^{-1} are mainly attributed to Lewis acid site (L) [23, 62–64]. The samples at room temperature showed a stronger intensity of the IR bands corresponding to both Brönsted and Lewis acid sites. The intensities corresponding to the Brönsted acid sites remained nearly constant with calcination of samples at 400 °C while those assigned to Lewis acid sites increased in intensity with calcination at 400 °C. It implies that both the Brönsted and Lewis acid sites of the PILCs catalysts are thermally stable at 400 °C. This observation was also in agreement with the previous work by Mnasri-Ghnimi et al. [23]. The characteristic acid strength for the pillared bentonite clay catalysts in the study was similar to the previous reports [23, 57, 64–66].

The thermal stability data of the clay catalysts determined from TGA are shown in Fig. 7. The thermograms in Fig. 7a show that the pillared clays are more thermally stable compared with the natural bentonite clay. The mixed metal oxide pillared clay show enhanced thermal stability over the single metal oxides. This can be attributed to the fact that during the heating of PILCs in the pillaring process, the introduced Al or Zr polycations yield rigid and thermal stable oxide species, which support the clay sheets apart and prevent their collapse [67–69]. The derivative thermogravimetric analysis (DTG) data presented in Fig. 7b was used to determine the number of steps and maximum temperatures of the mass loss for the samples. The data shows that both the natural and pillared bentonite clays thermally decompose in a stepwise way and two stages of weight loss at 36–150 °C and 576–721 °C were observed. In the first step, the loosely bonded water molecules were physical and chemical desorbed from the pillared bentonite clays samples. In the second step, the materials decomposed as a result of the desorption of remaining water within the crystal lattice, dihydroxylation of hydroxyl groups on the surface of the PILCs and degradation of formed oxides, therefore releasing a pillared metal from the bentonite clay interlayer [15, 69, 70]. No peaks were detected at temperatures higher than 750 °C, indicating that the structure of the materials sintered. As shown in Fig. 7b, there is a slight but noticeable difference in the DTG peak of each material. Raw bentonite clay and single metal oxides materials (Al-PILCs and Zr-PILCs) peaks were obtained at 58 °C, 61 °C and 63 °C, respectively. While on the other hand, the DTG peaks for Al/Zr-PILCs (1:3), Al/Zr-PILCs (1:1), Al/Zr-PILCs (3:1) and Al/Zr-PILCs (6:1) are observed approximately at 73 °C, 70 °C, 66 °C and 67 °C, respectively. This suggests that the pillaring of raw bentonite clay and addition of the second metal oxide to the single metal pillared bentonite clay may lead to a shift of the dihydroxylation temperature to a higher temperature region, which can be linked to the enhancement of the thermal stability observed with single and mixed bentonite pillared clay

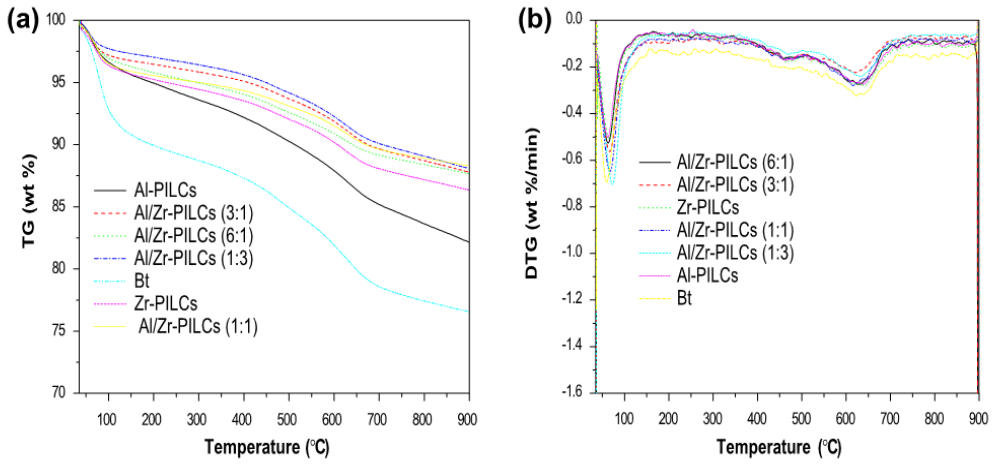


Fig. 7 TG (**a**) and DTG (**b**) curves of natural and pillared bentonite clay samples with single and mixed pillars

materials. Consequently, the TG analyses are in agreement with well-known thermal stability of the bentonite pillared clays materials up to 650 °C [44].

3.2 Catalytic wet air oxidation of phenol

The performances of the natural and pillared bentonite clay catalysts in the CWAO reaction for phenol and TOC conversions are shown in Fig. 8. Control experiments in the absence of the catalyst showed the oxidation of phenol and TOC to be negligible. The natural bentonite clay yields about 9% and 2% removal of phenol and TOC conversion, respectively, from solution after 120 min of reaction time which can be attributed to adsorption by the clay. The mixed metal oxides pillared bentonite clay (Al/Zr-PILCs) attain complete removal of phenol (100%) within 180 min compared with the single metal oxides (Al-PILCs or Zr-PILCs); Al-PILCs and Zr-PILCs as catalyst achieved 74% and 88%, respectively within 120 min. However, single metal oxides catalysts achieved 100% phenol removal when the reaction was prolonged to 180 min. Whereas up to 88% and 61% of TOC was converted after 180 min by mixed and single metal oxides pillared bentonite clay, respectively. The TOC conversion increased progressively till 120 min beyond which no significant conversions were obtained. The catalytic activities of the different pillared clay catalysts are in the order: Al-PILCs < Zr-PILCs < Al/Zr-PILCs (6:1) < Al/Zr-PILCs (1:3) < Al/Zr-PILCs (1:1) < Al/Zr-PILCs (3:1).

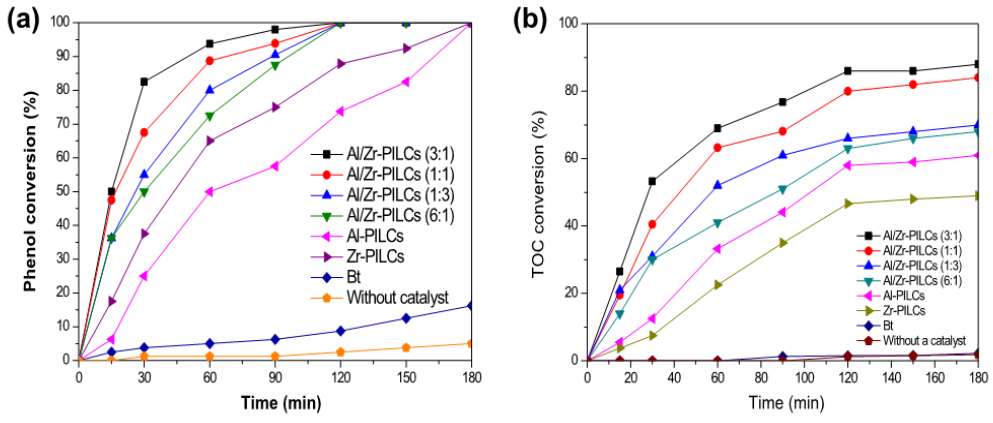


Fig. 8 Phenol (**a**) and TOC (**b**) conversions in the CWAO reaction of phenol over the natural and pillared bentonite clay samples (experimental conditions: 200 mL of reaction solution, 1000 mg/L, 0.4 g of catalyst, pH 3.0, 10 bar and 100 °C)

This trend can be attributed to an increase in the BET surface areas (61–230 m^2/g) with a corresponding increase in the number of active sites in the catalysts; the increasing positive charge (from zeta potential values) on the catalyst which increases the attraction between the catalyst and the negatively charged phenol in solution at acidic pH values, therefore increasing the adsorption of phenol on its surface, which consequently increases, the increasing stability of the pillared clays towards Zr^{4+} leaching played important role in phenol oxidation process as well as the enhancement of the surface acidity of the clay after pillaring, which is favourable for the phenol oxidation reaction. Therefore, the mixed metal oxides pillared clays (Al/Zr-PILCs) catalysts are highly effective for removal of phenol in aqueous solutions.

Table 3 summarizes a comparison of the results obtained in this work with other reported in the literature with different catalysts for CWAO of phenol. Different heterogeneous catalysts have been developed in the CWAO of phenol, such as transition metal (MnO_x-CeO_2), carbon materials (MWCNTs, GO, rGO) and noble metals catalysts (Ru, Pt…), main works from these contributions are illustrated in Table 3. These catalysts have proved their effectiveness for the CWAO of phenol and high resistance to metal leaching. Moreover, cerium-based heterogeneous catalysts have been widely studied due to the well-known oxygen storage capacity and high oxygen mobility of ceria, which improve the efficiency of CWAO of phenol. As presented in Table 3, Al/Zr-PILCs catalyst in our study compares favourably with all the catalysts except for graphene oxide (GO) catalyst, which shows poor performance. As indicated in Table 3, complete oxidation of phenol for the referenced catalysts can be obtained at relatively fast oxidation rates, however, the reaction conditions are high temperatures (> 140 °C) and high pressures (> 20 bar). Furthermore, the active phases of these catalysts are commonly costly. Therefore, the challenges of the development of robust heterogeous catalysts in CWAO under mild conditions can be overcome by the use of pillared clay catalysts such as Al/Zr-PILCs catalysts.

The experiments on the evolution of the intermediates in the CWAO of phenol over the Al/Zr-PILCs (3:1) catalyst were conducted and the results are illustrated in Fig. 9. Quintanilla et al. [75] proposed the hydroxylation of phenol takes place in ortho-oxidation and para-oxidation pathways and turning phenol into catechol and hydroquinone, which are both converted to p-benzoquinone. The oxidation of p-benzoquinone by hydroxyl radical results in ring opening with the formation of maleic and oxalic acids which further oxidize quickly to short-chain carboxylic acids such as formic, acetic and malonic acids. The short-chain carboxylic acids are then mineralized to CO_2 and H_2O. While Zapico et al. [76] suggested that phenol hydroxylation takes place involving a free radical mechanism through two routes; direct to CO_2 and H_2O and via organic intermediates. In this study, intermediates identified at the beginning of the reaction with HPLC during the phenol hydroxylation were mainly the aromatic ring compound hydroquinone and short chain carboxylic acids, such as formic, acetic, malonic, oxalic and maleic acids were generated during the reaction. Catechol and

Table 3 Comparison of the results of phenol oxidation with CWAO using different catalysts

Catalyst	Reactor	Conditions	Results	References
MWCNTs	Batch	T = 160 °C P = 20 bar [Ph]in = 1000 mg/L $t_{reaction}$ = 120 min	[Ph] = 100% [TOC] = 76%	[71]
MnO_x-CeO_2	Batch	T = 140 °C P = 20 bar [Ph]in = 1000 mg/L $t_{reaction}$ = 60 min	[Ph] = 100% [TOC] = 98%	[29]
GO	Batch	T = 155 °C P = 25 bar [Ph]in = 1000 mg/L $t_{reaction}$ = 120 min	[Ph] = 100% [TOC] = 84%	[72]
rGO	Batch	T = 160 °C P = 7 bar [Ph]in = 75 mg/L $t_{reaction}$ = 120 min	[Ph] = 50% [TOC] = 22%	[73]
(Ru,Pt)-TiO_2-CeO_2	Batch	T = 160 °C P = 20 bar [Ph]in = 2098 mg/L $t_{reaction}$ = 180 min	[Ph] = 100% [TOC] = 88%	[74]
Al/Zr-PILCs	Batch	T = 100 °C P = 10 bar [Ph]in = 1000 mg/L $t_{reaction}$ = 120 min	[Ph] = 100% [TOC] = 88%	This work

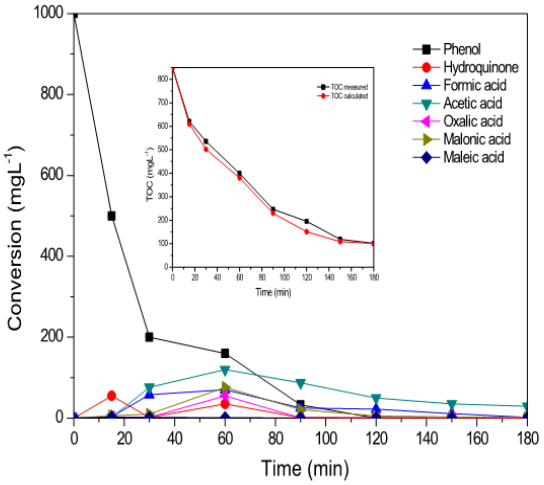


Fig. 9 Evolution of phenol and intermediates in the CWAO reaction of phenol over the Al/Zr-PILCs (3:1) (inset shows comparison between calculated and experimental TOC)

benzoquinone were not detected in the reaction as reported in the literature [71, 77, 78]. This can be attributed to the fact that these intermediates get rapidly oxidized, while the short chain carboxylic acids are continuously generated and accumulate in the oxidation reaction. As illustrated in Fig. 9, after 60 min of reaction, the short chain carboxylic acids almost completely disappear from the reaction mixture, whilst formic and acetic acids decrease more slowly. This suggests that the oxidation rate of both formic and acetic acids is the key step for total mineralization of phenol to CO_2 and H_2O. After 120 min reaction, most of the short-chain carboxylic acids were oxidized directly into CO_2 and H_2O. Similar results were reported by Yang et al. [72] and Ma et al. [29]. The comparison between the actual measured TOC and the TOC calculated from identified intermediates reveals that two curves TOC conversions against reaction time can be well fitted together.

3.3 Catalyst stability and reusability

The reusability of a catalyst is an important factor from the economic and environmental points of view and has been widely investigated in recent years. The stability and reusability of the Al/Zr-PILCs catalyst were studied using the catalyst with Al/Zr ratio of 3:1 under the optimum predetermined reaction conditions and reused six consecutive times after the first run, for the CWAO of phenol. The results presented in Table 4 show that the activity of the catalyst for the conversion of phenol remained steady after three reaction cycles and then declined very slightly from 100 to 95% in the seventh run. From the first use to third cycle reaction,

Table 4 Stability, leaching and basal spacing features of reused Al/Zr-PILCs catalyst in the removal of phenol and TOC over optimum conditions

No. of runs	Phenol removal in 120 min (%)	TOC conversion in 180 min (%)	Leaching of Zr^{4+} (Mg/L^{-1})	d_{001} (nm)
First use	100	88	0.001	1.92
Run 1	100	86	0.003	1.91
Run 2	100	86	0.005	1.91
Run 3	100	84	0.009	1.90
Run 4	98.8	80	0.010	1.88
Run 5	96.6	78	0.162	1.87
Run 6	95.3	75	0.283	1.87

almost the same TOC conversions are observed and then decreases down to 75% in the seventh run after 180 min reaction. These results indicate that the Al/Zr-PILCs were sufficiently stable and exhibit high reusability without a significant loss in its catalytic activity. Arena et al. [79] reported that catalyst deactivation in a CWAO of phenol can be due to fouling by carbonaceous deposits, active phase leaching and/or poisoning by adsorption of organic intermediates. Some authors have reported that leaching of the active phase is the most remarkable drawback of PILCs catalysts [80, 81]. The amount of Z^{4+} removed from the catalyst by leaching with the wastewater solution was determined and the results are presented in Table 4. Therefore, for the Al/Zr-PILCs catalyst used in this work, the slight decrease of catalyst activity can be attributed to a small amount of leaching of the active metals during the successive catalytic runs. However, it should be noted that a very negligible amount of Z^{4+} was removed from the catalyst as a result to leaching, indicating a strong interaction of the Z^{4+} with the pillared bentonite clay catalyst surfaces. Moreover, the decrease in TOC conversion caused the decrease of phenol removal, due to an increase of the refractory aromatic compounds [79, 82].

To determine if the catalyst is affected by the reaction conditions during its catalytic reuse XRD analysis was performed after each reaction cycle and the results presented in Table 4 and Fig. 10. The XRD patterns reveal that after six consecutive runs the structural stability of the catalyst was retained with similar crystallinity as that of the fresh catalyst. The intensity and positions of the peaks were consistent with those of the fresh catalyst. However, there was a slight decrease in the basal spacing of the used catalyst as shown in Table 4. The basal spacing values of the catalyst after six reuse cycles decreased slightly from 1.92 to 1.87 nm whilst there was observable change in BET surface area. The results show excellent reusability and stability of the catalyst for the CWAO of phenol over several cycles contributing towards green chemistry principles.

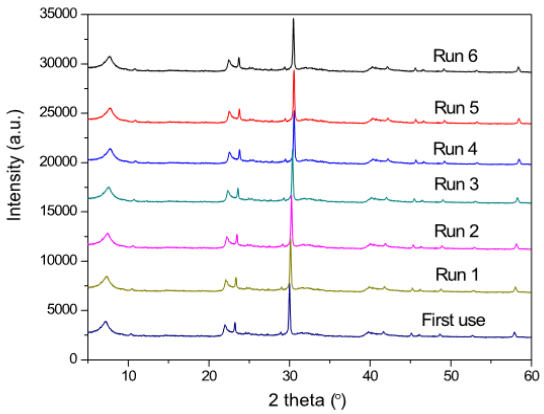


Fig. 10 XRD patterns of fresh and reused Al/Zr-pillared clay catalyst (Al/Zr ratio 3:1) under optimal experimental conditions

4 Conclusions

A series of Al/Zr-mixed pillars have been successful synthesized by direct addition of natural bentonite clay to the pillaring solution using ultrasound treatment during the formation of the pillaring solution and in the intercalation process. This synthesis method drastically reduces the synthesis time and volume of water used in the synthesis. Therefore, this method can be extensively used for preparation of pillared clays in the laboratory scale and provides possible economic benefits in the escalation of the preparation to an industrial production scale. The characterization of the synthesized PILCs materials exhibited that the basal spacing, BET surface area, pore volume, surface acidity and thermal stability of mixed Al/Zr-PILCs were greatly higher compared to single Al-PILCs, Zr-PILCs and natural bentonite clay. The Al/Zr-PILCs materials synthesized were microporous with outstanding structural properties. The Al/Zr-PILCs catalyst showed remarkable catalytic performance with 100% phenol and 88% TOC removals after CWAO of phenol under mild conditions (100 °C and 10 bars). The Al/Zr-PILCs composite with Al/Zr ratio of 3:1 Al:Zr was found to show optimum catalytic performance amongst the different ratios studied. In the CWAO of phenol over Al/Zr-PILCs catalyst, phenol is first oxidized into hydroquinone which is further oxidized into short-chain carboxylic acids that oxidize directly into carbon dioxide and water. Catalyst stability and its regeneration studies exhibited that the Al/Zr-PILCs composite catalyst demonstrated excellent chemical and structural stability with insignificant leaching of Zr^{4+}. Therefore, this study suggested that Al/Zr-pillared bentonite clay composite can be used as a potentially effective catalyst for CWAO of phenol.

Acknowledgements The authors wish to acknowledge financial support from the National Research Foundation (NRF)/Department of Science and Technology (DST) of South Africa under Professional Development Programme (PDP) Project No. 96719 and Mineral Science Council of South Africa (Mintek) under CWO of Wastewater Project No. ADE 164.

References

1. X. Sun, C. Wang, Y. Li, W. Wang, J. Wei, Treatment of phenolic wastewater by combined UF and NF/RO processes. Desalination **355**, 68–74 (2015)
2. S. Mohammadi, A. Kargari, H. Sanaeepur, K. Abbassian, A. Najafi, E. Mofarrah, Phenol removal from industrial wastewaters: a short review. Desalin. Water Treat. **53**, 2215–2234 (2015)
3. L.G.C. Villegas, N. Mashhadi, M. Chen, D. Mukherjee, K.E. Taylor, N. Biswas, A short review of techniques for phenol removal from wastewater. Curr. Pollut. Rep. **2**, 157–167 (2016)
4. E. Aneggi, A. Trovarelli, D. Goi, Degradation of phenol in wastewaters via heterogeneous Fenton-like Ag/CeO_2 catalyst. J. Environ. Chem. Eng. **5**, 1159–1165 (2017)
5. H. Ye, X. Zhang, Z. Zhao, B. Song, Z. Zhang, W. Song, Pervaporation performance of surface-modified zeolite/PU mixed matrix membranes for separation of phenol from water. Iran. Polym. J. **26**, 193–203 (2017)
6. E.S.Z. El-Ashtoukhy, Y.A. El-Taweel, O. Abdelwahab, E.M. Nassef, Treatment of petrochemical wastewater containing phenolic compounds by electrocoagulation using a fixed bed electrochemical reactor. Int. J. Electrochem. Sci. **8**, 1534–1550 (2013)
7. B. van Koppen, B. Schreiner, Moving beyond integrated water resource management: developmental water management in South Africa. Int. J. Water Resour. Dev. **30**, 543–558 (2014)
8. Department of Water Affairs, *Water for an Equitable and Sustainable Future* (Department of Water Affairs, Pretoria, 2013)
9. P. Kazemi, M. Peydayesh, A. Bandegi, T. Mohammadi, O. Bakhtiari, Stability and extraction study of phenolic wastewater treatment by supported liquid membrane using tributyl phosphate and sesame oil as liquid membrane. Chem. Eng. Res. Des. **92**, 375–383 (2014)
10. G. Yang, H. Chen, H. Qin, X. Zhang, Y. Feng, Effect of nitrogen doping on the catalytic activity of activated carbon and distribution of oxidation products in catalytic wet oxidation of phenol. Can. J. Chem. Eng. **95**, 1518 (2017)
11. J. Guo, M. Al-Dahhan, Activity and stability of iron-containing pillared clay catalysts for wet air oxidation of phenol. Appl. Catal. A **299**, 175–184 (2006)
12. J. Guo, M. Al-Dahhan, Catalytic wet oxidation of phenol by hydrogen peroxide over pillared clay catalyst. Ind. Eng. Chem. Res. **42**, 2450–2460 (2003)
13. M. Ding, S. Zuo, C. Qi, Preparation and characterization of novel composite AlCr-pillared clays and preliminary investigation for benzene adsorption. Appl. Clay Sci. **115**, 9–16 (2015)
14. A. Olaya, S. Moreno, R. Molina, Synthesis of pillared clays with Al_{13}-Fe and Al_{13}-Fe-Ce polymers in solid state assisted by microwave and ultrasound: characterization and catalytic activity. Appl. Catal. A **370**, 7–15 (2009)
15. J.T. Kloprogge, L.V. Duong, R.L. Frost, A review of the synthesis and characterisation of pillared clays and related porous materials for cracking of vegetable oils to produce biofuels. Environ. Geol. **47**, 967–981 (2005)
16. M.A. Vicente, A. Gil, F. Bergaya, Pillared clays and clay minerals. Handb. Clay Sci. **5**, 524 (2013)

17. J. Baloyi, T. Ntho, J. Moma, Synthesis and application of pillared clay heterogeneous catalysts for wastewater treatment: a review. RSC Adv. **8**, 5197–5211 (2018)
18. F. Tomul, The effect of ultrasonic treatment on iron–chromium pillared bentonite synthesis and catalytic wet peroxide oxidation of phenol. Appl. Clay Sci. **120**, 121–134 (2016)
19. V. Singh, V. Sapehiyia, G.L. Kad, Ultrasound and microwave activated preparation of ZrO_2-pillared clay composite: catalytic activity for selective, solventless acylation of 1, n-diols. J. Mol. Catal. A **210**, 119–124 (2004)
20. G. Fetter, P. Bosch, Microwave effect on clay pillaring, in *Pillared Clays and Related Catalysts* (Springer, New York, 2010), pp. 1–21
21. Z.U.O. Shufeng, Z. Renxian, Q.I. Chenze, Synthesis and characterization of aluminum and Al/REE pillared clays and supported palladium catalysts for benzene oxidation. J. Rare Earths **29**, 52–57 (2011)
22. C.B. Molina, J.A. Casas, J.A. Zazo, J.J. Rodriguez, A comparison of Al-Fe and Zr-Fe pillared clays for catalytic wet peroxide oxidation. Chem. Eng. J. **118**, 29–35 (2006)
23. S. Mnasri-Ghnimi, N. Frini-Srasra, Promoting effect of cerium on the characteristic and catalytic activity of Al, Zr, and Al–Zr pillared clay. Appl. Clay Sci. **88**, 214–220 (2014)
24. I. Fatimah, Preparation of ZrO_2/Al_2O_3-montmorillonite composite as catalyst for phenol hydroxylation. J. Adv. Res. **5**, 663–670 (2014)
25. W. Ye, B. Zhao, H. Gao, J. Huang, X. Zhang, Preparation of highly efficient and stable Fe, Zn, Al-pillared montmorillonite as heterogeneous catalyst for catalytic wet peroxide oxidation of Orange II. J. Porous Mater. **23**, 301–310 (2016)
26. G. Fetter, G. Heredia, L.A. Velázquez, A.M. Maubert, P. Bosch, Synthesis of aluminum-pillared montmorillonites using highly concentrated clay suspensions. Appl. Catal. A **162**, 41–45 (1997)
27. G. Fetter, G. Heredia, A.M. Maubert, P. Bosch, Synthesis of Al-intercalated montmorillonites using microwave irradiation. J. Mater. Chem. **6**, 1857–1858 (1996)
28. S.P. Katdare, V. Ramaswamy, A.V. Ramaswamy, Factors affecting the preparation of alumina pillared montmorillonite employing ultrasonics. Microporous Mesoporous Mater. **37**, 329–336 (2000)
29. C. Ma, Y. Wen, Q. Yue, A. Li, J. Fu, N. Zhang, H. Gai, J. Zheng, B.H. Chen, Oxygen-vacancy-promoted catalytic wet air oxidation of phenol from MnO_x–CeO_2. RSC Adv. **7**, 27079–27088 (2017)
30. E. Nissam, S. Sugunan, *Catalysis by Modified Pillared Clays and Porous Clay Heterostructures* (2014)
31. F. Tomul, S. Balci, Characterization of Al, Cr-pillared clays and CO oxidation. Appl. Clay Sci. **43**, 13–20 (2009)
32. R.E. Grim, *Clay Mineralogy*, 2nd edn. (McGraw-Hill, New York, 1968), pp. 185–224
33. W.M. Gitari, Attenuation of metal species in acidic solutions using bentonite clay: implications for acid mine drainage remediation. Toxicol. Environ. Chem. **96**, 201–217 (2014)
34. M. Benjelloun, P. Cool, T. Linssen, E.F. Vansant, Acidic porous clay heterostructures: study of their cation exchange capacity. Microporous Mesoporous Mater. **49**, 83–94 (2001)
35. H. Zhang, X. Liang, C. Yang, C. Niu, J. Wang, X. Su, Nano γ-Fe_2O_3/bentonite magnetic composites: synthesis, characterization and application as adsorbents. J. Alloy. Compd. **688**, 1019–1027 (2016)
36. W. Huang, Y.-K. Leong, T. Chen, P.-I. Au, X. Liu, Z. Qiu, Surface chemistry and rheological properties of API bentonite drilling fluid: pH effect, yield stress, zeta potential and ageing behaviour. J. Petrol. Sci. Eng. **146**, 561–569 (2016)
37. X. Peng, Z. Luan, F. Chen, B. Tian, Z. Jia, Adsorption of humic acid onto pillared bentonite. Desalination **174**, 135–143 (2005)
38. J. Zhou, P. Wu, Z. Dang, N. Zhu, P. Li, J. Wu, X. Wang, Polymeric Fe/Zr pillared montmorillonite for the removal of Cr (VI) from aqueous solutions. Chem. Eng. J. **162**, 1035–1044 (2010)
39. S.I. Rathnayake, W.N. Martens, Y. Xi, R.L. Frost, G.A. Ayoko, Remediation of Cr (VI) by inorganic-organic clay. J. Colloid Interface Sci. **490**, 163–173 (2017)
40. H. Ma, Y. Hei, L. Hua, Y. Guo, Y. Yang, C.-l. Yu, X.-R. Qiao, Fabrication of zirconium-pillared montmorillonite porous ceramic as adsorbents for Cr^{3+} removal and recycling. Ceram. Int. **42**, 14903–14909 (2016)
41. P. Kumararaja, K.M. Manjaiah, S.C. Datta, B. Sarkar, Remediation of metal contaminated soil by aluminium pillared bentonite: synthesis, characterisation, equilibrium study and plant growth experiment. Appl. Clay Sci. **137**, 115–122 (2017)
42. V. Masindi, M.W. Gitari, H. Tutu, M. DeBeer, Synthesis of cryptocrystalline magnesite–bentonite clay composite and its application for neutralization and attenuation of inorganic contaminants in acidic and metalliferous mine drainage. J. Water Process Eng. **15**, 2 (2015)
43. V. Masindi, W.M. Gitari, K.G. Pindihama, Synthesis of cryptocrystalline magnesite/bentonite clay composite and its application for removal of phosphate from municipal wastewaters. Environ. Technol. **37**, 603–612 (2016)
44. M. El Miz, S. Salhi, I. Chraibi, A. El Bachiri, M.-L. Fauconnier, A. Tahani, Characterization and adsorption study of thymol on pillared bentonite. Open J. Phys. Chem. **4**, 98 (2014)
45. S. Mnasri, N. Frini-Srasra, Influence of aluminium incorporation in the preparation of zirconia-pillared clay and catalytic performance in the acetalization reaction. Clay Miner. **47**, 453 (2012)
46. G. Fetter, V. Hernández, V. Rodríguez, M.A. Valenzuela, V.H. Lara, P. Bosch, Effect of microwave irradiation time on the synthesis of zirconia-pillared clays. Mater. Lett. **57**, 1220–1223 (2003)
47. F. Tomul, Effect of ultrasound on the structural and textural properties of copper-impregnated cerium-modified zirconium-pillared bentonite. Appl. Surf. Sci. **258**, 1836–1848 (2011)
48. F.T. Basoglu, S. Balci, Catalytic properties and activity of copper and silver containing Al-pillared bentonite for CO oxidation. J. Mol. Struct. **1106**, 382–389 (2016)
49. L.M. Wu, D.S. Tong, L.Z. Zhao, W.H. Yu, C.H. Zhou, H. Wang, Fourier transform infrared spectroscopy analysis for hydrothermal transformation of microcrystalline cellulose on montmorillonite. Appl. Clay Sci. **95**, 74–82 (2014)
50. S. Acemana, N. Lahav, S. Yariv, A thermo-FTIR-spectroscopy analysis of Al-pillared smectites differing in source of charge, in KBr disks. Thermochim. Acta **340**, 349–366 (1999)
51. F. Tomul, S. Balci, Synthesis and characterization of Al-pillared interlayered bentonites. Gazi Univ. J. Sci. **21**, 21–31 (2008)
52. B. Caglar, B.Q. Afsin, A. Tabak, E. Eren, Characterization of the cation-exchanged bentonites by XRPD, ATR, DTA/TG analyses and BET measurement. Chem. Eng. J. **149**, 242–248 (2009)
53. B. Caglar, B. Afsin, A. Tabak, E. Eren, Characterization of the cation-exchanged bentonites by XRPD, ATR, DTA/TG analyses and BET measurement. Chem. Eng. J. **149**, 242–248 (2009)
54. Y. Gao, W. Li, H. Sun, Z. Zheng, X. Cui, H. Wang, F. Meng, A facile in situ pillaring method—the synthesis of Al-pillared montmorillonite. Appl. Clay Sci. **88**, 228–232 (2014)
55. W. Schwieger, G. Lagaly, S.M. Auerbach, K.A. Carrado, P.K. Dutta, *Handbook of Layered Materials* (Marcel Dekker, Inc., New York, 2004)
56. P. Canizares, J.L. Valverde, M.R.S. Kou, C.B. Molina, Synthesis and characterization of PILCs with single and mixed oxide pillars prepared from two different bentonites. A comparative study. Microporous Mesoporous Mater. **29**, 267–281 (1999)
57. S.V. Awate, S.B. Waghmode, M.S. Agashe, Synthesis, characterization and catalytic evaluation of zirconia-pillared montmorillonite for linear alkylation of benzene. Catal. Commun. **5**, 407–411 (2004)

58. H. Jung, S.-M. Paek, J.-B. Yoon, J.-H. Choy, Zr K-edge XAS study on ZrO_2-pillared aluminosilicate. J. Porous Mater. **14**, 369–377 (2007)
59. S. Mnasri, N. Hamdi, N. Frini-Srasra, E. Srasra, Acid–base properties of pillared interlayered clays with single and mixed Zr–Al oxide pillars prepared from Tunisian-interstratified illite–smectite. Arab. J. Chem. (2014)
60. K.S.W. Sing, Reporting physisorption data for gas/solid systems with special reference to the determination of surface area and porosity (Recommendations 1984). Pure Appl. Chem. **57**, 603–619 (1985)
61. S.J. Gregg, K.S.W. Sing, *Adsorption, Surface Area and Porosity* (Academic Press, London, 1967)
62. M. Lefrancois, G. Malbois, The nature of the acidic sites on mordenite. J. Catal. **20**, 350–358 (1971)
63. M. Kojima, M.W. Rautenbach, C.T. O'Connor, Acidity characterization of ion-exchanged mordenite. J. Catal. **112**, 495–504 (1988)
64. B.T. Loveless, A. Gyanani, D.S. Muggli, Discrepancy between TPD-and FTIR-based measurements of Brønsted and Lewis acidity for sulfated zirconia. Appl. Catal. B **84**, 591–597 (2008)
65. F. Kooli, J. Bovey, W. Jones, Dependence of the properties of titanium-pillared clays on the hostmatrix: a comparison of montmorillonite, saponite and rectorite pillaredmaterials. J. Mater. Chem. **7**, 153–158 (1997)
66. C. Breen, A.T. Deane, J.J. Flynn, The acidity of trivalent cation-exchanged montmorillonite. Temperature-programmed desorption and infrared studies of pyridine and n-butylamine. Clay Miner. **22**, 169–178 (1987)
67. N. Rinaldi, A. Kristiani, Physicochemical of pillared clays prepared by several metal oxides, in *AIP Conference Proceedings*, pp. 020063
68. J.L. Valverde, P. Cañizares, M.R.S. Kou, C.B. Molina, Enhanced thermal stability of Al-pillared smectites modified with Ce and La. Clays Clay Miner. **48**, 424–432 (2000)
69. H.J. Chae, I.-S. Nam, S.W. Ham, S.B. Hong, Physicochemical characteristics of pillared interlayered clays. Catal. Today **68**, 31–40 (2001)
70. J. Pires, J. Francisco, A. Carvalho, M. Brotas, A.R. de Carvalho, C. Silva, B. Freire, de Castro, Development of novel pillared clays for the encapsulation of inorganic complexes. Langmuir **20**, 2861–2866 (2004)
71. S. Yang, X. Li, W. Zhu, J. Wang, C. Descorme, Catalytic activity, stability and structure of multi-walled carbon nanotubes in the wet air oxidation of phenol. Carbon **46**, 445–452 (2008)
72. S. Yang, Y. Cui, Y. Sun, H. Yang, Graphene oxide as an effective catalyst for wet air oxidation of phenol. J. Hazard. Mater. **280**, 55–62 (2014)
73. R.P. Rocha, A.G. Gonçalves, L.M. Pastrana-Martínez, B.C. Bordoni, O. Soares, J.J.M. Órfão, J.L. Faria, J.L. Figueiredo, A.M.T. Silva, M.F.R. Pereira, Nitrogen-doped graphene-based materials for advanced oxidation processes. Catal. Today **249**, 192–198 (2015)
74. A.E. de Los Monteros, G. Lafaye, A. Cervantes, G.Del Angel, J. Barbier Jr., G. Torres, Catalytic wet air oxidation of phenol over metal catalyst (Ru, Pt) supported on TiO_2–CeO_2 oxides. Catal. Today **258**, 564–569 (2015)
75. A. Quintanilla, J.A. Casas, A.F. Mohedano, J.J. Rodríguez, Reaction pathway of the catalytic wet air oxidation of phenol with a Fe/activated carbon catalyst. Appl. Catal. B **67**, 206–216 (2006)
76. R.R. Zapico, P. Marín, F.V. Díez, S. Ordóñez, Influence of operation conditions on the copper-catalysed homogeneous wet oxidation of phenol: development of a kinetic model. Chem. Eng. J. **270**, 122–132 (2015)
77. A. Santos, P. Yustos, A. Quintanilla, S. Rodrıguez, F. Garcıa-Ochoa, Route of the catalytic oxidation of phenol in aqueous phase. Appl. Catal. B **39**, 97–113 (2002)
78. G. Yang, H. Chen, H. Qin, X. Zhang, Y. Feng, Effect of nitrogen doping on the catalytic activity of activated carbon and distribution of oxidation products in catalytic wet oxidation of phenol. Can. J. Chem. Eng. **95**, 1518–1525 (2017)
79. F. Arena, R. Di Chio, B. Gumina, L. Spadaro, G. Trunfio, Recent advances on wet air oxidation catalysts for treatment of industrial wastewaters. Inorg. Chim. Acta **431**, 101–109 (2015)
80. H. Sassi, G. Lafaye, H.B. Amor, A. Gannouni, M.R. Jeday, J. Barbier, Wastewater treatment by catalytic wet air oxidation process over Al-Fe pillared clays synthesized using microwave irradiation. Front. Environ. Sci. Eng. **12**, 2 (2018)
81. S. Jafarinejad, *Cost-Effective Catalytic Materials for AOP Treatment Units* (2017)
82. M. Kurian, V.R. Remya, C. Kunjachan, Catalytic wet oxidation of chlorinated organics at mild conditions over iron doped nanoceria. Catal. Commun. **99**, 75–78 (2017)

Chapter 4

Synthesis and characterization of an efficient and stable Al/Fe pillared clay catalyst

This chapter has been published as: J. Moma, **J. Baloyi**, T. Ntho, Synthesis and characterization of an efficient and stable Al/Fe pillared clay catalyst for the catalytic wet air oxidation of phenol, RSC Adv. 8 (2018) 30115–30124. doi:10.1039/C8RA05825C.

J. Baloyi – 70% (conducted the research, wrote the first draft and addressed the reviewers comments);

T. Ntho – 15% (industrial (Mintek) supervisor, oversees the handling of experiments and obtained results);

J. Moma – 15% (academic (Wits) supervisor, reviewed the manuscript and approved the revised manuscript).

RSC Advances

PAPER

Check for updates

Cite this: *RSC Adv.*, 2018, **8**, 30115

Synthesis and characterization of an efficient and stable Al/Fe pillared clay catalyst for the catalytic wet air oxidation of phenol†

John Moma, *[a] Jeffrey Baloyi[ab] and Thabang Ntho[b]

Received 8th July 2018
Accepted 14th August 2018

DOI: 10.1039/c8ra05825c

rsc.li/rsc-advances

A facile method for synthesizing Al/Fe pillared clays (PILCs) from natural bentonite clay, by using ultrasonic treatment during the aging and intercalation steps, has been established. Single metal (Fe-PILCs and Al-PILCs) and mixed metal (Al/Fe-PILCs, with varying compositions of the pillaring precursors) pillared clays were prepared and characterized with a combination of chemical and instrumental methods. The pillared clays were evaluated as catalysts in the catalytic wet air oxidation (CWAO) of phenol and the mixed metal pillared clay catalysts, especially with an Al/Fe ratio of 3 : 1, were found to be highly active and stable, with superior properties such as surface areas, basal spacing, high porosity and thermal stability. The catalysts could also be reused several times without significant loss of activity. The results of the study show that Al/Fe-pillared clay catalysts are effective catalysts for the oxidation of phenol and removal of TOC in aqueous solutions. The main intermediate products in the CWAO of phenol were hydroquinone, pyrocatechol, and benzoquinone and oxalic, formic, malonic, oxalic, malonic and maleic acids.

1. Introduction

In recent times, a lot of research efforts have been dedicated to the development of efficient new 'green' technologies such as advanced oxidation processes (AOPs) for the removal of organic refractory pollutants from industrial effluents. Among several AOPs, the catalytic wet air oxidation (CWAO) using oxygen as the oxidative agent over a catalyst to initiate non-selective oxidation of refractory organic pollutants appears to be the most promising due to its effectiveness in converting organic compounds in industrial pollutants to CO_2 and H_2O.[1] The CWAO process is economic and environmentally friendly and more suitable for organic pollutants which are too dilute to be incinerated and too concentrated to be treated by a biological process.[1] CWAO is a green process which can operate at mild temperatures and pressures in the presence of a highly active catalyst, which positively influences the economics of the wastewater treatment operations.

However, the CWAO process has several drawbacks which limit its industrial application. These include the lack of stable, highly active and low cost catalysts (without noble metals). Therefore, a lot of research effort has been focused on the development of an active and robust catalyst, which can reduce the severity of the reaction conditions of the CWAO process, making it a possible commercial technology.[2,3] Clay minerals modified by pillaring have recently been found as potential catalytic materials for removal of refractory organic pollutants in wastewater. The clay minerals are abundant in nature, cheap and environmental friendly. The modification by pillaring involves intercalation of large polyoxocation in the interlayer space of the natural clay, which improves thermal and mechanical stability, porosity and BET surface area, basal spacing and accessibility to its acid sites.[1,4–6] The intercalation of clays using polyoxocation solutions containing two cations has been reported to improve thermal stability and catalytic properties.[7,8]

Nevertheless, the synthesis of pillared inter-layered clays (PILCs) using the conventional method has drawbacks such as prolonged synthesis times and high water consumption. This makes the pillaring process not economically scalable to industrial production. Therefore, the use of advanced green chemistry synthesis methods such as microwave radiation and ultrasound treatment has gained considerable attention with many studies aimed to reduce time and energy costs.[9] Timofeeva *et al.* reported that the micropore volume and the overall surface area of Al-PILCs can be affected by degree of hydrolysis of a pillaring solution (0.5 < OH/Al < 2.5) and the optimum OH/metal ratio was 2.2.[10] They discussed in details the effects of OH/(Fe + Al) ratio, aging time of Fe, and Al containing pillaring solution on physicochemical properties of Fe, Al-pillared clays. Shin *et al.*[11] observed the increase in total surface area,

[a]*Molecular Sciences Institute, School of Chemistry, University of the Witwatersrand, Johannesburg, South Africa. E-mail: john.moma@wits.acza*

[b]*Advanced Materials Division, MINTEK, 200 Malibongwe Drive, Randburg 2125, South Africa*

† Electronic supplementary information (ESI) available. See DOI: 10.1039/c8ra05825c

This journal is © The Royal Society of Chemistry 2018

micropore area and pore volume with aging time of the Al_{13}-solution because of the transformation of Al_{13}^{7+} into $Al_{24}O_{72}$ (Al_{13} dimer) and other polyoxocation. Gil *et al.*[12] reported that the higher Al/Fe and OH/(Al + Fe) ratios, the larger the amount of Al/Fe polyoxocation that forms in solution. Al/Fe-PILCs have been used in many studies as an effective catalyst in oxidation of phenol and chlorophenol in water by catalytic wet oxidation using hydrogen peroxide as oxidant.[13–16] Very limited studies have investigated the use of PILCs in the CWAO process using oxygen as oxidant, taking into account the drawbacks of the synthesis methods of the pillaring agents solutions.[1,3] Consequently, up to date, there is still great research interest to develop novel synthesis methods for PILCs that are economically viable. Ultrasonic treatment during the synthesis procedure has been reported to significantly reduce the synthesis time as well as water consumption. Numerous studies reported the use of ultrasound treatment method during aging of the pillaring solution and intercalation to decrease the synthesis time as well as the volume of water used in the pillaring process by approximately by 95%.[9,17,18]

Therefore, this study, Al/Fe-PILCs catalysts were synthesized using ultrasound treatment by direct addition of natural bentonite clay into the polyoxocation solutions containing Al and Fe metals followed by intercalation through ion exchange. The Al/Fe-PILCs were tested for CWAO of phenol in aqueous solutions. Finally, the catalyst stability and its regeneration were also investigated.

2. Materials and method

2.1 Materials

Bentonite clay was obtained from ECCA Holdings (Pty) Ltd., (Cape Town, South Africa). The natural bentonite clay was used without any further purification or cation exchange, sieving or refining. Analytical grade NaCl, Na_2CO_3, $Al(NO_3)_3 \cdot 9H_2O$, $Fe(NO_3)_3 \cdot 9H_2O$, HCl and NaOH were obtained from Merck Chemicals (Pty) Ltd. Phenol was obtained from Sigma Aldrich Chemical Co. Analytical-grade hydroquinone, benzoquinone, catechol, oxalic acid, acetic acid, maleic acid, malonic acid and formic acid used to prepare standards intermediates solutions were also purchased from Sigma-Aldrich Chemical Co. Acetic acid and methanol of chromatographic grade was obtained from Merck.

2.2 Preparation of Al/Fe pillared bentonite clay

2.2.1 Preparation of pillaring solutions. The Al pillaring solution was prepared by dropwise addition of NaOH solution (0.4 M, 500 mL) into a solution of $Al(NO_3)_3$ (0.4 M, 250 mL) under vigorous stirring. After continuous stirring for 120 min, the resulting solution was ultrasonicated at room temperature for 10 min. The Fe pillaring solution was also prepared by dropwise addition of NaOH solution (0.4 M, 500 mL) into a solution of $Fe(NO_3)_3$ (0.4 M, 250 mL) solution under vigorous stirring, followed by the same procedure as above. The mixed Al/Fe pillaring solutions with different Al/Fe molar ratios were prepared by slowly addition of NaOH (0.4 M) into a mixture of $Al(NO_3)_3$ (0.4 M, 250 mL) and $Fe(NO_3)_3$ (0.4 M, 250 mL) solutions under vigorous stirring until an $[OH^-]/[Al^{3+} + Fe^{3+}]$ molar ratio of 2 : 1 was reached. The concentrations used for the synthesis single and mixed pillared bentonite clay in this study was adapted from various literature reports.[19–22] Then the resulting solution was ultrasonicated for 10 min to obtain the Al/Fe pillaring agent solution.

2.2.2 Preparation of Al-PILCs, Fe-PILCs and Al/Fe-PILCs catalysts. The pillared clay catalysts were prepared from bentonite clay using ultrasonic treatment method according to the modified method described previously.[18] The exchange process of the bentonite clay was carried out with each of the pillaring solutions of Al, Fe or Al–Fe (Al/Fe molar ratios of 1 : 3, 1 : 1, 3 : 1 and 6 : 1). The dry natural bentonite clay was added directly into pillaring solutions at a ratio of 25 mL of pillaring solution per gram of clay and vigorously stirred at 25 °C for 30 min. The resulting suspension was ultrasonicated for 10 min at 25 °C to perform the ion exchange. The suspension was centrifuged and the solid component washed with high purity water (5 times each with 200 mL portions) to remove any unreacted nitrates. The solids obtained were oven-dried at 120 °C in air for 16 hours and calcined at 500 °C for 120 min. The prepared PILCs samples were referred as Al-PILCs, Fe-PILCs, Al/Fe-PILCs (1 : 3), Al/Fe-PILCs (1 : 1), Al/Fe-PILCs (3 : 1), Al/Fe-PILCs (6 : 1), respectively.

2.3 Catalysts characterization

The high-resolution scanning electron microscope (HRSEM) imaging and chemical analysis of the raw and PILCs samples were obtained using FEI Nova NanoSem 200. The chemical compositions of the samples were determined by semi-quantitative energy dispersive X-ray (EDX) spectrometry using an Oxford INCA instrument (Oxford instruments, UK). Zetasizer (Malvern Instruments, UK) was used to obtain zeta potential values of the samples at different pH values in order to determine their points of zero charge (pH_{zpc}). Cation exchange capacity (CEC) was determined using the Kjeldahl method described elsewhere.[6] 0.2 g of each material was saturated with 1 M ammonium acetate solution, followed by washing with methanol and five repeated washing with high purity water. The retained ammonium ions were then determined by the unit Kjeldahl method. The powder X-ray diffraction (PXRD) patterns of the samples were obtained from 5 to 80° of 2θ range by a high resolution Bruker AXS D8 X-ray advanced powder diffractometer with CoKα-radiation (40 kV, 40 mA, 1.78897 Å) using a LynxEye detector at scanning speed of 0.02° s^{-1}. The basal spacing (d_{001}) values were also determined using XRD patterns recorded. Isotherms of nitrogen adsorption–desorption of raw bentonite clay, Bt and PILCs were measured using the Micromeritics ASAP TriStar 3000 equipment. The samples were degassed under vacuum at 150 °C for 4 h. The specific surface area (S_{BET}) of the samples were obtained by the BET method and the total pore volume (V_t) was calculated at a relative N_2 pressure of $P/P^0 \sim 0.99$, at liquid nitrogen temperature of −196 °C. Pore size distribution in the mesopore range was calculated using the Barrett–Joyner–Halenda (BJH) method based on the desorption

This journal is © The Royal Society of Chemistry 2018

arm of the isotherms. Fourier transform infrared (FTIR) spectroscopic data was determined using a Varian 640-IR FTIR spectrometer with a miracle single bounce diamond ATR (attenuated total reflectance) cell from PIKE Technologies. The FTIR spectra of the samples were recorded at 25 °C between the wavenumbers ranging from 400 to 4000 cm^{-1} with resolution of 4 cm^{-1}. Thermogravimetric (TGA) analysis was carried out on simultaneous thermal analyser (STA) instrument (Perkin-Elmer model 6000) by heating about 5–10 mg of the samples under N_2 flowing at 20 mL min^{-1} at linear heating rate of 10 °C min^{-1} from 35 °C to 800 °C.

2.4 Catalytic wet air oxidation of phenol

The catalytic activities of Al-PILCs, Fe-PILCs and Al/Fe-PILCs catalysts were investigated using the CWAO of phenol solution as a model pollutant through a continuously stirred high-pressure stainless steel autoclave semi-batch reactor equipped with a magnetically driven stirrer. The initial pH of the phenol solutions was adjusted to the desired pH value of 3 by adding 1 M NaOH or HCl solutions prior to CWAO experiments. All experiments were performed at optimal values determined in our preliminary investigations as indicated in ESI (Fig. S3–S7†). The initial concentration of phenol solutions was prepared at 1000 mg L^{-1} and the amount of catalyst was 2 g L^{-1}. The reactor content was stirred vigorously for about 60 min in the dark at the desired temperature prior to the reaction. The air in the reactor was removed by purging the reactor system with pure nitrogen three times before nitrogen pressure of 5 bars was maintained for 5 min. The reactor content was heated to the desired temperature of 100 °C with the stirrer set at 800 rpm. Once the reactor content had reached the desired temperature, pure oxygen at the desired pressure at 10 bars was supplied to the reactor for the duration of the reaction. 5 mL samples were withdrawn periodically during the reaction and filtered using a micro filter of 0.45 μm pore size prior to analysis. The phenol concentration in the liquid samples was determined using high performance liquid chromatography (HPLC) method with an ODS-3 column and a UV detector (LC-10AD, Shimadzu, Kyoto, Japan). A methanol/water mixture (60/40 v/v) was used as mobile phase. The flow rate of the mobile phase was 1 mL min^{-1}. Total organic carbon (TOC) of the effluents was measured by a TOC analyzer to evaluate the mineralization degree in the CWAO of phenol. All experimental data analyses were conducted in triplicate, and the average values were used in the calculations.

2.5 Catalyst stability and its reusability studies

The metal leaching from the solid catalysts during CWAO of phenol reactions were determined by inductively coupled plasma-atomic emission spectrometer (ICP-AES) spectroscopy. The CWAO experiments were carried out in the same way as the main CWAO experiments at optimal conditions (catalyst loading of 2 g L^{-1} with 1000 mg L^{-1} initial phenol concentration solution at initial pH of 3). After determining the performance of the Al/Fe-PILCs catalyst in each reaction, the used catalyst was recovered by separating the catalyst solids from liquid phase at the end of each catalytic run. Then the solid catalyst was added into 100 mL of $CaCl_2$ solution (4%) to remove organics adsorbed on surface of the catalyst and stirred for 120 min at 25 °C and then washed with high purity water. The recovered catalysts were oven-dried at 120 °C for 5 hours, and characterized by PXRD and surface area analyses. The recovered catalyst was then reused for the same reaction under the same conditions.

3. Results and discussion

3.1 Physicochemical characterization

The surface morphology of the natural bentonite clay and PILCs catalysts samples are shown in ESI (Fig. S2†). According to SEM micrographs, the natural bentonite clay as well as the pillared bentonite clay samples showed a tightly packed pattern with rough surface. The EDS results showed the existence of Fe in the sheets of pillared bentonite clay catalysts. The mechanical structure of natural bentonite clay was not destroyed by the pillaring process (also confirmed by the XRD results). Table 1 shows the chemical composition of the natural and pillared bentonite clay samples, as obtained from EDS analysis. The chemical composition results revealed that the natural bentonite clay contained high amounts of oxides of Si^{4+} and Al^{3+} with exchangeable interlayer cations such as Na^+, Mg^{2+}, Ca^{2+}, K^+ and Fe^{3+}. The high content of Si/Al indicate the high amount of quartz and muscovite in the starting natural bentonite clay.[23] However, after modification by pillaring, the Si/Al ratio decreased as results of removal of the quartz. The high content of Na^+ than Ca^{2+} in the natural bentonite clay might be the indication that the interlamellar cation is sodium, therefore having a high swelling and cationic exchange capacities.[24] The increase of Al^{3+} and Fe^{3+} cations and the decrease of Na^+, Mg^{2+}, Ca^{2+} and K^+ exchangeable cations in the pillared bentonite clay

Table 1 Physicochemical characteristics of natural and pillared bentonite clay samples by EDX, CEC and XRD

Sample	Al/Fe ratio	Na (%)	Mg (%)	Al (%)	Si (%)	K	Ca	Fe	Si/Al	CEC (meq/100 g)	d_{001}
Bentonite	—	3.73	2.29	15.31	65.09	2.39	2.09	9.10	4.25	78.6	1.24
Al-PILCs	—	0.96	1.24	31.98	59.14	1.82	0.27	4.55	1.85	40	1.52
Fe-PILCs	—	0.93	1.22	13.73	52.42	1.42	0.16	30.12	3.82	27	1.56
Al/Fe-PILCs	1 : 3	0.96	2.08	19.98	56.80	56.80	0.13	18.61	2.84	23	1.59
Al/Fe-PILCs	1 : 1	0.97	1.35	21.88	57.19	57.19	0.15	17.01	2.61	20	1.61
Al/Fe-PILCs	3 : 1	0.91	1.25	20.55	57.70	57.70	0.14	17.97	2.81	21	1.69
Al/Fe-PILCs	6 : 1	0.86	1.79	21.78	56.75	56.75	0.15	16.99	2.61	31	1.64

samples confirmed the insertion of the Al^{3+} and Fe^{3+} Keggin ion between the bentonite clay sheets.

The cation exchange capacity (CEC) is one of the most significant properties of bentonite clay that is mainly related to the cation adsorption ability and surface functionalization. The CEC of natural and pillared bentonite clay was measured by the ammonium acetate exchange according to the Kjeldahl method and the results obtained are illustrated in Table 3. The CEC value of natural bentonite clay was about 78.6 meq/100 g which is in good agreement with well-known CEC value of South African natural bentonite clay of >60 meq/100 g.[23] As it can be seen in Table 1, the CEC values of single and mixed pillared clays samples shows a decrease (from 78.6 to 21 meq/100 g) compared to natural bentonite clay, therefore, demonstrating that the exchangeable cations were replaced by $A1^{3+}$ and Fe^{3+} pillars incorporated into the natural bentonite clay during pillaring process. Moreover, the decrease of CEC of the natural bentonite clay after pillaring suggests the irreversibility of cation exchange process.

The XRD patterns of the natural and pillared bentonite clay are shown in Fig. 1. The XRD results confirm the successful pillaring of the natural bentonite clay material in all cases. Table 1 shows the results of basal spacing (d_{001}) values of natural and pillared bentonite clay. The d_{001} values of all pillared bentonite clay samples increased after pillaring, which further confirmed the intercalation of the metal oxides pillars into the interlayer space of the bentonite clay. The basal spacing of the mixed metal oxide pillared clays are higher than those of the single metal oxide pillared clays as shown in Table 1. The increased basal spacing observed in the Al-PILCs can be attributed to the size of Al oligomers $[AlO_4Al_{12}(OH)_{24}(H_2O)_{12}]_7$ that was greater than the Fe oligomer $Fe_3(OH)_4^{5+}$.[14] The XRD patterns in Fig. 1 show well-defined reflections at 2 theta value of 7.40° which correspond to d_{001} value of 1.24 nm which is a typical characteristic peak of natural sodium bentonite clay, revealing that the predominant exchangeable cation could be sodium, as suggested by EDS analysis (see Table 1). Moreover, the natural bentonite clay matrices contain mineral impurities such as quartz, muscovite and calcite.[25,26] After modification by pillaring with Al and Fe, the (001) reflections shifted to lower 2 theta values, which resulted in an increase in d_{001} values from 1.24 nm to 1.69 nm. Meanwhile, no noticeable reflections of any crystalline phase of Fe oxides in Fe pillared bentonite clay samples are observed, as they would likely show a significantly lesser degree of crystallization. It is noteworthy that the natural bentonite clay structure was not negatively altered after pillaring, since the peaks observed in natural bentonite clay were retained, which is in agreement with the findings reported by Chen *et al.*[27] As reported by Jia *et al.* the ratio of Al/Fe influences the size of pillaring, and the sample with Al/Fe ratio 3 : 1 displays the highest basal spacing of pillared bentonite clay.[28] These findings were similar to those reported in the literature for single and mixed metal oxides of Al and Fe pillared bentonite clay.[1,29,30]

The pH point of zero charge (pH_{zpc}) of the catalyst is an important parameter to determine the pH at which the surface has net electrical neutrality and surface charge plays a main role in the adsorption of ionisable pollutants into catalyst from aqueous solutions. The surface charge results of the natural and pillared bentonite clay used in this study are shown in Fig. 2. According to the literature and the results obtained in this study the natural bentonite clay displayed negative zeta potential values without an isoelectric point over the entire pH range (1–10) studied.[23,27,31] The pH_{zpc} values of Al-PILCs, Fe-PILCs, Al/Fe-PILCs (1 : 3), Al/Fe-PILCs (1 : 1), Al/Fe-PILCs (3 : 1) and Al/Fe-PILCs (6 : 1) were found to be 5.4, 5.7, 3.3, 3.4, 3.7 and 4, respectively, whereas the pH_{zpc} value of natural bentonite clay was not observed. The negative zeta potential values of natural bentonite clay can be supported by the fact that bentonite clay particles comprise of a permanent negative charge arising from isomorphous substitution of structural Si^{4+} by Al^{3+} and OH groups pH dependent charge at the edges of the bentonite clay particles. Therefore, the obtained decrease in negative zeta potential from −28.6 to −17.5 mV with increasing H^+ ions in the solution can be attributed to pH dependent charge. However, after pillaring of natural bentonite clay with Al^{3+} and Fe^{3+}, the obtained pillared clay solid materials had positive zeta potential values at pH > 3.3 and pH < 5.7. The positive and negative zeta potential values of pillared clays at acidic and basic pH, respectively, can be attributed to predominant pillared

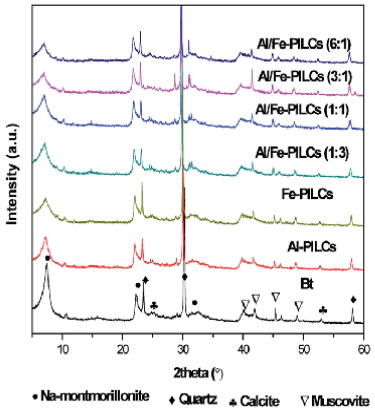


Fig. 1 X-ray diffraction spectra of natural and pillared bentonite samples clays.

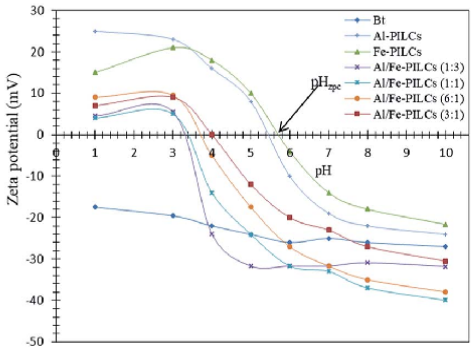


Fig. 2 Zeta potentials for different pH values of natural and pillared bentonite clay.

This journal is © The Royal Society of Chemistry 2018

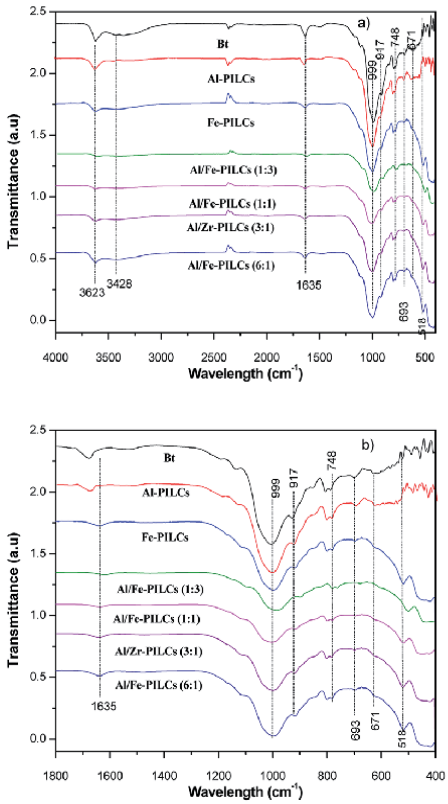


Fig. 3 FTIR spectra of natural (Bt) and pillared bentonite clay catalysts; (a) wide range wavelength and (b) low range wavelength.

bentonite clay surface species. For example $Fe(II,III)OH_2^+$ and $Al(III)H_2^+$ are predominant species at acidic pH whereas $Fe(II,III)O^-$ and $Al(OH)_4^-$ are predominant bentonite pillared clay surface species at basic pH. The pH_{zpc} values of single metal oxide pillared clay were found to be lower compared to mixed metal oxides pillared clay. This can be attributed to the fact that the mixed oxides of Al/Fe polyoxycations are presented as $\{[Al_xFe_y(OH)_z(H_2O)_n]^{(3x+3y-z)+}\}$, which is a predominant species on the surface of Al/Fe-PILCs and results in an increase of hydroxyl groups. This then causes a decrease of positive charges and pH_{zpc} values. The significance of these zeta potential values is that conversion of phenol is expected to be flexible below the obtained pH_{zpc} values of pillared clays since the net positively charged of pillared clays is likely to attract the phenol anions.

Shown in Fig. 3 is the FTIR analysis of natural and pillared bentonite clay. It can be seen from the FTIR spectra that there are no significant differences between the FTIR spectra of the natural and pillared bentonite clays, suggesting that the structure of natural bentonite clay was not affected by pillaring process. These findings are in agreement with both the SEM and XRD analysis results in this study. However, decreases of the peaks at 3623 cm^{-1} and in the range of 400 to 999 cm^{-1}, were observed for bentonite pillared clay catalysts, with more peak decrease in the mixed metal oxides compared to single metal oxides pillared catalysts. This can be attributed to the interactions between Al, Fe or Al/Fe mixed polyoxocations with Si–O group in the siloxane layers (silica tetrahedron plates) and Al–OH group in the alumina octahedral layers.[32,33] The absorption band located at 3623 cm^{-1} is ascribed to O–H stretching vibrations of non-hydrogen-bonded water region while the relatively weak absorption bands at 3428 cm^{-1} is also attributed to O–H stretching vibrations but of hydrogen-bonded water region.[34] The peak at 1635 cm^{-1} can be assigned to the H–O–H bending vibration.[34] The strong intense peak near 999 cm^{-1} corresponds to the in-plane Si–O–Si stretching vibrations.[28] The absorption band at 917 cm^{-1} is ascribed to Al–O(OH)–Al deformation, and the peaks situated at 518 cm^{-1}, 671 cm^{-1}, 693 cm^{-1} and 748 cm^{-1} corresponds to the deformation of Si–O–Fe, Si–O–Al, coupled Al–O and Si–O out of plane stretching vibration and Si–O–Mg, respectively.[28,34] The absorption bands corresponding to Fe–O–Fe vibration of Fe-bentonite were not detected. Similar findings were reported by Chen and Zhu who reported that this might be due to the characteristic stretching vibrations of natural bentonite clay mineral.[35]

The nitrogen adsorption–desorption measurements were investigated on both natural and pillared clays in order to determine porosity and BET surface area. The corresponding parameters such as BET surface area, total pore volume, micropores volume and pore diameter are summarised in Table 2. The obtained BET surface area and total pore volume of PILCs are much higher compared to natural bentonite clay. This indicates that the modification of natural bentonite clay by pillaring results in a significant increase in porosity and BET surface area. The BET surface areas of the mixed metal catalysts are higher than those of the single metal catalysts, which suggest that introduction of second metal ions greatly

Table 2 Surface properties of prepared catalysts and raw bentonite clay

Sample	Al/Fe ratio	S_{BET}[a] ($m^2\ g^{-1}$)	V_{pore}[b] ($cm^3\ g^{-1}$)	V_{mic}[c] ($cm^3\ g^{-1}$)	d_{pore}[d] (nm)
Bentonite	—	61	0.11	0.089	15.31
Al-PILCs	—	140	0.30	0.102	31.98
Fe-PILCs	—	147	0.32	0.099	13.73
Al/Fe-PILCs	1 : 3	175	0.34	0.110	19.98
Al/Fe-PILCs	1 : 1	190	0.35	0.111	21.88
Al/Fe-PILCs	3 : 1	200	0.37	0.113	20.55
Al/Fe-PILCs	6 : 1	169	0.33	0.105	21.78

[a] Specific surface area (S_{BET}). [b] Total pore volume at $P/P^0 \sim 0.99$. [c] Micropore volume. [d] Pore diameter.

improved the BET surface area and porosity. The increase in the BET surface areas of pillared natural bentonite samples may be attributed to the increase of micropores volume and enlarged total pore volume of micropores. The pore diameter of mixed metal composite catalysts greatly decreased compared to single metal catalysts, which positively impact the catalytic properties of mixed composite PILCs.

The thermograms and their derivative curves for both natural bentonite and the pillared bentonite clay samples carried out between 35 and 900 °C are shown in Fig. 4. As can be seen in Fig. 4, thermal analysis (TGA/DTG) of the natural bentonite clay and pillared bentonite clay samples showed a similar thermal behaviour, in which the mass loss for all the samples occurs in three stages. All the Al/Fe-PILCs samples display relatively small weight losses even at high temperatures compared with the Al and Fe-PILCs as well as the natural clay. As shown in Fig. 4 the TGA curves show an initial weight loss of 2.2%, 2.1%, 1.9%, 0.8%, 0.6%, 0.5% and 0.3% for natural bentonite, Al-PILCs, Fe-PILCs, Al/Fe-PILCs (1 : 3), Al/Fe-PILCs (1 : 1), Al/Fe-PILCs (3 : 1) and Al/Fe-PILCs (6 : 1), respectively, starting at 38 °C and ending at 156 °C. The major decomposition occurred above 554 °C and total weight loss at 900 °C was 23.5%, 18.1%, 12.3%, 12.0%, 11.8%, 10.5% and 9%, respectively for natural bentonite, Al-PILCs, Fe-PILCs, Al/Fe-PILCs (1 : 3), Al/Fe-PILCs (1 : 1), Al/Fe-PILCs (3 : 1) and Al/Fe-PILCs (6 : 1). This can be attributed to the fact that the Al and Fe polycations introduced in the layers of the clay form thermally stable oxides during the heat treatment in the pillaring process which prevents the collapse of the clay layers.[28,36] The derivative plot of the thermal gravimetric analysis (DTG) showed three peaks for natural bentonite clay, Al-PILCs, Fe-PILCs and Al/Fe-PILCs samples in the range of 36–150 °C, 388–487 °C and 576–721 °C. The peaks observed can be attributed to oxidation state of Al or Fe polycations used during the pillaring process.[28] For example oxidation state of Fe are Fe^{2+}, Fe^{3+} and Fe^{6+}, which resulted in three peaks. The first peak was due to the loss of physical adsorbed water molecules from the interlayer space.[29] The second small peak corresponds to the structural dehydroxylation of the clay mineral.[37] Finally the third step is attributed to the thermal decomposition of the layered pattern of the bentonite clay.[30,38] This is consistent with the literature where there are reports of the thermal stability of the bentonite pillared clays up to 650 °C.[39]

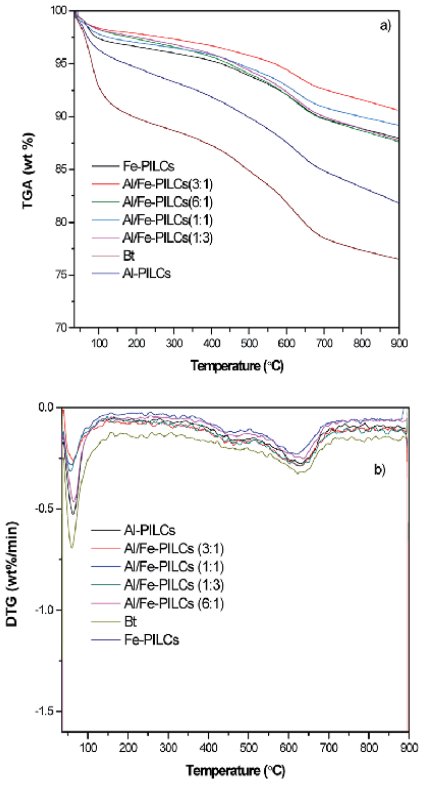


Fig. 4 Thermogravimetric analyses (TGA) (a) and their derivative plots (DTG) (b) for natural and pillared bentonite clay samples.

3.2 Catalytic wet air oxidation of phenol

The performance of the catalyst samples in the catalytic wet air oxidation of phenol are shown in Fig. 5. The conversion of phenol was negligible in the absence of catalyst, showing that phenol is extremely stable under non-catalysed reaction conditions. The conversion of phenol was very low (8%) in the presence of natural bentonite clay due to the absence of catalytic active sites and also due to highly negative charge of natural bentonite clay (as shown in Fig. 2) resulting in repulsion between its particles and negatively charged phenol. However, the pillared clay catalysts yield a very high phenol conversion, with the Al-PILCs and Fe-PILCs giving 74 and 85% conversion respectively over reaction time of 120 min and complete conversion at 180 min. The Al/Fe-PILCs showed higher activities with total conversion of phenol occurring at 120 min of reaction time. The order of the activities of the catalysts is Al-PILCs < Fe-PILCs < Al/Fe-PILCs (6 : 1) < Al/Fe-PILCs (1 : 3) < Al/Fe-PILCs (1 : 1) < Al/Fe-PILCs (3 : 1) with the most active catalyst being the Al/Fe-PILCs with a Al : Fe molar ratio of 3 : 1. Furthermore, TOC removal in the phenol oxidation by adsorption and in the absence of a catalyst (WAO) was negligible. In contrast, using pillared bentonite clay catalysts, the removal of TOC was significantly increased, 55%, 58%, 65%, 68%, 75% and 80% being achieved in less than 180 min with Al-PILCs, Fe-PILCs, Al/Fe-PILCs (6 : 1), Al/Fe-PILCs (1 : 3), Al/Fe-PILCs (1 : 1) and Al/Fe-PILCs (3 : 1), respectively. This observed trend in the performance of the catalysts can be attributed to the fact that pillaring of the clay imparts improved surface electrical properties as well as new functional groups in the clay. The zeta potentials of all the pillared clay samples were positive at pH below pH_{zpc} which indicate a positively charged surface of pillared clay samples. Therefore, the positive charge surface promotes the adsorption of phenol, which consequently increases oxidation of phenol on the catalyst surface. The larger BET surface area of the pillared clay samples also provides more active sites for oxidation reaction of phenol. The catalytic results show promise in the use of pillared clays as catalysts in catalytic wet oxidation reaction

This journal is © The Royal Society of Chemistry 2018

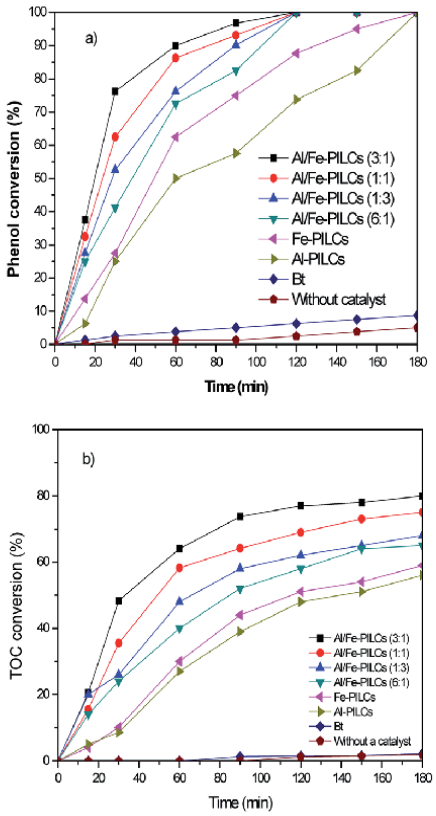


Fig. 5 Phenol (a) and TOC (b) conversions in the CWAO reaction of phenol over the natural and pillared bentonite clay samples (experimental conditions: 200 mL of reaction solution, 1000 mg L^{-1}, 0.4 g of catalyst, pH 3.0, 10 bar and 100 °C).

especially as the reaction here is carried out under mild conditions.

Table 3 summarizes a comparison of the performance of Al/Fe-PILCs catalyst in this study with some representative catalysts discussed in the literature for the CWAO of phenol in wastewater. To date very few published studies focused on the use of Al/Fe-PILCs in CWAO,[1,3] most of studies widely reported the use of Al/Fe-PILCs with costly hydrogen peroxide (H_2O_2) oxidant.[13–16,40] Therefore, the Al/Fe-PILCs in this study was also compared with other developed CWAO heterogeneous catalysts such as carbon materials (reduced graphene oxides, multi-walled carbon nanotubes…), noble metals catalysts (Ru, Pt…) and transition metal oxides (MnO_2, Fe_2O_3…).[41–43] As shown in Table 3, complete phenol oxidation and TOC removals can be accomplished at relatively faster oxidation rates, however, at high reaction conditions are temperatures (>100 °C) and pressures (>10 bar); these severe reaction conditions are strongly influenced by lack of robust catalysts which can be used under mild conditions.[44] In order to make CWAO process feasible at industrial scale, in the last decade a lot of attention has been paid to developing heterogeneous catalysts that can be used under mild conditions to reduce the costs for CWAO process. The Al/Fe-PILCs catalysts developed in this study show good catalytic performance under mild reaction conditions compared to most of the listed catalysts in Table 3. In generally the use of natural clay and transitional metal oxides as active phase reduces the preparation cost of the synthesized pillared clay catalysts in the present study.

According to the literature CWAO of phenol by hydroxyl radical takes place involving a free radical chain reaction.[45,46] Timofeeva *et al.* reported that the important step in the phenol oxidation in the presence of heterogeneous Fe-containing system is a formation of strong oxidation species such as $HO^{\bullet}$ radical compared to unreactive $O_2^{-\bullet}$ and $HO_2^{\bullet}$ radicals. The $HO^{\bullet}$ radical could rapidly oxidize the phenol through direct conversion to CO_2 and H_2O and *via* formation of aromatic intermediates such as hydroquinone and pyrocatechol.[47,48] Further hydroxylation of formed aromatics intermediates led to the formation of benzoquinone which transform into short-chain carboxylic acids such as maleic, malonic, oxalic, formic and acetic acids.[49] The intermediates of phenol oxidation were analyzed by HPLC and identified by comparison with selected commercial standards in this study. Fig. 6 shows the evolution of the intermediates and concentration profiles of phenol in the CWAO of phenol over Al/Fe-PILCs (Al : Fe = 3 : 1) as catalyst. The analysis of HPLC data detected the generation of intermediates such as hydroquinone and

Table 3 Performance comparison of various CWAO heterogeneous catalysts for phenol oxidation

Catalyst	Reactor	Conditions	Results	Ref.
MWCNTs	Batch	$T = 155$ °C, $P = 25$ bar, [pH] in = 1000 mg L^{-1}, $t_{reaction} = 120$ min	[pH] = 100%, [TOC] = 80%	42
GO	Batch	$T = 155$ °C, $P = 25$ bar, [pH] in = 1000 mg L^{-1}, $t_{reaction} = 120$ min	[pH] = 100%, [TOC] = 84%	41
$MnCeO_x$	Batch	$T = 150$ °C, $P = 9$ bar, [pH] in = 50 mg L^{-1}, $t_{reaction} = 60$ min	[pH] = 100%, [TOC] = 80%	44
(Ru,Pt)–TiO_2–CeO_2	Batch	$T = 160$ °C, $P = 20$ bar, [pH] in = 2098 mg L^{-1}, $t_{reaction} = 180$ min	[pH] = 100%, [TOC] = 88%	43
Al/Fe-PILCs	Batch	$T = 160$ °C, $P = 25$ bar, [pH] in = 2098 mg L^{-1}, $t_{reaction} = 180$ min	[pH] = 100%, [TOC] = 80%	1
Al/Fe-PILCs	Batch	$T = 100$ °C, $P = 10$ bar, [pH] in = 1000 mg L^{-1}, $t_{reaction} = 120$ min	[pH] = 100%, [TOC] = 80%	Current study

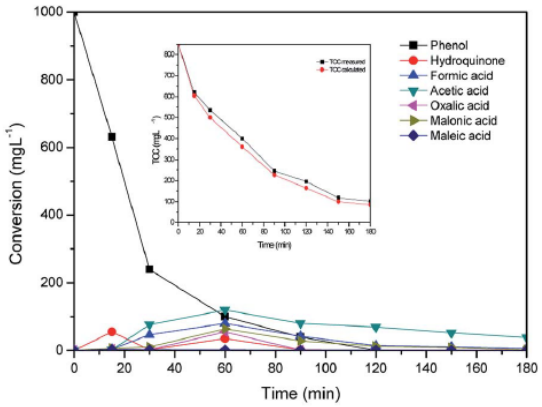


Fig. 6 Evolution of phenol and intermediates in the CWAO of phenol over the Al/Fe-PILCs (3 : 1).

short chain carboxylic acids (acetic and maleic acids) after 15 min of phenol oxidation reaction. At 60 min reaction time the concentration of the intermediates (maleic, acetic, formic, oxalic, malonic acids, as main intermediates, benzoquinone and pyrocatechol, as traces, below 10 mg L^{-1}) increase as phenol gets oxidized. However, after 120 min of the reaction the concentration of the intermediates becomes insignificant. The detected intermediates during the reaction did not accumulate in large quantities in the phenol reaction solution as they are rapidly oxidised by highly active hydroxyl radicals to form CO_2, H_2O and less harmful intermediates such as acetic acid. This behaviour can be attributed to the resistance of low-molecular-weight short chain carboxylic acids to CWAO, consistent with previous studies.[49,50] The Al/Fe pillared bentonite clay catalyst exhibited good catalytic activity in the CWAO of phenol, since complete oxidation of phenol was achieved with formation of less harmful intermediates. The content of these carboxylic acids intermediates can be calculated by TOC concentration and about 80% TOC conversion was obtained. The actual measured TOC and the calculated TOC by the identified intermediates were compared and results are shown in Fig. 6 (inset). As shown in Fig. 6 (inset), the two curves of TOC conversion with reaction time can be well fitted together, suggesting that the main intermediates are detected by HPLC in the CWAO of phenol in aqueous solution.

3.3 Catalyst stability and reusability

For practical applications, it is important to determine the stability and reusability of catalysts. The stability and reusability of the Al/Fe-PILCs (with Al/Fe ratio of 3 : 1) catalyst against metal leaching during the reaction was investigated in this work. To study the leaching of Fe^{3+} metal cations from pillared clay catalyst, concentration of total Fe^{3+} ions in the solution after 120 min of reaction time were measured and the results presented in Table 4. The catalyst was reused seven times to investigate its reusability. The results indicate that the concentration of Fe^{3+} ions leached in the solution after the reaction was ≤0.295 mg L^{-1} which is below the World Health Organization (WHO) maximum permissible level (0.3 mg L^{-1}) in drinking water after seven consecutive catalytic runs.[51] The results demonstrate that the pillared clay catalyst has good stability towards leaching of Fe^{3+} after the phenol oxidation reaction, since the leaching of Fe^{3+} was found to be negligible. The observed leaching could be attributed to the iron sites decorating the bentonite clay pillars, whereas the metal incorporated within the structure of the mixed bentonite clay pillars has been thought to be the most active in the catalytic wet air oxidation of phenol.[8] This confirms that the pillaring cations were well incorporated in the pillar structure of the catalyst. After seven consecutive reaction runs the phenol removal slightly decreased from 100 to 85% in 120 min reaction time. The slight decrease in catalytic activity can be attributed to the deposition of phenol on the catalyst surface during the reaction, which results in the blocking of the channels and, thus, to a decrease in the number of available active sites.[2] No significant decrease in surface area as well as in the d_{100} basal spacing of the catalyst is observed with each reuse. However, the TOC conversion decrease significantly from 80% to 50% with recycling times, suggesting that more hydroxylation instead of minimization of phenol took place with increasing consecutive reaction runs. Therefore, as shown in Table 3 three consecutive reaction runs for the Al/Fe-PILCs catalyst were attainable to achieve complete removal of phenol and 71% conversion of TOC in our studies. These results are in agreement with those published by Sassi *et al.* CWAO of phenol using Al/Fe-PILCs.[1] The oxidation of phenol was reported to be 95%, while 80% of TOC removal was obtained at 160 °C under 25 bar of pure oxygen after 180 min of reaction. Less than 0.7 mg L^{-1} of initial Fe species was leached out during the consecutive re-use of the catalyst, indicating that the Fe species were quite stable.

Table 4 Stability, leaching and basal spacing features of reused Al/Fe-PILCs catalyst in the removal of phenol and TOC over optimum conditions

No. of runs	Phenol removal in 120 min (%)	TOC conversion in 180 min (%)	Leaching of Fe^{3+} (mg L^{-1})	d_{001} (nm)
First use	100	80	0.175	1.69
Re-use 1	100	76	0.198	1.66
Re-use 2	100	71	0.214	1.65
Re-use 3	96	65	0.221	1.65
Re-use 4	91	57	0.263	1.64
Re-use 5	87	53	0.275	1.61
Re-use 6	85	50	0.295	1.68

This journal is © The Royal Society of Chemistry 2018

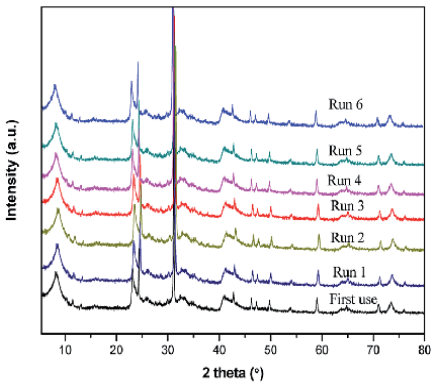


Fig. 7 PXRD patterns of the fresh and reused Al/Fe-pillared clay samples.

3.4 Structural studies of the catalyst after each catalytic run

The spent catalysts were characterized by PXRD to determine the effect of the catalyst re-use on its structure and morphology. Fig. 7 demonstrates results for structural stability of the catalyst after each consecutive catalytic run. After six reuse of the catalyst, its characteristic PXRD peaks are maintained, while there is gradual decrease in the basal spacing. Therefore, our preparation method which employs the use of ultrasonic treatment during the aging and intercalation steps results in a highly stabilized Fe^{3+} species in the pillared clay matrix.

4. Conclusions

Natural bentonite clay was successfully pillared with Al, Fe and Al/Fe polycations using ultrasonic treatment during the aging and the intercalation stages and tested for CWAO of phenol in aqueous solutions. This method resulted in a significant decrease in the consumption of water as well as synthesis time and the catalyst synthesis is performed at room temperature. The PXRD demonstrated an increase in the basal spacing up to 1.69 nm with a high thermal stability. The textual properties show an increase in BET surface area indicating that Al/Fe polycations inserted into the bentonite clay plays a crucial in increasing surface area. HRSEM confirms that this methodology allows interaction of Al/Fe polycations with the tetrahedral sheets of the bentonite clay, without destroying the structure of the clay. The pillared clay catalysts were found to completely oxidize phenol and 80% conversion of TOC in aqueous solution under mild conditions showing the potential of these catalysts to be used in removal of organic compounds from industrial wastewater streams. The analysis of intermediate products revealed the presence of hydroquinone, pyrocatechol, benzoquinone and oxalic, formic, malonic, oxalic, malonic and maleic acids. The Al/Fe-PILCs catalyst could be used in four consecutive reaction runs without significant loss of phenol catalytic activity and 65% conversion of TOC. Therefore, Al/Fe-PILCs catalysts were found to be promising catalysts for CWAO of phenol in aqueous solutions.

Conflicts of interest

There are no conflicts to declare.

Acknowledgements

The authors wish to acknowledge financial support from the National Research Foundation (NRF)/Department of Science and Technology (DST) of South Africa under Professional Development Programme (PDP) Project No. 96719 and Mineral Science Council of South Africa (Mintek) under CWO of Wastewater Project No. ADR31803.

References

1 H. Sassi, G. Lafaye, H. Ben Amor, A. Gannouni, M. R. Jeday and J. Barbier, *Front. Environ. Sci. Eng.*, 2018, **12**, 2.
2 J. Guo and M. Al-Dahhan, *Appl. Catal., A*, 2006, **299**, 175–184.
3 N. Ksontini, W. Najjar and A. Ghorbel, *J. Phys. Chem. Solids*, 2008, **69**, 1112–1115.
4 A. Olaya, S. Moreno and R. Molina, *Catal. Commun.*, 2009, **10**, 697–701.
5 A. Olaya, G. Blanco, S. Bernal, S. Moreno and R. Molina, *Appl. Catal., B*, 2009, **93**, 56–65.
6 S. Mnasri-Ghnimi and N. Frini-Srasra, *Appl. Clay Sci.*, 2014, **88–89**, 214–220.
7 J. Baloyi, T. Ntho and J. Moma, *RSC Adv.*, 2018, **8**, 5197–5211.
8 J. Herney-Ramirez, M. A. Vicente and L. M. Madeira, *Appl. Catal., B*, 2010, **98**, 10–26.
9 A. Olaya, S. Moreno and R. Molina, *Appl. Catal., A*, 2009, **370**, 7–15.
10 M. N. Timofeeva, S. T. Khankhasaeva, Y. A. Chesalov, S. V Tsybulya, V. N. Panchenko and E. T. Dashinamzhilova, *Appl. Catal., B*, 2009, **88**, 127–134.
11 Y.-S. Shin, S.-G. Oh and B.-H. Ha, *Korean J. Chem. Eng.*, 2003, **20**, 77–82.
12 A. Gil, L. M. Gandía and M. A. Vicente, *Catal. Rev.*, 2000, **42**, 145–212.
13 J. H. Ramírez, L. A. Galeano, G. Pinchao, R. A. Bedoya and A. Hidalgo, *J. Environ. Chem. Eng.*, 2018, **6**, 2429–2441.
14 N. R. Sanabria, M. A. Centeno, R. Molina and S. Moreno, *Appl. Catal., A*, 2009, **356**, 243–249.
15 A. Pérez, M. A. Centeno, J. A. Odriozola, R. Molina and S. Moreno, *Catal. Today*, 2008, **133–135**, 526–529.
16 C. B. Molina, J. A. Casas, J. A. Zazo and J. J. Rodríguez, *Chem. Eng. J.*, 2006, **118**, 29–35.
17 E. Ruiz-Hitzky and P. Aranda, *J. Sol-Gel Sci. Technol.*, 2014, **70**, 307–316.
18 F. Tomul, *Appl. Clay Sci.*, 2016, **120**, 121–134.
19 F. Tomul, *Chem. Eng. J.*, 2012, **185–186**, 380–390.
20 F. Tomul, *Ind. Eng. Chem. Res.*, 2011, **50**, 7228–7240.
21 F. Tomul and S. Balci, *Appl. Clay Sci.*, 2009, **43**, 13–20.
22 P. Tepmatee and P. Siriphannon, *Mater. Res. Bull.*, 2013, **48**, 4856–4866.
23 V. Masindi, M. W. Gitari, H. Tutu and M. DeBeer, *Journal of Water Process Engineering*, 2015, **8**, 227–240.

24 M. Vhahangwele and G. W. Mugera, *J. Environ. Chem. Eng.*, 2015, **3**, 2416–2425.
25 J. E. Aguiar, J. A. Cecilia, P. A. S. Tavares, D. C. S. Azevedo, E. R. Castellón, S. M. P. Lucena and I. J. Silva, *Appl. Clay Sci.*, 2017, **135**, 35–44.
26 J. Li, M. Hu, S. Zuo and X. Wang, *Curr. Opin. Chem. Eng.*, 2018, **20**, 93–98.
27 S. Chen, Y. Wu, G. Li, J. Wu, G. Meng, X. Guo and Z. Liu, *Appl. Clay Sci.*, 2017, **136**, 103–111.
28 H. Jia, S. Zhao, X. Zhou, C. Qu, D. Fan and C. Wang, *Arch. Environ. Prot.*, 2017, **43**(3), 82–90.
29 B. González, R. Trujillano, M. A. Vicente, A. Gil, V. N. Panchenko, E. A. Petrova and M. N. Timofeeva, *Appl. Clay Sci.*, 2017, **146**, 388–396.
30 P. Cañizares, J. L. Valverde, M. R. S. Kou and C. B. Molina, *Microporous Mesoporous Mater.*, 1999, **29**, 267–281.
31 S. Türker, F. Yarza, R. M. T. Sánchez and S. Yapar, *Colloids Surf., A*, 2017, **520**, 817–825.
32 J. Manjanna, T. Kozaki and S. Sato, *Appl. Clay Sci.*, 2009, **43**, 208–217.
33 J. Zhou, P. Wu, Z. Dang, N. Zhu, P. Li, J. Wu and X. Wang, *Chem. Eng. J.*, 2010, **162**, 1035–1044.
34 S. Kouraichi, M. El-Hadi Samar, M. Abbessi, H. Boudouh and A. Balaska, *Catal. Sci. Technol.*, 2015, **5**, 1052–1064.
35 J. Chen and L. Zhu, *Sep. Purif. Technol.*, 2009, **67**, 282–288.
36 T. Mishra, in *Pillared Clays and Related Catalysts*, ed. A. Gil, S. A. Korili, R. Trujillano and M. A. Vicente, Springer New York, New York, NY, 2010, pp. 99–128.
37 H. J. Chae, I.-S. Nam, S. W. Ham and S. B. Hong, *Catal. Today*, 2001, **68**, 31–40.
38 D. L. Guerra, C. Airoldi, V. P. Lemos and R. S. Angélica, *J. Hazard. Mater.*, 2008, **155**, 230–242.
39 M. El Miz, S. Salhi, I. Chraibi, A. El Bachiri, M. Fauconnier and A. Tahani, *Open J. Phys. Chem.*, 2014, **4**, 98–116.
40 S. Zhou, C. Zhang, X. Hu, Y. Wang, R. Xu, C. Xia, H. Zhang and Z. Song, *Appl. Clay Sci.*, 2014, **95**, 275–283.
41 S. Yang, Y. Cui, Y. Sun and H. Yang, *J. Hazard. Mater.*, 2014, **280**, 55–62.
42 S. Yang, X. Wang, H. Yang, Y. Sun and Y. Liu, *J. Hazard. Mater.*, 2012, **233–234**, 18–24.
43 A. E. de los Monteros, G. Lafaye, A. Cervantes, G. Del Angel, J. Barbier Jr and G. Torres, *Catal. Today*, 2015, **258**, 564–569.
44 F. Arena, C. Italiano and L. Spadaro, *Appl. Catal., B*, 2012, **115–116**, 336–345.
45 R. R. Zapico, P. Marín, F. V Díez and S. Ordóñez, *J. Environ. Chem. Eng.*, 2017, **5**, 2570–2578.
46 F. Stüber, J. Font, A. Fortuny, C. Bengoa, A. Eftaxias and A. Fabregat, *Top. Catal.*, 2005, **33**, 3–50.
47 A. Santos, P. Yustos, A. Quintanilla, S. Rodríguez and F. García-Ochoa, *Appl. Catal., B*, 2002, **39**, 97–113.
48 A. Quintanilla, J. A. Casas, A. F. Mohedano and J. J. Rodríguez, *Appl. Catal., B*, 2006, **67**, 206–216.
49 G. Yang, H. Chen, H. Qin, X. Zhang and Y. Feng, *Can. J. Chem. Eng.*, 2017, **95**, 1518–1525.
50 A. Eftaxias, J. Font, A. Fortuny, J. Giralt, A. Fabregat and F. Stüber, *Appl. Catal., B*, 2001, **33**, 175–190.
51 D. Pittet, B. Allegranzi and J. Boyce, *Infect. Control Hosp. Epidemiol.*, 2009, **30**, 611–622.

This journal is © The Royal Society of Chemistry 2018

Chapter 5

A novel synthesis method of Al/Cr pillared clay catalysts

This chapter has been reviewed for publication in Catalysis Letters as **Baloyi, J**., Ntho, T., & Moma, J. (2018). A Novel Synthesis Method of Al/Cr Pillared Clay and its Application in the Catalytic Wet Air Oxidation of Phenol. Catalysis Letters, 148(12), 3655-3668.

J. Baloyi – 70% (conducted the research, wrote the first draft and addressed the reviewers comments);

T. Ntho – 15% (industrial (Mintek) supervisor, oversees the handling of experiments and obtained results);

J. Moma – 15% (academic (Wits) supervisor, reviewed the manuscript and approved the revised manuscript).

Catalysis Letters (2018) 148:3655–3668
https://doi.org/10.1007/s10562-018-2579-x

A Novel Synthesis Method of Al/Cr Pillared Clay and its Application in the Catalytic Wet Air Oxidation of Phenol

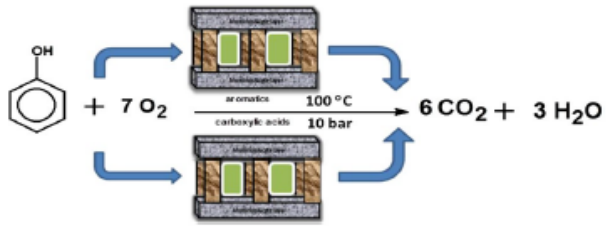
Jeffrey Baloyi[1,2] · Thabang Ntho[2] · John Moma[1]

Received: 15 August 2018 / Accepted: 26 September 2018 / Published online: 29 September 2018
© Springer Science+Business Media, LLC, part of Springer Nature 2018

Abstract

Natural bentonite clay was pillared with Al and Cr polycations (Al-PILCs and Cr-PILCs) as well as with both Al and Cr mixed polycations (Al/Cr-PILCs) at different Al/Cr molar ratios. The structural and textural properties of the pillared clay catalysts were characterized by various techniques, such as high resolution scanning electron microscopy with energy dispersive system, powder X-ray diffraction, adsorption–desorption of N_2 at – 196 °C, Fourier transform infrared spectroscopy, thermogravimetric analysis, cation exchange capacity and zeta potential. The obtained results showed that the intercalation of polycations in the interlamellar space of clay led to changes in the clay properties, basal spacing and specific surface area of a mixed PILCs were higher compared to single PILCs. Moreover, diffractograms of the Cr-PILCs confirmed the presence of a Cr_2O_3 phase. The catalytic wet air oxidation (CWAO) of the phenol was studied in a batchwise slurry reactor, at the experimental conditions of 100 °C temperature, 10 bar oxygen (O_2) partial pressure, at pH 3.0, 100 mg/L concentration and 0.4 g of catalyst. All catalysts were analysed to determine the conversion of phenol and removal of total organic carbon (TOC). The results showed that, Al-PILCs displayed higher removal of phenol and TOC conversion than Cr-PILCs. In the case of mixed Al/Cr-PILCs, maximum removal values of phenol and TOC conversion were achieved with Al/Cr molar ratio of 1:1. Moreover, aromatic intermediate products as catechol, hydroquinone and benzoquinones which are identified in the beginning of the phenol oxidation oxidized into short-chain carboxylic acids such as oxalic acid, maleic acid, formic acid, acetic acid and malonic acid. The obtained results demonstrate the potential of Al/Cr-PILCs catalyst as robust and cheap catalyst for CWAO of phenol under mild reaction conditions.

Graphical Abstract



Keywords Al/Cr-PILCs · Ultrasound treatment · Phenol · Catalytic wet air oxidation

1 Introduction

In recent years, pillared clays (PILCs) have received considerable attention for applications as catalysts and catalyst support due to their excellent catalytic properties such as high specific surface area, porous structure and high thermal stability [1–3]. The PILCs solids are obtained by separating the

Electronic supplementary material The online version of this article (https://doi.org/10.1007/s10562-018-2579-x) contains supplementary material, which is available to authorized users.

✉ John Moma
john.moma@wits.ac.za

Extended author information available on the last page of the article

clay layers through pillaring with an agent such as hydroxyl polycations of polynuclear metals (Al, Fe, Ti, Cr and Zr). These pillaring agents can be intercalated between adjacent layers of clay, maintaining the spacing between adjacent layers upon water removal and improving pore structure [4–6]. The pillaring process involves exchanging the interlayer polycations with large inorganic hydroxyl polycations of polynuclear cationic metals, which are converted into oxides that are strongly bonded to clay the after calcination. The common traditional method of PILCs synthesis, involves addition of metal ions, such as Al^{3+}, Zr^{4+}, Cr^{3+} and Fe^{3+}, into a basic solution ($NaCO_3$ or NaOH) and stirred at a certain temperature for hours (3–12 h), followed by 6–24 h or 1–5 days of aging at 60–80 °C to obtain hydroxyl polycations, which are pillaring agents solution. The precursor pillaring agent solution is added into the diluted clay mineral suspension (typical 2% in weight), which is followed by thermal treatment of intercalated clay mineral [7].

However, the preparation of PILCs as catalysts has not been extended to commercial scale, due to the difficulties involved in performing the laboratory synthesis procedure at industrial scale due to prolonged synthesis times and large amount of water involved [8, 9]. Numerous studies have made efforts to simplify the synthesis of PILCs, in order to lower the synthesis times and the volumes of water required. The use of concentrated clay suspensions (50 wt%) and direct addition of natural clay without purification into pillaring agent solution has been proposed as strategies used by various studies to decrease the volume of water required, while the synthesis time has been decreased by the use of microwave and ultrasound treatment method [6, 9–15]. These studies found that the volume of water required can be reduced by 70–95%, whereas the synthesis time can be decreased to 70–93%. In addition, PILCs composed of mixed polycations are reported to increase specific surface area, thermal stability and catalytic properties of the PILCs compared to a single polycations. Baloyi et al. [16] reported that in the mixed polycations PILCs, one of the polycations might be responsible for structural and thermal stability with the required pore structure, whereas the catalytically active sites might be enhanced by the correct choice of a second polycation. Gil et al. [17] found that Al-PILCs structural and acidic properties can be enhanced by the addition of a second polycation pillaring agent such as Fe, Cr, Ti and Zr, etc. The preparation of Cr-PILCs have attracted attention in the catalytic applications due to the different oxidation states of chromium [4]. However, numerous studies reported that Cr-PILCs are not stable at high temperatures. Mata et al. [18] reported a collapse of Cr-PILCs after calcination in air above 200 °C while Hopkins et al. [19] observed the collapse of Cr-PILCs basal spacing of 1.54 nm after calcination at 300 °C. Several reports have found that the thermal stability of Cr-PILCs was improved by the preparation of mixed chromium and aluminium pillars at different Al/Cr ratios because of high thermal stability of Al-PILCs [20, 21]. In the literature, limited studies have been reported on the synthesis of PILCs using methods such as ultrasound and microwave irradiation with direct use of natural dry clay without chemical treatment.

Phenol is an organic pollutant commonly found in industrial wastewater emitted from refineries, paint, coking operations, petrochemicals, pulp and paper, pharmaceuticals, resin manufacturing and plastics [1–4]. It was chosen as the model compound in this study, because of its refractory nature. Phenol is listed as priority water pollutants by the World Health Organisation (WHO) and it is considered toxic above 2 mg/L [15]. Phenol and its derivatives are common pollutants of ground water, because of its low biodegradability and toxic for animals and human beings [22]. Therefore, effective treatment of industrial wastewater contaminated by refractory organic compounds such as phenol is crucial. Catalytic wet air oxidation (CWAO) has attracted much attention for treatment of refractory organic compounds such as phenol that cannot be completely removed by conventional treatment methods. In CWAO, refractory organic compounds and oxidizable inorganic compounds can be oxidized with air or oxygen (O_2) at high operation temperature (150–325 °C) and pressure (0.5–20 MPa) in the presence of a robust catalyst.

In the current study, ultrasound treatment method was used both during the aging and the intercalation of pillaring agents to synthesize PILCs containing chromium and aluminium pillars with different Al/Cr molar ratios. Moreover, dry clay was directly added to the pillaring solutions without purification. Structural and textural properties of PILCs were characterized by PXRD, HRSEM-EDS, FTIR, TGA, Zetasizer and BET surface area measurements. The efficiency of these PILCs catalysts in the CWAO of phenol in aqueous phase under mild reaction conditions was investigated. Phenol oxidation intermediates generated by CWAO of phenol were identified and discussed.

2 Experimental

2.1 Materials and Reagents

All reagents used in this study were analytical grade and used without further purification. Natural bentonite (Bt) clay supplied by ECCA Holdings (Pty) Ltd from Cape Town, South Africa, with cation exchange capacity (CEC) of 78.6 meq/g, was used as starting material. Phenol (99.5%) was purchased from Sigma Aldrich Chemical Co. Sodium hydroxide (98.7%), hydrochloric acid (37%), aluminum nitrate nonahydrate, chromium (III) nitrate nonahydrate, acetic acid (99.0%) and HPLC-grade methanol were obtained

from Merck. All solutions were prepared with high purity water (resistivity 18.2 MΩcm) purified by a Milli-Q water system (Millipore).

2.2 Pillared Clay Catalysts Preparation

As previously described in the literature by Tumol et al. [15], the pillaring solutions were prepared by slowly adding NaOH solution (0.4 M, 500 mL) into $Al(NO_3)_3{\cdot}9H_2O$ (0.4 M, 250 mL) or $Cr(NO_3)_3{\cdot}9H_2O$ (0.4 M, 250 mL) solution under vigorous stirring at room temperature [23–26]. The NaOH was added at constant rate of approximately 5 mL/min to reach the final molar ratio of 2:1. The pillaring solutions were ultrasonicated for 10 min at room temperature prior to use. The mixed Al/Cr pillaring solutions with different molar ratios (Al/Cr mole ratios of 1:3, 1:1, 3:1 and 6:1) of Al/Cr were prepared by using the above procedure at room temperature. The intercalation was carried out by direct addition of dry clay into the single or mixed aluminium and zirconium pillaring solutions under vigorous stirring at room temperature for 30 min, using a ratio of 25 mL pillaring solution/1 g of clay. The ion exchange reaction was sped up by using ultrasonic treatment at 25 °C for 10 min. Finally, the solid fractions were separated by centrifugation for 8 min, washed several times with high purity water, oven-dried at 120 °C for 16 h, and then calcined in a muffle furnace at 500 °C for 2 h. The obtained pillared clay catalysts were denoted as Al-PILC, Cr-PILC, Al/Cr-PILC (1:3), Al/Cr-PILC (1:1), Al/Cr-PILC (3:1) and Al/Cr-PILC (1:1), respectively.

2.3 Characterization Techniques

The morphology and chemical composition of natural and pillared bentonite samples were characterized by high resolution scanning electron microscopy with an energy dispersive X-ray spectrometer (HRSEM–EDS, FEI Nova NanoSem). Powder X-ray diffraction (XRD) analysis was performed in a high resolution Bruker AXS D8 diffractometer with CoKα-radiation (40 kV, 40 mA, 1.78897 Å) in the 2θ range from 5° to 80° at scanning speed of 0.02°/s. Nitrogen adsorption–desorption measurements were performed at − 196 °C using Micromeritics ASAP TrisStar 3000 instrument. Prior to the measurement all samples were degassed under vacuum at 150 °C for 4 h. The specific surface area (S_{BET}) was determined using the Brunauer–Emmett–Teller (BET) method. The total pore volumes (V_t) were calculated at a relative N_2 pressure of $P/P_0 \sim 0.99$. While the pore size distribution was calculated using the Barrett–Joyner–Halenda (BJH) method based on the desorption branch of the isotherms. Fourier transform infrared (FTIR) spectrometer peaks were obtained from 4000 to 400 cm^{-1} over 200 scans using a Varian 640-IR FTIR spectrometer with a Miracle single bounce diamond attenuated total reflectance (ATR) cell from PIKE Technologies. Thermogravimetric (TG) and differential thermogravimetric (DTG) analyses were performed on a Perkin–Elmer model 6000 thermal analyzer. Samples were heated from 35 to 900 °C with nitrogen atmosphere, at a heating rate of 10°C/min under nitrogen flow rate of 20 mL/min. The surface charge of the samples were determined using a Nano Zetasizer (Malvern Instruments, UK). The cation exchange capacity (CEC) was determined by the ammonium acetate method using Kjeldhal technique.

2.4 Catalytic Wet Air Oxidation Experiments

The experimental studies were carried out in a 350 mL semi batch Teflon-lined autoclave reactor (Parr Instruments Co., model 4531M) equipped with a stirrer, an electric heating jacket, gas inlet and liquid sampling port. The temperature inside the reactor was measured by a thermocouple and a proportional-integral-derivative (PID) controller was used to keep the temperature constant inside the reactor. (A schematic of the experimental setup is presented in Figure S1). Prior to CWAO experiments, operational parameters were optimized from preliminary experiments (results are shown in Figs. S2–S7). The stirring speed was maintained at 800 rpm. The reaction temperature was set at 100 °C and the mixture inside the reactor was pressurized with 10 bar oxygen. In a typical run, the reactor was charged with aqueous suspension of phenol (200 mL, 1000 mg/L) and 2 g/L of catalyst at initial pH of 3. After air was purged in the reactor with pure nitrogen, the reactor system was pressurized with 5 bar of pure nitrogen pressure for 5 min. Once the desired temperature was reached, oxygen was introduced into the reactor immediately to get a 10 bar of total pressure. This point was set as the initial reaction time known as "zero time". Samples were withdrawn at regular intervals and immediately filtered using 0.45 µm once-off syringe filters to analyze the phenol concentration. All experiments were conducted in triplicates to check the reproducibility of the results. The data reported in this study were the average calculated from the repeat experiments. Experimental errors are less than 5% between repeat experiments throughout the study.

The stability and reusability of the best pillared clay catalyst was evaluated by successive use of the same catalyst sample in the phenol oxidation reaction. The experiments carried out using the same conditions as the above CWAO experiments. After each experimental run, the catalyst was recovered by centrifugation for the next use, added to 100 mL $CaCl_2$ solution (4%) and stirred for 120 min at room temperature to remove all adsorbed organics.

2.5 Analytical Methods

A high performance liquid chromatography (HPLC) (Shimadzu LC-10AD), equipped with an ODS-3 column and UV–Vis detector was used to determine the phenol concentration in solution. The mobile phase was composed of high purity water and methanol in a ratio of 60:40 (v/v) at a flow rate of 1 mL/min. The evolution of phenol intermediates during the reaction was analysed by HPLC following the procedure described by Ma et al. [5]. The total organic carbon (TOC) content was determined in filtered aliquots of the reaction mixture by Shimadzu TOC analyzer. The pH values of solutions were determined using a Mettler–Toledo FE 20 pH meter. The concentration of leachate Cr^{3+} was measured by inductively coupled plasma-atomic emission spectrometer (ICP-AES) spectroscopy.

3 Results and Discussion

3.1 Characterization Studies

SEM micrographs of the raw natural bentonite and the pillared bentonite clays synthesized using aluminium and chromium metal oxides are shown in Fig. 1. The results clearly indicate loosened and randomly distributed closely-packed structure after pillaring. The structure of all the pillared clay catalysts is similar to that of the natural bentonite clay indicating that the structure of the natural clay was not destroyed by pillaring with single or mixed metal oxide pillars. The energy dispersive X-ray spectroscopy (EDS) analysis of natural and pillared bentonites are presented in Table 1. EDS analysis clearly shows the presence of elements like Si, Al, Fe, Na, Mg, Ca, K and Cr in the samples. The Al and/ or Cr oxides metal contents increase as result of cation exchange with Na and Ca due to pillaring by Al, Cr and Al/Cr pillars. Therefore, confirming that the intercalation of Al or Cr is produced by a cation exchange reaction between the exchangeable small interlayer polycations in the interlayer space of bentonite clay and Al, Cr and Al/Cr pillars in solution. While the higher relative amount of Si/Al indicate the presence of quartz and muscovite [27, 28].

The cation exchange capacity (CEC) of the natural bentonite and pillared bentonite clay samples was measured by the ammonium acetate exchange according to the Kjeldhal method. Normally the CEC of natural bentonite clay is > 60 meq/100 g. The obtained CEC value of the bentonite clay in Table 1 is within the reported values of 75–80 meq/100 g for South African bentonite clay [29, 30]. As shown in Table 1, the CEC of the clay decrease with pillaring from 78.6 to 21 meq/100 g; the decrease attributable to the dissolution of octahedral cations of the 2:1 layers and protonation of the SiO groups. The low CEC values of the pillared bentonite clay indicate the irreversibility of cationic exchange of the intercalated polycations.

The zeta potential analysis results for natural and pillared bentonite clay in the variation of initial pH in the range 1 to 10 is indicated in Fig. 2. The surface charge of the natural bentonite clay exhibits highly negative zeta potential values over the entire pH range studied due to isomorphous substitution of structural Si^{4+} by Al^{3+} and pH dependent charge from the hydroxyl groups at the edges of the bentonite clay particles [31]. At pH 10, the zeta potentials of pillared clay catalysts have more negative charges than that of natural bentonite clay due to the high amount of hydroxyl (–OH) groups on pillared bentonite clay surface. However, the zeta potentials of the pillared clay catalysts decrease and convert to positive values with the decrease in initial pH values towards acidic conditions. This may be attributed to the increase in H^+ ions on the surface of pillared bentonite clay catalysts, which can effectively increase the electropositivity of the catalysts, therefore aiding anionic contaminants removal in aqueous solution [32]. Single metal (Al or Cr) polyoxycations pillared clays show a higher positive charge compared to mixed Al/Cr polyoxycations pillared clays, which may be attributed to the combination of more hydroxide ions (–OH) in the mixed Al/Cr polyoxycations ($\{[Al_xCr_y(OH)_z(H_2O)_n]^{(3x+3y-z)+}\}$).

The XRD patterns of the natural and pillared bentonite clay samples in the 5°–80° 2θ angle range are compared in Fig. 3. The corresponding basal spacing calculated by Bragg's law ($2d \sin\theta = n\lambda$, where d is the basal spacing, θ is the angle of diffraction, λ is the wavelength, and n is the path differences between the reflected waves, which equals an integral number of wavelength) at d_{001} smectites reflection are shown in Table 1. The XRD patterns reveal that natural bentonite clay is composed of Na-montmorillonite as principal crystalline phase, accompanied by other impurities such as quartz, muscovite and calcite. The detected crystalline phases for natural bentonite clay are in accordance with similar studies [30, 33]. After intercalation of Al, Cr or Al/Cr metal oxides pillars into the natural bentonite clay structure, the d_{001} peaks shifted slightly towards small 2θ values therefore increasing the basal spacing. Moreover, the d_{001} peak intensity decreases with pillaring compared to that of the natural bentonite clay. The XRD spectra of natural bentonite and pillared clay samples are very similar, suggesting that the structure of natural bentonite clay was not destroyed after pillaring process. In the case of Cr-PILC sample, the d_{001} diffraction peak collapses and the peaks around 18°, 18.5° and 37° can be ascribed to the presence of Cr_2O_3 in the diffractograms. This is in agreement with previous studies by De León et al. [20] and Chen et al. [34] who observed the d_{001} peak collapsing at temperatures above 300 °C. Therefore this can be attributed to the fact that the d_{001} plane in the Cr-PILC has tendency of losing the order

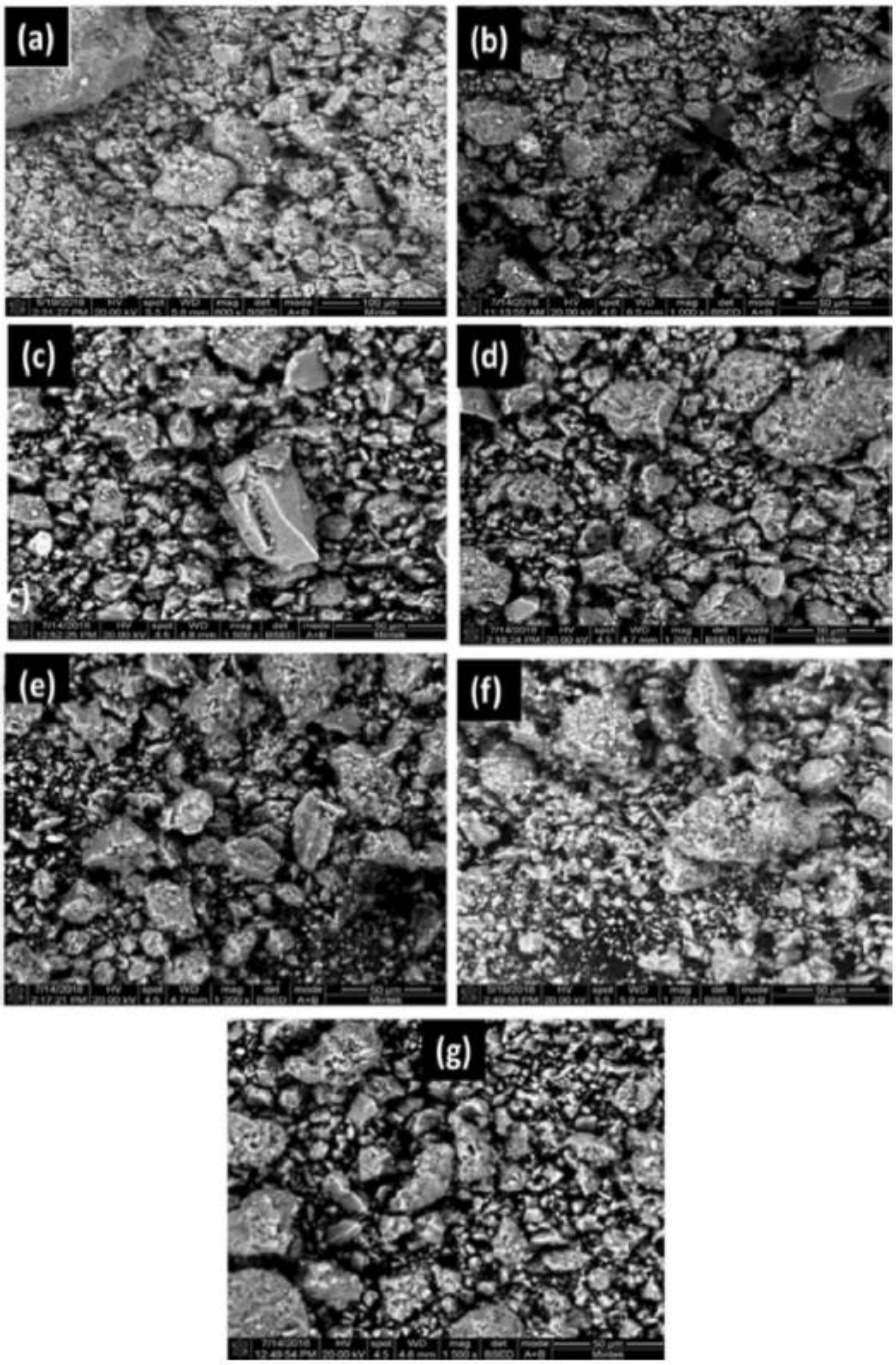


Fig. 1 HRSEM microphotographs of **a** Bt, **b** Al-PILC, **c** Cr-PILC, **d** Al/Cr-PILC (1:3), **e** Al/Cr-PILC (1:1), **f** Al/Cr-PILC (3:1) and **g** Al/Cr-PILC (6:1)

in the stacking of the pillared clay layers after calcination at 400–500 °C. The calcination temperature at 500 °C leads to appearance of the Cr_2O_3 phase shown by the peaks identified in Cr-PILCs, which are not detected in the corresponding exchanged mixed pillared bentonite clay (Al/Cr-PILCs).

Figure 4 shows the FTIR spectra (400–4000 cm^{-1}) recorded in transmission mode for natural bentonite clay and pillared bentonite clay samples. The peaks at 3583, 3294, 1630, 978, 906 and 561 cm^{-1} are typical of montmorillonite, while the peaks at 771 and 661 cm^{-1} corresponds to the presence of quartz [20]. The peak at 1487 cm^{-1} corresponds to the occurrence of small amounts of calcite or dolomite [35]. The peak at 3583 cm^{-1} is assigned to the OH-stretching vibration (Al-Al-OH) structural groups of montmorillonite. After pillaring of clay the Al-PILCs, Al-PILC (3:1) and Al-PILC (6:1) peaks at approximately 3583 cm^{-1} increase

Table 1 Physicochemical characteristics of natural and pillared bentonite clay samples by EDX, CEC and XRD

Sample	Al/Cr ratio	Na (%)	Mg (%)	Al (%)	Si (%)	K (%)	Ca (%)	Fe (%)	Cr (%)	Si/Al	CEC (meq/100 g)	d_{001} (nm)
Bentonite	–	3.73	2.29	15.31	65.09	2.39	2.09	9.10	0.00	4.25	78.6	1.24[a]
Al-PILC	–	0.96	1.24	31.98	59.14	1.82	0.27	4.55	0.00	1.85	40	1.52
Cr-PILC	–	0.95	1.13	11.42	58.54	1.16	0.16	4.21	22.13	5.13	30	0.90
Al/Cr-PILC	1:3	0.96	1.19	16.02	58.98	1.71	0.26	4.01	16.87	3.68	27	1.36
Al/Cr-PILC	1:1	0.97	1.22	19.02	59.01	1.61	0.21	4.38	13.58	3.10	21	1.50
Al/Cr-PILC	3:1	0.98	1.23	27.76	58.14	1.63	0.24	4.40	5.61	2.09	24	1.41
Al/Cr-PILC	6:1	0.93	1.21	29.19	59.11	1.68	0.26	4.45	3.17	2.03	33	1.38

[a]Basal spacing of non-calcined bentonite

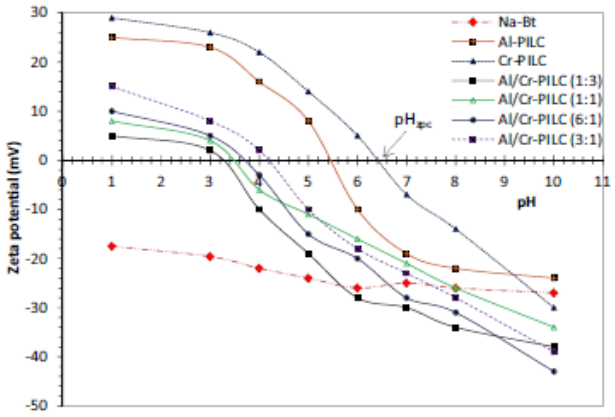


Fig. 2 Zeta potential (mV) of the natural and pillared bentonite clays as a function of pH

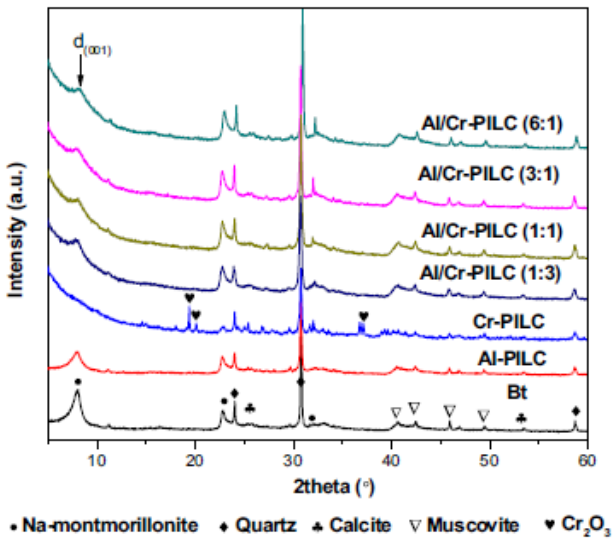


Fig. 3 X-ray diffractograms of the natural and pillared bentonite clay samples

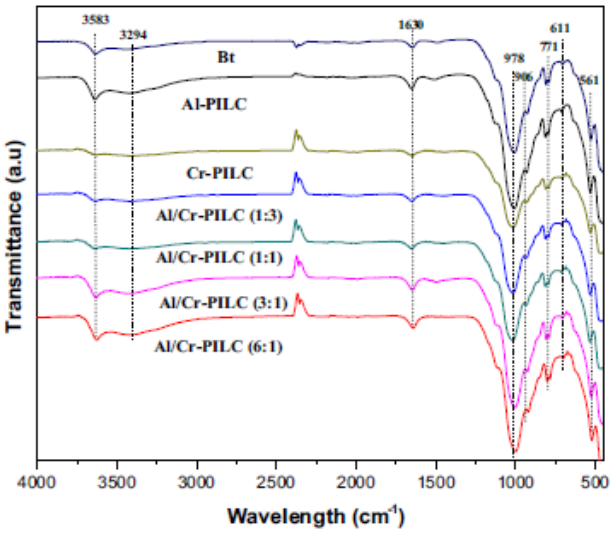


Fig. 4 FTIR spectra of natural and pillared bentonite clay samples

in intensity which is indicative of an improvement in the water retention capacity of the clay material due to pillaring. The intensities of Cr-PILC, Al-PILC (1:3) and Al-PILC (1:1) decrease and the peaks broaden. This decrease in the intensity of the peaks is attributed to the dehydration and dehydroxylation steps during pillaring [27]. The broadening of the peaks could be due to the introduction of additional –OH groups, as a result of the pillaring of the clay [35, 36]. The broad peak at 3294 cm^{-1} depicts the OH vibrational stretching of intercalated water in montmorillonite. The peak at 1630 cm^{-1} can be assigned to OH vibration bending of H–O–H. After the clay was pillared the intensities of the Al-PILC, Al-PILC (3:1) and Al-PILC (6:1) peaks at approximately 1630 cm^{-1} increased due to replacement of hydrated larger interlayer cations which decreases the –OH peaks. Moreover, the peaks at 1630 cm^{-1} shifted to higher wavelength (approximately between 1639 and 1660 cm^{-1}) due to pillaring process. The Si-O-Si stretching vibration in the tetrahedral structure of the bentonite clay peak is

observed at 978 cm^{-1}. The peaks at 906 and 771 cm^{-1} can be assigned to Al–Al–OH and Mg–Al–OH groups, respectively. After pillaring, intensities of these peaks at 978, 906 and 771 cm^{-1} decrease and the peaks shift to lower wavelengths. This shift can be attributed to the sharing of hydroxyl (OH) peaks between Al and Cr that are located in the octahedral positions [20, 27]. The Si–O–Mg and Si–O–Al species are donated by peaks at 561 and 661 cm^{-1} respectively. The FTIR spectral data provide evidence of the successful pillaring of the bentonite clay.

The textural characterization of natural and pillared bentonite clay, including the specific surface areas (S_{BET}), total pore volumes (V_p), mcro volume (V_{mic}) and average diameter of the pores (D_p) are presented in Table 2. The specific surface area of Al, Cr and Al/Cr increase significantly after pillaring process, which confirm that Al and Cr were efficiently intercalated into the interlayer space of bentonite clay sheets. Compared with the natural bentonite clay and single metal oxides pillars (Al or Cr), the mixed metal oxides pillars (Al/Cr) with different molar ratios exhibit higher specific surface areas. This shows that the mixed metal oxides pillars of Al/Cr polycations that formed were larger than the Al or Cr polycations, which is an indicative that bentonite clay layers were more separated and resulted in a more porous structures being formed. The specific surface area of Cr-PILCs increased slightly compared to starting natural clay, while the Al-PILCs increased significantly. This indicates a higher thermal stability of the Al-PILCs compared with the Cr-PILC which collapse with the loss of their interlaminar spacing at the calcination temperature of 500 °C. These results tally with the XRD analysis results in this study as well as with other studies in the literature [20, 21, 34]. The mixed metal oxides pillared clay of Al/Cr at the molar ratio of 1:1, shows a high specific surface area of 180 $m^2\ g^{-1}$. This proves that the mixed metal oxides pillars (Al/Cr) was more effective at increasing specific surface area than Al or Cr metal oxides pillars alone and the significance of introducing Al metal oxides pillars during the intercalation process to hinder the loss of specific surface area of Cr-PILC. Chen et al. [34] obtain similar results in which the optimum Al/Cr molar ratio in the pillaring process was determined to be 2:2. The micropore volumes, total pore volume and pore diameters of pillared bentonite clay materials increased with an increase in the specific surface area of pillared bentonite clay samples. The higher values of pore diameters and total pore volumes indicate that most of the total pores were formed from mesoporous structure. In conclusion it was observed that textural analyses of pillared bentonite clay confirm that the pillaring process led to the significant increase in the porosity, which is one of the most significant characteristics of the catalyst.

The TGA and DTG curves of the natural and pillared bentonite clays are shown in Fig. 5. The TGA curves of the pillared clay samples are similar to that of natural bentonite clay. The TGA and DTG curves recorded from 35 to 900 °C of the both natural and pillared bentonite clay show three stages of mass loss. The first step in the range of 49–170 °C is attributed to the loss of physically adsorbed water as well as the loosely bound water molecules present in the interlayer space of the pillared bentonite clay. The second step, at about 390–511 °C is related to the loss of water molecules coordinated to the pillars. It is worth noting that, at this stage, the removal of water is not associated with destruction of bentonite clay mineral structure indicating the high thermal stability of the clay which relates to their crystalline structure. Whereas the third step in the range of 548–704 °C can be ascribed to the breakdown of the clay crystal structure. At this temperature range, the loss in mass of the pillared bentonite clays peaks are lower compared to that of the natural clay, confirming the addition of Al and Cr amount during the pillaring and less volatiles. The observed differences in the TGA and DTG curves can be explained by the differences in the dehydration and dehydroxylation process, which can be ascribed to the presence of different species of Al and Cr in the interlayer and external surface, and also hydration energies differences [15].

Table 2 The textural characterization of prepared catalysts and raw bentonite clay

Sample	Al/Cr ratio	S^1_{BET} (m^2/g)	V^2_{pore} (cm^3/g)	V^3_{mic} (cm^3/g)	d^4_{pore} (nm)
Bentonite	–	61	0.11	0.089	10.1
Cr-PILC	–	67	0.13	0.091	9.6
Al-PILC	–	147	0.32	0.099	8.5
Al/Cr-PILC	1:3	150	0.29	0.1	8.1
Al/Cr-PILC	1:1	180	0.36	0.116	7.2
Al/Cr-PILC	3:1	168	0.33	0.111	7.8
Al/Cr-PILC	6:1	159	0.31	0.109	8.4

[1]Specific surface area (S_{BET})

[2]Total pore volume at $p/p^0 \sim 0.99$

[3]Micropore volume

[4]Pore diameter

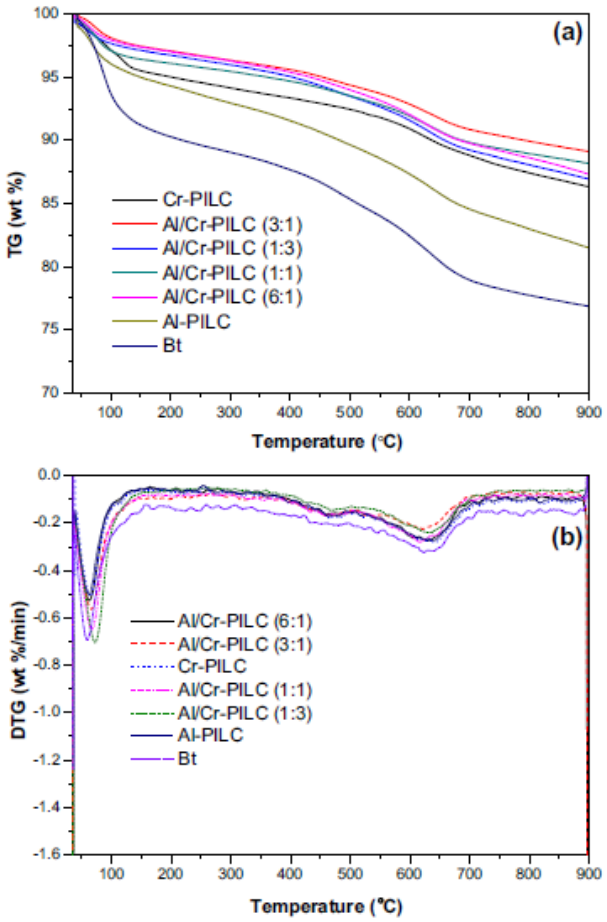


Fig. 5 TG (**a**) and DTG (**b**) curves of natural and pillared bentonite clay samples

The textural properties of Al/Cr-PILCs prepared in this study was compared with previously reported similar catalysts prepared by different methods in Table 1. From Table 1, with ultrasonic treatment, synthesis at room temperature and 20 min reaction time, 180 m^2/g and 1.50 nm of BET specific surface area and basal spacing, respectively, were achieved, whereas in a conventional synthesis method, low BET specific areas were reached in up to 7 days reaction times. Ding et al. [9] synthesized Al/Cr-PILCs catalysts using a one-step high-temperature and high-pressure (HTHP) method. They have found that after 4 h of calcination at 550 °C, the specific surface area and maximum basal spacing reached 266–362 m^2/g and 2.06 nm, respectively. Compared to conventional methods, the method significantly reduced the steps and material consumption. However, high temperatures, high pressures and long synthesis periods are required compared to ultrasonic treatment method. As in the case of the compared textural properties in Table 3, the beneficial effect of ultrasonic method on the Al/Cr-PILCs was observed. The obtained results can be explained by stability of Al/Cr-PILCs catalyst, which can be attributed to the uniform pillaring obtained by the use of ultrasonic treatment. Moreover, the use of ultrasonic treatment plays a role in accelerating the $[Al_{13}]^{7+}$ diffusion within the clay layers [14]. The use of ultrasonic treatment method present numerous advantages such as reduction of the synthesis time from days to less than 20 min. The method does not require any heat for the process, therefore, saving in costs and less safety risks. Finally, the addition of dry clay directly into pillaring solution results in less consumption of water and space required. Therefore, the textural properties of Al/Cr-PILCs catalyst herein is comparable and even better compared to other previous reported using conventional method.

3.2 Catalytic Wet Air Oxidation of Phenol

The catalytic activity of various pillared bentonite clay catalysts were investigated using phenol as a model pollutant and the results for phenol removal and total organic carbon (TOC) conversions are displayed in Fig. 6. It was found in the WAO (in the absence of catalyst) of phenol that the removal of phenol and TOC conversion were 9% and 2%, respectively, indicating that the phenol was stable under our

Table 3 Comparison of Al/Cr-PILCs catalyst textural properties with previously reported similar Al/Cr-PILCs catalysts prepared by different methods

Catalysts	Al/Cr ratio	Method of sythensis	Reaction conditions	S^1_{BET} (m^2/g)	d_{001} (nm)	CEC (meq/log)	Refs.
Al/Cr-PILC	1:1	Ultrasonic	T = 25 °C $t_{reaction}$ = 20 min pH 5	180	1.50	21	This work
Al/Cr-PILC	1:3	Convetional	T = 120 °C $t_{reaction}$ = 7 days	96	1.72	–	[27]
Al/Cr-PILC	2:5	HTHP	T = 140 °C $t_{reaction}$ = 36 h	362	2.06	–	[9]
Al/Cr-PILC	2:2	Conventional	T = 25 °C $t_{reaction}$ = 48 h	125	1.57	–	[34]

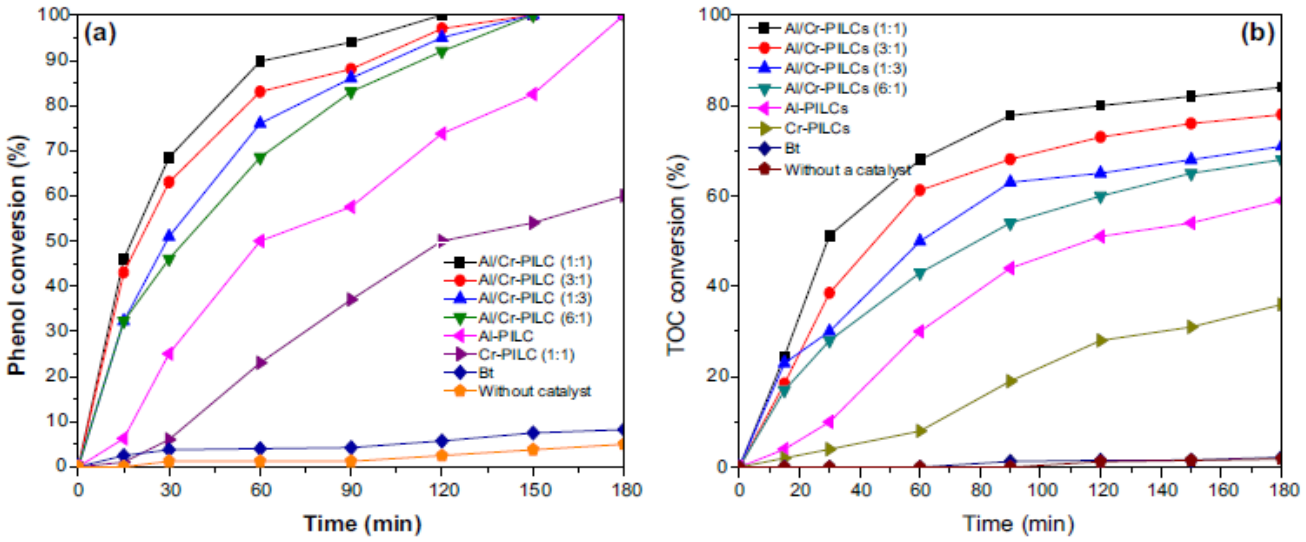


Fig. 6 Phenol (**a**) and TOC (**b**) conversions in the CWAO reaction of phenol over the natural and pillared bentonite clay samples (200 mL of reaction solution, 1000 mg/L phenol concentration, 0.4 g of catalyst, pH 3.0, 10 bar O_2 pressure and 100°C)

operating conditions. The adsorption experiments was studied under the same operating conditions using nitrogen in place of air. Under these conditions, 10% and 5% of phenol removal and TOC conversion, respectively, were adsorbed on the catalysts, which could be ascribed to the large specific surface area of the catalysts which results in an increase number of active sites in the catalysts. The phenol removal and TOC conversion using natural bentonite clay were found to be 8% and 2%, respectively, which was almost inactive toward the CWAO of phenol. In contrast, the use of the various pillared clays as catalysts yielded good catalytic activities towards phenol removal and TOC conversion in the CWAO reaction with the mixed metal oxides being the most active catalysts. After 120 min reaction, the phenol removal reached 92%, 95%, 97% and 100% over the Al/Cr-PILC (6:1), Al/Cr-PILC (1:3), Al/Cr-PILC (3:1) and Al/Cr-PILC (1:1) catalysts, respectively. High mineralization of the phenol was obtained and approximately 84% TOC conversion was achieved within 180 min of the reaction in using Al/Cr-PILC (1:1) catalyst. The TOC conversion decreased from 84 to 36%, with minimum in case of Cr-PILC. The TOC conversion values decreased in the following order: Al/Cr-PILC (1:1) > Al/Cr-PILC (3:1) > Al/Cr-PILC (1:3) > Al/Cr-PILC (6:1) > Al/Cr-PILC > Cr-PILC. The performance of mixed pillared clay catalysts specifically Al/Cr-PILC (1:1) catalyst can be attributed to the highest surface area (180 m^2/g), which contribute to more active sites in the CWAO process. The high thermal stability of the Al/Cr-PILCs prevented the collapse of the bentonite clay interlayer structure during the calcination step of the pillaring process, the increasing stability of the pillared clay towards Cr^{3+} leaching and possible enhancement of surface acidity of the clay after pillaring, that is significant for the oxidation of phenol as reported in our previous studies [23]. Moreover, the increased positively charged surface of the Al/Cr-PILCs favored electrostatic attraction between the catalyst and negatively charged phenoxide ion in solution at acidic pH values, thus, enhancing the adsorption of phenol on its surface.

The catalytic activities of the various catalysts in the CWAO reaction of phenol are summarized in Table 4. In the literature, there are no data available on the application of Al/Cr-PILCs as catalysts in the CWAO processes. As chromium being a good oxidant catalyst due to its different oxidation states, in literature, there are limited studies where Al/Cr-PILCs was used as a catalyst in oxidation reactions [20, 21, 27, 34]. The use of noble metals (Pt, Ru…), transition metal oxides (TiO_2, CeO_2…) and carbon materials (GO, r-GO…) for CWAO of phenol has been carried out by numerous researches and their works show that these catalysts give high activity [37–41]. Rocha et al. [37] investigated the use of Pt/TiO_2-Ceria as catalysts for the CWAO of phenol and found that Pt/TiO_2-Ceria catalyst showed 96% of phenol conversion and complete TOC conversion. It was also reported that the presence of Ce in the catalysts prevents deactivation of the catalysts due to carbon deposition on the surface. Davies et al. [41] applied Pt/SiC catalyst for CWAO of phenol in aqueous solutions and the catalyst displayed good performance and was very durable for CWAO of phenol, achieving 99.95% phenol removal and 95% TOC conversion at a reaction temperature of 160 °C and total pressure of 7 bar. Yang et al. [37] reported on a CWAO of phenol in a batch reactor using CeO_2-TiO_2 catalysts and the

Table 4 Summary of the comparative study for phenol oxidation with CWAO using different catalysts

Catalyst	Operating conditions	Pollutant	Results	Refs.
Pt/TiO_2/Ceria	T = 160 °C P = 10 bar Batch experiments $t_{reaction}$ = 2 h	Phenol (1000 mg/L)	[Ph] = 96% [TOC] = 100%	[37]
Pt/SiC	T = 160 °C P = 7 bar Batch experiments $t_{reaction}$ = 5 h	Phenol (1000 mg/L)	[Ph] = 99.95% [TOC] = 95%	[41]
CeO_2-TiO_2	T = 150 °C P = 30 bar Batch experiments $t_{reaction}$ = 150 min	Phenol (1000 mg/L)	[Ph] = 100% [TOC] = 80%	[39]
MnO_x-CeO_2	T = 100 °C P = 10 bar Batch experiments $t_{reaction}$ = 60 min	Phenol (1000 mg/L)	[Ph] = 100% [TOC] = 77%	[38]
GO	T = 155 °C P = 25 bar Batch experiments $t_{reaction}$ = 40 min	Phenol (1000 mg/L)	[Ph] = 100% [TOC] = 84%	[40]
r-GO	T = 155 °C P = 25 bar Batch experiments $t_{reaction}$ = 120 min	Phenol (1000 mg/L)	[Ph] = 100% [TOC] = 80%	[40]
Al/Cr-PILC(1:1)	T = 100 °C P = 10 bar Batch experiments $t_{reaction}$ = 120 min	Phenol (1000 mg/L)	[Ph] = 100% [TOC] = 80%	[This work]

CeO_2-TiO_2 mixed oxides catalysts display the higher activity. Phenol removal and TOC conversion were about 100% and 77% after 120 min in the CWAO of phenol at reaction temperature of 150 °C and the total pressure of 30 bar. Low cost metal oxides, such as MnO_x-CeO_2 have been reported by Arena et al. [38] as more active catalysts in the CWAO of phenol at low temperature as 100 °C and total pressure of 10 bar. It was found that the complete phenol removal was achieved within 40 min reaction time, while 80% of TOC conversion was achieved after 60 min. This high catalytic activity of the MnO_x-CeO_2 catalysts was attributed to the rapid adsorption of phenol and its intermediates. However, MnO_x-CeO_2 catalysts were reported to suffer from deactivation because of deposition of carbon on the catalyst surface. Yang et al. [40] used graphene oxide (GO) and chemically reduced graphene oxides in the absence of any metals, in the catalytic wet air oxidation (CWAO) of phenol in a batch reactor. The GO was reported to have the highest catalytic activity, with complete removal of phenol achieved after 40 min, and 84% TOC conversion was obtained after 120 min at reaction temperature of 155 °C and total pressure of 25 bar. While complete phenol oxidation and 80% TOC conversion was achieved over r-GO.

As shown in Table 3 noble metal catalysts containing Ru and Pt catalysts, have shown the best catalytic activities in terms of phenol removal and TOC conversion in the CWAO of phenol. Whereas, the metal oxides such as CeO_2 have been reported to attract a lot attention, due to their good chemical and thermal stability and resistance to both acidic and basic media [37]. However, these best catalytic activities are obtained at high operation conditions of CWAO reaction and using expensive metals. Therefore, considering the low cost of Al, Cr and natural clays, the use of Al/Cr-PILC (1:1) catalyst synthesized in this study appeared to be the most promising for CWAO of phenol.

Since Al/Cr-PILC (1:1) catalyst exhibited the highest catalytic performance in the reaction, it was further considered for the study of the evolution of reaction intermediates. The yield of intermediates in the course of the phenol CWAO reaction was monitored and the evolution profiles of the identified intermediates are indicated in Fig. 7. The identification of intermediates during phenol oxidation was performed by HPLC analyses by direct comparison of retention times with the corresponding standards. The main intermediates identified were pyrocatechol, benzoquinone, hydroquinone, oxalic acid, maleic acid, formic acid, acetic acid and malonic acid. These intermediates have been identified by several other studies for phenol oxidation conducted using CWAO process [42, 43]. Refractory aromatic ring compounds such as hydroquinone are formed at

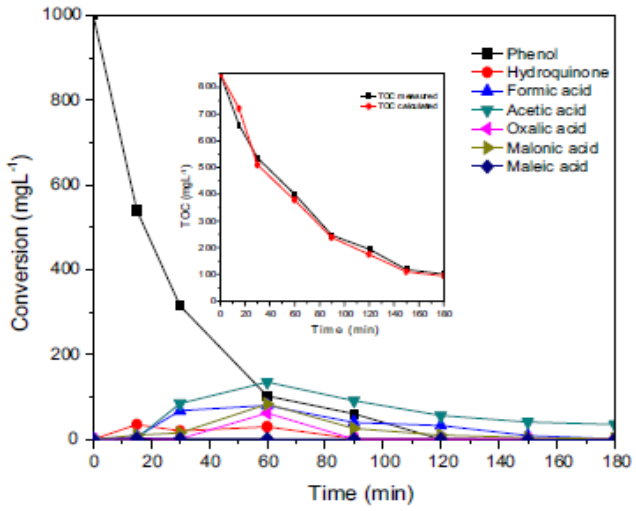


Fig. 7 Evolution of phenol and intermediates in the CWAO reaction of phenol over the Al/Cr-PILC (1:1)

the beginning of the CWAO reaction. Then some aromatic intermediates such as pyrocatechol and benzoquinone were detected in the middle of the phenol oxidation reaction. The aromatic intermediates need to be oxidized since they are more toxic than phenol itself [44]. In this study the colour of the phenol solution was observed to change during the reaction; the colourless phenol solution at the beginning turned light brown to dark brown then light brown. The dark brown colour can be attributed to the formation of benzoquinone. The light brown solution turned colourless due to oxidation of benzoquinone to short chain carboxylic acids [45, 46]. With the increase in phenol oxidation reaction time, short chain carboxylic acids such as oxalic acid, maleic acid, formic acid, acetic acid and malonic acid are formed in the reaction. Hydroquinone showed its highest concentration after about 15 min of the reaction whilst all the other intermediated were highest in concentration at about 60 min all of which are further oxidized. Acetic and oxalic acids concentrations decrease more slowly, suggesting that these short chain acids are more difficult to oxidize at these operation conditions. These results are in agreement with the work of Guo [44]. and Ma et al. [18]. The formation of polymeric compounds during the CWAO of phenol as reported Zapico et al. [43], was quantified by means of the TOC measurements. The detailed radical nature of phenol CWAO mechanism has been already well documented in the literature [47–50] and the discussion of our reaction mechanism experimental results were limited to our findings in this study. The proposed reaction mechanism is based on the work of Santos et al. [48] for phenol CWAO mechanism. Through the identified intermediates in our study it can be suggested that phenol oxidation proceeds through

Table 5 Stability, leaching and basal spacing features of reused Al/Cr-PILC catalyst in the removal of phenol and TOC over optimum conditions

No. of runs	Phenol removal in 120 min (%)	TOC conversion in 180 min (%)	Leaching of Cr^{3+} (Mg L^{-1})	d_{001} (nm)
First use	100	84	0.065	1.50
Re-use 1	100	81	0.096	1.48
Re-use 2	100	80	0.110	1.47
Re-use 3	98	77	0.118	1.44
Re-use 4	95	74	0.124	1.44
Re-use 5	91	71	0.160	1.40
Re-use 6	87	67	0.297	1.38

the ortho-oxidation pathway and para-oxidation pathway to catechol and hydroquinone as the first step. Hydroquinone is converted to p-benzoquinone, while the conversion of hydroquinone to o-benzoquinone is considered negligible, since o-benzoquinone was not detected by HPLC in our study. The aromatic intermediates break down into open cleavage products such as maleic acid, which oxidize into short chain carboxylic acids such as formic, malonic, acetic and oxalic acids. At the end of the reaction acetic, formic and oxalic acids break down into and CO_2 and H_2O. Figure 7 (inset) compares calculated and measured TOC for the measured concentrations of phenol and the quantified intermediates identified in the reaction solution with time. The difference between the TOC calculated and TOC measured is considered to correspond to the unidentified intermediates, mostly the solid polymer formed in the reaction [43]. Based on the results obtained there are no differences between the measured and calculated throughout the reaction, suggesting that all the reaction intermediates were identified or possible contribution of unidentified soluble compounds is considered negligible.

3.3 Catalyst stability and reusability

The Al/Cr-PILC catalyst with ratio of 1:1 was used six consecutive times for the CWAO of phenol solution to evaluate its stability and reusability, and the results are presented in Table 5. After four runs the phenol removal efficiency was still above 98%, suggesting that no significant loss of the catalytic activity occurred. However, the TOC conversion noticeably decreased from 84 to 67%, indicating that more hydroxylation instead of phenol mineralization occurred with the catalyst reuse. Therefore, it is recommended that four runs for the catalyst was feasible in order to achieve almost complete phenol removal and 74% TOC conversion under studied conditions. There was a negligible decrease in the catalyst BET surface area from 180 to 172 m^2/g after the successive reuse indicating negligible change in the surface

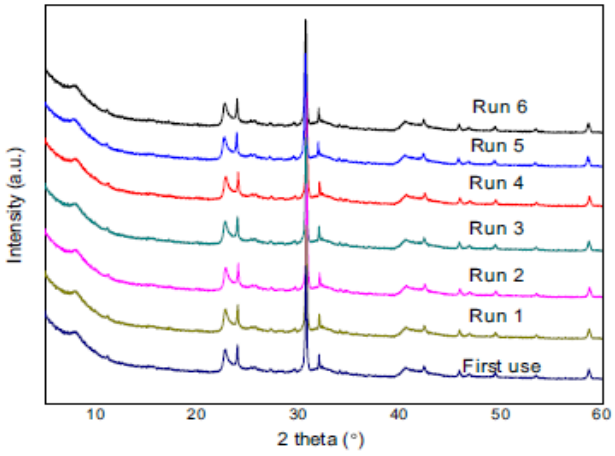


Fig. 8 XRD patterns of fresh and reused Al/Cr-pillared clay catalyst (Al/Cr ratio 1:1) under optimal experimental conditions

composition of the catalyst during use. This result suggests that the noticeable decrease in Al/Cr-PILCs catalytic activity for the consecutive oxidation reaction runs was unlikely caused by surface area pore site blockage. The Cr^{3+} leaching concentration was less than 1 mg/L after six times catalyst reuse, which exhibited high stability of the Al/Cr-PILCs catalyst. The results of the catalytic activities and stability of the Al/Cr- PILCs catalyst revealed that they are good catalyst and have the sufficient stability in the CWAO of phenol reaction. Therefore, making Al/Cr-PILCs catalyst promising materials for treatment of refractory organic pollutants.

The structure of the catalyst after each catalytic run was evaluated by XRD analysis and the results are indicated in Table 5 and Fig. 8. No evident decline of basal spacing was observed after the consecutive reaction runs. The excellent stability of the basal spacing might be due to the stable structure of the catalyst. The XRD patterns before and after the consecutive use showed no obvious change in the position of the d_{001} basal spacing of the Al/Cr-PILC catalyst. These results showed that the Al/Cr-PILC catalyst had great stability and good reusability.

4 Conclusions

The method of hydrolysis and ion exchange were successfully achieved by direct addition of the clay into the pillaring solution using ultrasound both during the formation of the pillaring solution and in the intercalation process, respectively. The preparation method used in this study significantly reduced the synthesis time and the water consumption required compared to traditional method discussed in the literature, indicating advantages of potential scale-up of the pillared clay preparation.

The results of the CWAO experiments showed that all tested pillared clay catalysts were active in both removal of phenol and TOC conversion. The highest conversion was obtained with Al/Cr ratio of 1:1 Al/Cr, since 100% phenol removal was achieved after 120 min, and 84% TOC conversion was obtained after 180 min under the low temperature and oxygen partial pressure conditions of 100 °C and 10 bar in the oxidation of phenol by CWAO. Aromatic intermediates such as catechol, hydroquinone and benzoquinones were obtained and it was found that these intermediate compounds oxidized into short-chain carboxylic acids such as oxalic acid, maleic acid, formic acid, acetic acid and malonic acid. And these short-chain carboxylic acids were then oxidized directly into carbon dioxide and water. The reusability of the catalyst showed superior catalytic activity and stability under our operating conditions. Moreover, in all experimental runs, chromium leaching was found to be less than 1 mg/L, which was lower than the maximum allowed by legislation.

Acknowledgements We kindly acknowledge the financial support of the National Research Foundation (NRF)/ Department of Science and Technology (DST) of South Africa under Professional Development Programme (PDP) Project No. 96719 and Mineral Science Council of South Africa (Mintek) under CWO of Wastewater Project No. ADE 164.

References

1. Ye W, Zhao B, Gao H, Huang J, Zhang X (2016) Preparation of highly efficient and stable Fe,Zn,Al-pillared montmorillonite as heterogeneous catalyst for catalytic wet peroxide oxidation of Orange II. J Porous Mater 23:301–310. https://doi.org/10.1007/s10934-015-0082-y
2. Sassi H, Lafaye G, Ben Amor H, Gannouni A, Jeday MR, Barbier J (2017) Wastewater treatment by catalytic wet air oxidation process over Al-Fe pillared clays synthesized using microwave irradiation. Front Environ Sci Eng 12:2. https://doi.org/10.1007/s11783-017-0971-1
3. Zhu J, Wen K, Wang Y, Ma L, Su X, Zhu R, Xi Y, He H (2018) Superior thermal stability of Keggin-Al30pillared montmorillonite: A comparative study with Keggin-Al13pillared montmorillonite. Microporous Mesoporous Mater 265:104–111. https://doi.org/10.1016/j.micromeso.2018.02.007
4. Li J, Hu M, Zuo S, Wang X (2018) Catalytic combustion of volatile organic compounds on pillared interlayered clay (PILC)-based catalysts. Curr Opin Chem Eng 20:93–98. https://doi.org/10.1016/j.coche.2018.02.001
5. Moma J, Baloyi J, Ntho T (2018) Synthesis and characterization of an efficient and stable Al/Fe pillared clay catalyst for the catalytic wet air oxidation of phenol. RSC Adv 8:30115–30124. https://doi.org/10.1039/C8RA05825C
6. Vicente MA, Gil A, Bergaya F (2013) Pillared clays and clay minerals. In: Bergaya F, Lagaly G (eds.) Handbook of Clay Science. Elsevier, Amsterdam, pp. 523–557. https://doi.org/10.1016/B978-0-08-098258-8.00017-1
7. Bergaya F, Aouad A, Mandalia T (2006) Pillared clays and clay minerals. Dev Clay Sci 1:393–421. https://doi.org/10.1016/S1572-4352(05)01012-3

8. Aouad A, Mandalia T, Bergaya F (2005) A novel method of Al-pillared montmorillonite preparation for potential industrial up-scaling. Appl Clay Sci 28:175–182. https://doi.org/10.1016/j.clay.2004.02.003
9. Ding M, Zuo S, Qi C (2015) Preparation and characterization of novel composite AlCr-pillared clays and preliminary investigation for benzene adsorption. Appl Clay Sci 115:9–16. https://doi.org/10.1016/j.clay.2015.07.020
10. Olaya A, Blanco G, Bernal S, Moreno S, Molina R (2009) Synthesis of pillared clays with Al–Fe and Al–Fe–Ce starting from concentrated suspensions of clay using microwaves or ultrasound, and their catalytic activity in the phenol oxidation reaction. Appl Catal B 93:56–65. https://doi.org/10.1016/j.apcatb.2009.09.012
11. Sivaiah MV, Petit S, Brendlé J, Patrier P (2010) Rapid synthesis of aluminium polycations by microwave assisted hydrolysis of aluminium via decomposition of urea and preparation of Al-pillared montmorillonite. Appl Clay Sci 48:138–145. https://doi.org/10.1016/j.clay.2009.11.016
12. Sanabria NR, Molina R, Moreno S (2009) Effect of Ultrasound on the structural and textural properties of Al–Fe pillared clays in a concentrated medium. Catal Lett 130:664. https://doi.org/10.1007/s10562-009-9956-4
13. Rahmani F, Haghighi M, Estifaee P (2014) Synthesis and characterization of Pt/Al_2O_3–CeO_2 nanocatalyst used for toluene abatement from waste gas streams at low temperature: Conventional vs. plasma–ultrasound hybrid synthesis methods. Microporous Mesoporous Mater 185:213–223. https://doi.org/10.1016/j.micromeso.2013.11.019
14. Duong LV, Kloprogge JT, Frost RL, van Veen JAR (2007) An improved route for the synthesis of Al13-pillared montmorillonite catalysts. J Porous Mater 14:71–79. https://doi.org/10.1007/s10934-006-9010-5
15. Tomul F (2016) The effect of ultrasonic treatment on iron–chromium pillared bentonite synthesis and catalytic wet peroxide oxidation of phenol. Appl Clay Sci 120:121–134. https://doi.org/10.1016/j.clay.2015.11.007
16. Baloyi J, Ntho T, Moma J (2018) Synthesis and application of pillared clay heterogeneous catalysts for wastewater treatment: a review. RSC Adv 8:5197–5211. https://doi.org/10.1039/C7RA12924F
17. Gil SA, Korili R, Trujillano MA, Vicente (2011) A review on characterization of pillared clays by specific techniques. Appl Clay Sci 53:97–105. https://doi.org/10.1016/j.clay.2010.09.018
18. Mata G, Trujillano R, Vicente MA, Belver C, Fernández-García M, Korili SA, Gil A (2007) Chromium-saponite clay catalysts: Preparation, characterization and catalytic performance in propene oxidation. Appl Catal A 327:1–12. https://doi.org/10.1016/j.apcata.2007.04.021
19. Corporation GM (1977) United States Patent 19
20. De León MA, Santos CDL, Latrónica L, Cesio AM, Volzone C, Castiglioni J, Sergio M (2014) High catalytic activity at low temperature in oxidative dehydrogenation of propane with Cr–Al pillared clay. Chem Eng J 241:336–343. https://doi.org/10.1016/j.cej.2013.10.086
21. Cañizares P, Valverde JL, Kou MRS, Molina CB (1999) Synthesis and characterization of PILCs with single and mixed oxide pillars prepared from two different bentonites. A comparative study. Microporous Mesoporous Mater 29:267–281. https://doi.org/10.1016/S1387-1811(98)00295-9
22. Gągol M, Przyjazny A, Boczkaj G (2018) Wastewater treatment by means of advanced oxidation processes based on cavitation: a review. Chem Eng J 338:599–627. https://doi.org/10.1016/j.cej.2018.01.049
23. Baloyi J, Ntho T, Moma J (2018) Synthesis of highly active and stable Al/Zr pillared clay as catalyst for catalytic wet oxidation of phenol. J Porous Mater. https://doi.org/10.1007/s10934-018-0667-3
24. Tomul F (2012) Adsorption and catalytic properties of Fe/Cr-pillared bentonites. Chem Eng J. https://doi.org/10.1016/j.cej.2012.01.094
25. Tomul F (2011) Synthesis, characterization, and adsorption properties of Fe/Cr-pillared bentonites. Ind Eng Chem Res 50:7228–7240. https://doi.org/10.1021/ie102073v
26. Tepmatee P, Siriphannon P (2013) Effect of preparation method on structure and adsorption capacity of aluminum pillared montmorillonite. Mater Res Bull 48:4856–4866. https://doi.org/10.1016/j.materresbull.2013.06.066
27. Tomul F, Balci S (2009) Characterization of Al, Cr-pillared clays and CO oxidation. Appl Clay Sci 43:13–20. https://doi.org/10.1016/j.clay.2008.07.006
28. Grim RE (1968) Clay mineralogy. McGraw-Hill, New York, p 596
29. Vhahangwele M, Mugera GW (2015) The potential of ball-milled South African bentonite clay for attenuation of heavy metals from acidic wastewaters: simultaneous sorption of Co^{2+}, Cu^{2+}, Ni^{2+}, Pb^{2+}, and Zn^{2+} ions. J Environ Chem Eng 3:2416–2425. https://doi.org/10.1016/j.jece.2015.08.016
30. Masindi V, Gitari MW, Tutu H, DeBeer M (2015) Efficiency of ball milled South African bentonite clay for remediation of acid mine drainage. J Water Process Eng 8:227–240. https://doi.org/10.1016/j.jwpe.2015.11.001
31. Gu L, Xu J, Lv L, Liu B, Zhang H, Yu X, Luo Z (2011) Dissolved organic nitrogen (DON) adsorption by using Al-pillared bentonite. Desalination 269:206–213. https://doi.org/10.1016/j.desal.2010.10.063
32. Huang W, Chen J, He F, Tang J, Li D, Zhu Y, Zhang Y (2015) Effective phosphate adsorption by Zr/Al-pillared montmorillonite: insight into equilibrium, kinetics and thermodynamics. Appl Clay Sci 104:252–260. https://doi.org/10.1016/j.clay.2014.12.002
33. Li K, Lei J, Yuan G, Weerachanchai P, Wang J-Y, Zhao J, Yang Y (2017) Fe-, Ti-, Zr- and Al-pillared clays for efficient catalytic pyrolysis of mixed plastics. Chem Eng J 317:800–809. https://doi.org/10.1016/j.cej.2017.02.113
34. Chen D, Cen C, Feng J, Yao C, Li W, Tian S, Xiong Y (2016) Co-catalytic effect of Al-Cr pillared montmorillonite as a new SCR catalytic support. J Chem Technol Biotechnol 91:2842–2851. https://doi.org/10.1002/jctb.4899
35. Bel Hadjltaief H, Da Costa P, Galvez ME, Ben Zina M (2013) Influence of operational parameters in the heterogeneous photo-Fenton discoloration of wastewaters in the presence of an iron-pillared clay. Ind Eng Chem Res 52:16656–16665. https://doi.org/10.1021/ie4018258
36. Kloprogge JT (2017) Infrared and raman spectroscopies of pillared clays. In: Gates WP, Kloprogge JT, Madejová J, Bergaya F (eds.) Infrared Raman spectroscopy of clay minerals. Elsevier, Amsterdam, pp 411–446. https://doi.org/10.1016/B978-0-08-100355-8.00012-6
37. Rocha MAL, Del G, Ángel G, Torres-Torres A, Cervantes A, Vázquez A, Arrieta JN, Beltramini (2015) Effect of the Pt oxidation state and Ce^{3+}/Ce^{4+} ratio on the Pt/TiO_2-CeO_2 catalysts in the phenol degradation by catalytic wet air oxidation (CWAO). Catal Today 250:145–154. https://doi.org/10.1016/j.cattod.2014.09.016
38. Arena F, Negro J, Parmaliana A, Spadaro L, Trunfio G (2007) Improved $MnCeO_x$ systems for the catalytic wet oxidation (CWO) of phenol in wastewater streams. Ind Eng Chem Res 46:6724–6731. https://doi.org/10.1021/ie0701118
39. Yang S, Zhu W, Wang J, Chen Z (2008) Catalytic wet air oxidation of phenol over CeO_2-TiO_2 catalyst in the batch reactor and the packed-bed reactor. J Hazard Mater 153:1248–1253. https://doi.org/10.1016/j.jhazmat.2007.09.084

40. Yang S, Cui Y, Sun Y, Yang H (2014) Graphene oxide as an effective catalyst for wet air oxidation of phenol. J Hazard Mater 280:55–62. https://doi.org/10.1016/j.jhazmat.2014.07.051
41. Davies D, Golunski S, Johnston P, Lalev G, Taylor SH (2018) Dominant effect of support wettability on the reaction pathway for catalytic wet air oxidation over Pt and Ru nanoparticle catalysts. ACS Catal 8:2730–2734. https://doi.org/10.1021/acscatal.7b04039
42. Delgado JJ, Chen X, Pérez-Omil JA, Rodríguez-Izquierdo JM, Cauqui MA (2012) The effect of reaction conditions on the apparent deactivation of Ce–Zr mixed oxides for the catalytic wet oxidation of phenol. Catal Today 180:25–33. https://doi.org/10.1016/j.cattod.2011.03.069
43. Zapico RR, Marín P, Díez FV, Ordóñez S (2017) Assessment of phenol wet oxidation on CuO/γ-Al_2O_3 catalysts: competition between heterogeneous and leached-copper homogeneous reaction paths. J Environ Chem Eng 5:2570–2578. https://doi.org/10.1016/j.jece.2017.04.050
44. Guo J, Al-Dahhan M (2005) Modeling catalytic trickle-bed and upflow packed-bed reactors for wet air oxidation of phenol with phase change. Ind Eng Chem Res 44 (17): 6634–6642. https://doi.org/10.1021/ie050335v
45. Álvarez PM, McLurgh D (2002) Plucinski, copper oxide mounted on activated carbon as catalyst for wet air oxidation of aqueous phenol. 1. Kinetic and mechanistic approaches. Ind Eng Chem Res 41:2147–2152. https://doi.org/10.1021/ie0104464
46. Quintanilla A, Menéndez N, Tornero J, Casas JA, Rodríguez JJ (2008) Surface modification of carbon-supported iron catalyst during the wet air oxidation of phenol: Influence on activity, selectivity and stability. Appl Catal B 81:105–114. https://doi.org/10.1016/j.apcatb.2007.11.034
47. Arena F, Italiano C, Spadaro L (2012) Efficiency and reactivity pattern of ceria-based noble metal and transition metal-oxide catalysts in the wet air oxidation of phenol, Appl Catal B. https://doi.org/10.1016/j.apcatb.2011.12.035
48. Santos A, Yustos P, Quintanilla A, Rodríguez S, García-Ochoa F (2002) Route of the catalytic oxidation of phenol in aqueous phase. Appl Catal B 39:97–113. https://doi.org/10.1016/S0926-3373(02)00087-5
49. Zazo JA, Casas JA, Mohedano AF, Gilarranz MA, Rodríguez JJ (2005) Chemical pathway and kinetics of phenol oxidation by Fenton's reagent. Environ Sci Technol 39:9295–9302. https://doi.org/10.1021/es050452h
50. Lal K, Garg A (2015) Catalytic wet oxidation of phenol under mild operating conditions: development of reaction pathway and sludge characterization. Clean Technol Environ Policy 17:199–210. https://doi.org/10.1007/s10098-014-0777-9

Affiliations

Jeffrey Baloyi[1,2] · Thabang Ntho[2] · John Moma[1]

[1] Molecular Science Institute, School of Chemistry, University of the Witwatersrand, P/Bag 3, WITS 2050, Johannesburg, South Africa

[2] Advanced Materials Division, MINTEK, Private Bag X3015, Randburg 2125, South Africa

Chapter 6

Influence of operational parameters and kinetic modelling in a batch reactor

This chapter has been accepted for publication in Iranian Journal of Chemistry and Chemical Engineering (IJCCE) as: **J. Baloyi**, T. Ntho and J. Moma, Influence of operational parameters and kinetic modelling of catalytic wet air oxidation of phenol by Al/Zr pillared clay catalyst.

J. Baloyi – 70% (conducted the research, wrote the first draft and addressed the reviewers' comments);

T. Ntho – 15% (industrial (Mintek) supervisor, oversees the handling of experiments and obtained results);

J. Moma – 15% (academic (Wits) supervisor, reviewed the manuscript and approved the revised manuscript).

Influence of operational parameters and kinetic modelling of catalytic wet air oxidation of phenol by Al/Zr pillared clay catalyst.

Jeffrey Baloyi [1, 2], Thabang Ntho [2] and John Moma [1,*]

[1] Molecular Science Institute, School of Chemistry, University of the Witwatersrand, P/Bag 3, WITS 2050, Johannesburg, South Africa

[2] Advanced Materials Division, MINTEK, Private Bag X3015, Randburg 2125, South Africa

***** Corresponding author: Email: john.moma@wits.ac.za; Tel.: +27-11-717-6741

ABSTRACT: *Single and mixed oxide Al/Zr-pillared clay (Al/Zr-PILC) catalysts were synthesized and tested for catalytic wet air oxidation (CWAO) of aqueous phenol solution under milder conditions, in a semi-batch reactor. The catalysts were synthesized from natural bentonite clay using ultrasonic treatment during the aging and intercalation steps and were characterized by means of high resolution scanning electron microscopy-energy dispersive angle X-ray spectrometry (HRSEM-EDX), powder X-ray diffraction (p-XRD), nitrogen adsorption/desorption, Fourier Transforms Infrared Spectroscopy (FTIR) and zeta potential. Successful pillaring of aluminium and zirconium oxides into the clay was confirmed by p-XRD with increased basal spacing (1.92 nm) and higher specific surface area (230 m^2/g). The influence of stirrer speed (200-1000 rpm), catalyst dosage (1-3 g/L), initial pH (1-3), initial phenol concentration (500-1500 mg/L), effect of temperature (80-150 °C) and oxygen pressure (5-15 bar) was evaluated on phenol conversion and their reaction kinetics. At the optimum conditions of initial pH of 3, catalyst dosage of 2 g/L, initial phenol concentration of 1000 mg/L, reaction temperature of 100 °C and oxygen pressure of 10 bar , the complete removal of phenol was achieved by Al/Zr-PILC within 120 min. The CWAO process was well described by first-order power rate law kinetics model. The apparent activation energy of the reaction calculated by Arrhenius equation was 21.306 kJ mol^{-1}.*

KEYWORDS: *Kinetic modelling; Al/Zr pillared clay; phenol removal; catalytic wet air oxidation.*

INTRODUCTION

Wastewater containing phenol represent a threat to human beings and aquatic life, being regenerated by industrial processes such as petrochemicals, pharmaceuticals, resin manufacturing and refineries in the range of 200-1500 mg/L [1, 2]. Since phenol is stable, refractory, non-biodegradable, toxic to living organism at very low concentration and poisonous to soil microbes, their discharge into the environment without treatment poses severe environmental and health problems. Given these reasons, the treatment of phenol wastewater is important before being released into the environment. Advanced oxidation processes (AOPs) specifically catalytic wet air oxidation (CWAO), appears as one of the preferred feasible and effective methods for the removal of non-biodegradable refractory organic compounds such as phenol [3]. In general, CWAO is a liquid phase oxidation process in which oxygen or air is used to oxidize refractory organic compounds into carbon dioxide and water in the presence of suitable solid catalyst, without any toxic gaseous emission. CWAO process can be operated at mild temperature and pressure conditions, which are very attractive process economics. Unfortunately, the lack of stable and active catalysts, which results in high capital investment and high operating costs limits the large scale application of CWAO.

Noble metal supported catalysts have been reported to be active for the CWAO treatment of refractory organic contaminants, however, the main disadvantage for these catalysts are costs, deactivation, sintering, leaching and deposition of carbonaceous material on the catalysts surface [4, 5]. The use of pillared interlayered clays (PILC) as heterogeneous catalysts in CWAO has been proposed due to their excellent physiochemical, abundant, low cost, simplicity of the pillaring process and catalytic properties. However, traditional process for synthesis of PILC involves prolonged times (1-5 days) and large amount of water (2 wt. % suspension), and such requirements significantly hinder the scale-up of the pillaring process to industrial scale [6, 7]. Many strategies such as use of concentrated clay suspension, dry clay, addition of dry clay to pillaring solutions have been proposed as ways of overcoming the above mentioned problems. Microwave irradiation and ultrasonic treatment during the synthesis of PILC, in which the aging and ion exchange processes occur within minutes (5-30 minutes) has also been reported. The use of mixed metal oxides for the pillaring of the clay has been found to improve properties of PILC compared to single metal oxide [7, 8].

However, CWAO process using PILC heterogeneous catalysts is not only influenced by origin and features of the catalysts but also the operational parameters used. Therefore, in order to determine the feasibility of CWAO for practical use, it is crucial to investigate influence of operational parameters on the efficiency of CWAO on the removal of refractory organic pollutants.

In this context, the objective of this study is to synthesize single and mixed Al/Zr-PILC catalysts from South African natural bentonite clay using ultrasonic treatment during the pillaring and intercalation steps and test them as heterogeneous catalysts for CWAO of phenol. The influence of several significant operation parameters such as stirrer speed, catalyst dosage, initial pH, initial phenol concentration, reaction temperature and oxygen pressure on the CWAO of phenol have also been studied in detail.

EXPERIMENTAL SECTION

Catalyst synthesis

The starting material was natural clay from deposit of Cape Town bentonite mine (Western Cape Province, South Africa). The cation exchange capacity (CEC) of natural clay was 78.6 meq/g. The natural clay was used as received without further purification. The pillaring agent solution was prepared by the slow addition of a NaOH solution (0.4 M, 500 mL) into a 250 mL of 0.4 M $Al(NO_3)_3 \cdot 9H_2O$ or $Zr(NO_3)_4.5H_2O$ at room temperature under vigorous stirring for 120 min until an $[OH^-]/[Al^{3+}$ or Zr^{4+} or $Al^{3+} + Zr^{4+}]$ molar ratio of 2:1 was achieved. The solution was then ultrasonicated for 10 min at 25 °C. The resulting pillaring agent solution was then added directly into dry bentonite clay, at ratio of 3.33 mmol of (Al + Zr)/g sodium bentonite (25 mL pillaring solution/1 g) and stirred at 25 °C for 30 min. The resulting dispersion was ultrasonicated for 10 min at room temperature to perform ion exchange, followed by filtering, washing with high purity water (5 times with 200 mL portions) and centrifuged at 4000 rpm for 8 min. The obtained solids were oven-dried overnight at 120 °C and calcined at 500 °C for 120 min in a muffle furnace.

Characterization of the catalysts

High resolution scanning electron microscopy (HRTEM) was performed on a FEI Nova NanoSem 200 from FEI Company. The elemental analysis was performed by EDX which

was equipped to HRSEM. Powder X-ray diffractograms (p-XRD) were recorded on a high resolution Bruker AXS D8 X-ray advanced powder diffractometer using CoKα-radiation (40 kV, 40 mA, 1.78897 Å) and scanning in the range of 2θ over 5 to 80° at scanning speed of 0.02°/s. Brunauer−Emmett−Teller (BET) specific surface areas, average pore diameters, pore volumes and Barrett-Joiner-Halenda (BJH) pore size distribution of the catalyst samples were determined by N_2 adsorption/desorption at −196 °C using a Micrometrics ASAP Tristar 3000 unit. The samples were place in the sample holder and degassed in a vacuum at 150 °C for 4 h before analysis. FTIR spectroscopic measurements were performed on a Varian 640-IR FTIR spectrometer with a Miracle single bounce diamond ATR cell from PIKE Technologies. Zeta potential was determined by Zetasizer Nano ZS (Malvern Instruments, UK) and the Cation exchange capacity (CEC) was obtained using Kjeldhal technique.

Catalytic oxidation of phenol solutions

The CWAO experiments were carried out in a 350 mL high-pressure autoclave "semi-batch type" reactor (Parr model 4531M) equipped with a magnetic stirrer to eliminate mass transfer limitations of oxygen from the gas to liquid phase. The reactor was fitted with a removable glass lining and loaded with 250 mL of aqueous phenol solution (500-1500 mg/L) at desired initial pH over the range of 3-4 and a desired amount of a catalyst (1-3 g/L). After reaching the adsorption/ desorption equilibrium, the reaction mixture inside the reactor was purged with N_2 and then heated to the desired temperature between 80 to 150 °C. Once the desired temperature was reached, pure oxygen pressure (5-15 bar) was introduced into the reactor and a first sample was withdrawn for analysis in which it was set as "zero time". Thereafter, liquid samples were withdrawn at regular time intervals by a syringe and immediately filtered by 0.45 μm pore size nylon micro filter into a HPLC vial. All experiments were conducted in triplicate and the average data used. The concentrations of phenol were analyzed with an HPLC system (LC-10AD, Shimadzu, Kyoto, Japan) using an ODS-3 column and UV detector at a detection wavelength of 254 nm. The mobile phase was a mixture of methanol and water (60:40, v/v) slightly acidified with 0.1% acetic acid at a flow rate of 1 mL/min and 20 μL injection volume. The evolution of phenol intermediates during the reaction were analysed by HPLC following the method described by Ma et al. [9]. Total organic carbon (TOC) was measured to determine the mineralization degree of phenol by a Shimadzu TOC analyzer.

Kinetic study

The CWAO reaction kinetics for the phenol oxidation reaction is required to provide complete interpretation of the data obtained in the semi-batch reactor. Many researchers [2, 3, 10, 11] in the literature have described the oxidation rates of phenol oxidation using a simple power law expression. All experimental data were fitted to a power rate law and represented by the following equation:

$$r_a = -\frac{dC_{ph}}{dt} = k_1 \cdot C_{O_2}.\ C_{ph}^{a} \quad (1)$$

where r_a is the rate of phenol oxidation reaction; α is the reaction order with respect to phenol; Co_2 is the oxygen concentration; k_1 is the intrinsic reaction rate constant. Assuming a constant concentration of oxygen, the power rate law becomes

$$-\frac{dC_{ph}}{dt} = k_{ap} \cdot\ C_{ph}^{a} \quad (2)$$

The majority of authors previously reported that the CWAO of pure phenol oxidation reaction follows first-order kinetics with respect to the phenol concentration [2, 3, 12-16]. Assuming a first order reaction with respect to phenol concentration, Equation 2 can be integrated for α = 1 to become:

$$-ln\ C_{ph}\ =\ k_{ap}.t + \times \quad (3)$$

$$-ln\left(\frac{C_{ph}}{C_{0\,ph}}\right) = k_{ap}\,t \quad (4)$$

where k_{ap} (min^{-1}) is the apparent first-order kinetic rate constant, which can be determined from the slope of $-ln(\frac{C_{ph}}{C_{o\,ph}})$ versus *t*, C_{ph} and $C_{0\,ph}$ represent both the final and initial concentration of phenol, respectively.

Activation energy

Assuming an Arrhenius dependence of temperature, apparent activation energy of phenol conversion can be expressed as follows

$$k_{ap} = k_0 \exp\left[-\frac{E_a}{RT}\right] \quad (5)$$

Eq. (5) can be written in the logarithmic form:

$$\ln k_{ap} = \ln k_0 - \frac{E_a}{RT} \quad (6)$$

where E_a is apparent activation energy (kJ mol^{-1}); k_o is pre-exponential factor (min^{-1}); k_{ap} is apparent reaction rate constant (min^{-1}); T is the reaction temperature (K); R is the universal gas constant (8.314 J mol^{-1} K^{-1}).

RESULTS AND DISCUSSION

Catalysts characterization

The chemical composition of natural clay and pillared clay catalysts, as determined by EDS, are reported in Table 1S in the supplementary materials. The chemical weight composition of natural clay confirms SiO_2 and Al_2O_3 as the major constituents of the natural clay with other mineral oxides impurities such as Na_2O, CaO, MgO, K_2O and Fe_2O_3. The high content of Si and Al oxides revealed the existence of quartz and muscovite, whereas the high content oxides of Na compared to Ca confirmed that the natural bentonite is in the sodium form (Na^+) [17, 18]. After the pillaring process the aluminium and zirconium oxides content in the pillared clay catalysts increased from 15.31 to 31.98 wt% and from 0 to 38.19 wt% respectively. The SEM micrographs of natural clay and pillared clay are presented in Fig. 1. The morphology of natural and pillared bentonite clay have tightly packed patterns with porous and rough surface. There are no observable differences in the morphology of the surface of natural and pillared bentonite clays. It is noteworthy that the natural bentonite clay structure was still intact after pillaring process, thus, indicating that the mechanical structure of natural bentonite clay was not affected by the pillaring process.

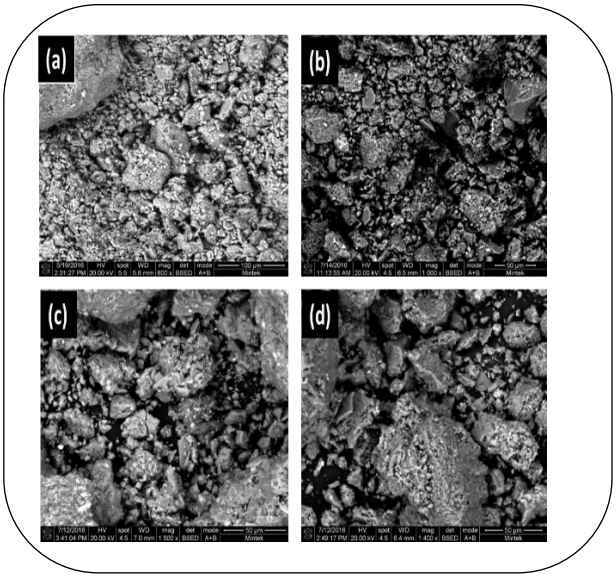


Fig. 1: HRSEM micrographs of (a) Na-Bt, (b) Al-PILC, (c) Zr-PILC and (d) Al/Zr-PILC (3:1).

The surface area, total pore volume, micropore volume and pore diameter of natural and pillared bentonite clays are shown in Table 2S. The expansion of natural bentonite clay structure and desegregation of the bentonite clay particles during the pillaring process leads to a significant increase of the specific surface area and porosity in the pillared bentonite clay catalysts. The increase in the specific surface area and porosity for the single metal oxides (Al or Zr) pillared bentonite clay samples were lower compared to mixed metal oxides (Al/Zr) pillared catalysts. The specific surface area and the micropore volume of natural bentonite clay increased from 61 to 230 m^2/g and 0.089 to 0.115 cm^3/g respectively with the high increase in the surface area for pillared bentonite clay indicating successful pillaring of Al and Zr metal oxides species into the silicate layers of the bentonite clay. These results are in agreement with previous reports by different researchers [8,19-23].

To study the nature of the change of charge on the surface of materials, their zeta potentials were measured. The zeta potential values of natural clay and pillared bentonite clay at different pH values are shown in Fig. 2. The point of zero charge for different samples was determined by plotting the zeta potential values of the suspension as function of pH values [24]. As can be seen, the natural bentonite clay has negative zeta potential values in the pH range of 1 to 10. The high permanent negative charge on the basal surface of Na-Bt clay particles might arise from high degree of isomorphous substitution of structural Si^{4+} in the tetrahedral layer by Fe^{3+} or Al^{3+} while Al^{3+} in the octahedral layer is substituted by Fe^{2+} or Mg^{2+} [25] as well as the pH independent charge arising from the hydroxyl groups at the edges

of the natural bentonite clay particles. The decrease in negative zeta potential from 27 to 17.5 mV with increasing pH values (H^+ ions) in the solution can be attributed to this pH independent charge. In contrast, the pillared bentonite clays have higher zeta potentials than natural bentonite clay, which reflect that positive charges have been introduced into natural bentonite clay during the intercalation process resulting in less negatively charged pillared bentonite clays. This might be attributed to the formed oxide pillars between Na-Bt layers due to the hydration of zirconium or aluminium polycations intercalated into the interlamellar space upon calcination.

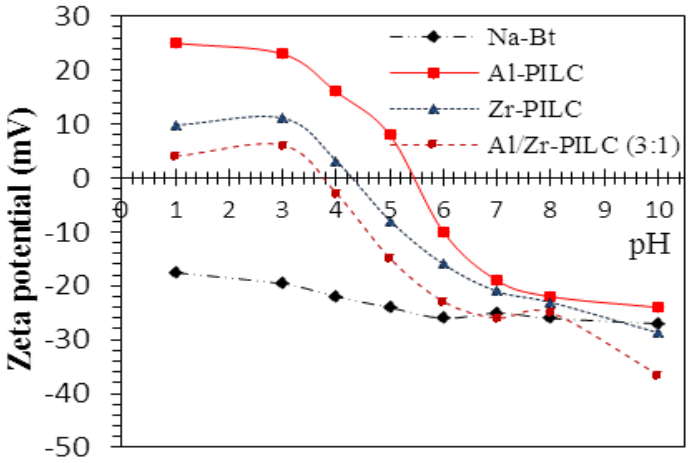


Fig. 2: Zeta potential (mV) values as a function of pH for natural and pillared bentonite clay.

XRD patterns of both the natural and pillared bentonite clays are shown in Fig. 3. The XRD data confirms that the natural bentonite clay contains Na-montmorillonite with other impurities such as quartz, muscovite and calcite. A shift of the signal related to (001) sodium montmorillonite planes at $2\theta = 8.8^{\circ}$ to $2\theta = 7.3 - 6.88^{\circ}$ was observed. The basal *d*-spacing (d_{001}) and 2 theta angle values for materials are listed in Table 3S in the supplementary material. The basal *d*-spacing (d_{001}) increased from 1.56 nm in the natural bentonite to 1.72-1.92 nm in the pillared bentonite clay due to pillaring process. This shift is expected due to expansion of the interlayer space of the natural bentonite clay after pillaring process, thus, indicating a successful intercalation of active metal oxides clusters (Al, Zr or Al/Zr) into silicate layers.

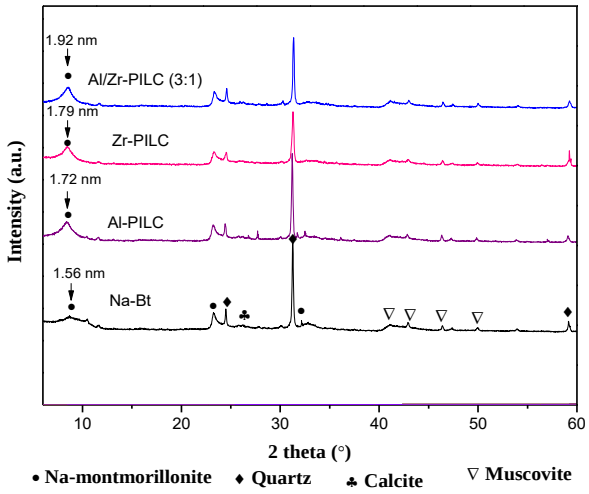


Fig. 3: XRD spectra of natural bentonite clay and pillared bentonite clay samples.

FTIR spectroscopy further confirmed the effectiveness of the pillaring process. The FTIR spectra (400 – 4000 cm^{-1}) of both the natural and pillared bentonite clay materials are shown in Fig. 4. The FTIR spectrum of the natural bentonite clay exhibits two peaks at 3583 and 3294 cm^{-1} in the –OH stretching region. These two peaks correspond to –OH stretching vibrations of structural hydroxyl groups in the bentonite clay and water molecules (H-bonded water) present in the interlayer [26-28]. After pillaring, these peaks at 3583 and 3294 cm^{-1} appeared broadened and their intensity decreased due to the existence of Keggin-OH and Keggin-H_2O stretches and hydration of interlayer water molecules, respectively [29, 30]. The peak near 1630 cm^{-1} corresponds to H-O-H bending vibration of water, while the peak at approximately 978 cm^{-1} corresponds to the siloxane (Si-O-Si) group stretching vibration in the tetrahedral structure of the bentonite clay [27, 31], but the peak shifted to higher wavelength (978 to 1088 cm^{-1}) due to pillaring in all the pillared materials. The peaks at 906 and 771 cm^{-1} can be assigned to Al-OH and MgO-H stretching vibrations, respectively [27]. The peaks resulting from Si-O bending and Al-O stretching vibration are observed at 561 and 611 cm^{-1} respectively [6].

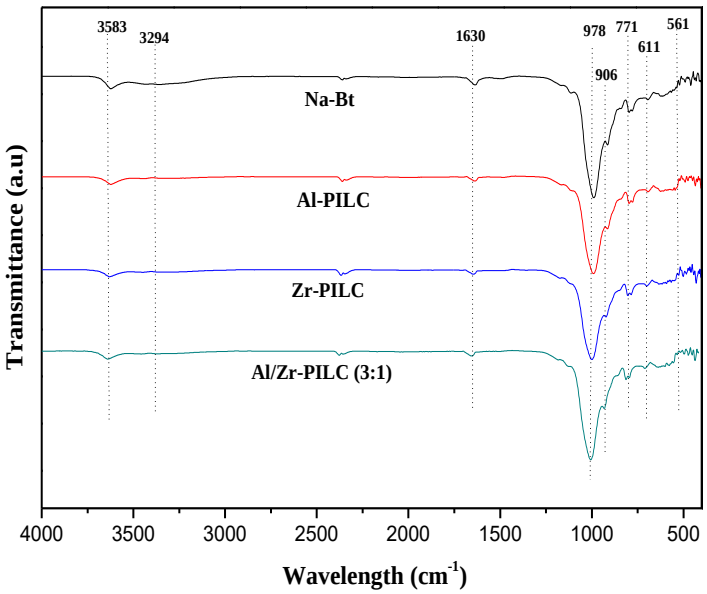


Fig. 4: FTIR spectra of natural bentonite clay and different pillared bentonite clay samples.

Pyridine has been used as a probe molecule to study the chemical nature of acidic sites in the natural and pillared bentonite clay samples [8, 21,]. As shown in Fig. 5 the FT-IR spectra of adsorbed pyridine base molecule in the region of 1650 -1400 cm^{-1} were utilized to discriminate the Lewis and Brönsted acid sites on the samples. Following the pyridine adsorption on natural and pillared bentonite samples, the peaks at 1443, 1491, 1522, 1541, 1558 and 1635 cm^{-1} were observed. The peaks at 1443 and 1541 cm^{-1} represent the pyridine molecules interacted with Brönsted (B) acid sites [8, 21] whereas the peaks at 1491, 1522 and 1635 cm^{-1} represent the pyridine molecules interacted with the Lewis acid site (L) [8, 32-34]. Moreover, the peak at 1558 cm^{-1} mainly corresponds to the pyridine species held by both the Brönsted and Lewis sites [8, 21, 32-34]. The presence of the Brönsted acid sites on the surface acidity of the pillared bentonite clay, is reported to be favorable for the phenol oxidation reaction [8, 31,].

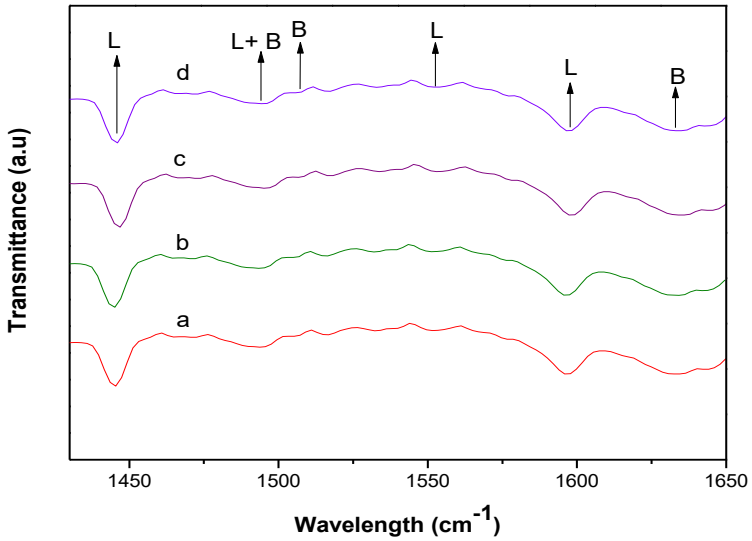


Fig. 5: FTIR spectra of the pyridine adsorbed of the bentonite samples (a) Bt, (b) Al-PILC, (c) Zr-PILC and (d) Al/Zr-PILC (3:1).

CWAO of phenol and the evolution of intermediates

Figure 6(a) shows the phenol conversion with reaction time over natural bentonite clay and pillared bentonite clay. A control experiment (without any catalysts) was carried and 9% of phenol removal was achieved after 120 min, while more than 74% of phenol removal was achieved in the presence of pillared clay catalysts. It can be concluded that the non-catalytic wet air oxidation (WAO) of phenol was not active under these operating conditions. The adsorption experiment was also carried out to test the phenol removal due to adsorption over pillared clay catalysts and only 3% of phenol was removed. However, when using pillared bentonite clay as catalysts in the CWAO, removal of phenol increased significantly with increasing reaction time and the phenol removal were 74%, 88% and 100% after 120 min reaction for Al-PILC, Zr-PILC and Al/Zr-PILC (3:1), respectively. It can thus be concluded that the pillared clays are efficient catalysts in the CWAO of phenol. Figure 6(b) indicates the TOC removal in the CWAO of phenol. The TOC removal in the phenol oxidation by adsorption and in the absence of a catalyst was negligible. In contrast, the removal of TOC was significantly increased, 49%, 61% and 88% being achieved in less than 180 min with Al-PILC, Zr-PILC and Al/Zr-PILC (3:1), respectively, under pillared bentonite clay.

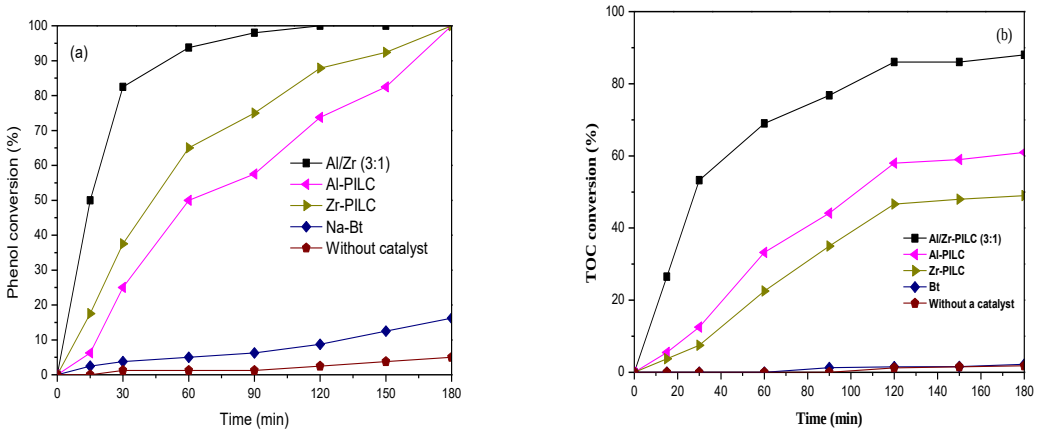


Fig. 6: CWAO of phenol over different catalysts (a) and TOC removal (b) under optimized experimental conditions (200 mL phenol solution, 1000 mg/L phenol concentration, 0.4 g of catalyst, 10 bar oxygen pressure, pH 3.0 and 100 °C reaction temperature).

The experiments on the evolution of the intermediates in the CWAO of phenol over the Al/Zr-PILCs (3:1) catalyst were conducted and the results are shown in Fig. 7. The analysis of the reaction products revealed the presence of the following main intermediates; hydroquinone, acetic acid, formic acid, malonic acid, oxalic acid and maleic acid. The refractory aromatic intermediates such as hydroquinone was identified by HPLC analysis at the beginning of the experiments, and all of them show maximum concentrations within 90 min reaction time. Therefore, the results suggest that these compounds are intermediates, which are further oxidized into short chain carboxylic acids. Moreover, catechol and benzoquinone were not detected in the reaction as reported in the literature [39-41]. This can be due to the fact that these aromatic intermediates get rapidly oxidized, while the short chain carboxylic acids are continuously generated and accumulate in the oxidation reaction. As shown in Fig. 7, after 60 min, the short chain carboxylic acids almost completely disappear from the reaction mixture, whereas formic and acetic acids decline more slowly. Therefore, suggesting that the oxidation rate of both formic and acetic acids is the key step for total mineralization of phenol to CO_2 and H_2O. After 120 min reaction, short-chain carboxylic acids were oxidized directly into CO_2 and H_2O. These results are in agreement with the findings reported by Guo and Al-Dahhan [42].

The effectiveness of the oxidation of phenol has also been analysed in terms of TOC removal measured and calculated from intermediates. Fig. 7 (insert) shows the evolution of TOC actual measured and calculated with reaction time; the difference between these two values corresponds to the unidentified intermediates. The measured TOC removal has been depicted

together with the calculated TOC corresponding to phenol and the analyzed intermediates; the two curves TOC removal against reaction time can be fitted together.

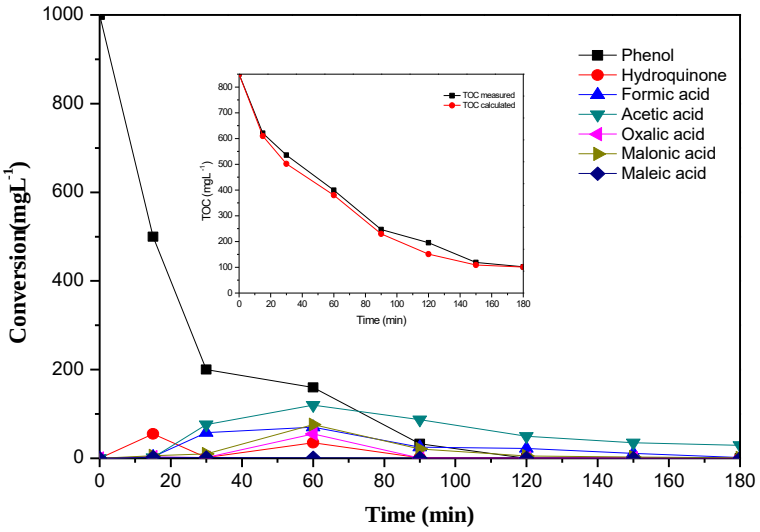


Fig. 7: Evolution of phenol and intermediates in the CWAO reaction of phenol over the Al/Zr-PILC (3:1) (insert shows comparison between calculated and experimental TOC).

Influence of the operational parameters and kinetic study for the CWAO of phenol

In order to obtain efficient CWAO of phenol and their kinetic analysis, the influence of the crucial operational parameters such as mass transfer, initial pH, catalyst dosage, initial phenol concentration, reaction temperature and oxygen partial pressure were evaluated. In studying the kinetics of a chemical reaction that is surface-catalysed, it is important to evaluate the relative contributions of mass transfer and true surface reaction. A diffusion-controlled reaction rate will be greatly affected by changes in the degree of agitation. In order to study the dependence of the reaction on the stirring rate on the conversion of phenol, the stirring rate was varied between 200 – 1000 rpm) at 100 °C using 2 g/L catalyst and 1000 mg/L as initial phenol concentration for 150 min reaction time. As shown in Fig. 8, the increase in phenol conversion rate shows a mass transfer regime from 200 to 600 rpm. However, further increase in stirring speed beyond 600 rpm did not increase the phenol conversion rate, which suggests that mass transfer limitation has no effect on the phenol conversion rate over that range. Consequently, all other kinetic study experiments were carried out at 600 rpm to ensure a kinetically controlled regime.

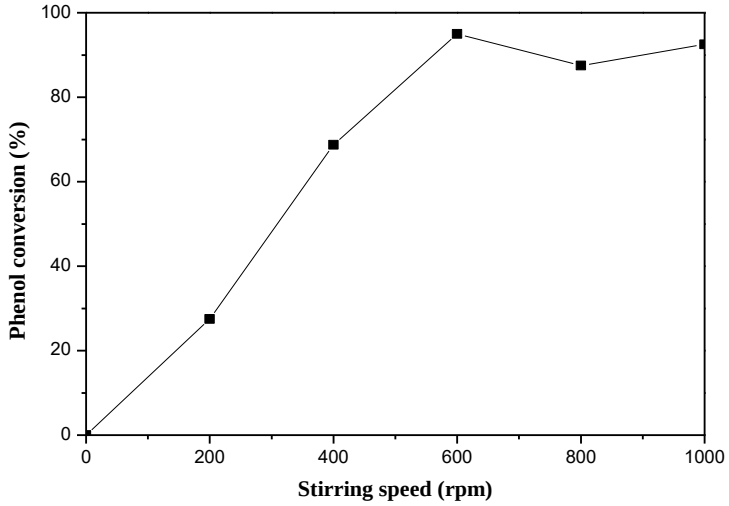


Fig. 8: Effect of mass transfer on the conversion of phenol in aqueous solution. Experimental conditions: phenol, 1000 mg/L; volume, 200 mL; catalyst loading, 2 g/L; reaction time, 150 min; partial oxygen pressure, 10 bar; temperature, 100 °C.

The initial pH of the phenol solution is an important parameter influencing the oxidation of phenol on the CWAO process [35, 89]. The effect of initial solution pH was studied at pH values of 3, 3.5 and 4 as shown in Fig. 9. The conversion of phenol decreases with increasing initial solution pH; the results obtained indicate that optimum pH for maximum phenol conversion in the pH range studied, is pH 3. All reactions for studying the kinetics of the reaction were therefore carried out at pH 3. In view of the fact that CWAO of phenol occurs on the catalyst surface, the process is primarily driven by electrostatic forces. Zeta potential measurements at different pH values provide key information to understanding the interaction and affinity between the catalyst and the phenol solution. As shown in Fig. 2, the point of zero charge for optimum Al/Zr-PILC (3:1) was at pH 3.8. Therefore, the catalyst surface will be positively charged for pH < 3.8, negatively charged for pH > 3.8 and neutral for pH = 3.8, while phenol with pKa of 9.95 is reported to be charged negatively under acidic conditions (studied pH range). Then the conversion of phenol is dependent on the distribution of the species of phenol and the surface charge of Al/Zr-PILC and the existence of cations or anions in the solution. In the studied pH range, phenol is in its non-ionic form; the adsorption onto the catalyst surface is maximized, while there is a minimization of water solubility. The charge attraction between the positively charged Al/Zr-PILC particles and negatively charged phenol molecules increases the affinity of phenol molecules with Al/Zr-PILC particles.

The results of the effect of pH on conversion rate constant were investigated and the results are indicated in the inset of Fig. 9. The experimental data presents good first-order kinetic behaviour. As shown in Fig. 9 (insert), the highest reaction rate constant is obtained at pH 3 where the phenol conversion rate reached 94% within 60 min. However, increase in pH beyond 3 resulted in the decrease of the reaction rate constant values; consequently decrease in the conversion of phenol efficiency (79%). Therefore, the optimal pH of 3 was chosen in this work.

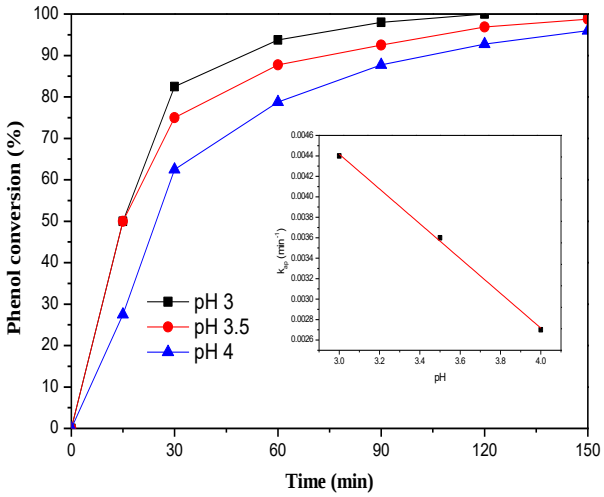


Fig.9: Effect of initial pH on conversion of phenol in aqueous solution (a) and the corresponding effect on rate constant (b). Experimental conditions: phenol, 1000 mg/L; volume, 200 mL; catalyst loading, 2 g/L; reaction time, 150 min; partial oxygen pressure, 10 bar; temperature, 100 °C.

To investigate the effect of the phenol solution concentration on the reaction, it was varied from 500 to 1500 mg/L. As shown in Fig. 10, the phenol conversion decreases with increasing initial concentration of phenol. The decrease in phenol conversion at higher initial phenol concentrations can be as a result of competition for the catalyst active sites by the phenol reactant in solution as well as an increase in mass transfer limitation of phenol and consequently a decrease in the rate at which phenol molecules adsorb on the catalyst surface from solution. The results are in consistent with those obtained by other researchers [4, 42-44], indicating that the catalytic activity of phenol decreases with increasing initial phenol concentration. The effect of initial phenol concentration on apparent kinetic rate constant is shown in the inset of Fig. 10. The results display a good linear relationship of apparent rate constant as a function of initial phenol concentration. The phenol conversion was fitted using first-order kinetic, as confirmed by the observed straight line. The inset of Fig. 10 shows that

the apparent kinetic rate constant decreased with increase of initial phenol concentration. Accordingly, there is a slight increase in apparent kinetic rate constant from 0.0803 min^{-1} to 0.1098 min^{-1} over the initial phenol concentration from 1000 to 500 mg/L. As a result, 1000 mg/L was chosen as the optimal initial phenol concentration in this study.

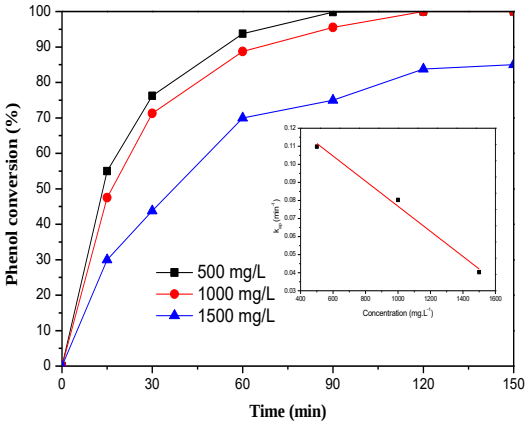


Fig. 10: Effect of initial concentration of phenol in aqueous solution (a) and the corresponding effect on rate constant (b). Experimental conditions: volume, 200 mL; catalyst loading, 2 g/L; pH, 3.0; reaction time, 150 min; partial oxygen pressure, 10 bar; temperature 100 °C.

The optimum catalyst dosage in the reactor was investigated by varying the catalyst mass for the reaction between 1 – 3 g/L of phenol solution maintaining the other parameters constant. Figure 11 show the dependence of the phenol conversion as a function of catalyst amount. An increase in phenol conversion is observed with an increasing catalyst amount from 1 to 2 g/L. However, a further increase to 3 g/L results in a decrease in the phenol conversion. The decrease in conversion with an increase in catalyst amount can be attributed to a decrease in catalyst active sites as a result of agglomeration of the excess catalyst particles in the slurry. A free-radical chain reaction for CWAO of phenol has been proposed by some researchers [45-47]. In this mechanism the competition between free radical formation and free radical termination is expected to take place and both rates increase with an increase in catalyst amount. The results indicate that the free radical formation rate is higher at a lower catalyst loading, while at excessive higher catalyst loading, free radical termination rate dominates the reaction. Therefore, 2 g/L catalyst dosage can be considered optimum for obtaining maximum phenol conversion in the studied range and subsequent experiments were performed at 2 g/L. The effect of catalyst dosage on the apparent kinetic rate constant of phenol is shown in the inset of Fig. 12. The linear trend of apparent kinetic rate constant as

function of catalyst loading shown in Fig. 12 (inset) indicates that the reaction obeys first-order kinetics. The apparent kinetic rate constant increased from 0.0127 min^{-1} to 0.0432 min^{-1} with the increase in catalyst mass from 1 to 2 g/L and then decreased to 0.0297 min^{-1} with a catalyst mass of 3 g/L. Therefore, the highest apparent kinetic rate constant was observed at catalyst loading of 2 g/L with phenol conversion rate of 94% within 120 min.

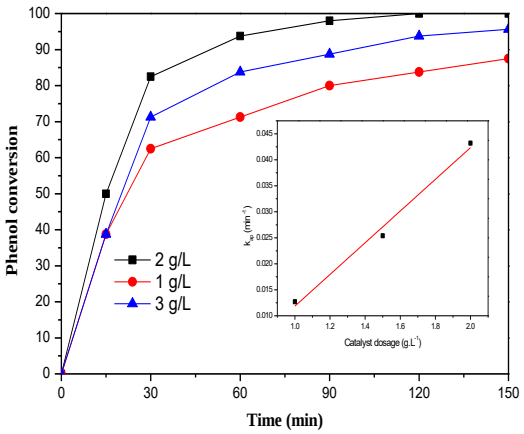


Fig. 12: Effect of catalyst dosage on conversion of phenol in aqueous solution (a) and the corresponding effect on rate constant (b). Experimental conditions: phenol, 1000 mg/L; volume, 200 mL; pH, 3.0; reaction time, 150 min; partial oxygen pressure, 10 bar; temperature, 100 °C.

In order to investigate the effect of temperature on the CWAO of phenol in aqueous solution catalysed by the Al/Zr pillared clay catalyst, the experiments with different temperatures (80 °C, 100 °C and 120 °C) were set up. Fig. 12 shows that the phenol conversion increases with temperature. It is observed that at lower temperatures, the required reaction time was longer than at high temperature. However, at longer reaction times, the difference in phenol conversions at 100 °C and 120 °C are not significantly different. The reaction temperature of 100 °C was considered the optimal reaction temperature in the study. This trend suggests that the reaction temperature strongly affects the CWAO of phenol and can be ascribed to intermediate compounds such as aromatics and organic acids which are reported by other researches to be produced during the reaction [4, 46, 47]. When all these organic compounds are removed, the remaining aliphatic compounds (mainly carboxylic acids) become resistant to oxidation or occur at low rate, even at high temperatures, and the overall oxidation process decreases. In comparison with actual industrial CWAO operation temperature between 200 to 325 °C, the lower reaction temperature required by Al/Zr-pillared clay catalyst would possibly result in high energy cost savings. The influence of reaction temperature on the

apparent kinetic reaction rate constant was investigated as shown in the inset of Fig. 12. A linear relation between the apparent rate constant and the reaction temperature is observed and it is evident that the apparent rate constant of phenol conversion increases with reaction temperature.

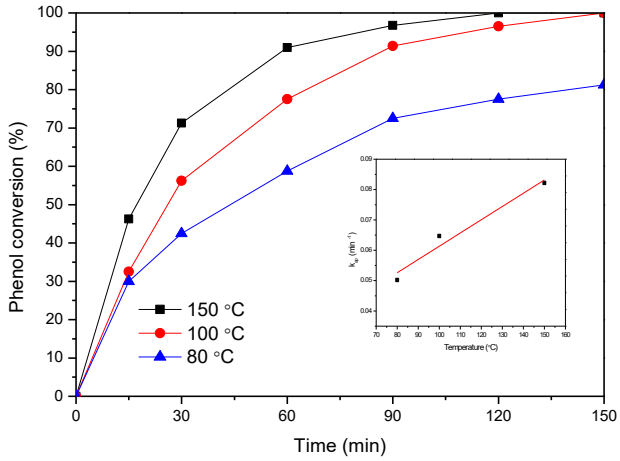


Fig. 12: Effect of reaction temperature on conversion of phenol in aqueous solution (a) and the corresponding effect on rate constant (b). Experimental conditions: phenol, 1000 mg/L; volume, 200 mL; pH, 3.0; reaction time, 180 min; partial oxygen pressure, 10 bar; catalyst loading, 2 g/L.

The effect of oxygen partial pressure on the phenol conversion rate was studied by varying different pressures from 5 to 15 bar and the results are presented in Fig. 13. There is an increase in the phenol conversion with increasing oxygen partial pressure. The phenol conversion reached 74% at 5 bar of oxygen partial pressure while complete removal of phenol was reached at 10 and 15 bar after 120 min reaction time. This is as a result of the fact that the concentration and solubility of the oxygen gas increase with increasing pressure resulting in a faster phenol oxidation rate. This effect might be correlated to the availability of liquid oxygen to the active site of the pillared clay catalysts. According to the Henry's law, the partial pressure of oxygen in the gas phase is directly proportional to the oxygen dissolved in the liquid phase. However, an increase in the oxygen partial pressure from 10 to 15 bar does not result in a significant increase in the phenol conversion. And consequently, the oxygen partial pressure of 10 bar was considered as the optimum value in this study. The effect of oxygen partial pressure on the kinetic reaction rate constant of phenol oxidation was investigated and the results are shown in the inset of Fig. 13. There is a linear relationship of apparent rate constant as function of oxygen partial pressure confirming that the experimental

data obtained can be described by the first-order kinetic model. An increase in the kinetic reaction rate constant with the oxygen partial pressure was observed.

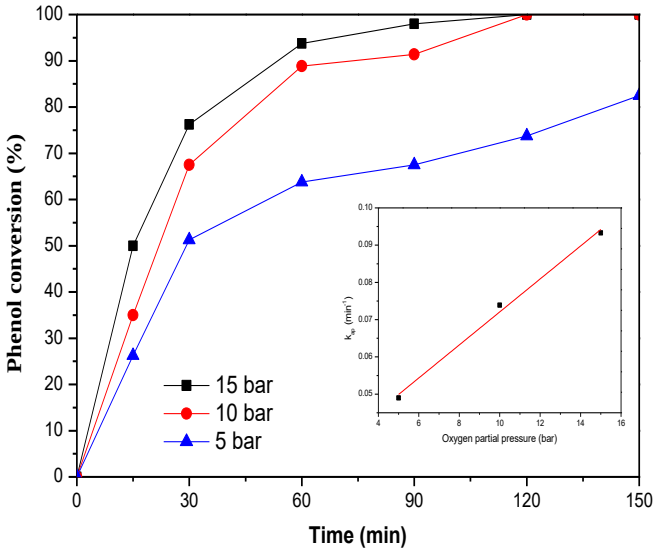


Fig. 13: Effect of oxygen partial pressure on conversion of phenol in aqueous solution (a) and the corresponding effect on rate constant (b). Experimental conditions: phenol, 1000 mg/L; volume, 200 mL; pH, 3.0; reaction time, 180 min; temperature, 100 °C; catalyst loading, 2 g/L.

Activation Energy

In order to determine the apparent activation energy, the experiments were carried out under the predetermined optimal experimental conditions at the three different temperatures. The Arrhenius plot obtained is shown in Fig. 14. The plot presents a good linear relationship (R^2 = 0.9875) between ln k_{ap} and 1/T indicating that the experimental data follow the Arrhenius-type behaviour. The slope and intercept of the straight line were used to determine apparent activation energy (E_a) and pre-exponential factor (k_0), respectively. To the best of our knowledge, there is no study published in the open literature in which these kinetic parameters are reported on the CWAO of phenol using Al/Zr-pillared clay catalysts. However, the kinetics of phenol oxidation using Al/Fe-pillared extrudates has been reported with an apparent activation energy of 53.306 kJ mol^{-1} [4]. It should be noted that such kinetic approach does not correspond to actual intrinsic kinetics since extrudates were used and not powder catalysts as in our study. The observed apparent activation energy and pre-exponential factor of phenol oxidation were found to be 21.306 kJ mol^{-1} and 0.512 min^{-1}, which were lower than 24.62 to 176 kJ mol^{-1} values obtained in other studies using different catalyst systems [2, 12, 14, 48-51]. These results indicate that the CWAO of phenol using

Al/Zr pillared clay catalyst requires a relatively low activation energy compared to other systems studied; and can be easily achieved.

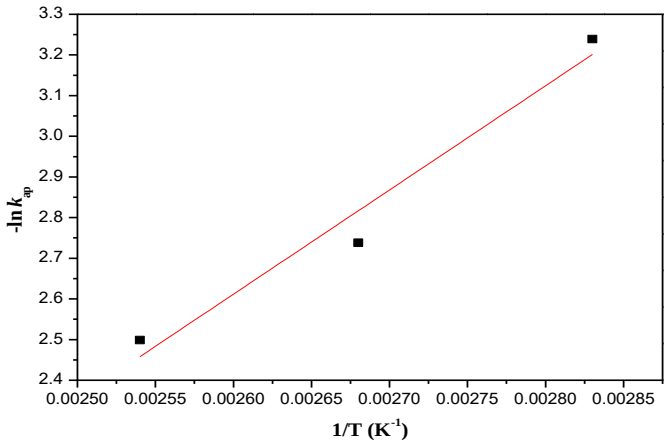


Fig. 14: *Arrhenius plot for determining E_a (apparent activation energy) and k_o (pre-exponential factor) for the CWAO of phenol in aqueous solution. (1000 mg/L phenol; 200 mL volume; pH 3; 100 °C reaction temperature; catalyst loading, 2 g/L).*

CONCLUSIONS

The natural bentonite clay was successfully pillared with single and mixed metal oxides of Al and Zr using ultrasonic treatment. Its catalytic performance was evaluated in the CWAO of phenol in an aqueous solution by semi-batch reactor. XRD analysis confirmed the successful pillaring of bentonite clay. The incorporation of Al^{3+} and Zr^{4+} species into pillared bentonite clay was confirmed by EDX. The results of characterization of synthesized catalysts indicated that the basal spacing, BET surface area, pore volume, surface acidity and thermal stability of mixed Al/Zr-PILC was significantly higher than single Al-PILC, Zr-PILC and natural bentonite clay.

Furthermore, the study indicates the potential of pillared bentonite clay catalysts for the removal of phenol from aqueous solutions under mild reaction conditions of the CWAO process. And the Al/Zr-PILC composite with metal Al:Zr ratio of 3:1 was found to be very active among different pillared catalysts and the complete removal of phenol from solution was achieved within 120 min. The CWAO process was affected by reaction parameters, such as initial pH, catalyst loading, initial phenol concentration reaction temperature and oxygen partial pressure. The optimal reaction parameters were achieved at initial pH 3,

catalyst loading of 2 g/L, phenol concentration of 1000 mg/L at reaction temperature of 100 °C and 10 bar oxygen partial pressure. The experimental results indicate that the phenol oxidation can be described by first-order kinetics, with apparent activation energy of 21.306 kJ mol^{-1}. The Al/Zr-PILC composite catalyst exhibited good results for removal of phenol in aqueous solution at mild condition by CWAO and has the potential to substitute the expensive noble metal catalysts.

Acknowledgements

The authors are grateful to the National Research Foundation (NRF)/ Department of Science and Technology (DST) of South Africa (Project code. 96719) and Mineral Science Council of South Africa (Mintek) (Project code. ADR 31803) for financial support.

REFERENCES

[1] J. Baloyi, T. Ntho, J. Moma, Synthesis and application of pillared clay heterogeneous catalysts for wastewater treatment: a review, RSC Advances, 8 (2018) 5197-5211.

[2] M.F. Abid, G.M. Alwan, L.A. Abdul-Ridha, Study on Catalytic Wet Air Oxidation Process for Phenol Degradation in Synthetic Wastewater Using Trickle Bed Reactor, Arabian Journal for Science and Engineering, 41 (2016) 2659-2670.

[3] A. Eftaxias, J. Font, A. Fortuny, A. Fabregat, F. Stüber, Kinetics of phenol oxidation in a trickle bed reactor over active carbon catalyst, Journal of Chemical Technology and Biotechnology, 80 (2005) 677-687.

[4] J. Guo, Catalytic wet oxidation over pillared clay catalyst in packed-bed reactors: Experiments and modeling, (2005).

[5] F. Arena, C. Italiano, L. Spadaro, Efficiency and reactivity pattern of ceria-based noble metal and transition metal-oxide catalysts in the wet air oxidation of phenol, Applied Catalysis B: Environmental, 115 (2012) 336-345.

[6] F. Tomul, Effect of ultrasound on the structural and textural properties of copper-impregnated cerium-modified zirconium-pillared bentonite, Applied Surface Science, 258 (2011) 1836-1848.

[7] H. Sassi, G. Lafaye, H.B. Amor, A. Gannouni, M.R. Jeday, J. Barbier, Wastewater treatment by catalytic wet air oxidation process over Al-Fe pillared clays synthesized using microwave irradiation, Frontiers of Environmental Science & Engineering, 12 (2018) 2.

[8] S. Mnasri-Ghnimi, N. Frini-Srasra, Promoting effect of cerium on the characteristic and catalytic activity of Al, Zr, and Al–Zr pillared clay, Applied Clay Science, 88 (2014) 214-220.
[9] C. Ma, Y. Wen, Q. Yue, A. Li, J. Fu, N. Zhang, H. Gai, J. Zheng, B.H. Chen, Oxygen-vacancy-promoted catalytic wet air oxidation of phenol from MnO x–CeO 2, RSC Advances, 7 (2017) 27079-27088.
[10] A. Fortuny, C. Bengoa, J. Font, A. Fabregat, Bimetallic catalysts for continuous catalytic wet air oxidation of phenol, Journal of hazardous materials, 64 (1999) 181-193.
[11] A. Eftaxias, Catalytic wet air oxidation of phenol in a trickle bed reactor: kinteics and reactor modelling, Universitat Rovira i Virgili, 2002.
[12] A. Pintar, J. Levec, Catalytic oxidation of organics in aqueous solutions: I. Kinetics of phenol oxidation, Journal of catalysis, 135 (1992) 345-357.
[13] A. Fortuny, C. Bengoa, J. Font, F. Castells, A. Fabregat, Water pollution abatement by catalytic wet air oxidation in a trickle bed reactor, Catalysis Today, 53 (1999) 107-114.
[14] M. Safaa, Catalytic Wet Air Oxidation of phenolic compounds in wastewater in a trickle bed reactor at high pressure, (2009).
[15] A. Quintanilla, J.A. Casas, J.J. Rodriguez, M.T. Kreutzer, F. Kapteijn, J.A. Moulijn, Kinetics of the wet oxidation of phenol over an Fe/activated carbon catalyst, International Journal of Chemical Reactor Engineering, 5 (2007).
[16] A. Quintanilla, J.A. Casas, J.J. Rodriguez, Catalytic wet air oxidation of phenol with modified activated carbons and Fe/activated carbon catalysts, Applied Catalysis B: Environmental, 76 (2007) 135-145.
[17] F. Tomul, S. Balci, Characterization of Al, Cr-pillared clays and CO oxidation, Applied Clay Science, 43 (2009) 13-20.
[18] R.E. Grim, Clay Mineralogy. 2nd edn McGraw-Hill Book Company, New York, (1968) 185-224.
[19] W. Schwieger, G. Lagaly, S.M. Auerbach, K.A. Carrado, P.K. Dutta, Handbook of layered materials, in, Marcel Dekker, Inc., New York, 2004.
[20] P. Canizares, J.L. Valverde, M.R.S. Kou, C.B. Molina, Synthesis and characterization of PILCs with single and mixed oxide pillars prepared from two different bentonites. A comparative study, Microporous and mesoporous materials, 29 (1999) 267-281.

[21] S.V. Awate, S.B. Waghmode, M.S. Agashe, Synthesis, characterization and catalytic evaluation of zirconia-pillared montmorillonite for linear alkylation of benzene, Catalysis communications, 5 (2004) 407-411.
[22] H. Jung, S.-M. Paek, J.-B. Yoon, J.-H. Choy, Zr K-edge XAS study on ZrO2-pillared aluminosilicate, Journal of Porous Materials, 14 (2007) 369-377.
[23] S. Mnasri, N. Hamdi, N. Frini-Srasra, E. Srasra, Acid–base properties of pillared interlayered clays with single and mixed Zr–Al oxide pillars prepared from Tunisian-interstratified illite–smectite, Arabian Journal of Chemistry, (2014).
[24] H. Zhang, X. Liang, C. Yang, C. Niu, J. Wang, X. Su, Nano γ-Fe 2 O 3/bentonite magnetic composites: Synthesis, characterization and application as adsorbents, Journal of Alloys and Compounds, 688 (2016) 1019-1027.
[25] S.I. Rathnayake, W.N. Martens, Y. Xi, R.L. Frost, G.A. Ayoko, Remediation of Cr (VI) by inorganic-organic clay, Journal of Colloid and Interface Science, 490 (2017) 163-173.
[26] J. Madejová, FTIR techniques in clay mineral studies, Vibrational spectroscopy, 31 (2003) 1-10.
[27] P. Kumararaja, K.M. Manjaiah, S.C. Datta, B. Sarkar, Remediation of metal contaminated soil by aluminium pillared bentonite: Synthesis, characterisation, equilibrium study and plant growth experiment, Applied Clay Science, 137 (2017) 115-122.
[28] F.T. Basoglu, S. Balci, Catalytic properties and activity of copper and silver containing Al-pillared bentonite for CO oxidation, Journal of Molecular Structure, 1106 (2016) 382-389.
[29] L.M. Wu, D.S. Tong, L.Z. Zhao, W.H. Yu, C.H. Zhou, H. Wang, Fourier transform infrared spectroscopy analysis for hydrothermal transformation of microcrystalline cellulose on montmorillonite, Applied Clay Science, 95 (2014) 74-82.
[30] S. Acemana, N. Lahav, S. Yariv, A thermo-FTIR-spectroscopy analysis of Al-pillared smectites differing in source of charge, in KBr disks, Thermochimica Acta, 340 (1999) 349-366.
[31] W. Ye, B. Zhao, H. Gao, J. Huang, X. Zhang, Preparation of highly efficient and stable Fe, Zn, Al-pillared montmorillonite as heterogeneous catalyst for catalytic wet peroxide oxidation of Orange II, Journal of Porous Materials, 23 (2016) 301-310.
[32] M. Lefrancois, G. Malbois, The nature of the acidic sites on mordenite, Journal of Catalysis, 20 (1971) 350-358.

[33] M. Kojima, M.W. Rautenbach, C.T. O'Connor, Acidity characterization of ion-exchanged mordenite, Journal of Catalysis, 112 (1988) 495-504.
[34] B.T. Loveless, A. Gyanani, D.S. Muggli, Discrepancy between TPD-and FTIR-based measurements of Brønsted and Lewis acidity for sulfated zirconia, Applied Catalysis B: Environmental, 84 (2008) 591-597.
[35] I. Fatimah, Preparation of ZrO2/Al2O3-montmorillonite composite as catalyst for phenol hydroxylation, Journal of Advanced Research, 5 (2014) 663-670.
[36] G. Fetter, G. Heredia, L.A. Velázquez, A.M. Maubert, P. Bosch, Synthesis of aluminum-pillared montmorillonites using highly concentrated clay suspensions, Applied Catalysis A: General, 162 (1997) 41-45.
[37] G. Fetter, G. Heredia, A.M. Maubert, P. Bosch, Synthesis of Al-intercalated montmorillonites using microwave irradiation, Journal of Materials Chemistry, 6 (1996) 1857-1858.
[38] S.P. Katdare, V. Ramaswamy, A.V. Ramaswamy, Factors affecting the preparation of alumina pillared montmorillonite employing ultrasonics, Microporous and Mesoporous Materials, 37 (2000) 329-336.
[39] A. Santos, P. Yustos, A. Quintanilla, S. Rodrıguez, F. Garcıa-Ochoa, Route of the catalytic oxidation of phenol in aqueous phase, Applied Catalysis B: Environmental, 39 (2002) 97-113.
[40] G. Yang, H. Chen, H. Qin, X. Zhang, Y. Feng, Effect of nitrogen doping on the catalytic activity of activated carbon and distribution of oxidation products in catalytic wet oxidation of phenol, The Canadian Journal of Chemical Engineering, 95 (2017) 1518-1525.
[41] S. Yang, X. Li, W. Zhu, J. Wang, C. Descorme, Catalytic activity, stability and structure of multi-walled carbon nanotubes in the wet air oxidation of phenol, Carbon, 46 (2008) 445-452.
[42] J. Guo, M. Al-Dahhan, Catalytic wet oxidation of phenol by hydrogen peroxide over pillared clay catalyst, Industrial & engineering chemistry research, 42 (2003) 2450-2460.
[43] A. Yadav, A.K. Teja, N. Verma, Removal of phenol from water by catalytic wet air oxidation using carbon bead–supported iron nanoparticle–containing carbon nanofibers in an especially configured reactor, Journal of Environmental Chemical Engineering, 4 (2016) 1504-1513.
[44] Q. Wu, X. Hu, P.-l. Yue, Kinetics study on catalytic wet air oxidation of phenol, Chemical engineering science, 58 (2003) 923-928.

[45] S.S. Lin, D.J. Chang, C.-H. Wang, C.C. Chen, Catalytic wet air oxidation of phenol by CeO2 catalyst—effect of reaction conditions, Water Research, 37 (2003) 793-800.
[46] F. Arena, C. Italiano, A. Raneri, C. Saja, Mechanistic and kinetic insights into the wet air oxidation of phenol with oxygen (CWAO) by homogeneous and heterogeneous transition-metal catalysts, Applied Catalysis B: Environmental, 99 (2010) 321-328.
[47] L. Chang, I.P. Chen, S.-S. Lin, An assessment of the suitable operating conditions for the CeO2/γ-Al2O3 catalyzed wet air oxidation of phenol, Chemosphere, 58 (2005) 485-492.
[48] A. Pintar, J. Levec, Catalytic liquid-phase oxidation of refractory organics in waste water, Chemical engineering science, 47 (1992) 2395-2400.
[49] A. Santos, P. Yustos, A. Quintanilla, F. Garcia-Ochoa, Kinetic model of wet oxidation of phenol at basic pH using a copper catalyst, Chemical engineering science, 60 (2005) 4866-4878.
[50] J.F. Akyurtlu, A. Akyurtlu, S. Kovenklioglu, Catalytic oxidation of phenol in aqueous solutions, Catalysis Today, 40 (1998) 343-352.
[51] F. Stüber, I. Polaert, H. Delmas, J. Font, A. Fortuny, A. Fabregat, Catalytic wet air oxidation of phenol using active carbon: performance of discontinuous and continuous reactors, Journal of Chemical Technology and Biotechnology, 76 (2001) 743-751.

Chapter 7

Cordierite honeycomb washcoated with Al/Zr pillared bentonite catalyst: mechanistic studies, reaction pathway and kinetic modelling

This chapter has been submitted for publication under Applied Catalysis B: Environmental as: **J. Baloyi**, T. Ntho and J. Moma, Catalytic wet air oxidation of phenol by cordierite honeycomb washcoated with Al/Zr pillared bentonite.

J. Baloyi – 70% (conducted the research, wrote the first draft and addressed the reviewers' comments);

T. Ntho – 15% (industrial (Mintek) supervisor, oversees the handling of experiments and obtained results);

J. Moma – 15% (academic (Wits) supervisor, reviewed the manuscript and approved the revised manuscript).

Catalytic wet air oxidation of phenol by cordierite honeycomb washcoated with Al/Zr pillared bentonite

S.J Baloyi [a, b], J.A Moma[a], and T.A Ntho [b]

a Molecular Science Institute, School of Chemistry, University of the Witwatersrand, P/Bag 3, WITS 2050, Johannesburg, South Africa.
b Advanced Materials Division, Mintek, Private Bag X3015, Randburg 2125, South Africa

---

The use of monolithic catalysts to the oxidation of phenol in wastewaters is a crucial issue for practical applications in order to minimize the pressure drop in the flow reactor. Herein, cordierite monoliths coated with Al/Zr pillared bentonite clay powder were synthesized, characterized and tested in phenol oxidation. The pillared clay powder and the washcoat layers were characterized by techniques such as HRSEM, N_2 adsorption–desorption and XRD. Ultrasound experiments used to estimate the coating adherence show that the washcoated Al/Zr pillared bentonite powder is well anchored on the cordierite. Kinetics of catalytic wet air oxidation (CWAO) of phenol was studied over monolithic catalyst using a flow reactor. The complete removal of phenol and 91% TOC conversion were observed in the presence of monolithic catalyst at optimal conditions. After 140 h long reaction the catalyst exhibited a negligible changes in removal of phenol and TOC conversion, showing that the catalyst was very stable and highly reactive. The high specific surface area, good dispersion and reducibility of the pillared clay mixed oxides coated as a thin layer over the cordierite monolith led to the higher catalytic activity observed in phenol oxidation. During the CWAO of phenol reaction, aromatic ring intermediates (*p*-benzoquinone, catechol acid and hydroquinone) and short chain carboxylic acids (oxalic acid, maleic acid, formic acid, acetic acid and malonic acid) were identified. Kinetic parameters of the model that describes the formation and oxidation of intermediate aromatic compounds and short chain carboxylic acids were determined. The obtained experimental data results were described sufficiently with respect to phenol conversion. The proposed CWAO of phenol kinetic model account for internal and external diffusion limitations, assuming the pseudo-first order reaction. Therefore, synthesized monolithic catalysts have great potential for application in CWAO of phenol, since the materials used in the process are inexpensive, abundant and require minimal modifications.

Keywords: Pillared clay washcoating; flow reactor; reaction pathway and kinetics; phenol; catalytic wet air oxidation (CWAO).

1. Introduction

The development of inexpensive and stable catalytic materials for treatment of wastewater is increasingly becoming a priority in environmental catalysis research. The current demands involves the use of inexpensive catalytic materials, robust, economic and environmental friendly wastewater treatment processes. In this context, catalytic wet air oxidation (CWAO) have emerged as one of the most promising processes to remove highly refractory organic compounds that are non-biodegradable in wastewater. CWAO operates under mild reaction conditions such as reaction temperature in the range of 100 - 200 °C and pressure of 5 - 30 bar using oxygen as environmental friendly oxidant [1]. CWAO generate strongly oxidative hydroxyl radical from oxygen decomposition to easily degrade refractory organic pollutant molecules. However, the development of low-costly active, selective and stable catalytic materials still remains the main disadvantage for a wide application and commercialisation of CWAO processes [2].

Wastewater originating from petroleum refinery, pharmaceutical, agricultural, pulp and paper mills, petrochemical and ceramic plants, coal conversion activities, dyes, pesticides and phenolic resins are one of the major water intensive industries which generate high amount of very hazardous wastewater [3]. Phenol and its derivatives are difficult to degrade by conventional biological treatment due to their poor biodegradability, high toxicity and ecological aspects, hence the phenol effluent wastewater should be treated by advance oxidation processes (AOPs) such as CWAO [4]. The presence of discharged phenol in water bodies represents a serious health hazard to humans, animals, plants and microorganisms. Moreover, phenol presents carcinogenic and mutagenic potential for humans. Phenol is very harmful to organisms even at low concentrations and great attention has been paid to removal of phenol in aqueous effluents.

Many studies on the CWAO of phenol involve the use of costly noble metals deposited on various supports [5], transition metal oxides [6] and pillared interlayered clays (PILCs) catalysts [7]. In the past decade PILCs appear to be promising catalytic materials in wastewater treatment application due to their low cost, high catalytic activity, highly stable to leaching and environmental safety [8,9]. However, industrial scale development of the CWAO pillared clay catalysts depends on the ability to conform the powder PILCs catalysts from laboratory scale to commercial shapes scale such as pellets, spheres, trefoils and monoliths. Therefore, there is

a great necessity for creative strategies which should enable PILCs to be engineered to "designer catalysts" for applications in sustainable wastewater treatment processes. For practical purposes, PILCs catalytic powders must be fixed on a shaped substrate. At present, many studies in the literature found the monolithic supported catalysts very attractive due to high mechanical strength, enhanced heat transfer performance, higher catalytic activity with less active components and a faster response to changing conditions [10]. Honeycomb cordierite ($2Al_2O_3 \cdot 2MgO \cdot 5SiO_2$) ceramics is the most common and popular monolithic structure because of its superior hydrothermal stability, economic reasons and plasticity. It is therefore selected as the monolith substrate in this study. For practical purpose washcoating of honeycomb cordierite with PILCs powder catalysts deems to be necessary. And the PILCs powder as active component of the monolithic catalyst greatly influences the final catalytic activity. The monolithic catalyst as a novel kind of catalyst presents excellent operational properties such as, high mechanical strength, convenient to install or uninstall the monolithic catalyst into or out of the reactor, a low thermal expansion coefficient and low pressure drop when used in a fixed bed reactor.

In the current study, cordierite monolith substrate was used due to their beneficial properties in order to support a low cost active PILCs catalyst for the CWAO of phenol in aqueous solution. For the preparation of structured monolithic catalyst, Al/Zr-PILCs as the active phase taking into account our previous studies by Baloyi et al. [11], in which Al/Zr-PILCs catalyst was found to be highly active and stable catalyst for CWAO of phenol in aqueous solution. Therefore Al/Zr-PILCs/cordierite monolith have been synthesized and characterized by high resolution scanning electron microscopy (HRSEM), Energy-dispersive X-ray spectroscopy (EDX), N_2 adsorption-desorption, X-ray diffraction (XRD) and ultrasound test to investigate morphologies, chemical composition, BET surface areas, structure phase identification and mechanical stability of coating, respectively. The synthesized monolithic catalyst was used in CWAO using phenol as selected model pollutant in flow reactor at mild temperature (120 – 160 °C) and oxygen pressure (5 – 15 bar). The aim of selecting mild reaction conditions was to reduce the severity of CWAO conditions which may decrease capital and operating cost of the overall wastewater treatment. The phenol oxidation reaction intermediates were identified and a reaction pathway and kinetic model were proposed. To best of our knowledge, the application of Al/Zr-PILCs/cordierite monolith catalysts for this reaction has not been previously reported.

2. Experimental

2.1 Materials

Natural South African sodium bentonite clay from deposit of Cape bentonite mine (Cape Town, Western Cape province, South Africa) was used as starting material to prepare powder pillared clay catalyst. The natural bentonite clay was used as received without any further purification or cation exchange. The main physicochemical characteristics of the bentonite clay were specific surface area (S_{BET}), 61 m^2/g, total pore volume (V_{total}), 0.11 cm^3/g, basal spacing (d_{001}), 1.24 nm and cation exchange capacity (CEC), 78.6 meq/100 g. Other physiochemical characteristics are described in details elsewhere [11]. The cordierite honeycomb monoliths used in this study were obtained from Mintek. The supplied cordierite honeycomb monoliths with a square cell density of 400 cells per square inch (cpsi). A photographic image of a monolith section before and after washcoating is shown in Fig.1. All chemicals reagents which were used in this study, e.g., NaCl, Na_2CO_3, $Al(NO_3)_3 \cdot 9H_2O$, $Fe(NO_3)_3 \cdot 9H_2O$, $Zr(NO_3)_4 \cdot 5H_2O$, $Cr(NO_3)_3 \cdot 9H_2O$, C_6H_5OH, HCl and NaOH were of analytical grade, purchased from Merck Chemicals (Pty) Ltd. High purity water (resistivity 18.2 MΩcm) purified by a Milli-Q water system (millipore) in the Mintek laboratory was used throughout this study.

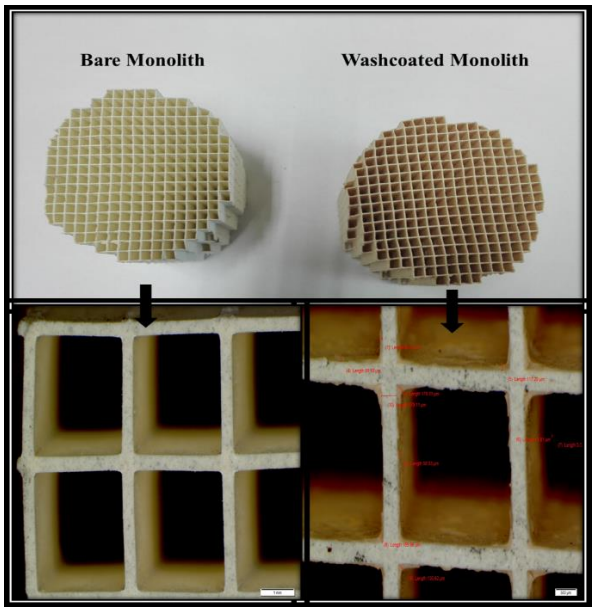


Fig. 1. Photographic images of monolith section used for SEM-EDX before and after washcoating in this study.

2.2 Powder catalyst preparation

The powder pillared clay catalyst samples used in the washcoating of cordierite honeycomb monoliths was prepared by ion exchange method. The pillaring and intercalation procedures have been described in more details in previous works using Al^{3+}/Zr^{4+} intercalating pillaring agents [11]. The molar ratio of 3:1 mixed metal oxides of Al^{3+}:Zr^{4+} was used, as optimised in our previous studies [11]. In an attempt to further improve the specific surface area of the pillared powder catalyst, the powder catalyst was acid activated using 25 v/v% sulphuric acid at 100 °C for 4 h [12]. The obtained suspension was thoroughly washed with high purity water (until pH > 4) and then oven-dried overnight at 120 °C. The prepared pillared clay catalyst sample was referred as Al/Zr-PILCs.

2.3 Optimization of the slurry and monolith washcoating

The cordierite honeycomb monoliths were washcoated in accordance to the modified dip-coating method that was used by other researches for washcoating of cordierite monolith [12,13]. The cordierite honeycomb monoliths were cut to the dimensions of the plug flow reactor column test attains cylindrical samples with 5.5 cm diameter and 5 cm length. The slurry was prepared according to the modified ball-milling procedure reported by Cristiani et al. [14]. The washcoated cordierite honeycomb monoliths catalysts were prepared from the Al/Zr-PILCs slurry which was accomplished using the Netzsch-Feinmahltechnik GmbH LME1 wet grinding ball mill and ceria stabilized zirconia beads. The mixture containing Al/Zr-PILCs powder, high purity water and 30 wt. % silica solution (molar ratio of 1:2:1.5 of Al/Zr-PILCs powder, high purity water and 30 wt. % silica sol, respectively was used) was milled. The silica solution was used in order to improve the binding strength. Milling was done in order to attain required particle size (2 – 5 μm). The Al/Zr-PILCs was separated from the grinding beads by fluidisation method and oven-dried overnight at 120 °C. Then the milled Al/Zr-PILCs slurry was stabilised by mixing with high purity water in a jacketed reaction flask and kept under vigorous stirring for 180 min at room temperature. In order to obtain active Al/Zr-PILCs catalyst slurry the pH was controlled between 3 and 4 using concentrated nitric acid.

Prior to washcoating the cordierite honeycomb monoliths were pre-treated with 20 v/v% oxalic acid. The cordierite honeycomb monoliths samples were then immersed in oxalic acid solution

for 8 h at room temperature to remove impurities and also roughening the surface. Then the cordierite honeycomb monoliths samples were thoroughly washed with high purity water, air-dried in an oven overnight at 120 °C and calcined in muffle furnace at 500 °C for 2 h under air. The cordierite honeycomb monoliths were dipped into the slurry prepared above for different immersion times (1, 5 and 10 min) and excess slurry was blown out with compressed air. The monoliths were immersed in the slurry for up to 3 times to attain the expected Al/Zr-PILCs loading of 15 to 35 wt. %. Then monoliths catalysts were oven-dried in air at 120 °C for 30 min and finally calcined at 500 °C for 2 h. The catalyst obtained was named Al/Zr-PILC-M.

2.4 Mechanical stability test of washcoat

The mechanical stability test of monolith catalysts was done in order to evaluate the adherence of the pillared clay coating into cordierite honeycomb monolith. The adherence of the Al/Zr pillared clay coated onto the cordierite honeycomb monolith was evaluated by an ultrasonic method [14,15] using digital ultrasonic cleaner (Model UD200 SH-6L). The washcoated monolith catalysts of different Al/Zr pillared clay loadings were put in a beaker containing acetone and submitted to ultrasonic treatment (160 W, 25 kHz). After 60 min, the samples were taken out from ultrasonic cleaner, oven-dried at 120 °C for 30 min and then the weight loss was measured by the following equation:

$$\Delta w(\%) = \frac{(w_b - w_a)}{w_a} \times 100\% \quad (1)$$

Where, Δw is the percentage weight loss of the coating obtained by measuring the weight (w) of the monolith before (w_b) and after (w_a) ultrasonic treatment.

2.5 Characterization techniques

2.5.1 X-ray diffraction

X-ray diffraction (XRD) analysis of all samples was performed on Bruker AXS D8 X-ray advanced powder diffractometer. Diffraction patterns were recorded by using a LinxEye detector with CoKα-radiation (1.78897 Å) over a 2θ range from 5 to 80° at 40 kV and 40 mA with step angle increment of 0.02°/s. The crystal phases of the samples were confirmed according to JCPDS reference.

2.5.2 Scanning electron microscopy (SEM) and energy dispersive spectrometer (EDS)

The surface morphology of the starting pillared clay powder as well as of the cordierite honeycomb monoliths catalysts were carried out in a FEI Nova NanoSem 200 high-resolution scanning electron microscope (HRSEM) coupled with energy dispersive spectrometer (EDS) analysis. The elemental chemical analysis was performed using an OXFORD INCA (Oxford instruments, UK) apparatus.

2.5.3 Textural properties

The textural properties was assessed by N_2 adsorption–desorption isotherms experiments conducted at –196 ˚C using a Micromeritics Tristar 3000 instrument. Prior to the measurement, the samples were degassed at 150 °C for 4 h under vacuum. The specific surface area (S_{BET}) of the samples were calculated by the BET equation while the pore volume and pore size distribution were calculated using the Barrett–Joyner–Halenda (BJH) method based on the desorption branch of the isotherms.

2.6 Experimental set-up

Fig. 2 illustrates a schematic of experimental rig design of high pressure monolith reactor setup. The lab-scale rig was made up of stainless steel reactor column and designed to operate at pressure up to 30 bar. The experimental rig consists of a 6 cm inside diameter and 3 mm wall thickness, liquid and gas delivery system, gas-liquid separator and effluent measurement system. A cylindrical furnace covered the length of the reactor to maintain uniform temperature inside the reactor and the heating tape was arranged along the length of liquid and gas lines. The high pressure monolith reactor is operated in co-current down-flow mode, where pure oxygen is introduced co-currently with phenol into the reactor. The liquid flow rates were controlled by a peristaltic pump, which insured the delivery of a liquid solutions from the feed tank to the top of the reactor at the desired flow rate. The gas flow rates were controlled by a mass flow controller (MFC) linked to a control box and the pure oxygen/air required was

delivered from a pressurised gas cylinder. The pure oxygen is mixed with phenol solution at the top of the rector and subsequently down-flow co-currently through the pre-packing materials to the catalyst bed. Two monolith blocks were packed in between post and pre packing sections supported by a stainless steel screen with mesh openings large enough to hinder particles crossing. For uniform radial liquid distribution over the reactor cross-section of silica sand from the top layer was placed before the monolith catalyst bed. The post packing materials at the bottom of the reactor was also a silica sand with a stainless steel screen placed at the outlet of the reactor column. The reactor effluent passed through the pneumatic actuator before flowing into a liquid/gas separator, which allowed liquid to be collected at the bottom and the gas to be sent to GC analysis connected online.

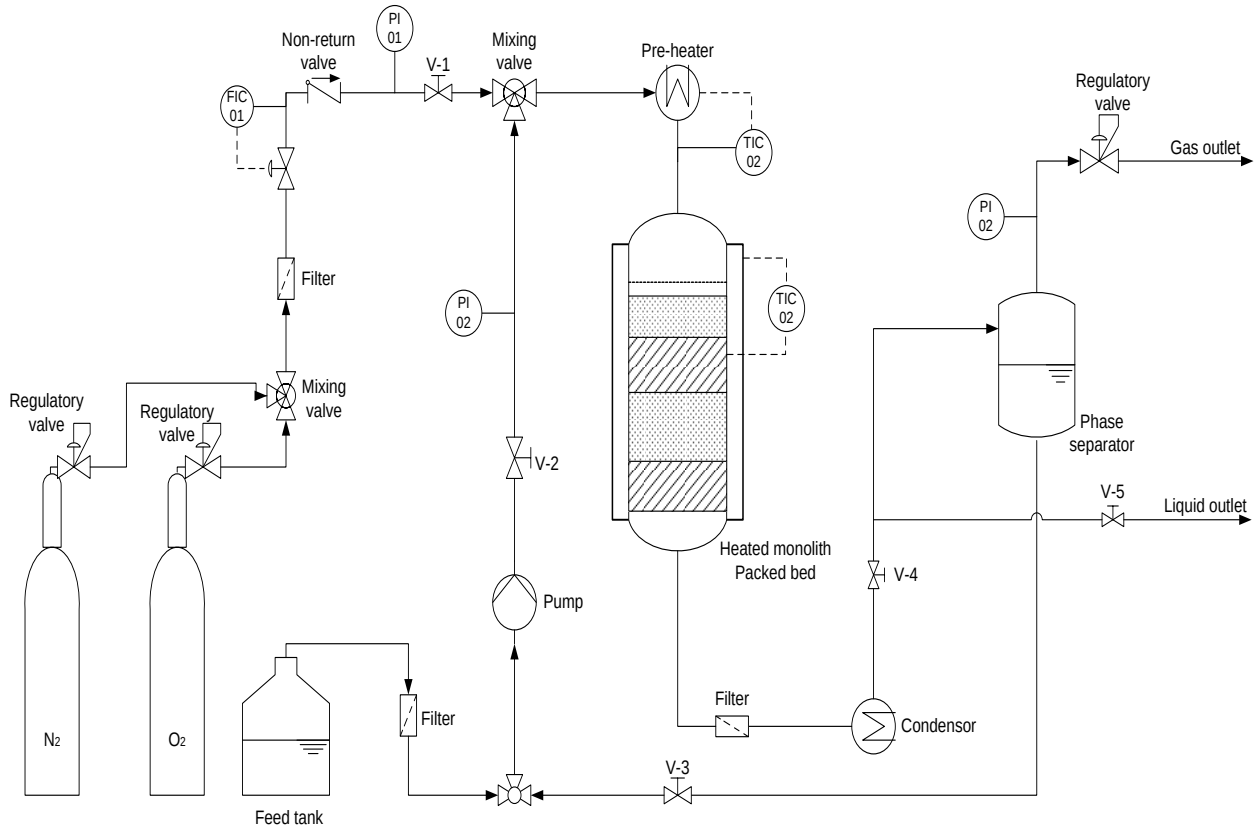


Fig. 2. Process and instrumentation diagram of the monolith reactor experimental rig.

2.7 Catalytic activity measurements procedure and operating conditions

The catalytic activity of Al/Zr-PILCs monolith for the CWAO of phenol in aqueous solution was investigated in a continuous high pressure monolith reactor operated in down flow mode. The long stainless steel reactor column was loaded with two monolith pieces and charged with phenol solution, as well as pure oxygen. The pure oxygen gas is supplied from an oxygen cylinder, while the liquid is delivered to the reactor through peristaltic pump from feed tank and both lines were preheated with electrical tape heater (Heraeus-Witrmann GmbH Heidelberg, type MS6) which was connected to a temperature controller (Yang Ming CX TA 3000) prior entering the reactor. The liquid and gas reactants enters the reactor in different inlet and mixed immediately at the top section of the reactor then contact the reactor bed as combined liquid-gas stream flow. The combined stream was heated in the pre-packing materials to a desired temperature and the heterogeous CWAO reaction is expected to take place after the combined stream contacted the catalyst bed. The reaction temperature was measured by two thermocouples inserted inside the heating furnace and into the packed bed through top reactor inlet evenly spaced along the reactor column length. After passing through the reactor column, the hot effluent was cooled in a condenser, which is operated with water as the coolant, then flow through the gas-liquid high-pressure separator. The stainless steel mesh demister was place in the top flange of the separator to trap the liquid mist from the effluent gas stream. The pressure build up in the gas and liquid inlet and outlet streams was prevented by pressure indicator and safety valve. The liquid outlet at the bottom of the separator was controlled by a micrometric valve, which allowed for sampling of a liquid collected in the separator. Samples were withdrawn during the reaction and taken for analysis. The gas stream from the separator will be discharged through a back-pressure controller which maintained constant pressure in the reactor. Control experiments in absence of Al/Zr-PILCs monolith catalyst, with the bare monolith and packing materials were performed at the same operating conditions as the main experiments. The operating conditions and the operational range are listed in Table 1. In order to have a good comparison with what has been found in the literature, operational conditions used in this study were kept in consistent with what was used by Davies et al. [14].

Table 1
Kinetics experiments operational conditions and monolith reactor dimensions.

Reactor variable	Value
Temperature (°C)	120 – 160
Pressure (bar)	5 – 15
Flow rate of liquid (mL/min)	5 – 20
Flow rate of gas (%)	20 – 100
Initial phenol concentration (mg/L)	1000 – 2000
Reactor diameter (i.d/o.d, m)	(0.056/0.065)
Length of reactor (cm)	43
Length of the bed catalyst (cm)	10
Bed porosity	77.2
Construction materials	Stainless steel

2.8 Analytical methods

The catalytic activity of the pillared clay materials in CWAO was evaluated by the removal of phenol. Phenol and by-products concentration were determined by means HPLC method with an ODS-3 column and a UV detector (LC-10AD, Shimadzu, Kyoto, Japan). A mixture of 60/40 (V/V) of methanol to water (slightly acidified/0.1% acetic acid was added) was used as a mobile phase. For all compounds, the flow rate of the mobile phase was 1 ml/min. The column was operated at a constant temperature of 30 °C. Prior to injection into the analytical HPLC column, the samples were filtered in order to remove fines. Detection of the compounds was performed using UV absorbance at a wavelength of 254 nm. Detection of low molecular weight carboxylic acids was performed with the UV absorbance method at a wavelength of 210 nm. In the end, sample measurement of wavelength was switched to 254 nm to detect phenol correctly, to obtain the concentration profiles of phenol and intermediates. To properly separate phenol from the partial oxidation products, single compounds were quantitatively identified by injecting pure samples of the expected partial oxidation products. The established phenol calibration curve was regularly checked with standard phenol solutions to correct deviations in column performance. The intermediates in the reaction products were identified by comparison with their corresponding pure commercial samples. Then, the calibration curves for each

intermediate detected were established in the concentration ranges that they were found in the reaction products. Phenol conversion Xph was calculated by the following expression:

$$X_{ph} = \frac{C_{ph,in} - C_{ph,out}}{C_{ph,in}} \quad (2)$$

where $C_{ph,in}$ is the inlet phenol concentration and $C_{ph,out}$ the outlet phenol concentration measured during CWAO or adsorption experiments.

The amount of total organic carbon (TOC) in liquid samples was measured using a TOC analyser (O-I Analytical, 1010 model) equipped with a reactor and non-dispersive infrared detector (NDIR). TOC was determined as the difference between total carbon (TC) and total inorganic carbon (TIC) measured. The instrument was set up for analysis of samples with organic carbon concentrations up to 100 ppm. Hence, all samples were diluted as required. The instrument was calibrated using standards (five standards with concentration up to 100 ppm of organic carbon concentration) prepared using potassium hydrogen phthalate. The samples were then injected automatically using an auto sampler into the instrument reaction chamber. In the reaction chamber, the samples were reacted with acid (5% w/v ortho phosphoric acid) to convert any remaining inorganic carbon (CO_3^{2-}) to CO_2, which was then removed by nitrogen (instrument grade). The remaining organic carbon was then oxidised to CO_2 using sodium persulphate (200 g/L) and UV light. The CO_2 liberated was then detected using IR detector, and was used to evaluate the amount of organic carbon in the sample. As phenol, TOC conversion was calculated as:

$$X_{TOC} = \frac{C_{TOC,in} - C_{TOC,out}}{C_{TOC,in}} \quad (3)$$

where $C_{TOC,in}$ is the inlet total organic content and $C_{TOC,out}$ outlet total organic content.

3 Results and discussion

3.1 Washcoat mechanical stability testing

In order to study the mechanical stability of the monolithic catalysts, the adhesion strength of Al/Zr-PILCs coated onto the honeycomb cordierite monolith pieces was evaluated by an

ultrasonic test method. For this purpose, cordierite monoliths were dip-coated up to 5 times and between 13 and 39 wt. % catalyst loading were washcoated into the cordierite monolith pieces. Table 2 indicate the different mass loadings, mass loss and thickness of the coating and coating times required to achieve desired mass loading under ultrasonic vibration with a power of 160 W of 25 kHz exerted for 60 min. As shown in Table 2 the adhesion tests provided excellent results with the weight loss of less than 1 wt. % for all different dip-coating times, therefore illustrating strong adhesion between the coating and cordierite honeycomb monolith substrate. The obtained results are in agreement with other studies in the literature on clays coated on a cordierite monoliths [12,16], with an insignificant weight loss after a long ultrasonic treatment. The evaluation of the Al/Zr-PILCs load on monolith pieces is one of the key factors in the preparation process of the monolithic catalysts. The characteristic dimensions of the coating showing the minimum and maximum thickness are shown by a cross-section cut of an Al/Zr-PILCs coated monolith, seen with a metallurgical microscope (shown in Fig. S1 supplementary materials). Table 2 shows the thickness of coating at different loadings, as expected the thickness of coating was found increasing with the loading of Al/Zr-PILCs slurry. It can be concluded that the thickness of coating during the monolith washcoating is strongly influenced by Al/Zr-PILCs slurry concentration and the coating times. These findings display how good the mechanical properties of the monolithic catalysts.

Table 2

Mechanical stability test of monolithic catalyst and loading of Al/Zr-PILCs into monolith.

Coating times	Mass loaded (wt. %)	Thickness of coating (μm)	Weight loss (%)
1	13	61.89	0.01
2	20	62.61	0.08
3	26	63.25	0.10
4	33	64.75	0.20
5	39	64.96	0.80

3.2 Characterization of the Al/Zr-PILCs monolith catalyst

3.2.1 X-ray diffraction (XRD)

The XRD patterns of the monolithic (Al/Zr-PILCs-M) catalyst as well as for the reference samples used in this study at wide angle XRD and low angle XRD patterns are shown in Fig. 3, respectively. As it can be seen from Fig. 3, bare cordierite has characteristic diffraction peaks at 12°, 21°, 25°, 30°, 33°, 35°, 40°, 41°, 50°, 64° and 68°; accordance with previous results [10,17]. The XRD patterns of natural clay and powder pillared clay catalysts used as reference samples are in good agreement with our previous studies [11] and their detailed discussions can be found in our previous work. In comparing the XRD patterns of pure and oxalic acid pre-treated cordierite monoliths in Fig. 3, it can be seen that the intensity of oxalic acid pre-treated monolith was relatively higher than pure monolith. On the other hand weak diffraction peaks were observed for oxalic acid pre-treated Al/Zr-PILCs compared to pure Al/Zr-PILCs. Moreover, it can be observed that after acidification of powder Al/Zr-PILCs catalyst the Na-montmorillonite peak at 33° was destroyed. These results shows that oxalic acid is less destructive in attacking the cordierite monolith than powder Al/Zr-PILCs. This findings is also in good agreement with results obtained by other authors [18] who studied the preparation of high surface area cordierite monolith by oxalic acid treatment. In order to clearly check the possible presence of the Al/Zr-PILCs coated on the cordierite monolith more clearly, Fig. 3b compiles the XRD patterns of coated cordierite monolith as well as the acid pre-treated bare cordierite monolith and acid pre-treated powder pillared clay samples at low angle. It was observed that, Al/Zr-PILCs crystalline phases can be detected with corresponding peaks to cordierite monolith however with decreased peak intensity. This can be attributed to mixed Al/Zr polyoxocations, which is likely to be present as $\{[Al_xZr_y(OH)_z(H_2O)_n]^{(3x+4y-z)+}\}$, this polyoxocation solution may penetrate the cordierite monolith pores after acid solution and form very thin layers of amorphous [11,17]. Moreover, the decreased peak intensity can be ascribed to the amorphous phase of a pure silica used as binder during washcoating of cordierite monoliths [18].

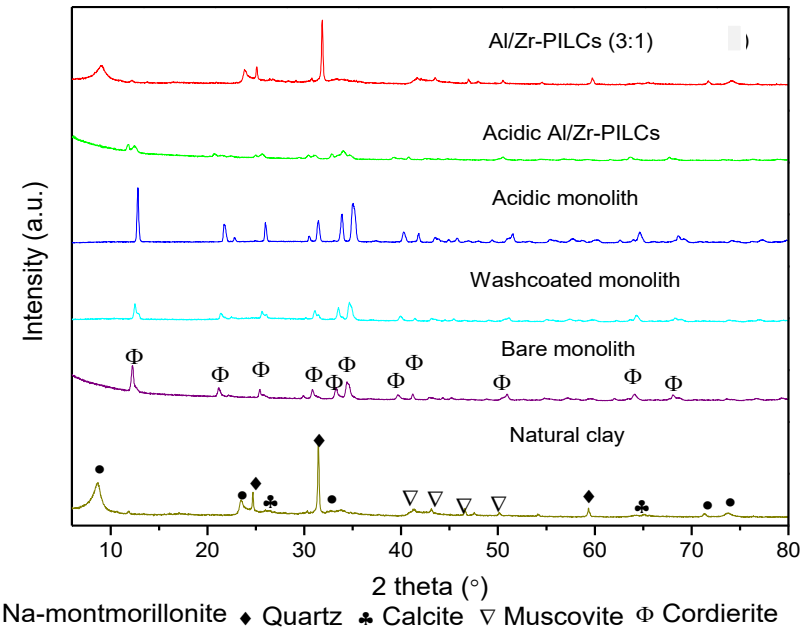


Fig. 3. XRD patterns for the reference natural clay, bare cordierite monolith and Al/Zr-PILCs powder and washcoated monolith (Al/Zr-PILCs-M).

3.2.2. Surface morphology and EDS characterization

Fig. 4 display the surface morphology of the bare cordierite monolith and wash-coated cordierite monolith that was treated by dilute oxalic acid as examined by SEM. The surface morphology of the natural bentonite clay and Al/Zr-PILCs catalysts samples used in this study are shown in Fig. S2 (supplementary materials) SEM micrographs. The surface morphology of these materials are explained details in our previous studies [11]. As can be seen from the images (Fig. 4a-b), the bare cordierite monolith presented a coarse and rough surface, which is favorable for wash-coating process. Fig. 4c-d shows the SEM images of Al/Zr-PILCs-M catalyst, the micrographs of the channel walls show that the Al/Zr-PILCs powder catalysts was well deposited on the channel walls and the washcoat is observed in all the corners of the cross section of washcoated cordierite monolith. Nevertheless, a thin catalytic layer of the Al/Zr-PILCs with interconnected surface cracks was also observed. The cracks in the corners of the monolith channels can be due to the differences in thermal expansion between the cordierite monolith and the Al/Zr-PILCs powder, whereas the cracks in the coat layer can be formed during a too fast drying step [19]. It was reported in the literature that the drying step requires

a careful control of temperature and moisture and the steps must be slow enough to prevent ruptures and cracks [20]. However, it noteworthy that the observed cracks did not significantly affect the stability of the monolithic catalysts, since the stable active component sheets were formed on the cordierite monolith surface, as shown by the results of mechanical stability test in Table 2. In Table 3 energy dispersive spectrometer (EDS) results for different samples are presented. As shown in Table 3, the cordierite monolith elements such as Al, Mg and Si were detected. The EDS analysis confirmed the presence of the Zr and Fe elements in the cordierite monolithic catalyst walls. It noteworthy that the Zr and Fe that was detected in the cordierite monolithic catalyst are most likely from the Al/Zr-PILCs powder used.

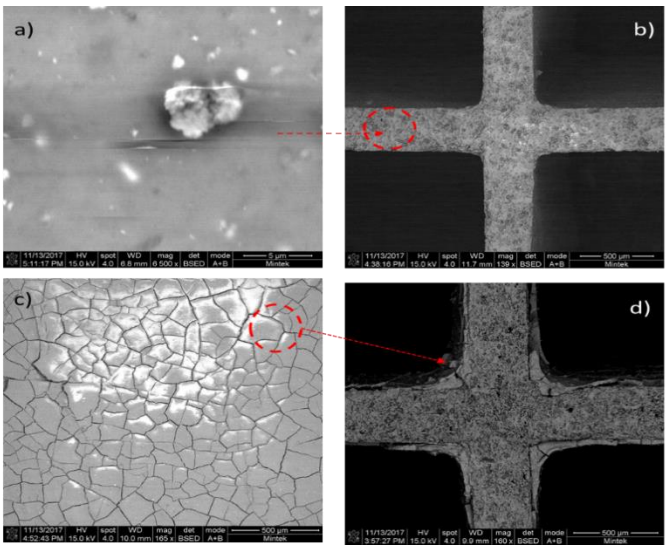


Fig. 4. Comparison between HRSEM images of (a) uncoated cordierite monolith, (b) cross section of uncoated monolith, (c) wash-coated cordierite monolith and (d) cross section of washcoated monolith.

Table 3

Elemental composition estimated by SEM–EDS analysis.

Sample	Na (%)	Mg (%)	Al (%)	Si (%)	K (%)	Ca (%)	Fe (%)	Zr (%)
Natural Clay	3.73	3.29	15.31	65.09	2.39	1.09	9.10	0.00
Bare monolith	0.00	15.37	24.93	59.70	0.00	0.00	0.00	0.00
Al/Zr-PILCs	0.26	1.29	36.65	54. 47	1.41	0.04	1.61	17.31
Al/Zr-PILCs-M	0.12	15.83	27.98	57.24	0.02	0.01	0.16	15.58

3.2.3. Textural characterization

The N_2 adsorption and desorption isotherms analyses of the bare cordierite monolith support and monolithic catalyst (33 wt. % Al/Zr-PILCs-M) were carried out and the results are shown in Fig. 4. The pore size distribution curve of the monolithic catalyst is presented in the inset as well as the cordierite monolith is also shown for comparison. It was observed that the shape of this isotherm exhibited typical IV type N_2 sorption isotherms (IUPAC classification), which suggests the existence of mesopores [23]. The mesoporous texture was also exhibited from average pore size which is approximately 23 nm. According to classification of hysteresis loops from IUPAC [23], the typical H2-type hysteresis loops between the adsorption-desorption isotherms are observed, indicating the existence mesoporous of ink bottle shaped pores.

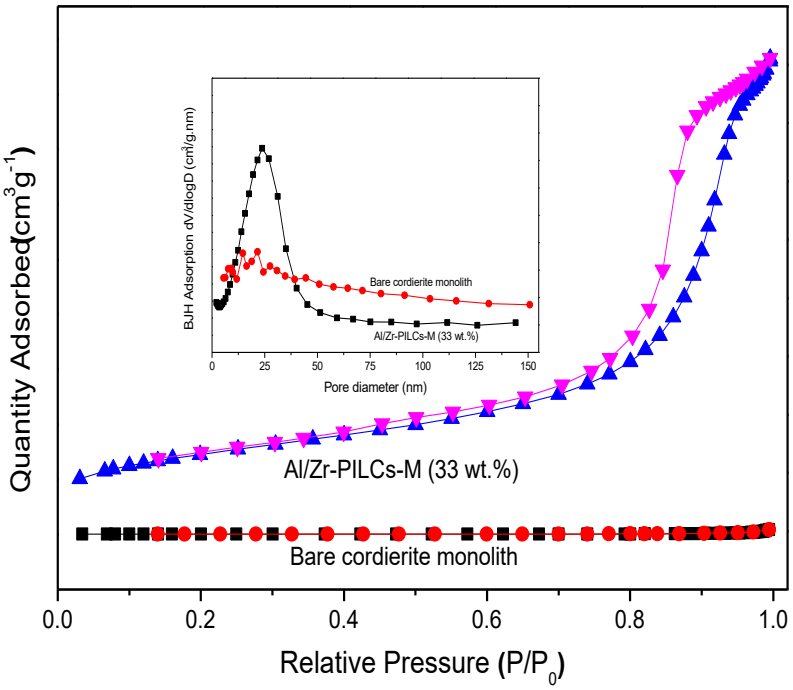


Fig. 4. N_2 adsorption–desorption isotherms of bare monolith and washcoated cordierite monolith. The inset shows the pore size distribution of the monolithic catalyst calculated from the adsorption isotherm.

The BET specific surface areas data was obtained from Brunauer–Emmett–Teller (BET) method and the pore volume and pore size distribution were derived from the adsorption isotherms using the Barret–Joyner–Halanda (BJH) method. The results of the BET specific surface area, pore volume and pore diameter data are listed in Table 4. The BET specific surface

area and pore volume of the powder catalyst and bare cordierite monolith was found increasing after oxalic acid treatment. Shigapov et al. [18] reported that increased pore volume and high specific surface area of cordierite monolith can be obtained by oxalic acid treatment of bare cordierite monolith. It was also found that acid treatment with oxalic acid does not significantly reduce the mechanical stability of the cordierite monolith, which can have a negative effect towards the practical application of the monolithic catalyst. Other studies in the literature also reported that oxalic acid treatment increase the specific surface area and pore volume of the cordierite and also promoted the dispersion of active phase and the activity of the catalysts [12,18]. Han et al. [12] claimed that the layered structure of montmorillonite clay was destroyed, after acid treatment and structural aluminium was dissolved and removed, resulting in reforming porous structure and increasing specific surface area, pore volume and pore size. The specific surface area of Al/Zr-PILCs powder before acid treatment was 230 m^2/g, whereas the bare cordierite monolith support showed negligible BET specific surface area (< 1 m^2/g). The reported BET specific surface area (0.16 m^2/g) in our studies is in accordance with typical BET specific surface area reported in literature for bare cordierite monolith [21]. The BET specific surface area, pore volume and pore size of the Al/Zr-PILCs-M (33 wt. %) increased significantly compared with bare cordierite monolith from 26 m^2/g, 0.033 cm^3/g and 4.9 nm to 160 m^2/g, 0.32 cm^3/g and 5.9 nm, respectively. The obtained results can be ascribed to acidic Al/Zr-PILCs catalyst and SiO_2 in silica solution. The acidic Al/Zr-PILCs catalyst helped increasing the specific surface area due to higher specific surface area of acidic Al/Zr-PILCs, whereas silica solution acted as binder, therefore favouring the loading of acidic Al/Zr-PILCs powder and the formation of new mesopores structure [12]. The high BET specific surface area for monolithic catalysts prepared in this study is significant for practical use of these materials in heterogeneous catalysis.

Table 4

Textural parameters of the catalysts measured by N_2 adsorption and desorption isotherms.

Sample	S^1_{BET} (m^2/g)	V^2_{pore} (cm^3/g)	d^4_{pore} (nm)
Bare cordierite	0.16	0.0002	4.82
Bare cordierite (acid pre-treated)	26	0.033	4.9
Al/Zr-PILCs (3:1)	230	0.38	7.1
Al/Zr-PILCs	242	0.41	7.9
Al/Zr-PILCs-M (33 wt. %)	160	0.32	5.9

[1]Specific surface area (SBET); [2]Total pore volume at p/p0 ~ 0, 99; [4]Pore diameter.

3.3 Catalytic stability and preliminary test

Before performing the reaction studies, preliminary test was conducted in the plug flow reactor, aimed to study the catalyst stability, influence of non-catalytic wet oxidation of phenol, influence of a pressure drop and influence of phenol solution feed flow rate on the performance of this continuous flow monolithic reactor for the CWAO of phenol. The experiments were carried out at 140 °C reaction temperature and 10 bar of oxygen partial pressure, 1500 mg/L of initial phenol concentration and catalyst bed of 10 cm at pH = 4. At optimal operating conditions, pressure drop in the continuous plug flow reactor was found negligible. An experiment without monolithic catalyst was carried out to investigate the non-catalytic wet oxidation process. In this experiment, no phenol removal and TOC conversion was achieved, after 5 h of reaction time. Therefore, it can be claimed that the effect of the non-catalytic wet oxidation of phenol can be neglected in this study. An adsorption experiment, using nitrogen instead of oxygen, was also investigated. The phenol conversion and TOC removal was approximately 3% and 1%, respectively. The effect of gas flow rate was studied by varying the gas flow rate (20, 40, 60, 80 and 100%). The obtained results are presented in Fig. 5(a), as it can be seen both phenol removal and TOC conversion increased as the gas flow rate was increased gradually from 20 to 80%. A maximum phenol removal and TOC conversion were noticed at gas flow rate of 80%, beyond which the gas flow rate slightly decreased. Therefore, 80% gas flow rate was selected for further studies in this work. The effects of residence time on phenol removal and TOC conversion over different phenol flow rate was investigated (5 mL/min to 20 mL/min) under optimal operating parameters, the results are presented in Fig. 5(a). As it can be seen in Fig. 5(a), the phenol removal and TOC conversions were noticeably

decreased from 100% to 70% and 91% to 60%, respectively, with the phenol feed flow rate increasing from 5 mL/min to 20 mL/min. The obtained results can be ascribed to the less hydroxyl radicals being generated at high feed flow rate due to shorter residence time of phenol solution within the reactor. Moreover, with increasing phenol feed flow rate, the colour of the phenol solution slowly changed from colourless to light brown, and then to dark brown. The observed change in colour can be attributed to the oxidation of phenol solution (colourless) to by-products such as benzoquinone which is dark brown in colour, therefore, confirming incomplete removal of phenol at high flow rate.

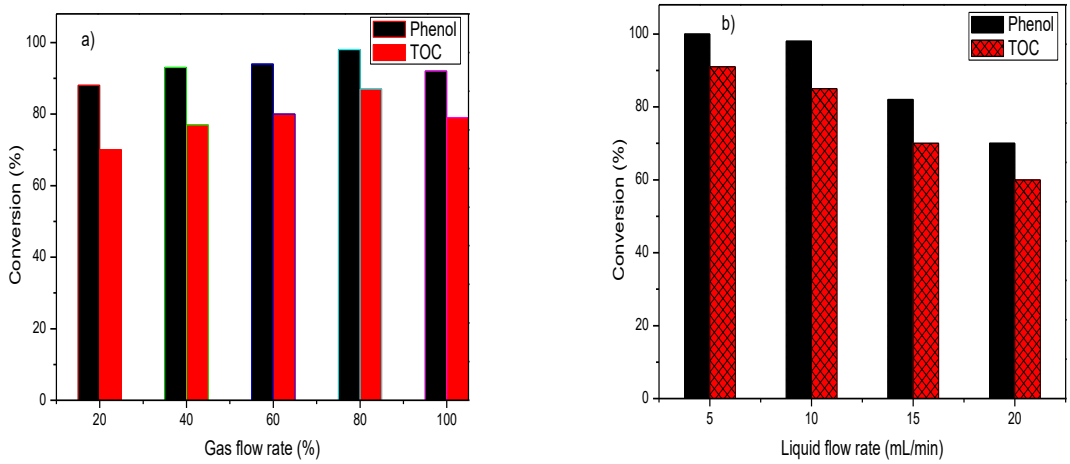


Fig. 5. Effect of phenol feed flow rates on the monolithic catalytic performance, (a) gas flow rate and (b) liquid feed flow rate.

The catalysts used in CWAO of organic pollutants may suffer severe deactivation during the reaction, therefore, prior to the reaction rate studies the special attention was paid to study the stability of the monolithic catalyst. In order to evaluate the monolithic catalyst stability, the long term (140 h) experiment was carried out in a monolithic plug flow reactor operated in a continuous flow mode at optimum reaction conditions. The profiles of removal of phenol and TOC conversions in the liquid effluent during experimental run is shown in Fig. 6. As can be seen in Fig. 6, approximately 97% and 85% removal of phenol and TOC conversion, respectively was achieved after 140 h reaction. The phenol removal and TOC conversion slightly decreased from 100% to 97% and 91% to 85%, respectively during 140 h, which showed high catalyst stability. The obtained results can be ascribed to beneficial effect from chemical interactions between the cordierite monolith support and the Al/Zr-PILCs catalytic layer. The insignificant leaching (< 0.283) of Zr metal in Al/Zr-PILCs catalyst after six cycles

was reported in our previous studies [11]. Since the negligible changes in removal of phenol and TOC conversion were observed during 140 h of reaction, consequently, it can be concluded that the monolithic catalyst revealed a high stability in the reaction conditions in this study.

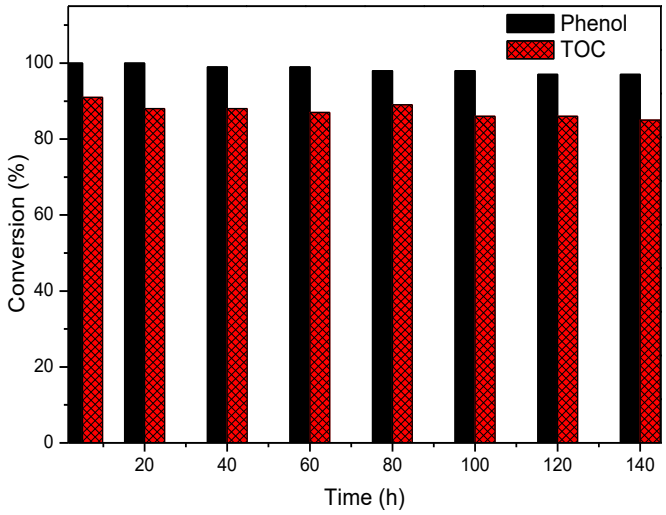


Fig. 6. Stability of monolithic catalyst in the removal of phenol and TOC conversion in long term experiment over optimum conditions.

3.4. Influence of operation conditions

3.3.1. Effect of temperature

In order to study the effect of reaction temperature on CWAO of phenol, experiments were conducted at 120 °C, 140 °C and 160 °C, respectively, while keeping other operational conditions constant. Fig. 7 (a) and (b) shows the relationship between reaction temperature and phenol removal and TOC conversion in 300 min. As can be seen in Fig. 7 (a), the removal of phenol increased gradually with increased in reaction temperature and shows complete removal of phenol at 160 °C. As the reaction temperature increases from 120 °C to 140 °C, phenol removal increased from 82% to 98.5% and complete removal was obtained at 160 °C. The effect of different reaction temperature on TOC conversion was studied and the obtained results are shown in Fig. 7 (b). As it can be seen in Fig. 7 (b), TOC conversion increased from 67% to 91% with increase in reaction temperature from 120 °C to 160 °C after 4 h reaction time. However, insignificant difference of phenol removal and TOC conversion at 140 °C and 160 °C was observed, therefore in this study reaction temperature of 140 °C was considered the

optimal reaction temperature. The obtained results showed that the increase in temperature had increased the rate hydroxylation at monolithic catalyst active sites and generated more hydroxyl radicals, resulting in higher collision frequency between phenol molecules and hydroxyl radicals. The observed slightly increase in phenol removal and TOC conversion at higher temperature can be attributed to self-scavenging of hydroxyl radicals. Mohite et al. [22] also observed an increase in the phenol removal and TOC conversion with the increase in temperature.

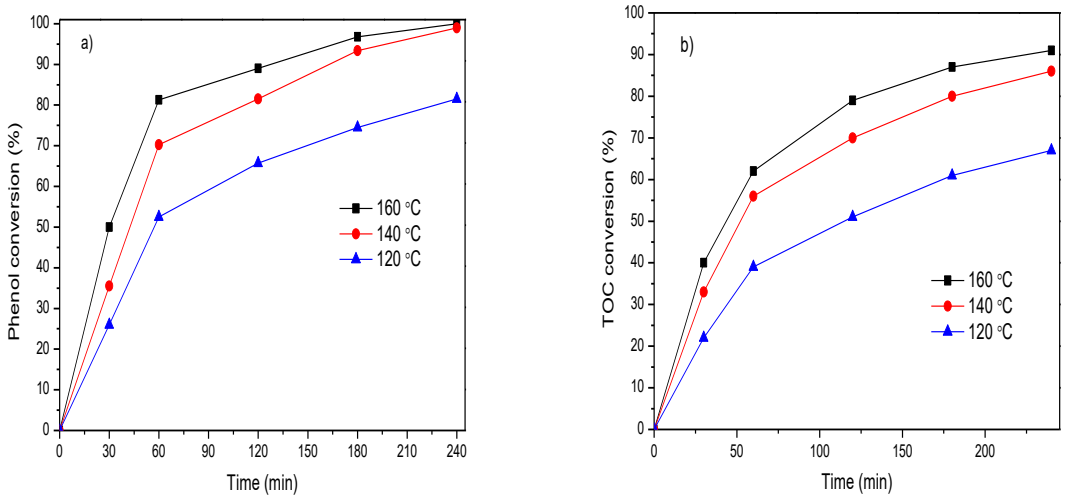


Fig. 7. Effect of temperature on (a) phenol (%) and (b) TOC conversion (%) as function of time over monolithic catalyst. (Reaction conditions: 1500 mg/L of phenol concentration, 10 bar oxygen partial pressure and feed flow rate of 5 mL/min).

3.3.2. Effect of oxygen partial pressure

The effect of oxygen partial pressure on phenol removal and TOC conversion was studied in the range of 5, 10 and 15 bar and the results are shown in Fig. 8. As can be seen from Fig. 8 (a), increasing oxygen partial pressure from 5 to 15 bar the removal of phenol increased from 76 to 100% and the results showed a good agreement with what have been reported in literature [23]. The observed significant increase on phenol removal with increasing oxygen partial pressure can be attributed to increasing density and solubility of the gas. This effect might be correlated to the availability of liquid oxygen to the active site of the monolithic catalyst. According to the Henry's law, the partial pressure of oxygen in the gas phase is directly proportional to the oxygen dissolved in the liquid phase. When the oxygen partial pressure was

increased from 10 to 15 bar, the phenol removal was insignificantly enhanced by approximately 2%. Therefore, the oxygen partial pressure of 10 bar was considered as the optimum value in this study. Fig. 8 (b) shows the TOC conversion for CWAO reactions at the same operating oxygen partial pressure as above. As shown in Fig. 8 (b), the TOC conversion increased with an increase in oxygen partial pressure was observed, when the oxygen partial pressure was less than 10 bar, it had a relatively significant effect on TOC conversion. The TOC conversion enhanced from 70 to 86% when the oxygen partial pressure increased from 5 to 10 bar. This was due to the rising of oxygen concentration in the solution which generate more hydroxyl free radical, thereby increasing TOC conversion. However, when oxygen partial pressure was increased more than 10 bar, an increase in the reaction pressure has no significant influence in TOC conversion (4% increase). Therefore, further increase in oxygen partial pressure above 10 bar tends to affect the phenol removal only by a slight margin. This can be ascribed to saturation of oxygen on the surface of monolithic catalyst while the concentration of the hydroxyl free radical was kept constant. Though it was observed that the CWAO reaction was favoured at higher oxygen partial pressure (15 bar), in order to reduce the severity of the CWAO reaction, the 10 bar oxygen partial pressure was used throughout the investigation. A similar behavior was observed by other researches in literature [40, 41].

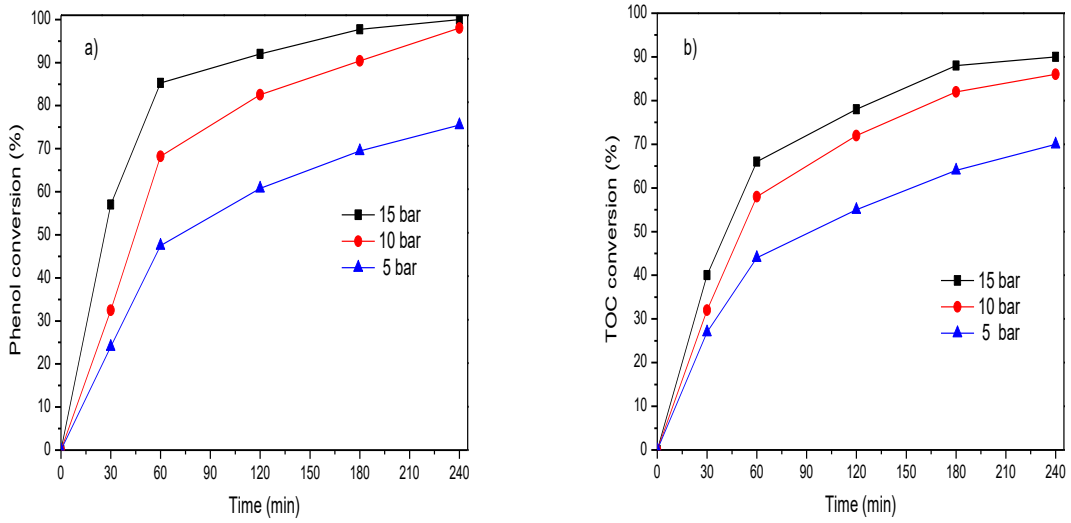


Fig. 8. Effect of oxygen partial pressure on the CWAO of (a) phenol (%) and (b) TOC conversion (%) as function of time over monolithic catalyst. (Reaction conditions: 1500 mg/L of phenol concentration, 140 °C reaction temperature and 5 mL/min feed flow rate).

3.3.3. Effect of the initial phenol concentration

The effect of the initial phenol concentration on the phenol removal and TOC conversion was studied in the range (1000, 1500 and 2000 mg/L), with keeping other operational parameters constant and the results are shown in Fig. 9. Fig. 9(a) shows only a slight difference, up to 5% in initial phenol conversion between the experiments carried out different initial phenol concentration. Therefore, the initial phenol concentration had very little impact on the phenol removal. With increasing the initial phenol concentration from 1000 mg/L to 2000 mg/L, the phenol removal increased from 95 to 100%, respectively, after 240 min reaction. The obtained results shows that the efficiency of the hydroxyl radical oxidation could be enhanced at higher initial phenol concentration. The results reported in our studies are in good agreement with what have been reported in a continuous mode operation, in the literature [24–30]. Eftaxias et al. [31] reported the CWAO of phenol over activated carbon in a trickle bed reactor, where almost complete phenol removal at 5000 mg/L was attained at 160 °C. Suárez-Ojeda et al. [24] investigated the influence of temperature and oxygen partial pressure on the continuous CWO of phenol, o-cresol and 2-chlorophenol, also employing activated carbon as catalyst. Stüber et al. [29] studied the CWAO of phenol in a trickle bed reactor and complete phenol removal was achieved at initial phenol concentration of 2500 mg/L. The obtained results are of great contribution towards industrial scale, since the studied concentrations simulated industrial applications. For example phenols are reported to be present in various wastewater industries, such as refineries (6-500 mg/L), coking operations (28–3,900 mg/L), coal processing (9–6,800 mg/L), pharmaceuticals (0.1-1600 mg/L)and petrochemical plants (2.8–1,220 mg/L) from low to high concentrations [1,8]. Fig. 9(b) shows the influence of initial phenol concentration in solution over the TOC conversion. As presented in Fig. 9(b), TOC conversion increased as the initial phenol concentration increased. Insignificant differences between the initial phenol concentration of 1000 mg/L to 2000 mg/L was observed, the TOC conversion increased from 84 to 90%, respectively. Similar results were reported by Guo et al. [28], who investigated TOC conversion over initial phenol concentration of 1000 mg/L to 2000 mg/L and found 90% TOC conversion at 170 °C. They further reported that the differences in TOC conversion between the studied concentrations were insignificant. Lin et al. [32] reported a maximum TOC conversion in the range of 400 to 2500 mg/L initial phenol concentration after 3 h reaction time

at 15 bar. Moreover, it was reported that only 2 h reaction time was needed to achieve maximum TOC conversion at initial phenol concentration of 400 to 1000 mg/L, 3 h for 2500 mg/L and longer reaction time for 5000 mg/L.

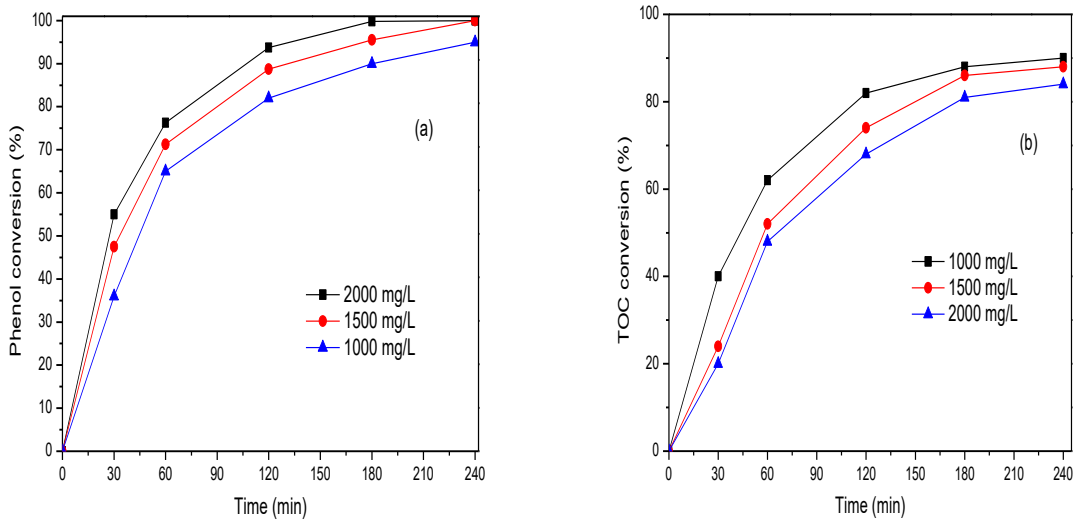


Fig. 9. Effect of initial phenol concentration on the CWAO of (a) phenol (%) and (b) TOC conversion (%) as function of time over monolithic catalyst. (Reaction conditions: 10 bar oxygen partial pressure, 140 °C reaction temperature and 5 mL/min feed flow rate).

3.4. Intermediates evolution and reaction pathway for the CWAO of phenol

The assessment of the reaction intermediates evolution and reaction pathway involved in the oxidation of phenol by CWAO is significant. Fig. 10 shows the evolution of the intermediates upon CWAO of phenol over the monolithic catalyst at 140 °C and 10 bar oxygen partial pressure after 240 min reaction time. As shown in Fig. 10, the reaction main intermediates detected by HPLC at the beginning of the reaction in this study were hydroquinone, formic, acetic, malonic, oxalic and maleic acids. Some known possible aromatic ring compounds such as catechol and benzoquinone were not detected at the beginning of the experiments in this study, which can be attributed to the fact that these phenol reaction intermediates shows high oxidation rate, whereas the short chain carboxylic acids are continuously generated and accumulated in the oxidation reaction. These phenol reaction intermediates were reported in various studies in literature and also detected in our previous studies [11,33]. Devlin et al. [1] also identified the intermediates compounds such as hydroquinone, catechol, formic, acetic,

malonic, oxalic and maleic acids during CWAO of phenol at 200 °C. Quintanilla et al. [3] studied the phenol reaction intermediates and identified aromatic ring intermediates such as *p*-benzoquinone, *p*-hydroxybenzoic acid and very low amounts of hydroquinone as primary oxidation intermediates that are further oxidized to short chain carboxylic acids (mainly maleic, malonic, acetic and formic acids). In their studies short chain carboxylic acids showed to be highly resistance to further oxidation to CO_2 and H_2O after complete oxidation of phenol, it was further suggested that these acids were being responsible of the TOC remaining after complete removal of phenol. As shown in Fig. 10, when the phenol oxidation reaction time was increased, aromatic compounds such as catechol and benzoquinone were identified in very low amounts ($\leq$ 10 mg/L) and short chain carboxylic acids such as oxalic acid, maleic acid, formic acid, acetic acid and malonic acid were also detected at very low concentration. This suggesting that these short chain carboxylic acids are reaction intermediates that are further oxidized to CO_2 and H_2O. However, it was noticed that short chain carboxylic acids such as acetic acid concentration decreases slowly, therefore, it can be assumed that oxidation rate of both acetic acids is the key step for total mineralization of phenol to CO_2 and H_2O.

Moreover, the TOC conversion was calculated from the concentration of the different reaction intermediates identified by HPLC, in which 91% TOC conversion was attained. Fig. 10 (inset) compare the TOC conversion values measured directly with the TOC analyser and the TOC conversion values calculated from the concentrations of the different reaction intermediates identified by HPLC. The two curves of TOC conversion with reaction time can be well fitted together, indicating that all reaction intermediates had been accurately detected and quantified in the CWAO of phenol.

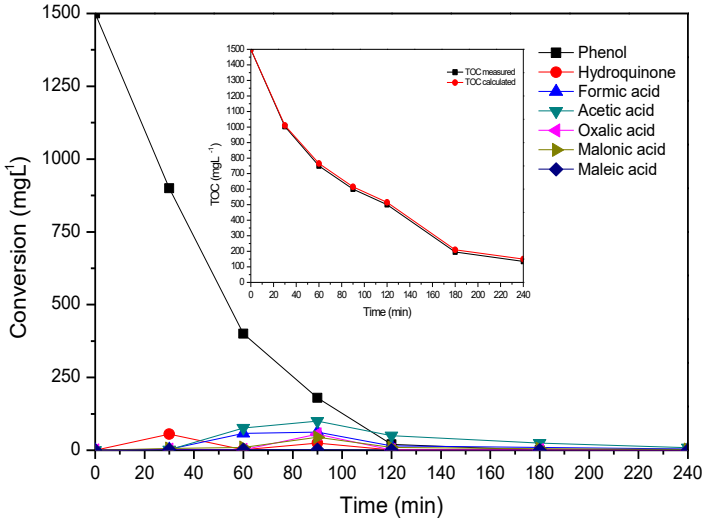


Fig. 10. Evolution of phenol and intermediates upon CWAO of phenol at 140 °C under 10 bar.

Possible catalytic reaction pathway for CWAO process of phenol in the continuous plug flow reactor was proposed based on the reaction intermediates products identified by HPLC analysis above. Fig. 11 shows a proposed reaction pathway in this study using monolithic catalyst at 140 °C under 10 bar. The discussion of our reaction pathway experimental results were limited to our findings in this study, since the detailed radical nature of phenol CWAO mechanism has been already well documented in the literature [34–37]. As can be seen in Fig. 11, hydroxylation of phenol takes place in ortho-oxidation pathway and para-oxidation pathway to catechol and hydroquinone as first step. Hydroquinone was converted to p-benzoquinone, while o-benzoquinone was not identified in our studies. Zazo et al. [36] reported that the presence of p-benzoquinone can be explained by the dihydroxybenzenes and benzoquinones which are in redox equilibrium in acid media. They further reported that the formation of o-benzoquinone was not possible to be identified in the phenol CWAO reaction since this compound is unstable in aqueous solution and there are no commercial standards available. After first step, both catechol and hydroquinone follow the same oxidation route, ring-opening of these aromatic intermediates compounds by oxidation of hydroxyl radical leads to the formation of maleic acid which further oxidized quickly to short-chain carboxylic acids such as oxalic acid and malonic acid. Acetic acid was generated from malonic acid while formic acid was generated from oxalic acid, which were final oxidized to H_2O and CO_2 [36,38,39]. According to the formed CWAO of phenol intermediates, the reaction pathway of phenol was in good agreement with the result in the literature [3].

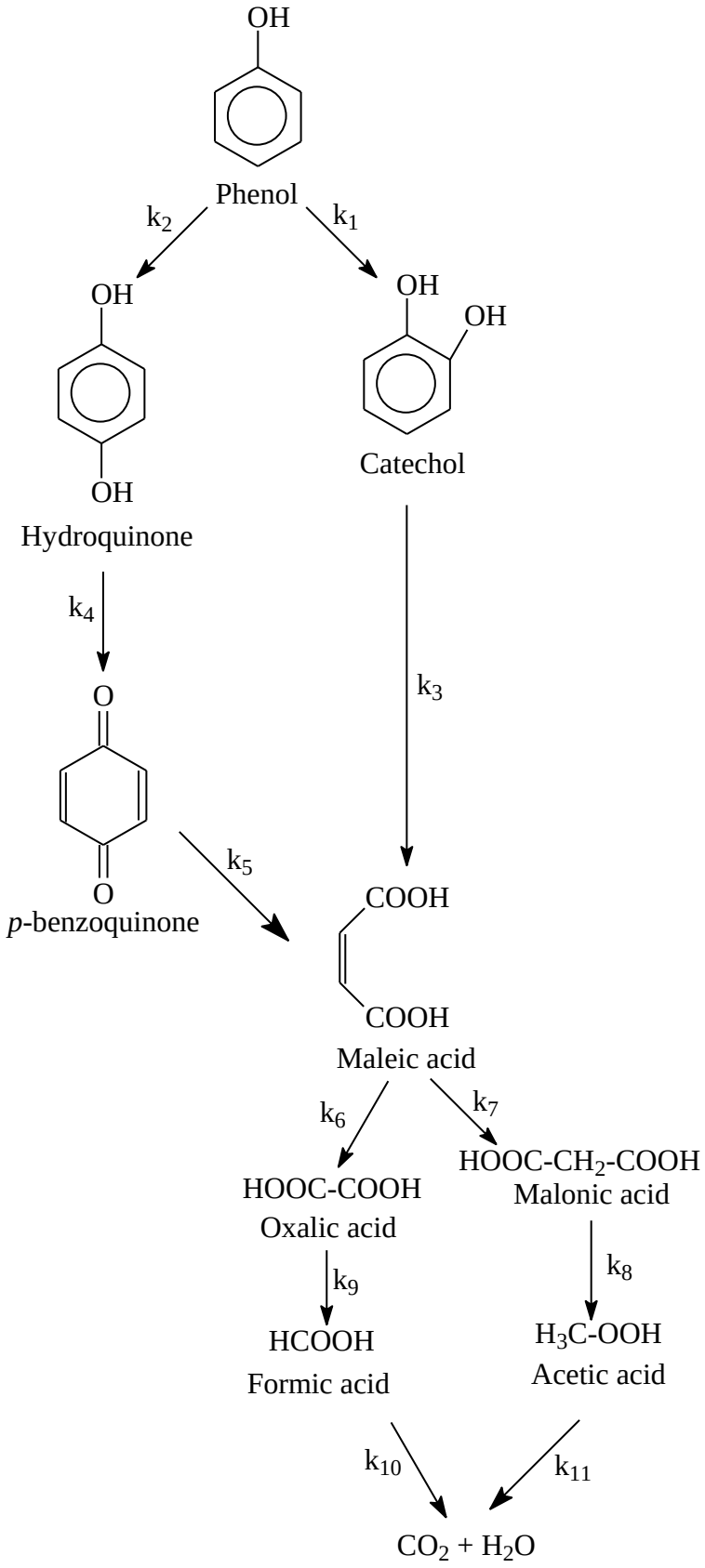


Fig. 11. Proposed reaction pathway for the CWAO of phenol.

3.5. Kinetic modelling of phenol CWAO in a plug flow reactor

The development of the experimental based kinetic model will be a step forth from lab-scale studies to industrial scale CWAO wastewater treatment process. The kinetic model that can describe both the phenol oxidation and formation and consumption of intermediate oxidation products has been used in order to optimize the description of oxidative destruction of phenol. The respective kinetic model for phenol oxidation in a continuous plug flow reactor using monolithic catalyst was based on that proposed by Oxana et al. [40]. The reaction kinetic equations describing overall phenol oxidation reaction consisting of phenol oxidation into intermediates and further oxidation of formed intermediates into simply chain carboxylic acids to CO_2 and H_2O were proposed based on reaction pathway shown in Fig. 11. The CWAO of phenol kinetic model involved 9 equations and 11 rate constants, the kinetic constants are apparent since the effect of oxygen was not included:

$$\frac{dC_{phenol}}{dt} = -(k_1 + k_2) \cdot C_{phenol} \quad (1)$$

$$\frac{dC_{catechol}}{dt} = k_1 \cdot C_{phenol} - k_3 \cdot C_{catechol} \quad (2)$$

$$\frac{dC_{hydroquinone}}{dt} = k_2 \cdot C_{phenol} - k_4 \cdot C_{hydroquinone} \quad (3)$$

$$\frac{dC_{p-benzoquinone}}{dt} = k_4 \cdot C_{hydroquinone} - k_5 \cdot C_{p-benzoquinone} \quad (4)$$

$$\frac{dC_{maleic}}{dt} = k_3 \cdot C_{catechol} + k_5 \cdot C_{p-benzoquinone} - k_6 \cdot C_{maleic\ acid} - k_7 \cdot C_{maleic\ acid} \quad (5)$$

$$\frac{dC_{malonic\ acid}}{dt} = k_6 \cdot C_{maleic\ acid} - k_8 \cdot C_{malonic\ acid} \quad (6)$$

$$\frac{dC_{oxalic\ acid}}{dt} = k_6 \cdot C_{maleic\ acid} - k_9 \cdot C_{oxalic\ acid} \quad (7)$$

$$\frac{dC_{formic\ acid}}{dt} = k_9 \cdot C_{oxalic\ acid} - k_{10} \cdot C_{formic\ acid} \quad (8)$$

$$\frac{dC_{acetic\ acid}}{dt} = k_8 \cdot C_{malonic\ acid} - k_{11} \cdot C_{acetic\ acid} \quad (9)$$

The above kinetic equations confirmed (results not shown here) that the best description of the experimental results was provided by two oxidation routes via oxidation of phenol into aromatic intermediates and further oxidation of aromatic intermediates to short-chain carboxylic acids through the following kinetic equations:

$$W_{ph} = k_1 \exp\left(-\frac{E_1}{RT}\right) \frac{C_{ph} C_{cat} C_{O_2}}{1 + k_2 C_{O_2} + k_3 \left(C_{ph} + C_i\right)^2} \quad (10)$$

$$W_i = k_4 \exp\left(\frac{E_2}{RT}\right) \frac{C_{ph} C_{cat} C_{O_2}}{1 + k_5 C_{O_2} + k_6 \left(C_{ph} + C_i\right)^2} \quad (11)$$

Taking into account the external and internal diffusion limitations, the above kinetic equations were used to calculate apparent oxidation rate of phenol.

A continuous flow plug reactor used in the experimental runs can be described by the following equation:

$$\frac{dC_i}{d_\tau} = v_i W_{app} \quad (12)$$

where *Ci* is the concentration of reactants, τ is the residence time, v_i is the stoichiometric coefficient, i is the index of reactants and W_{app} is the apparent rate of phenol oxidation (calculated using equations (10) and (11) taking into account both the external and internal diffusion limitations).

The apparent reaction rate was reduced to the pseudo-first-order equation with respect to concentration of phenol:

$$W_{app} = k_{app} C_{ph} \quad (13)$$

$$k_{app} = \frac{1}{1/\beta S_{ex} + 1/k^*} \quad (14)$$

where β is the coefficient of external mass transfer, S_{ex} is the external specific surface area and k^* is the reaction rate constant. The Sherwood number was used to calculate β:

$$\beta = \frac{ShD}{d_{eq}} \quad (15)$$

where D is the diffusion coefficient of phenol in water and d_{eq} is the equivalent hydraulic diameter in a catalyst bed [40]:

$$Sh = 3.66\left(1 + 0.095ReSc\frac{d_{eq}}{L}\right)^{0.45} \quad (16)$$

$$Re = \frac{ud_{eq}\rho}{\mu} \quad (17)$$

$$Sc = \frac{\mu}{\rho D} \quad (18)$$

where L is the monolith length, Re is the Reynolds number, Sc is the Schmidt number, μ is the linear rate of the reaction flow, ρ is the flow density and μ is the flow viscosity.

The rate constant for the oxidation of phenol taking into account the internal diffusion inhibition was calculated by the following equations:

$$k^* = \upsilon\frac{w}{C_{ph}} \quad (19)$$

$$\nu = \frac{1}{\varphi} \quad (20)$$

$$\varphi = \frac{d_{gr}}{2}\sqrt{\frac{w}{C_{ph}D_{eff}}} \quad (21)$$

where υ is the efficiency factor, φ is the Thiele modulus, D_{eff} is the effectiveness coefficient of phenol diffusion in catalyst pores, w is the phenol reaction intrinsic rate calculated by Eq. (10).

Fig. 12 shows the results of the numerical calculations. As shown in Fig. 12 the experimental dependencies of phenol conversion against flow rates are correctly described. There is a good agreement between experimental and calculated data. This can be ascribed to the accuracy of the Eq. 16, used for external mass transfer coefficient estimation (insignificant coefficient description error) and accuracy of efficiency factor calculations because of easy shape of honeycomb catalyst. Therefore, the proposed kinetic model provides an adequate description of the monolithic honeycomb efficiency and support the obtained experimental evidence of the effectiveness of used monolithic catalyst in this study.

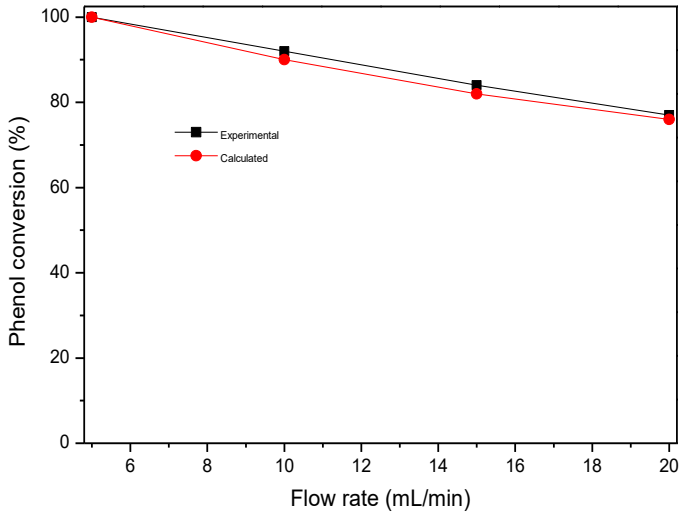


Fig. 12. Experimental and calculated phenol conversion at different flow rate.

Conclusions

In this work, cordierite honeycomb monolithic supports were coated successfully with inexpensive pillared clay catalyst by slurry wet coating using silica solution as the binder and used for the catalytic wet air oxidation of phenol in aqueous solution. The synthesized novel composite catalysts were characterized by XRD, N_2 adsorption-desorption isotherms and HRSEM-EDX techniques. The BET specific surface area and mean pore size of the monolithic catalysts obtained by N_2 adsorption–desorption isotherm studies shows that the catalyst are mesoporous by showing type IV adsorption isotherms. The HRSEM characterization results confirmed the active components were well deposited on the channel walls and the washcoat is observed in all the corners of the washcoated monolith cross section, while the EDX revealed the presence of the Zr and Fe elements in the cordierite monolithic catalyst walls. The novel composite catalysts exhibited good mechanical stability after ultrasound treatment, however, cracks were formed on the coat layer and in the corners of the channels due to a difference in thermal expansion and during a too fast drying step. Future studies we will concentrate on overcoming this problem by optimizing the temperature and moisture control during drying step. The XRD patterns confirmed the different diffraction peaks for the monolithic catalysts and all reference materials.

Monolithic catalysts exhibited good catalytic performance with 100% phenol removal and 91% TOC conversion after the CWAO of phenol at optimal conditions. The optimal operating conditions were 1500 mg/L of initial phenol concentration, 10 bar of partial oxygen pressure. Moreover, it is noteworthy that the monolithic catalyst showed perfect stability in the CWAO of phenol over the prolonged activity test. The reaction pathway in CWAO of phenol over monolithic catalysts in a plug flow reactor was proposed based on hydroxyl radical reacting with phenol and then converting it to aromatics intermediates compounds such as catechol, hydroquinone and p-benzoquinone. The aromatics intermediates further oxidised into short chain carboxylic acids such as maleic acid, malonic, oxalic and formic acids. Finally, these short chain carboxylic acids are decomposed to carbon dioxide and water. Kinetics of CWAO of phenol was studied in a plug flow reactor over monolith catalysts based on the phenol reaction pathway proposed in this study. Kinetic parameters of the model that describes the formation and oxidation of intermediate aromatic compounds and short chain carboxylic acids were determined. The obtained experimental data results were described sufficiently with respect to phenol conversion. The proposed CWAO of phenol kinetic model account for internal and external diffusion limitations, assuming the pseudo-first order reaction. Therefore, the proposed approach can be used for scaling-up the CWAO of phenol in plug flow reactor. This study provides an efficient approach for the treatment of phenol containing wastewater by CWAO process over monolithic catalysts.

List of acronyms

W_{ph}	Phenol reaction rate	$mol.L^{-1}s^{-1}$
W_i	Intermediate reaction rate	$mol.L^{-1}s^{-1}$
E_2 &E_1	Activation energy	$K.J.mol^{-1}$
R	Gas constant	$J.mol^{-1}K^{-1}$
T	Temperature	K
C_{ph}	Phenol concentration	$mol.L^{-1}$
C_{cat}	Catalyst concentration	$mol.L^{-1}$
C_{O2}	Oxygen concentration	$mol.L^{-1}$
C_i	Intermediates concentration	$mol.L^{-1}$

k_1 to k_{11}	Rate constant	$mol.L^{-1}s^{-1}$
k_{2i}, k_{3i}, k_{5i} & k_{6i}	Adsorption constant	$L.mol^{-1}$
τ	Residence time	s
W^{APP}	Phenol oxidation rate	$mol.L^{-1}s^{-1}$
K^{APP}	Pseudo first order rate constant	$mol.L^{-1}s^{-1}$
β	Coefficient external mass transfer	$mol/(s. \cdot m^2)/(mol/m^3)$
S_{ex}	External specific surface area of the catalyst	m^{-1}
k^*	Reaction rate constant	$mol.L^{-1}s^{-1}$
D	Diffusion coefficient	m^2/s
d_{eq}	Equivalent hydraulic diameter	m
L	Monolith length	mm
Re	Reynolds number	
Sc	Schmidt number	
u	Linear rate of reaction flow	m/s
ρ	Flow density	kg/m^3
μ	Flow viscosity	kg/m.s
Sh	Sherwood number	
υ	Efficiency factor	
φ	Thiele modulus	
D_{eff}	Effective coefficient of diffusion	mm^2/s
w	Intrinsic rate of reaction	$mol.L^{-1}s^{-1}$

Acknowledgement

The authors wish to acknowledge financial support from the National Research Foundation (NRF)/ Department of Science and Technology (DST) of South Africa under Professional Development Programme (PDP) Project No. 96719 and Mineral Science Council of South Africa (Mintek) under CWO of Wastewater Project No. ADE 164.

References

[1] L. Zhou, H. Cao, C. Descorme, Y. Xie, Phenolic compounds removal by wet air oxidation based processes, Front. Environ. Sci. Eng. 12 (2017) 1. doi:10.1007/s11783-017-0970-2.

[2] F. Arena, C. Italiano, A. Raneri, C. Saja, Mechanistic and kinetic insights into the wet air oxidation of phenol with oxygen (CWAO) by homogeneous and heterogeneous transition-metal catalysts, Appl. Catal. B Environ. 99 (2010) 321–328. doi:https://doi.org/10.1016/j.apcatb.2010.06.039.

[3] A. Quintanilla, J.A. Casas, A.F. Mohedano, J.J. Rodríguez, Reaction pathway of the catalytic wet air oxidation of phenol with a Fe/activated carbon catalyst, Appl. Catal. B Environ. 67 (2006) 206–216. doi:https://doi.org/10.1016/j.apcatb.2006.05.003.

[4] R.R. Zapico, P. Marín, F. V Díez, S. Ordóñez, Assessment of phenol wet oxidation on CuO/γ-Al2O3 catalysts: Competition between heterogeneous and leached-copper homogeneous reaction paths, J. Environ. Chem. Eng. 5 (2017) 2570–2578. doi:https://doi.org/10.1016/j.jece.2017.04.050.

[5] A.E. de los Monteros, G. Lafaye, A. Cervantes, G. Del Angel, J.B. Jr., G. Torres, Catalytic wet air oxidation of phenol over metal catalyst (Ru,Pt) supported on TiO2–CeO2 oxides, Catal. Today. 258 (2015) 564–569. doi:https://doi.org/10.1016/j.cattod.2015.01.009.

[6] S. Yang, W. Zhu, J. Wang, Z. Chen, Catalytic wet air oxidation of phenol over CeO2-TiO2 catalyst in the batch reactor and the packed-bed reactor, J. Hazard. Mater. 153 (2008) 1248–1253. doi:https://doi.org/10.1016/j.jhazmat.2007.09.084.

[7] J. Moma, J. Baloyi, T. Ntho, Synthesis and characterization of an efficient and stable Al/Fe pillared clay catalyst for the catalytic wet air oxidation of phenol, RSC Adv. 8 (2018) 30115–30124. doi:10.1039/C8RA05825C.

[8] J. Baloyi, T. Ntho, J. Moma, Synthesis and application of pillared clay heterogeneous

catalysts for wastewater treatment: a review, RSC Adv. 8 (2018) 5197–5211. doi:10.1039/C7RA12924F.

[9] F. Tomul, Adsorption and catalytic properties of Fe/Cr-pillared bentonites, Chem. Eng. J. 185–186 (2012) 380–390. doi:https://doi.org/10.1016/j.cej.2012.01.094.

[10] B. Liu, J. Du, X. Lv, Y. Qiu, C. Tao, Washcoating of cordierite honeycomb with vanadia-tungsta-titania mixed oxides for selective catalytic reduction of NO with NH3, Catal. Sci. Technol. 5 (2015) 1241–1250. doi:10.1039/c4cy01179a.

[11] J. Baloyi, T. Ntho, J. Moma, Synthesis of highly active and stable Al/Zr pillared clay as catalyst for catalytic wet oxidation of phenol, J. Porous Mater. (2018). doi:10.1007/s10934-018-0667-3.

[12] L. Han, Y. Wang, J. Zhang, Z. Lei, C. Huang, B. Chen, Acidic Montmorillonite/Cordierite Monolithic Catalysts for Cleavage of Cumene Hydroperoxide, Chinese J. Chem. Eng. 22 (2014) 854–860. doi:https://doi.org/10.1016/j.cjche.2014.06.006.

[13] L. Tang, Z. Zhao, Y. Wei, J. Liu, Y. Peng, K. Li, Study on the coating of nano-particle and 3DOM LaCoO3 perovskite-type complex oxide on cordierite monolith and the catalytic performances for soot oxidation: The effect of washcoat materials of alumina, silica and titania, Catal. Today. 297 (2017) 131–142. doi:https://doi.org/10.1016/j.cattod.2017.06.016.

[14] D.M. Gómez, J.M. Gatica, J.C. Hernández-Garrido, G.A. Cifredo, M. Montes, O. Sanz, J.M. Rebled, H. Vidal, A novel CoOx/La-modified-CeO2 formulation for powdered and washcoated onto cordierite honeycomb catalysts with application in VOCs oxidation, Appl. Catal. B Environ. 144 (2014) 425–434. doi:https://doi.org/10.1016/j.apcatb.2013.07.045.

[15] J. Hwang, H.-J. Ha, J. Ryu, J.-J. Choi, C.-W. Ahn, J.-W. Kim, B.-D. Hahn, W.-H. Yoon, H. Lee, J.-H. Choi, Enhancement of washcoat adhesion for SCR catalysts to convert nitrogen oxide using powder spray coating of TiO2 on metallic honeycomb substrate, Catal. Commun. 94 (2017) 1–4. doi:https://doi.org/10.1016/j.catcom.2017.02.002.

[16] M. Tahir, Photocatalytic carbon dioxide reduction to fuels in continuous flow monolith photoreactor using montmorillonite dispersed Fe/TiO2 nanocatalyst, J. Clean. Prod. 170 (2018) 242–250. doi:https://doi.org/10.1016/j.jclepro.2017.09.118.

[17] H. Zhou, Y. Su, W. Liao, W. Deng, F. Zhong, Preparation, characterization, and properties of monolithic Fe/Al2O3/cordierite catalysts for NO reduction with C2H6, Appl. Catal. A Gen. 505 (2015) 402–409.

[18] A.N. Shigapov, G.W. Graham, R.W. McCabe, M.P. Peck, H.K. Plummer, The preparation of high-surface-area cordierite monolith by acid treatment, Appl. Catal. A Gen.

182 (1999) 137–146. doi:https://doi.org/10.1016/S0926-860X(99)00003-4.

[19] M.B. Adamowska, P. Da Costa, Structured Pd / γ-Al 2 O 3 Prepared by Washcoated Deposition on a Ceramic Honeycomb for Compressed Natural Gas Applications, J. Nanoparticles. 2015 (2014) 10–12. doi:http://dx.doi.org/10.1155/2015/601941.

[20] E. García-Bordejé, F. Kapteijn, J.A. Moulijn, Preparation and characterisation aspects of carbon-coated monoliths, Catal. Today. 69 (2001) 357–363. doi:https://doi.org/10.1016/S0920-5861(01)00392-3.

[21] B.M. Sollier, L.E. Gómez, A. V Boix, E.E. Miró, Oxidative coupling of methane on cordierite monoliths coated with Sr/La2O3 catalysts. Influence of honeycomb structure and catalyst-cordierite chemical interactions on the catalytic behavior, Appl. Catal. A Gen. 550 (2018) 113–121. doi:https://doi.org/10.1016/j.apcata.2017.10.023.

[22] R.G. Mohite, A. Garg, Performance of heterogeneous catalytic wet oxidation for the removal of phenolic compounds: Catalyst characterization and effect of pH, temperature, metal leaching and non-oxidative hydrothermal reaction, J. Environ. Chem. Eng. 5 (2017) 468–478. doi:https://doi.org/10.1016/j.jece.2016.12.024.

[23] J. Guo, M. Al-Dahhan, Activity and stability of iron-containing pillared clay catalysts for wet air oxidation of phenol, Appl. Catal. A Gen. 299 (2006) 175–184. doi:https://doi.org/10.1016/j.apcata.2005.10.039.

[24] M.E. Suárez-Ojeda, A. Fabregat, F. Stüber, A. Fortuny, J. Carrera, J. Font, Catalytic wet air oxidation of substituted phenols: Temperature and pressure effect on the pollutant removal, the catalyst preservation and the biodegradability enhancement, Chem. Eng. J. 132 (2007) 105–115. doi:https://doi.org/10.1016/j.cej.2007.01.025.

[25] B. Larruy, A. Ayude, J. Font, A. Fortuny, C. Bengoa, A. Fabregat, F. Stüber, Gas feed composition modulation in phenol CWAO over active carbon, Chem. Eng. Sci. 62 (2007) 5564–5566. doi:https://doi.org/10.1016/j.ces.2007.01.079.

[26] M. Santiago, F. Stüber, A. Fortuny, A. Fabregat, J. Font, Modified activated carbons for catalytic wet air oxidation of phenol, Carbon N. Y. 43 (2005) 2134–2145. doi:https://doi.org/10.1016/j.carbon.2005.03.026.

[27] S. Morales-Torres, A.M.T. Silva, A.F. Pérez-Cadenas, J.L. Faria, F.J. Maldonado-Hódar, J.L. Figueiredo, F. Carrasco-Marín, Wet air oxidation of trinitrophenol with activated carbon catalysts: Effect of textural properties on the mechanism of degradation, Appl. Catal. B Environ. 100 (2010) 310–317. doi:https://doi.org/10.1016/j.apcatb.2010.08.007.

[28] J. Guo, M. Al-Dahhan, Modeling Catalytic Trickle-Bed and Upflow Packed-Bed

Reactors for Wet Air Oxidation of Phenol with Phase Change, Ind. Eng. Chem. Res. - IND ENG CHEM RES. 44 (2005).

[29] F. Stüber, J. Font, A. Fortuny, C. Bengoa, A. Eftaxias, A. Fabregat, Carbon materials and catalytic wet air oxidation of organic pollutants in wastewater, Top. Catal. 33 (2005) 3–50. doi:10.1007/s11244-005-2497-1.

[30] M.A.L. Rocha, G. Del Ángel, G. Torres-Torres, A. Cervantes, A. Vázquez, A. Arrieta, J.N. Beltramini, Effect of the Pt oxidation state and Ce3+/Ce4+ ratio on the Pt/TiO2-CeO2 catalysts in the phenol degradation by catalytic wet air oxidation (CWAO), Catal. Today. 250 (2015) 145–154. doi:https://doi.org/10.1016/j.cattod.2014.09.016.

[31] A. Eftaxias, J. Font, A. Fortuny, J. Giralt, A. Fabregat, F. Stüber, Kinetic modelling of catalytic wet air oxidation of phenol by simulated annealing, Appl. Catal. B Environ. 33 (2001) 175–190. doi:https://doi.org/10.1016/S0926-3373(01)00178-3.

[32] S.S. Lin, D.J. Chang, C.-H. Wang, C.C. Chen, Catalytic wet air oxidation of phenol by CeO2 catalyst—effect of reaction conditions, Water Res. 37 (2003) 793–800. doi:https://doi.org/10.1016/S0043-1354(02)00422-0.

[33] R.S.C. Advances, Synthesis and characterization of an efficient and stable Al/Fe pillared clay catalyst for the catalytic wet air oxidation of phenol, (n.d.).

[34] F. Arena, C. Italiano, L. Spadaro, Efficiency and reactivity pattern of ceria-based noble metal and transition metal-oxide catalysts in the wet air oxidation of phenol, Appl. Catal. B Environ. 115–116 (2012) 336–345. doi:https://doi.org/10.1016/j.apcatb.2011.12.035.

[35] A. Santos, P. Yustos, A. Quintanilla, S. Rodríguez, F. García-Ochoa, Route of the catalytic oxidation of phenol in aqueous phase, Appl. Catal. B Environ. 39 (2002) 97–113. doi:https://doi.org/10.1016/S0926-3373(02)00087-5.

[36] J.A. Zazo, J.A. Casas, A.F. Mohedano, M.A. Gilarranz, J.J. Rodríguez, Chemical Pathway and Kinetics of Phenol Oxidation by Fenton's Reagent, Environ. Sci. Technol. 39 (2005) 9295–9302. doi:10.1021/es050452h.

[37] K. Lal, A. Garg, Catalytic wet oxidation of phenol under mild operating conditions: development of reaction pathway and sludge characterization, Clean Technol. Environ. Policy. 17 (2015) 199–210. doi:10.1007/s10098-014-0777-9.

[38] X. Li, Y. Cui, Y. Feng, Z. Xie, J.-D. Gu, Reaction pathways and mechanisms of the electrochemical degradation of phenol on different electrodes, Water Res. 39 (2005) 1972–1981. doi:https://doi.org/10.1016/j.watres.2005.02.021.

[39] D. Duprez, F. Delanoë, J. Barbier, P. Isnard, G. Blanchard, Catalytic oxidation of

organic compounds in aqueous media, Catal. Today. 29 (1996) 317–322. doi:https://doi.org/10.1016/0920-5861(95)00298-7.

[40] O.P. Taran, A.N. Zagoruiko, A.B. Ayusheev, S.A. Yashnik, R. V Prihod'ko, Z.R. Ismagilov, V. V Goncharuk, V.N. Parmon, Wet peroxide oxidation of phenol over Cu-ZSM-5 catalyst in a flow reactor. Kinetics and diffusion study, Chem. Eng. J. 282 (2015) 108–115. doi:https://doi.org/10.1016/j.cej.2015.02.064.

Chapter 8

General conclusions and recommendations

In this study numerous pillared clay catalysts were synthesized, tested and screened for their catalytic activity in CWAO of phenol in a batch and plug-flow reactor. It was revealed from an intensive literature review of the CWAO and pillared clay catalysts that there was room for development in terms of synthesizing an active and robust catalyst. Moreover, the reduction of prolonged synthesis times (1-5 days) and large amount of water (2 wt. % suspension) used in a process as such requirements significantly hinder the scale-up of the pillaring process to industrial scale. The desired catalysts must reduce the severity of the reaction conditions of the CWAO process.

The main objective, therefore, was to apply a novel pillared clay catalysts prepared from natural bentonite clay for treatment of phenol in aqueous solution by CWAO at mild reaction conditions. Three pillared clay-based heterogeneous catalysts, Al/Zr-PILCs, Al/Fe-PILCs and Al/Cr-PILCs were synthesized from natural bentonite and screened for their efficiency in removal of phenol in aqueous medium. The method of hydrolysis and ion exchange were successfully achieved by direct addition of the clay into the pillaring solution using ultrasound both during the formation of the pillaring solution and in the intercalation process, respectively. The synthesize method used in this study significantly reduced the synthesis time and the water consumption required compared to traditional method discussed in the literature, indicating advantages of potential scale-up of the pillared clay. Therefore, this method can be extensively used for synthesis of pillared clays in the laboratory scale and provides possible economic benefits in the escalation of the preparation to an industrial production scale. The characterization of the synthesized PILCs materials exhibited that the basal spacing, BET surface area, pore volume and thermal stability of mixed metal polycations were greatly higher compared to single metal polycations and natural bentonite clay. The PXRD demonstrated an increase in the basal spacing up to 1.92 nm with a high thermal stability. The textual properties show an increase in BET surface area indicating that mixed metal polycations inserted into the

bentonite clay plays a crucial role in increasing surface area. HRSEM confirms that this methodology allows interaction of mixed metal polycations with the tetrahedral sheets of the bentonite clay, without destroying the structure of the clay.

The PILCs catalysts screening process in a batch reactor was aimed to attain the best catalyst for phenol CWAO reaction. It was discovered that all mixed metal PILCs catalysts strongly oxidized phenol and provided much activity in terms of phenol removal and TOC conversion. The Al/Zr-PILCs, Al/Fe-PILCs and Al/Cr-PILCs composites with metal ratios of 3:1 (Al:Zr), 3:1 (Al:Fe) and 1:1 (Al:Cr), respectively, were found to be very active among different pillared catalysts and a complete phenol removal and more than 80% of TOC conversion was achieved within 120 min. However, Al/Zr-PILCs catalyst with ratio of 3:1 promoted phenol removal and TOC conversion to a much higher catalytic activity and stability. A significant effect of the studied variables such as reaction temperature, oxygen partial pressure, initial phenol concentration, catalyst loading, initial solution pH and reaction time was observed and has a direct influence on the CWAO of phenol. The analysis of intermediate products revealed the presence of hydroquinone, pyrocatechol, benzoquinone and oxalic, formic, malonic, oxalic, malonic and maleic acids. All synthesized PILCs catalyst could be used in four consecutive reaction runs without significant loss of phenol catalytic activity and above 65% TOC conversion. The kinetic study of the best catalyst was carried out and experimental results indicate that the phenol oxidation can be described by first-order kinetics, with apparent activation energy of 21.306 kJ mol^{-1}. For practical purpose, this led to a more comprehensive study being carried out on a plug-flow reactor using cordierite honeycomb monolithic supports coated with Al/Zr-PILCs with ratio of 3:1.

The cordierite honeycomb monolithic supports were coated successfully with inexpensive pillared clay catalyst by slurry wet coating using silica solution as the binder and used for the CWAO of phenol in aqueous solution. The synthesized novel composite catalysts were characterized by XRD, N_2 adsorption-desorption isotherms and HRSEM-EDX techniques. The BET specific surface area and mean pore size of the monolithic catalysts obtained by N_2 adsorption–desorption isotherm studies shows that the catalyst are mesoporous by showing type IV adsorption isotherms. The HRSEM characterization results confirmed the active components were well deposited on the channel walls and the washcoat is observed in all the corners of the washcoated monolith cross section, while the EDX revealed the presence of the Zr and Fe elements in the cordierite monolithic catalyst walls. The novel composite catalysts

exhibited good mechanical stability after ultrasound treatment, however, cracks were formed on the coat layer and in the corners of the channels due to a difference in thermal expansion and during a too fast drying step. The XRD patterns confirmed the different diffraction peaks for the monolithic catalysts and all reference materials.

The monolithic catalyst showed excellent catalytic activity with complete phenol removal and 91% TOC conversion after the CWAO of phenol at optimal conditions (140 °C and10 bar). Moreover, it is noteworthy that the monolithic catalyst showed perfect stability in the CWAO of phenol over the prolonged activity test. The reaction pathway in CWAO of phenol over monolithic catalysts in a plug flow reactor was proposed based on hydroxyl radical reacting with phenol and then converting it to aromatics intermediates compounds such as catechol, hydroquinone and p-benzoquinone. The aromatics intermediates further oxidised into short chain carboxylic acids such as maleic acid, malonic, oxalic and formic acids. Finally, these short chain carboxylic acids are decomposed to carbon dioxide and water. Kinetics of CWAO of phenol was studied in a plug flow reactor over monolith catalysts based on the phenol reaction pathway proposed in this study. Kinetic parameters of the model that describes the formation and oxidation of intermediate aromatic compounds and short chain carboxylic acids were determined. The obtained experimental data results were described sufficiently with respect to phenol conversion. The proposed CWAO of phenol kinetic model account for internal and external diffusion limitations, assuming the pseudo-first order reaction. Therefore, the proposed approach can be used for scaling-up the CWAO of phenol in plug flow reactor.

To conclude, novel pillared clay catalysts were successful prepared from natural bentonite clay for treatment of phenol in aqueous solution by CWAO at mild reaction conditions. Moreover, on developing a successful novel pillared clays-based catalysts, the commissioning of a plug-floe reactor was carried out successful. The novel PILCs catalysts attained complete removal of phenol and more than 80% TOC conversion in a mild reaction conditions. Future study is recommended to concentrate on overcoming the problem associated with the cracks that were formed on the coat layer and in the corners of the channels of monolithic catalysts due to a difference in thermal expansion and during a too fast drying step. This can be achieved by optimizing the temperature and moisture control during drying step. Although, the objectives of the current study have been achieved, it is recommended to study different flow conditions in order to understand flow dynamics of different flow regimes. Also using the advanced

analysis tool such as computational fluid dynamics (CFD) to stimulate the behaviour of the reactor system.

APPENDICES

The following is a **list of abbreviations** that were used in the thesis:

AOPs	Advance oxidation processes
CWAO	Catalytic wet air oxidation
HRSEM	High resolution scanning electron microscopy
EDX	Energy-dispersive X-ray spectroscopy
CEC	Cation exchange capacity
MFC	Mass flow controller
TOC	Total organic carbon
TC	Total carbon
TIC	Total inorganic carbon
BJH	Barret–Joyner–Halanda
BET	Brunauer–Emmett–Teller
FTIR	Fourier transform infrared spectroscopy
PXRD	Powder X-ray diffraction
TCD	Thermal conductivity detector
TGA-DTA	Thermogravimetric analysis with differential thermal gravimetry
wt. %	Weight percentage

Supplementary materials

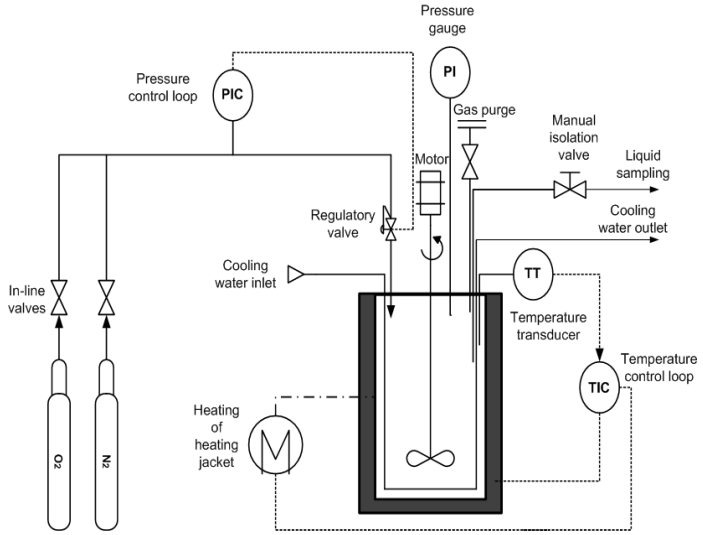


Fig. S1: Experimental set up for phenol oxidation semi-batch reactor system.

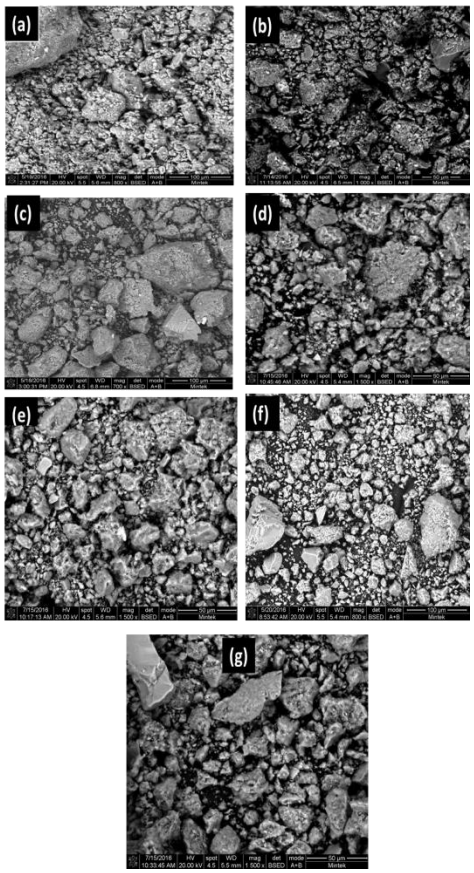


Fig. S2: HRSEM micrographs of: (a) Natural bentonite clay, (b) Al-PILCs, (c) Fe-PILCs, (d) Al/Fe-PILCs (1:3), (e) Al/Fe-PILCs (1:1), (f) Al/Fe-PILCs (3:1) and (g) Al/Fe-PILCs (6:1).

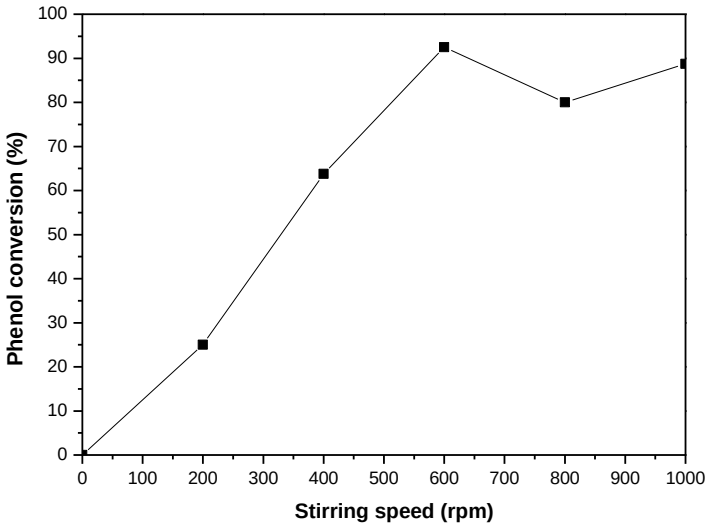


Fig. S3: Effect of mass transfer on the conversion of phenol in aqueous solution. (phenol conc, 1000 mg/L; volume, 200 mL; catalyst loading, 2 g/L; reaction time, 150 min; partial oxygen pressure, 10 bar; temperature, 100 °C).

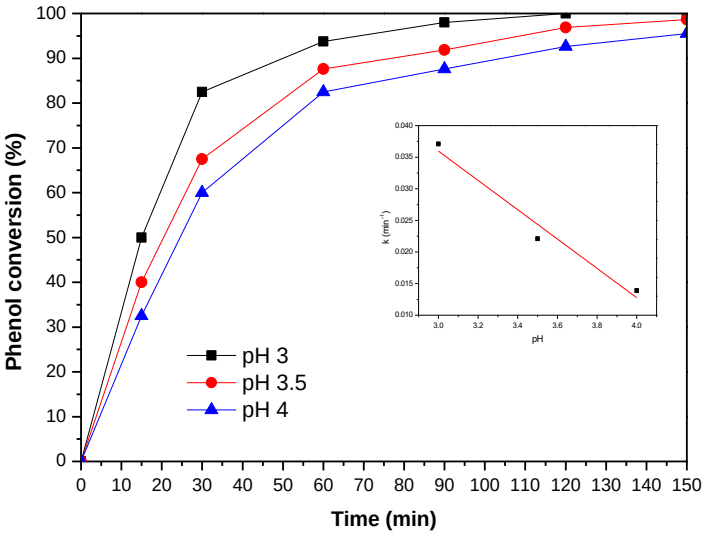


Fig. S4: Effect of initial pH on conversion of phenol in aqueous solution. (phenol conc, 1000 mg/L; volume, 200 mL; catalyst loading, 2 g/L; reaction time, 150 min; partial oxygen pressure, 10 bar; temperature, 100 °C).

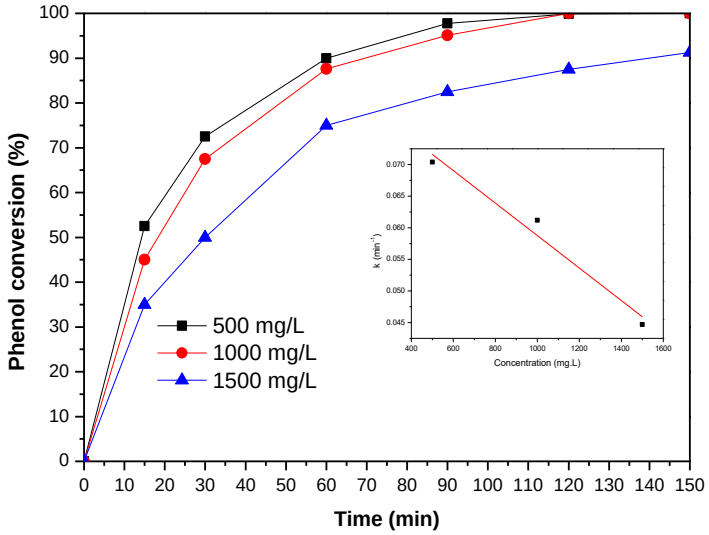


Fig. S5: Effect of initial concentration of phenol in aqueous solution. (volume, 200 mL; catalyst loading, 2 g/L; pH, 3.0; reaction time, 150 min; partial oxygen pressure, 10 bar; temperature 100 °C).

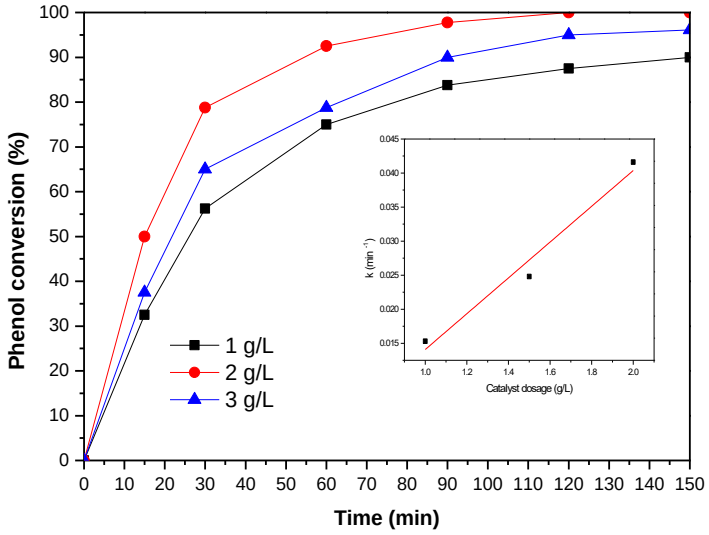


Fig. S6. Effect of catalyst mass on conversion of phenol in aqueous solution. (phenol concentration, 1000 mg/L; volume, 200 mL; pH, 3.0; partial oxygen pressure, 10 bars; temperature, 100 °C).

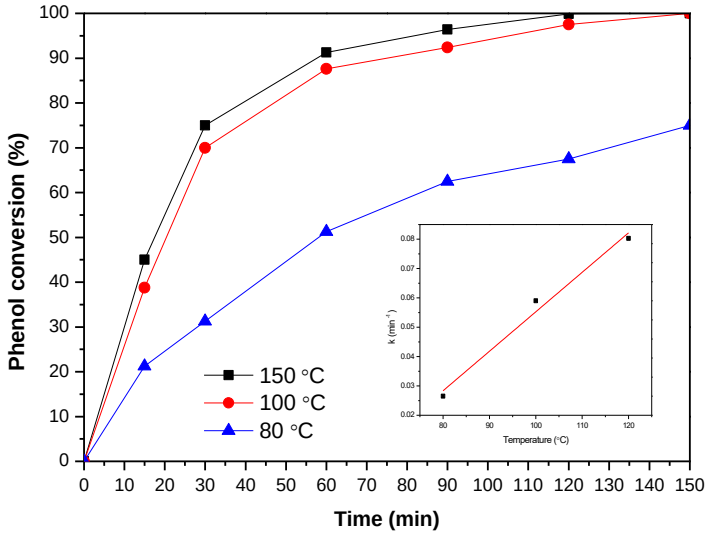


Fig. S7. Effect of reaction temperature on conversion of phenol in aqueous solution. (phenol concentration, 1000 mg/L; volume, 200 mL; pH, 3.0; reaction time, 180 min; partial oxygen pressure, 10 bar; catalyst loading, 2 g/L).

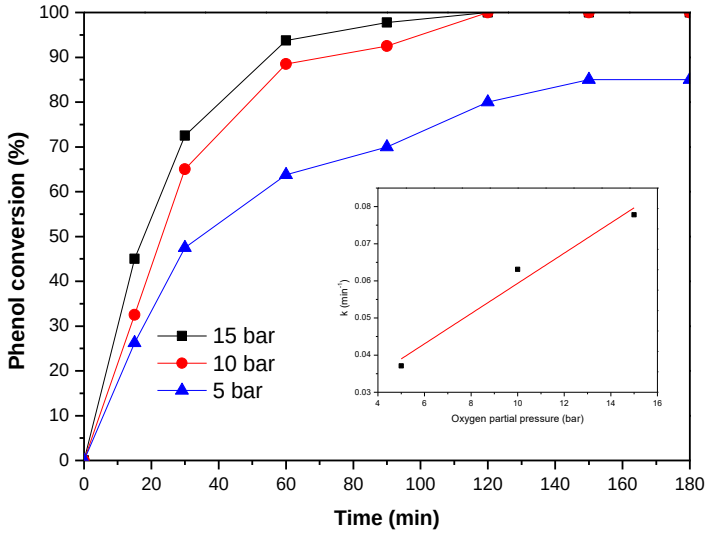


Fig. S8. Effect of oxygen partial pressure on conversion of phenol in aqueous solution (phenol concentration, 1000 mg/L; volume, 200 mL; pH, 3.0; reaction time, 180 min; temperature, 100 °C; catalyst loading, 2g/L).

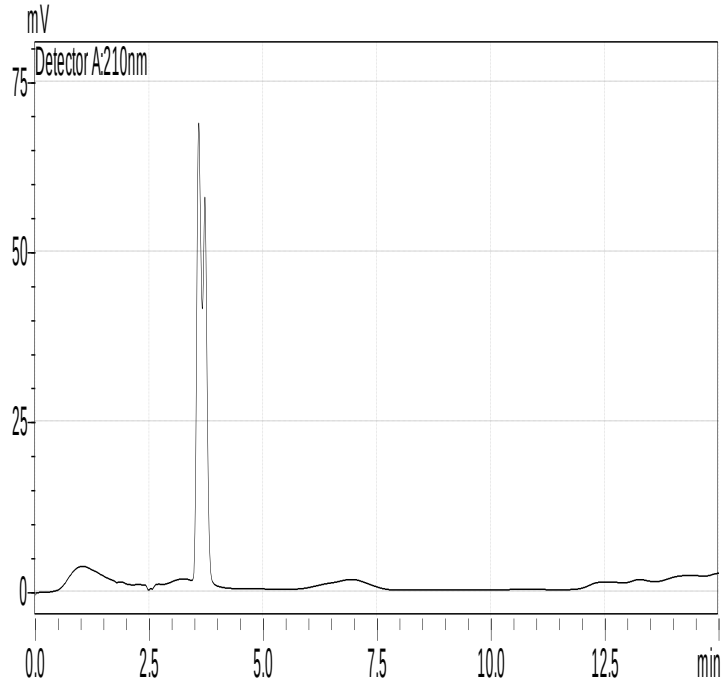


Fig. S9. HPLC calibration curve for phenol.

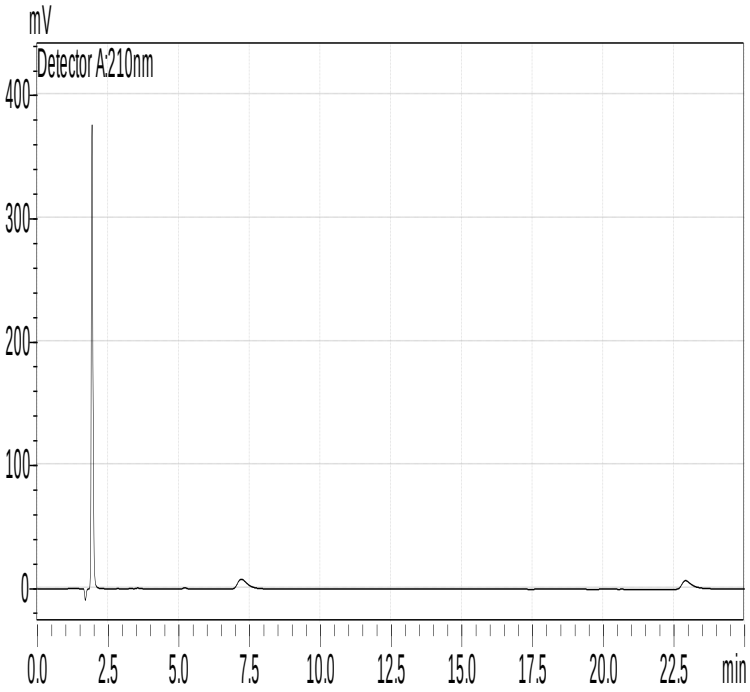


Fig. S10. HPLC calibration curve for acetic acid.

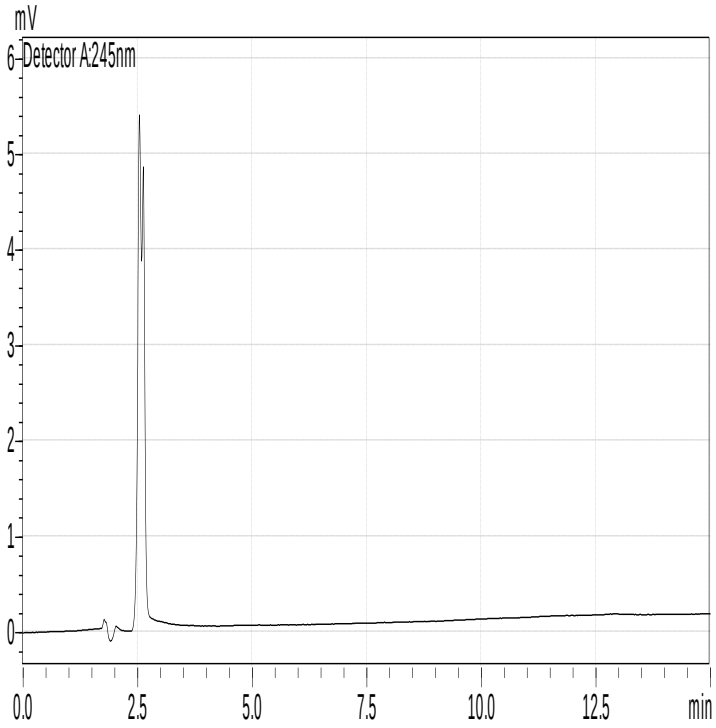


Fig. S11. HPLC calibration curve for formic acid.

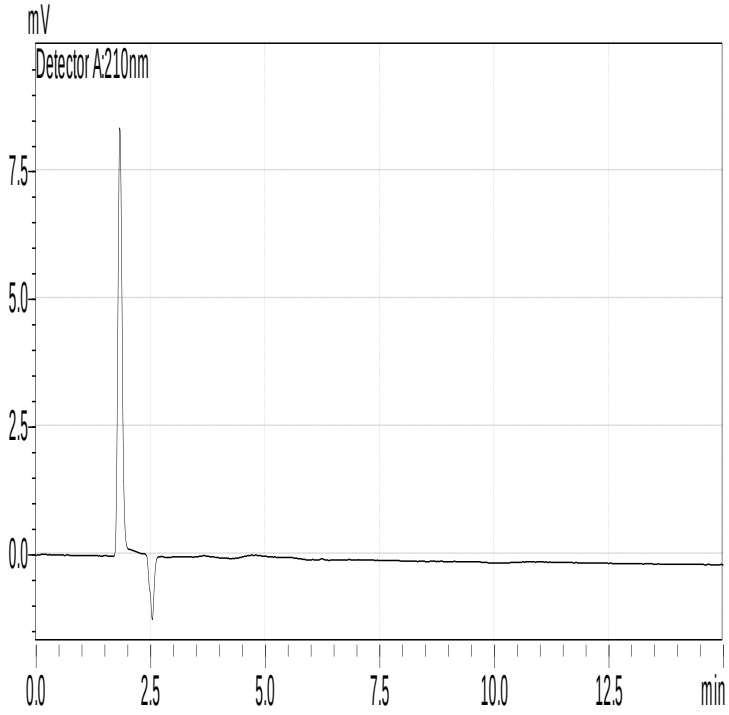


Fig. S12. HPLC calibration curve for maleic acid.

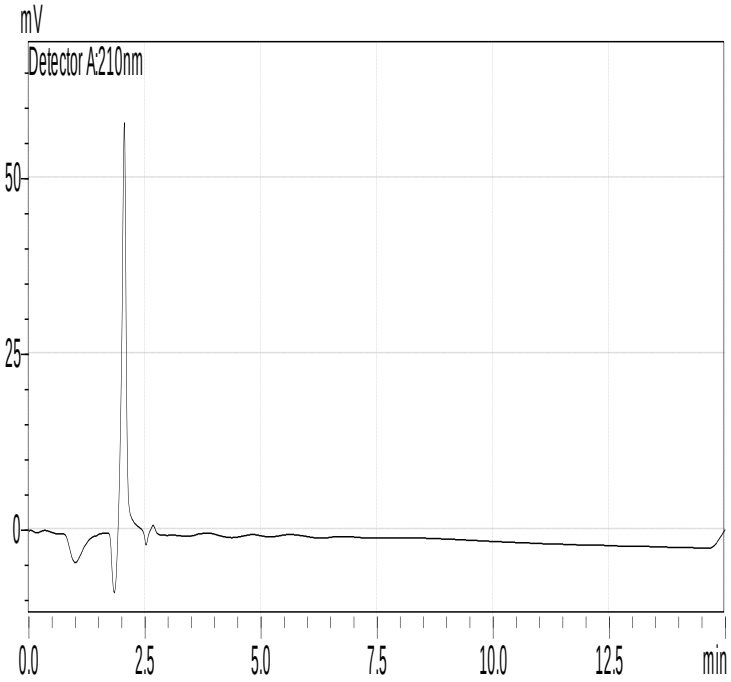


Fig. S13. HPLC calibration curve for hydroquinone.

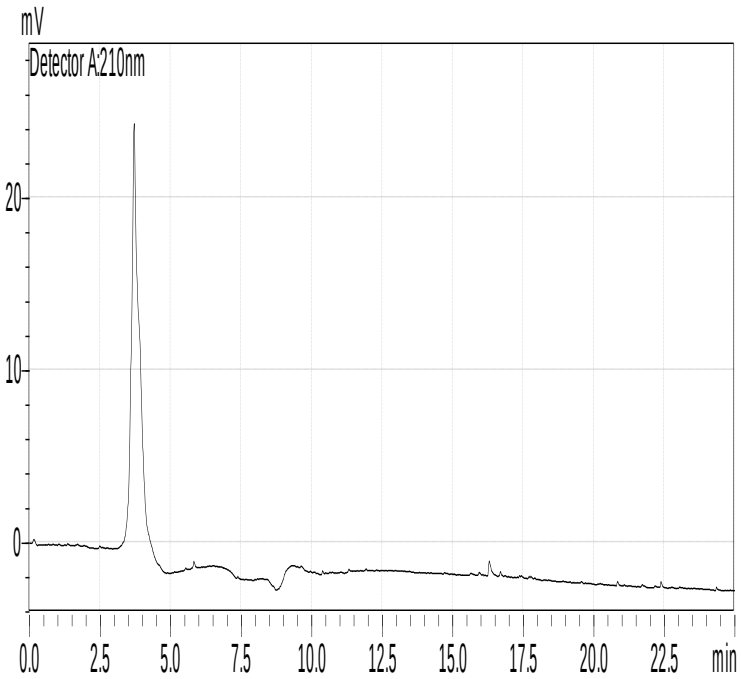


Fig. S14. HPLC calibration curve for pyrocatechol.

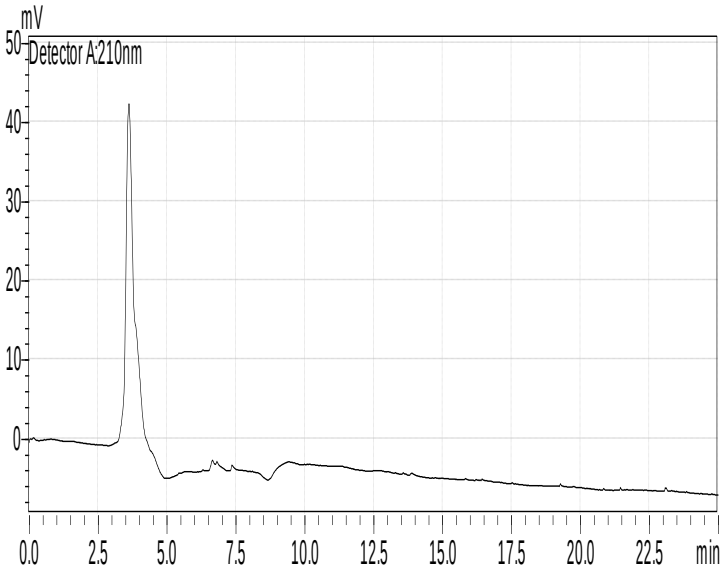


Fig. S15. HPLC calibration curve for benzoquinone.

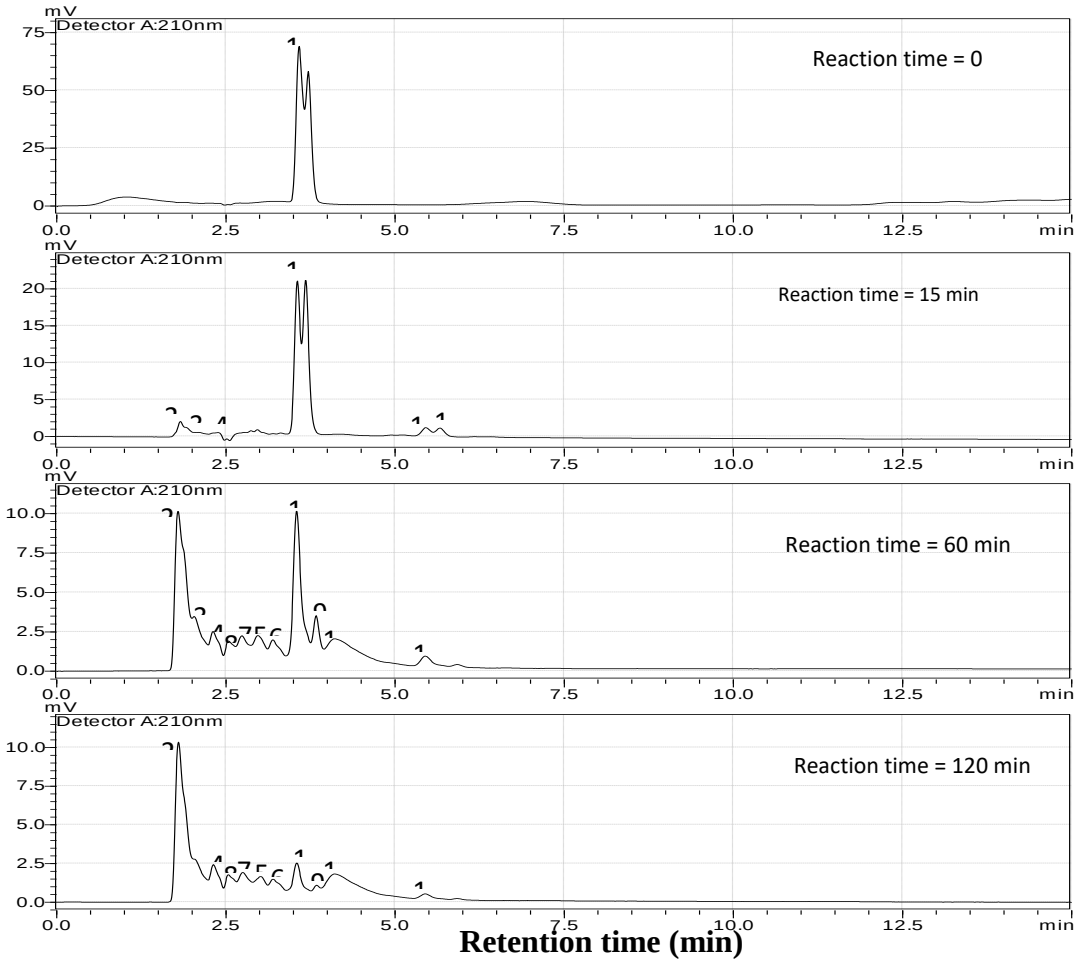


Fig. S16. Typical liquid chromatograms of phenol and intermediates in liquid sample. 1. Phenol; 2. Acetic acid; 3. Hydroquinone; 4. Maleic acid; 5. Benzoquinone; 6. Pyrocatechol; 7. Malonic acid; 8. Formic acid; 9. Oxalic acid.

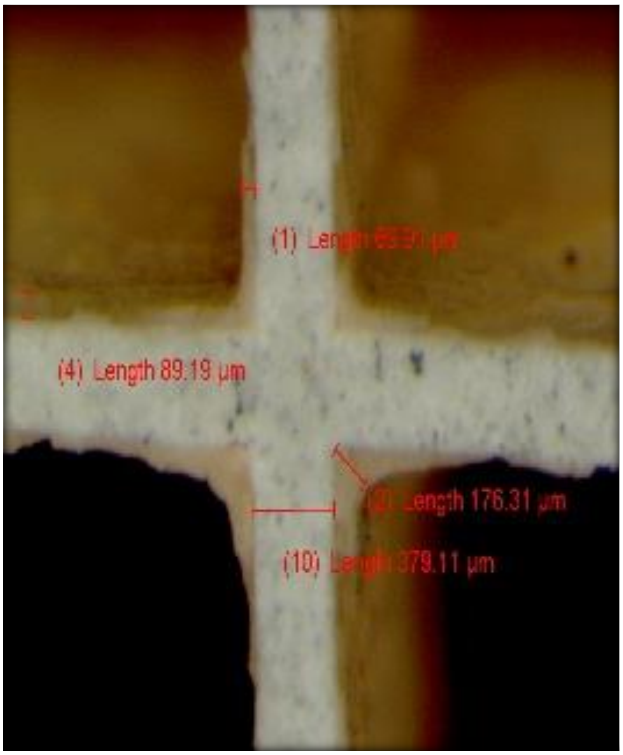


Fig. S17. Cross-section cut of a Al/Zr-PILCs-coated monolith seen with a metallurgical microscope.

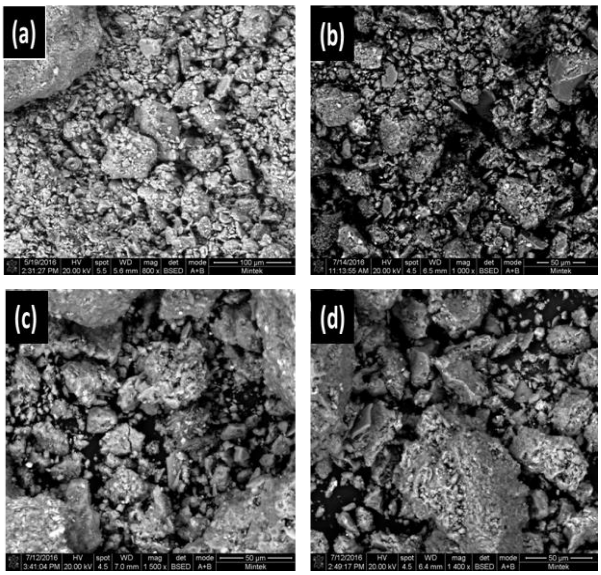


Fig. S18. HRSEM micrographs of (a) Na-Bt, (b) Al-PILC, (c) Zr-PILC and (d) Al/Zr-PILC (3:1)

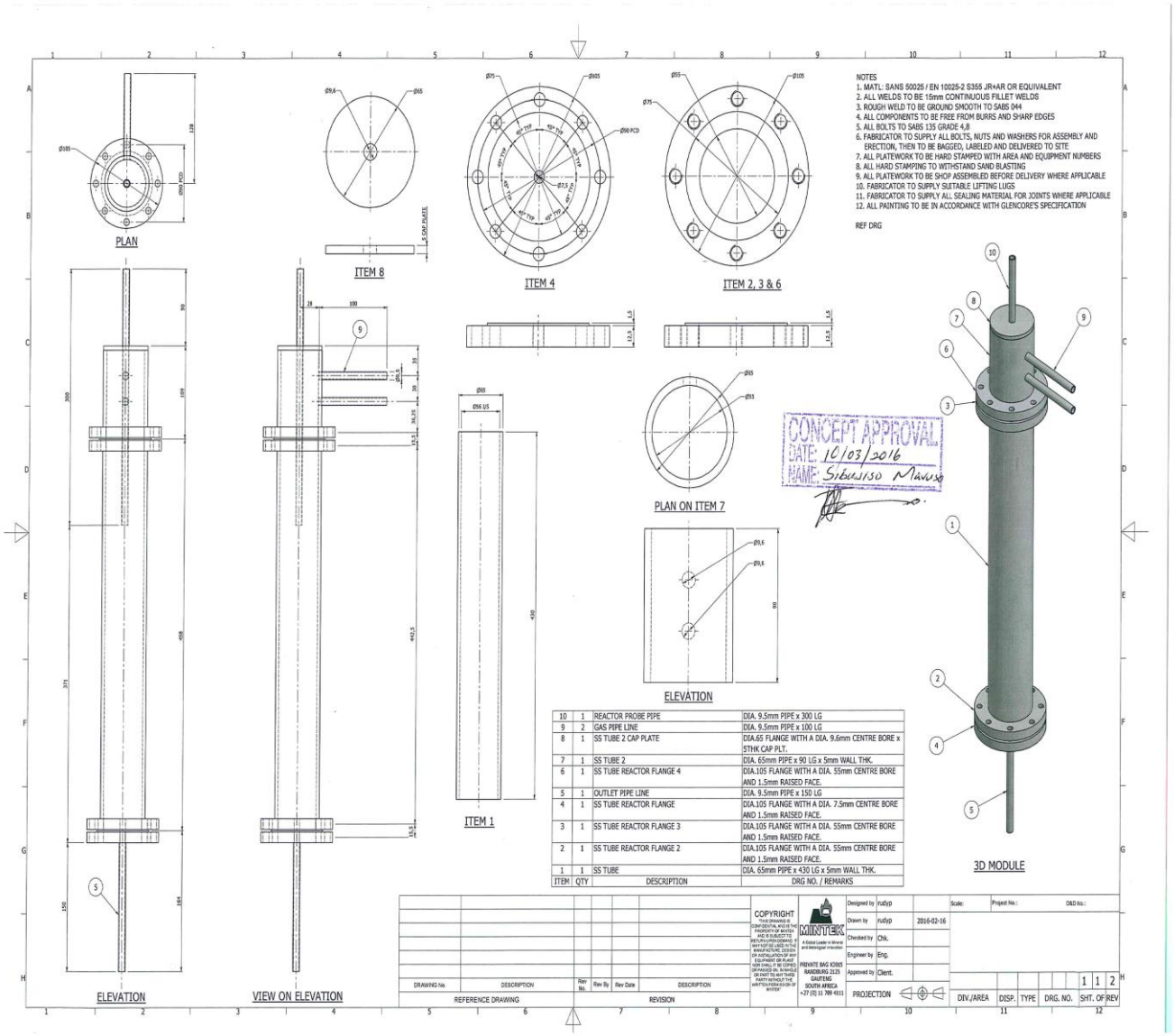


Fig. S19. Designed continuous flow reactor tube.